U.S. Department of Commerce
Weather Bureau

U.S. Department of Army
Corps of Engineers

HYDROMETEOROLOGICAL REPORT NO. 37

METEOROLOGY OF HYDROLOGICALLY CRITICAL STORMS IN CALIFORNIA

Prepared by
ROBERT L. WEAVER
Hydrometeorological Section
Hydrologic Services Division
U.S. Weather Bureau

Washington, D.C.
December 1962

HYDROMETEOROLOGICAL REPORTS

(Nos. 6–22 Numbered Retroactively)

*No. 1. Maximum possible precipitation over the Ompompanoosuc Basin above Union Village, Vt. 1943.
*No. 2. Maximum possible precipitation over the Ohio River Basin above Pittsburgh, Pa. 1942.
*No. 3. Maximum possible precipitation over the Sacramento Basin of California. 1943.
*No. 4. Maximum possible precipitation over the Panama Canal Basin. 1943.
*No. 5. Thunderstorm rainfall. 1947.
*No. 6. A preliminary report on the probable occurrence of excessive precipitation over Fort Supply Basin, Okla. 1938.
*No. 7. Worst probable meteorological condition on Mill Creek, Butler and Hamilton Counties, Ohio. 1937. (Unpublished.) Supplement, 1938.
*No. 8. A hydrometeorological analysis of possible maximum precipitation over St. Francis River Basin above Wappapello, Mo. 1938.
*No. 9. A report on the possible occurrence of maximum precipitation over White River Basin above Mud Mountain Dam site, Wash. 1939.
*No. 10. Maximum possible rainfall over the Arkansas River Basin above Caddoa, Colo. 1939. Supplement, 1939.
*No. 11. A preliminary report on the maximum possible precipitation over the Dorena, Cottage Grove, and Fern Ridge Basins in the Willamette Basin, Oreg. 1939.
*No. 12. Maximum possible precipitation over the Red River Basin above Denison, Tex. 1939.
*No. 13. A report on the maximum possible precipitation over Cherry Creek Basin in Colorado. 1940.
*No. 14. The frequency of flood-producing rainfall over the Pajaro River Basin in California. 1940.
*No. 15. A report on depth-frequency relations of thunderstorm rainfall on the Sevier Basin, Utah. 1941.
*No. 16. A preliminary report on the maximum possible precipitation over the Potomac and Rappahannock River Basins. 1943.
*No. 17. Maximum possible precipitation over the Pecos Basin of New Mexico. 1944. (Unpublished.)
*No. 18. Tentative estimates of maximum possible flood-producing meteorological conditions in the Columbia River Basin. 1945.
*No. 19. Preliminary report on depth-duration-frequency characteristics of precipitation over the Muskingum Basin for 1- to 9-week periods. 1945.
*No. 20. An estimate of maximum possible flood-producing meteorological conditions in the Missouri River Basin above Garrison Dam site. 1945.
*No. 21. A hydrometeorological study of the Los Angeles area. 1939.
*No. 21A. Preliminary report on maximum possible precipitation, Los Angeles area, California. 1944.
*No. 21B. Revised report on maximum possible precipitation, Los Angeles area, California. 1945.
*No. 22. An estimate of maximum possible flood-producing meteorological conditions in the Missouri River Basin between Garrison and Fort Randall. 1946.
*No. 23. Generalized estimates of maximum possible precipitation over the United States east of the 105th meridian, for areas of 10, 200, and 500 square miles. 1947.
*No. 24. Maximum possible precipitation over the San Joaquin Basin, Calif. 1947.
*No. 25. Representative 12-hour dewpoints in major United States storms east of the Continental Divide. 1947.
*No. 25A. Representative 12-hour dewpoints in major United States storms east of the Continental Divide. 2d edition. 1949.
*No. 26. Analysis of winds over Lake Okeechobee during tropical storm of August 26–27, 1949. 1951.
*No. 27. Estimate of maximum possible precipitation, Rio Grande Basin, Fort Quitman to Zapata. 1951.
*No. 28. Generalized estimate of maximum possible precipitation over New England and New York. 1952.
*No. 29. Seasonal variation of the standard project storm for areas of 200 and 1,000 square miles east of 105th meridian. 1953.
No. 30. Meteorology of floods at St. Louis. 1953. (Unpublished.)
No. 31. Analysis and synthesis of hurricane wind patterns over Lake Okeechobee, Florida. 1954.
No. 32. Characteristics of United States hurricanes pertinent to levee design for Lake Okeechobee, Florida. 1954.
No. 33. Seasonal variation of the probable maximum precipitation east of the 105th meridian for areas from 10 to 1,000 square miles and durations of 6, 12, 24, and 48 hours. 1956.
No. 34. Meteorology of flood-producing storms in the Mississippi River Basin. 1956.
No. 35. Meteorology of hypothetical flood sequences in the Mississippi River Basin. 1959.
No. 36. Interim report—Probable maximum precipitation in California.
No. 37. Meteorology of hydrologically critical storms in California. 1962.
No. 38. Meteorology of flood-producing storms in the Ohio River Basin. 1961.

---

* Out of print.

HYDROMETEOROLOGICAL REPORT NO. 37

METEOROLOGY OF HYDROLOGICALLY CRITICAL STORMS IN CALIFORNIA

U.S. DEPARTMENT OF COMMERCE
WEATHER BUREAU
Washington
December 1962

TABLE OF CONTENTS

TABLE OF CONTENTS
(Cont'd.)

TABLE OF CONTENTS
(Cont'd.)

FIGURES

FIGURES (Cont'd.)

FIGURES (Cont'd.)

FIGURES (Cont'd.)

Chapter I

PURPOSE, SCOPE AND AUTHORIZATION

Purpose of report

The purpose of this report is to describe the more significant meteorological aspects of hydrologically critical storms in California. Hydrometeorological Report No. 36, "Interim Report - Probable Maximum Precipitation in California" (1), and the present report are companion publications directed to different aspects of the same over-all investigation. This report takes stock of major precipitation storms in the record with emphasis on recent storms not previously reviewed in Hydrometeorological Reports; HMR 36* applies the established storm and climatic characteristics to estimating probable maximum precipitation.

It is timely to review what presently available data reveal about the characteristics of Pacific Coast precipitation storms, aside from the immediate application to probable maximum precipitation estimates, and to lay the groundwork for assimilating new kinds of observations. Paramount among the new channels of information are radar and satellite observations, which give good promise of increasing understanding of the complex nature of meteorological processes in an area where storm data over the contiguous ocean are sparse and where the nature of approaching storms is markedly modified by the effect of terrain.

Scope of report

The second chapter classifies hydrologically critical large-area cool-season storms by synoptic types and describes in some detail the most recent of these storms. Subsequent chapters cover the synoptic aspects and relation to precipitation of the storm components of wind, moisture transport and convergence as well as the effect of topographic lifting on these components. Included in chapter VI is a discussion of intense local storms which do not fall clearly into the classification of chapter II, and have not been previously described in detail in the meteorological literature.

Description of the hydrologically critical storm

In this report the term "hydrologically critical storm" refers in a general way to storms which from the standpoint of precipitation intensity, duration, or area result in high flows on streams. The term "major storm," used to designate storms important from all three standpoints, is the subject of the main body of this report. "Minor storms" are those of lesser duration and/or intensity.

---

*Hydrometeorological Report No. 36 is referred to frequently in the present paper and will be abbreviated "HMR 36."

1. Precipitation characteristics. As a matter of convenience in discussing its causes and characteristics, precipitation is referred to as (1) orographic precipitation, that due to lifting of a flow of air by a mountain barrier and thus of primary importance over most of the area of California, or (2) convergence precipitation, caused by upward motion due to the storm itself. Intensity of orographic precipitation is dependent on the rate of climb of moist air above a topographic barrier. The general flow of moist air approximately normal to the principal barriers is discussed in chapter III. The nature of the terrain of California with wide variations in the steepness and height of slopes, orientation of valleys, and other topographic features results in a wide variation in orographic precipitation. A general discussion of terrain effects is found in chapter IV. Less important features are mentioned elsewhere. Convergence precipitation in major storms is primarily dependent on time and space variation of the wind. Frontal lifting and release of instability are frequently concurrent factors but are also frequently of relatively minor importance. These factors are discussed in chapter V.

2. Hydrologic characteristics. Flood potential of a storm derives not only from the immediate precipitation but also from the antecedent meteorological conditions. Snow accumulation and prior saturation of the soil can substantially augment storm runoff as compared to that which would occur with dry ground and/or little or no snow. Flood potential varies also with man-induced factors such as channel improvements, occupation of flood plain, and reservoir storage capacity and method of operation. Thus appraisal of the magnitude of a storm from the hydrologic standpoint is based on other factors in addition to precipitation. An example of differences in flooding in two central Sierra storms with somewhat comparable precipitation but contrasting antecedent conditions (in December 1884 and December 1955) is discussed in chapter II. This report deals only with the meteorological factors concurrent with the precipitation storm and regards as hydrologically critical any storm which produced outstandingly high precipitation whether significant flooding resulted or not.

Authorization

The authorization of this study is contained in a memorandum from the Office of Chief of Engineers to the Weather Bureau, referred to in the introduction of HMR 36. The Corps of Engineers supported the preparation of this report by the Weather Bureau.

Chapter II

TYPES AND SYNOPTIC FEATURES OF MAJOR CALIFORNIA STORMS

An important feature of the general circulation in many major California winter storms is the predominance of meridional flow at the expense of zonal flow, wherein storm tracks are diverted around, or terminated by, blocking Highs which establish themselves at middle and high latitudes in varying degrees of intensity. Such patterns permit maximum anomalies of some meteorological elements.

The first section of this chapter (2-A) classifies major California storms of this century, and some recent minor ones, on the basis of this feature of blocking and discusses briefly the resulting synoptic patterns as they affect California precipitation. The list of major storms was compiled from those which were unusual from the standpoint of both intensity and duration of precipitation over an extensive area. High intensity precipitation of short duration and/or small area can be described more adequately on other bases, even though in a few instances it is part of a major storm.

Major storms subsequent to 1940 are discussed in 2-B in some detail, with reference to synoptic developments. /The December 1884 and December 1955 storms are compared in 2-C./ Three storms resulting in very heavy rain locally are reviewed in 2-D.

2-A. STORM TYPE CLASSIFICATION

Storms are grouped under three main headings, depending on the longitude, from west to east, respectively, of upstream or downstream blocking patterns which are effective prior to and/or during the course of the storm. This in turn determines the latitude of approach of the storms toward the coast, as follows:

Low-latitude type. Blocking in mid-Pacific between longitude 160W and 180W, or about the longitude of the eastern Aleutians. Storms reach the coast from a low latitude under the block. This is primarily a type for precipitation in the northern half of California.

High-latitude type. Blocking in the eastern Pacific east of longitude 160W. Storms reach California from a high latitude near the coast. This is mainly a storm type for the southern half of California.

The latitude at which blocking is least effective in these two types is referred to as the latitude of breakthrough of surface fronts.

Mid-latitude type. Low pressure in the central and eastern Pacific, with varying degrees of blocking over western North America, as storms move

across the Pacific at middle latitudes. Their direction of approach as they near the coast is influenced by both the general offshore circulation and the effectiveness of the continental block. Three directions of approach serve in a general way to subdivide this type, namely, south, southwest, and west. This type includes both Northern and Southern California storms in about the same number.

Charts are shown for each subtype of the three main types (figures 2-1 through 2-11), illustrating the tracks of surface Lows (solid lines) and location of ridges and blocking Highs (long dashed lines), along with a sketch of one or more positions of surface fronts during the storm (short dashed lines).

2-A-1. Low-latitude type storms

This type involves blocking at the longitude of the eastern Aleutians, or between longitude 160W and 180W. A feature common to all Low-latitude type storms is a wave chain extending toward the coast from the Hawaiian Islands, usually the result of a breakthrough under the mid-Pacific block. There may or may not be a following breakthrough at high latitudes, a basis for subdivision of the type. Storms of this type affecting California are with rare exceptions centered in the northern two-thirds of the State. They are characterized by strong gradients in a southwest flow of moist stable air from a rather distant low-latitude source, with a minimum of interruption by intrusion of air from a more northerly source.

Complete blocking at high latitudes. A Low of varying intensity and position occupies the southern Gulf of Alaska during the storm (figure 2-1). It is maintained by cold outbreaks from the interior of Alaska and is surrounded by an intense crescent-shaped High centered over Alaska and extending both southward from the eastern Aleutians over the ocean and southeastward into the central United States. The storm track from the western Pacific is diverted under this mid-Pacific block so that it reaches a point a little north of the Hawaiian Islands before swinging toward higher latitudes, on its way to the California coast.

The storm may be initiated in one of two ways. At the beginning of the storm, the first wave on a wave chain oriented northeast-southwest may reach the coast after passing under the block at a low latitude, as in the January 1906 storm. Or, as on December 20, 1955, completion of the wave chain may depend upon a southwestward extension from the coast toward the region of breakthrough north of Honolulu of a frontal boundary the origin of which is a cold surge from the interior of Alaska. In either case, waves move along the frontal boundary to the south of the Alaskan Gulf Low and approach the coast usually only partially occluded, so that just south of the wave chain a strong persistent flow of moist stable air from a low latitude is established. In this flow, convergence precipitation due to inertial effects contributes significantly to rainfall totals. The duration of this arrangement depends on the maintenance and stability of position of the Gulf Low, as well as the block to the west. Usually termination follows a partial filling and southeastward shift of the Gulf Low so as to allow the wave chain to move southeastward across the storm area.

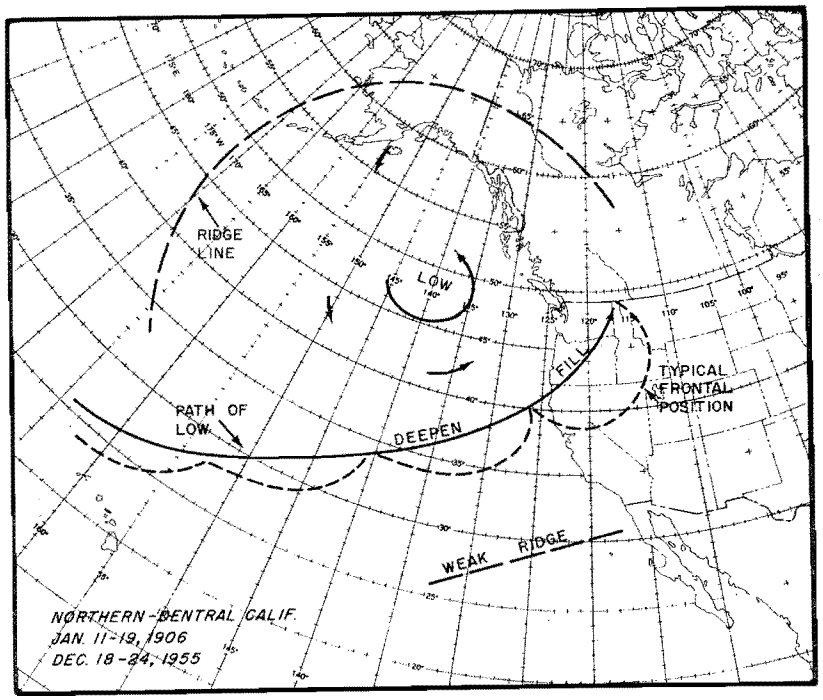

Fig. 2-1. LOW-LATITUDE TYPE, WITH BLOCKING AT HIGH LATITUDES. Solid lines, typical paths of Lows; short dashed lines, typical frontal positions; long dashed lines, typical orientation of ridges of high pressure. Dates of storms of this type listed on corner of figure.

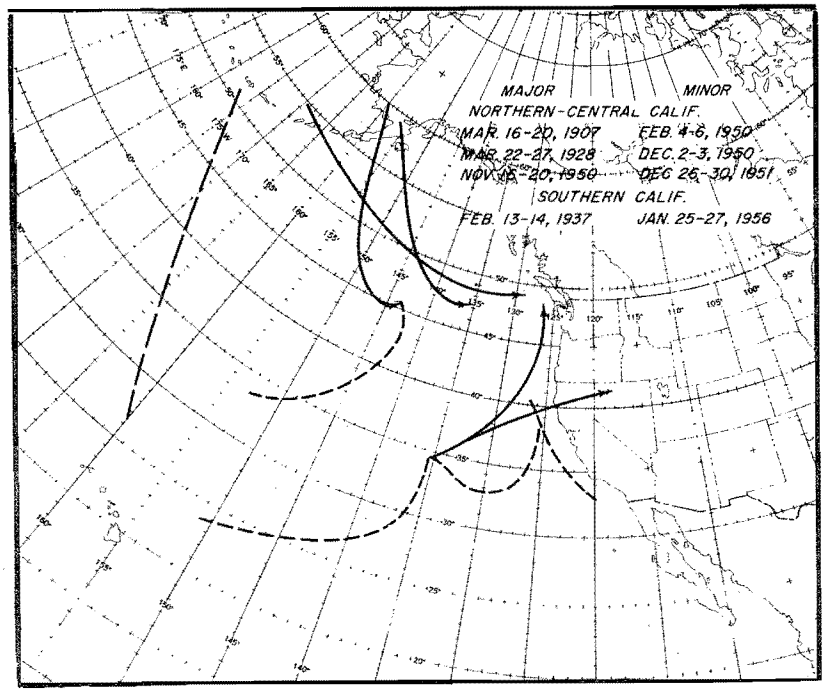

Fig. 2-2. LOW-LATITUDE TYPE, WITH BREAKTHROUGH AT HIGH LATITUDES. For legend see figure 2-1.

Breakthrough at high latitudes. This type is essentially the same as described above except that breakthrough shifts from a low to a high latitude (figure 2-2). At the beginning of the storm, the wave chain extends northeastward from near Hawaii to the coast. West of Hawaii the chain has already been terminated by southward shift of the block. The high latitude portion of the block is weak enough at that time so that fronts may pass through it across western Alaska or the eastern Aleutians and enter the Gulf of Alaska, where deepening and a varying amount of stagnation of the center occurs.

Variation in position and orientation of the track of the high latitude breakthrough and later movement of the Gulf Low affects the relation between this Low and the wave chain to the south, giving considerable variation in the later phases of the storm sequence both in duration and manner of termination. A more nearly west-to-east track will result in a minimum of stagnation and tend to shift the center of activity into British Columbia, Washington, and Oregon, with ridging offshore. A more north-south orientation, if too far to the west, will permit ridging northward over California. If it is farther east so as to maintain a trough near the coast, waves may continue to form but not deepen intensely. The January 25-27, 1956 minor storm was centered over Southern California by a southeastward displacement of the main features of this type.

In most instances, the formation of the initial wave chain was the result of a low-latitude breakthrough, as described above. In one exception, the November 1950 storm, a stagnant Low near Honolulu took the place of the low-latitude breakthrough; this Low was drawn northeastward toward an elongated front that had originated as a cold surge into the Gulf of Alaska and that extended southwestward from the coast, as described in the December 1955 storm. The resulting circulation brought a flow of tropical air into Central California from east of Honolulu that was stable and very moist, especially at upper levels.

2-A-2. High-latitude type storms

The heading suggests the initial latitude of approach. The longitude of the Pacific block in this type is east of longitude 160W, thus placing the point of origin of storms close to the Pacific Coast of North America. Low centers form off the British Columbia or Washington coasts as cyclogenesis within a crescent-shaped block.

High-latitude type storms, with few exceptions, cause heaviest precipitation in Southern California, a reflection of the limitations imposed upon the Low tracks by the blocking pattern and upon moisture in air that is of recent polar origin at higher latitudes.

No breakthrough - NNW-SSE orientation. The title of the type suggests the approximate orientation of the trajectory of the Low; southward along the coast, then toward the east or northeast (figure 2-3). The storm is preceded by a fast-moving storm from the northwest into the southern Great Basin

Plateau, leaving a residual Low center off the Washington coast. Intensification of the ridge to the west and northwest of this Low completes the block prior to the main storm and forms a crescent-shaped High around it. The Low moves southward and deepens off the Central California coast (to about 1000-mb in the 1916 storms), then moves inland and recurves toward the northeast as limitations to its movement are imposed by the nearly stationary High around it. Offshore deepening on the trailing cold front extends the trough southward and delays passage of the cold front and the shift to west winds across Southern California. As the deepening Low center moves inland, the flow from the south and southwest into Central and Southern California becomes very strong, although because of the limited trajectory of the air moisture is not as high as in most Mid-latitude type storms. Duration of heavy rain in these storms is limited to this period, about 1 day.

No breakthrough - north-south orientation. The pattern is similar to the preceding one except that the orientation of the crescent-shaped ridge requires a north-south track of the Lows along the coast, followed by a reversal in direction toward north. For Southern California storms, the latitude of reversal is that of Northern California (figure 2-4). For storms centered in Northern California, the pattern described above is displaced northward so that reversal in direction of the offshore Low occurs off the Washington coast (figure 2-5).

Most features of this type are common to both Northern and Southern California. The southward extension of the offshore trough permits waves to move north-northeastward toward the coast, prolonging the southerly flow. The convergence component of rain due to these waves is an important part of the total. In both the December 1921 and January 1911 storms, the storm began with a trapped Low emerging from the southwest as pressure fell to the north.

The above description applies to the main part of the December 18-27, 1921 storm, that is, through the 22d. The remaining period involved a sequence with a more nearly NNE-SSW orientation. The offshore trough had moved through Southern California on the 22d, with the Low stagnant off the Oregon coast. A weak surge of colder air from the Aleutians (a temporary weakening of the block there) entered the back side of the stagnant Low and swung around toward the coast. When the surface front of this surge had reached the coast, with a northeast-southwest orientation offshore, waves forming on it resulted in small but deep Lows reaching the Central California coast from the southwest on the 25th and 26th, but quickly filling after moving inland.

Mid-latitude breakthrough. This type, if it affects the entire state, causes heaviest rain in the southern part. It involves air masses of great temperature contrast and results in formation of deep Lows at the coast with extremely high surface pressure gradients (figure 2-6). The area of activity gradually shifts southward.

Initially a deepening Low moves down the British Columbia coast and southeastward into Washington. But by this time a weakening of the Pacific

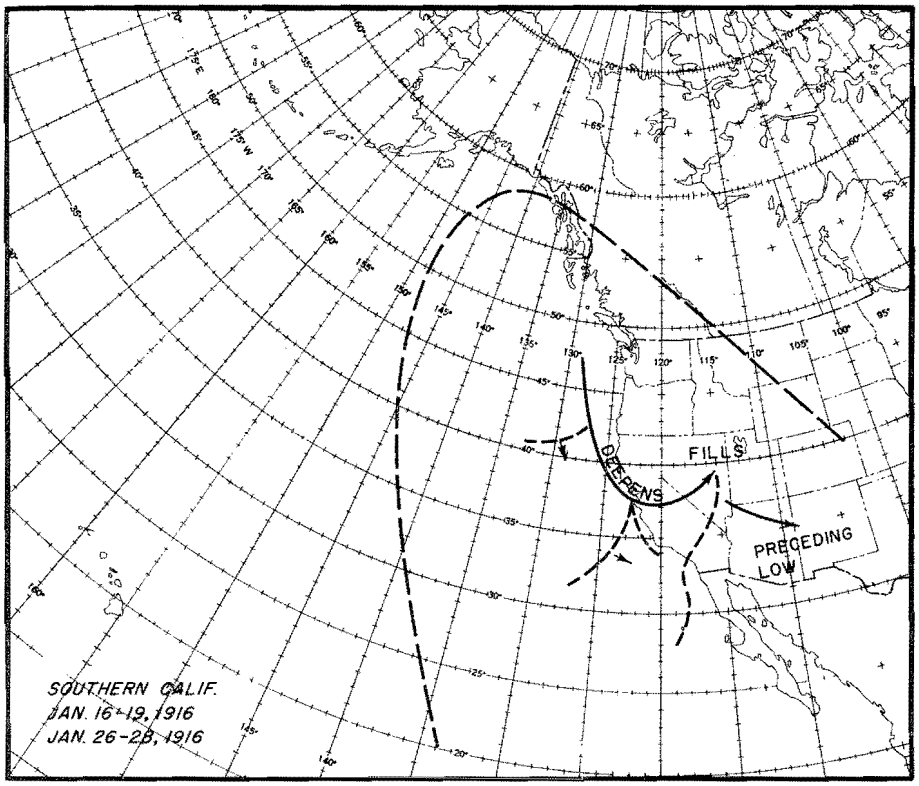

Fig. 2-3. HIGH-LATITUDE TYPE, NO BREAKTHROUGH. NNW-SSE ORIENTATION. For legend see figure 2-1.

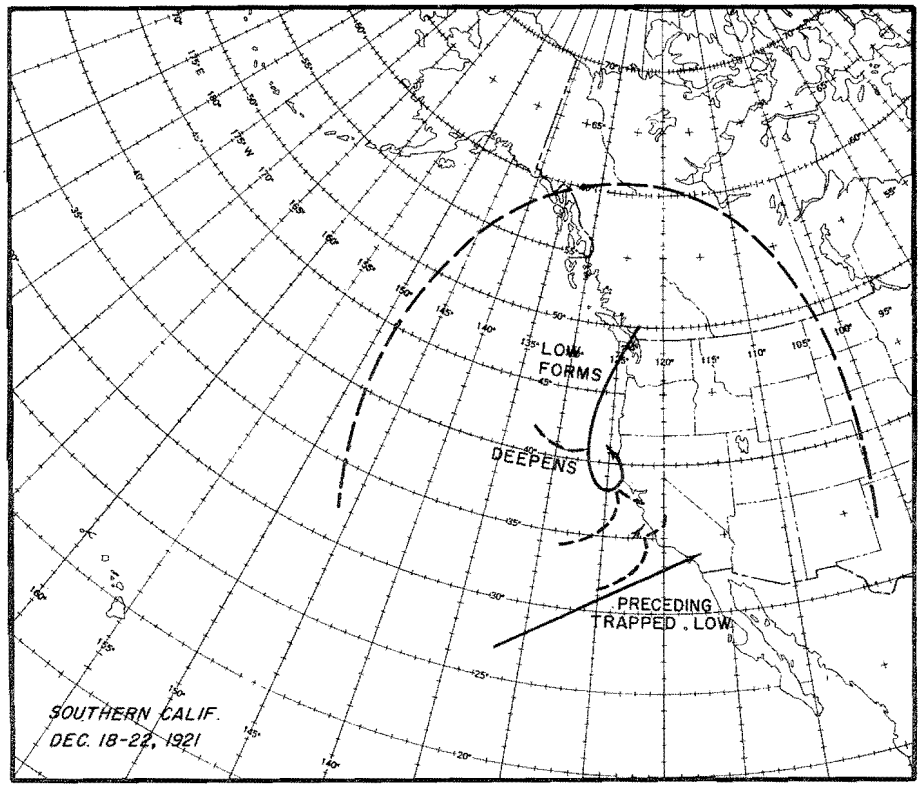

Fig. 2-4. HIGH-LATITUDE TYPE, NO BREAKTHROUGH. NORTH-SOUTH ORIENTATION. SOUTHERN CALIFORNIA. For legend see figure 2-1.

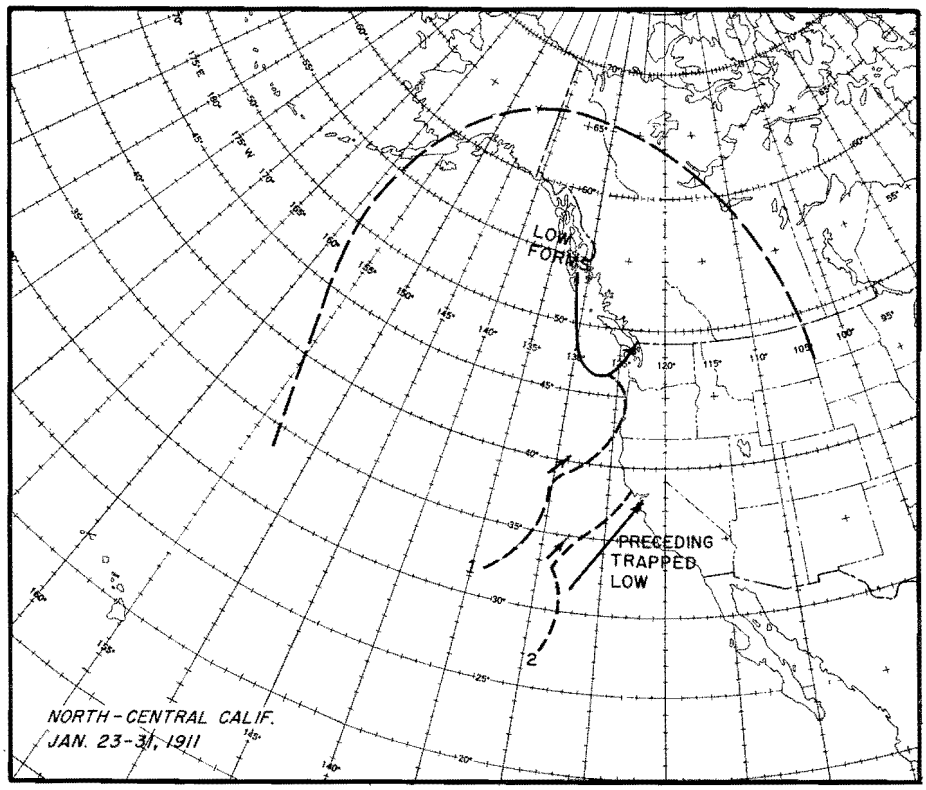

Fig. 2-5. HIGH-LATITUDE TYPE, NO BREAKTHROUGH. NORTH-SOUTH ORIENTATION. NORTHERN CALIFORNIA. For legend see figure 2-1.

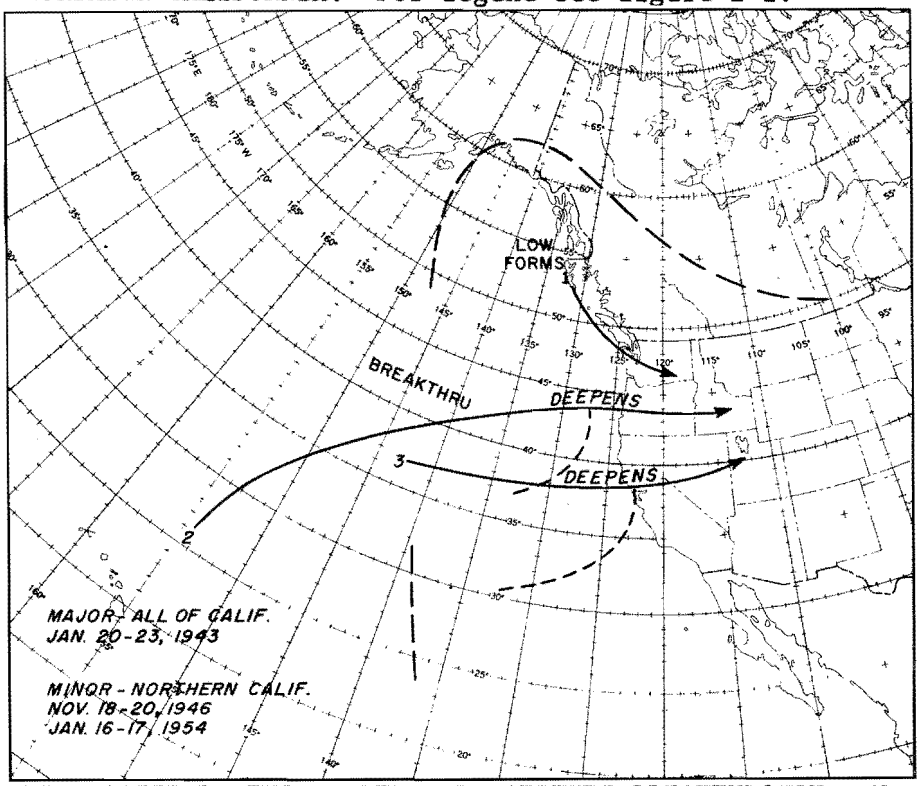

Fig. 2-6. HIGH-LATITUDE TYPE, WITH MID-LATITUDE BREAKTHROUGH. Numbers refer to sequence of Lows. For legend see figure 2-1.

block has permitted a mid-latitude breakthrough of a weak Pacific storm from west or southwest. As it moves toward the coast, rapid deepening occurs when cold Arctic air flowing southwestward off the Washington coast enters its circulation. The center moves rapidly eastward, followed by a southward shift of cold air to its rear.

The depth of centers as they reach the coast, as well as their latitude and number, influences the rainfall distribution. In the January 1943 storm, the first Pacific breakthrough involved warm air in a Low which had moved northward from near Honolulu on the back side of the block prior to eastward movement (figure 2-23a). Because of the great contrast between this air and the cold air flowing off the coast of British Columbia, the storm center became so deep at the coast that, although it entered in Oregon, strong pressure gradient extended southward through Southern California. The second Low center entered near San Francisco about 36 hours later, with strong gradients and moderately high dew points in Central and Southern California. It prolonged the storm to nearly 3 days' duration.

The convergence mechanisms in such a storm are intense as a result of deep Low centers moving across the area, strong winds in changing pressure fields with which they are not in balance, and marked frontal effects.

2-A-3. Mid-latitude type storms

The broad-scale circulation during these storms is more nearly zonal than in the other types. Blocking in the Pacific is replaced by areas of low pressure. The three directions that title the subheadings of this type suggest, in a general way, the direction of approach of Lows just offshore and the average direction from which the flow enters California as storms cross the Pacific from a westerly direction at middle latitudes. The blocking effect of a continental High is greatest with the Southerly subtype and least with the Westerly, a zonal type. Anomalies in moisture decrease in the same manner.

Southerly. Deep Lows crossing the eastern Pacific at middle latitudes, or forming there, are diverted northward some distance offshore by the continental block (figures 2-7 and 2-8). This maintains a very high pressure gradient along the coast. The high values of surface dew point result from an air trajectory from south-southwest from a low latitude at high speeds. Only after the final front passes inland is this warm flow cut off, since prior to this time it has either entered directly as tropical air or has been modified by lengthy flow at a low latitude so as to be almost indistinguishable from tropical air. Frontal systems reaching the coast prior to the final one have rapidly undergone frontolysis.

Southwesterly. This is the most common storm type, both in Northern and Southern California.

1. Northern California. The depth and position of the center of the offshore circulation is influenced by successive occluding Lows from the

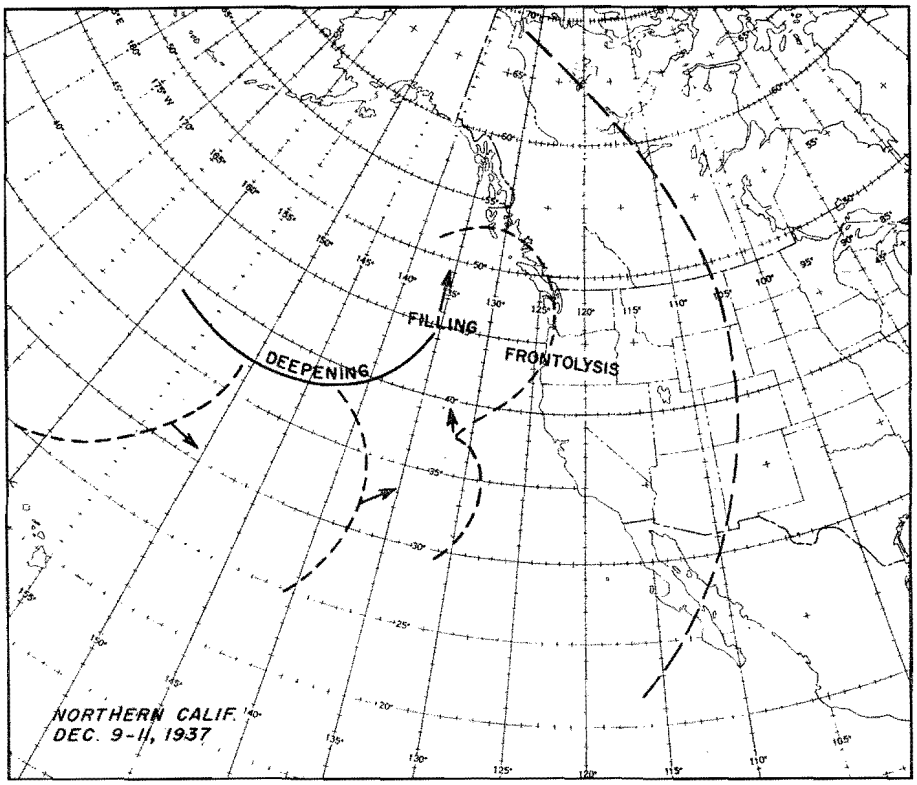

Fig. 2-7. MID-LATITUDE SOUTHERLY TYPE. NORTHERN CALIFORNIA. For legend see figure 2-1.

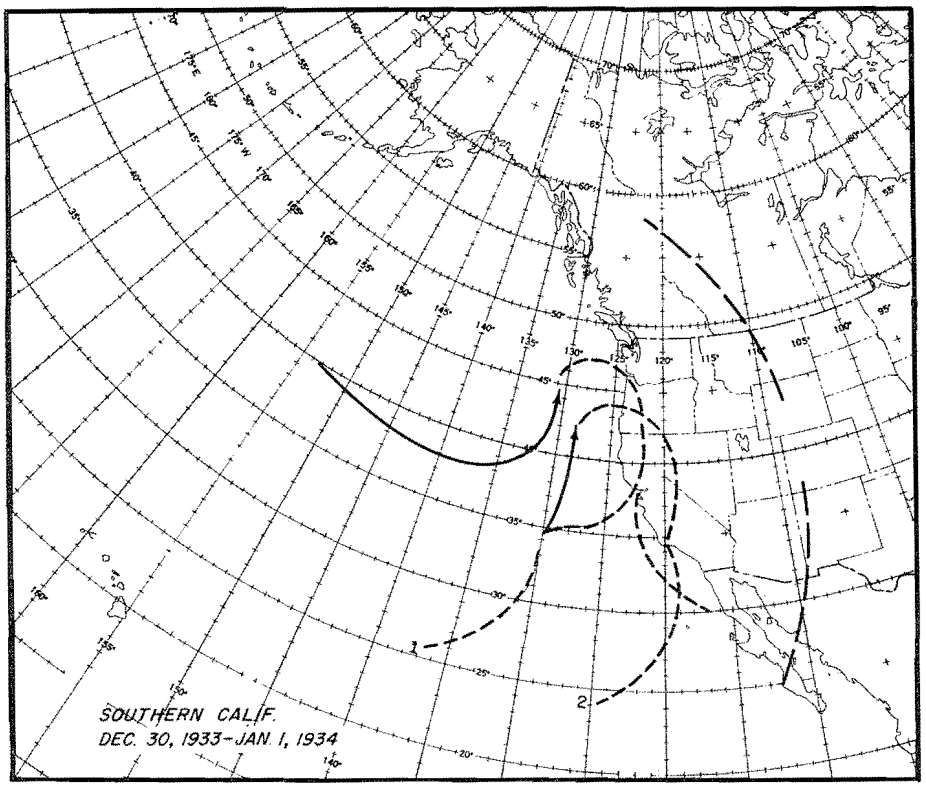

Fig. 2-8. MID-LATITUDE SOUTHERLY TYPE. SOUTHERN CALIFORNIA. Numbers refer to sequence of Lows. For legend see figure 2-1.

west that deepen on entering the eastern Pacific but tend to rotate around a mean offshore position as the occluded fronts enter the coast from the southwest and impinge against the continental High (figure 2-9). The frequency and orientation of the occlusions is such that there is only brief decrease in strength of flow between them. The long trajectory of polar air at low latitudes prior to reaching the coast provides modification to the point that its characteristics approach those of tropical air, although not to the extent of the Southerly type. Tropical air appears to be involved only rarely, and then quite briefly in connection with the warm sector of a wave development.

In the February 1940 storm, waves formed on the polar front closer to the coast than indicated in figure 2-9, and were less completely occluded at the coast than in other storms. In the January 1909 storm, Low centers formed at a lower latitude than indicated in figure 2-9, as a result of extension of the Alaskan High southward from the Aleutians, and later deepened in the southern Gulf of Alaska.

2. Southern California. Four storms of this type, each of which produced a prolonged southwest flow of moist air over Southern California, are described (figures 2-10a, 2-10b, and 2-10c). Their common characteristic was a southeastward shift of the long-wave trough close to the coast as compared to its position in Northern California storms of this type.

February 13-16, 1927 and February 28-March 3, 1938. With a deep semi-stationary Low in the southern Gulf of Alaska, a chain of occluding waves passed around its southern periphery at a fairly low latitude before approaching the coast (figure 2-10a). The blocking continental High was well to the north, permitting a breakthrough of these storms south of it, across Southern California and into the southern Plateau.

April 4-8, 1926. A strong ridge was present in the central Pacific. Weak storm centers crossed this ridge at middle latitudes, deepened as they moved southeastward to a low latitude in the eastern Pacific where they recurved to the northeast and entered the Central California coast at approximately 24-hour intervals as completely occluded fronts (figure 2-10b).

February 17-21, 1914. A storm center, crossing to the north of a similar mid-Pacific ridge, stagnated and filled in the Gulf of Alaska, but a new storm center forming on the southward trailing front at a low latitude, set up a southwest-northeast wave chain into Central California and a persistent moist flow into Southern California (figure 2-10c).

Westerly: Northern California. This is a strong zonal type involving relatively minor storms (figure 2-11). The Pacific High is well developed in mid-Pacific. Storms passing out of a long-wave trough farther west speed north of this ridge toward southeast into an offshore long-wave trough, and intensify off the Washington-Oregon coast. Frontal systems leave the main Low offshore and pass eastward across all of California, followed by a weak surface ridge of high pressure. The time interval between storms is 24 to 36 hours.

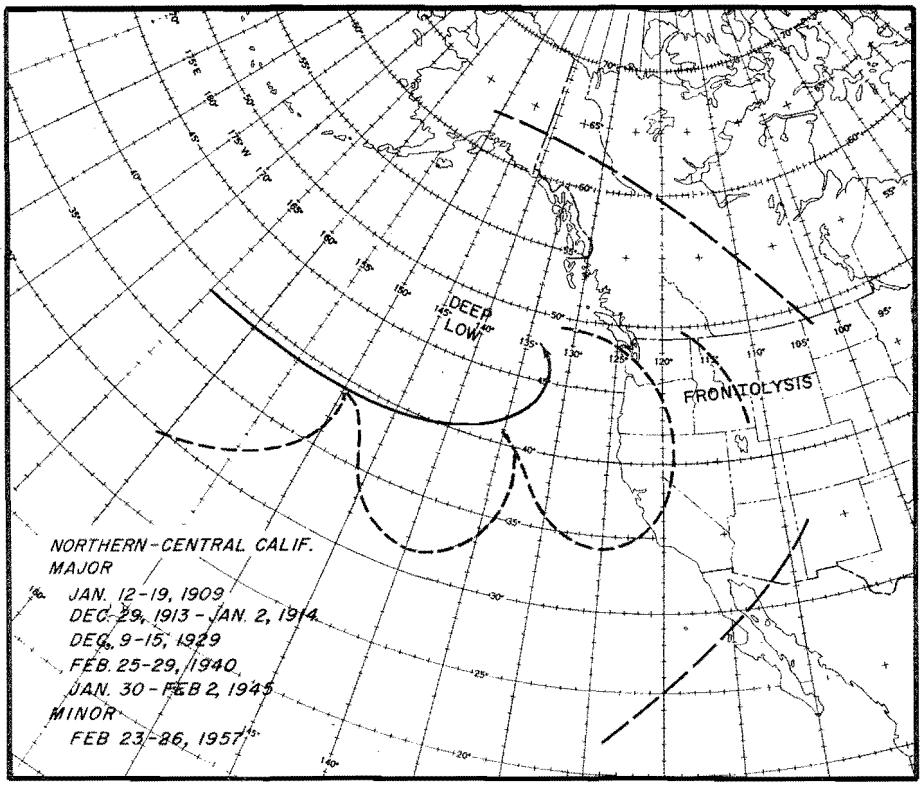

Fig. 2-9. MID-LATITUDE SOUTHWESTERLY TYPE. NORTHERN-CENTRAL CALIFORNIA. For legend see figure 2-1.

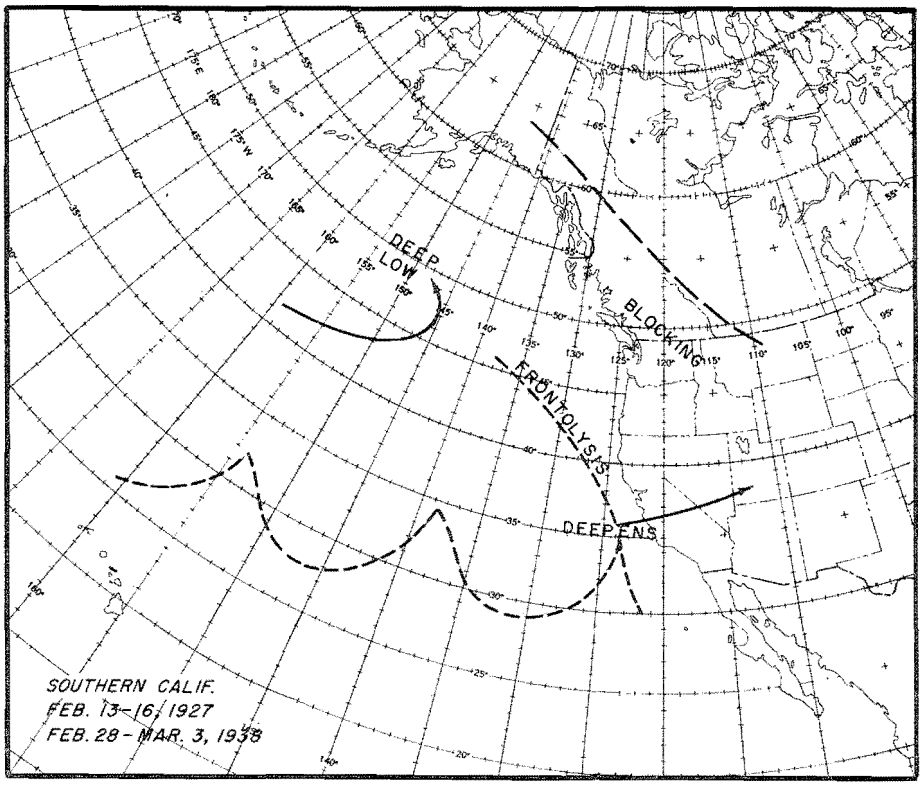

Fig. 2-10a. MID-LATITUDE SOUTHWESTERLY TYPE. SOUTHERN CALIFORNIA. For legend see figure 2-1.

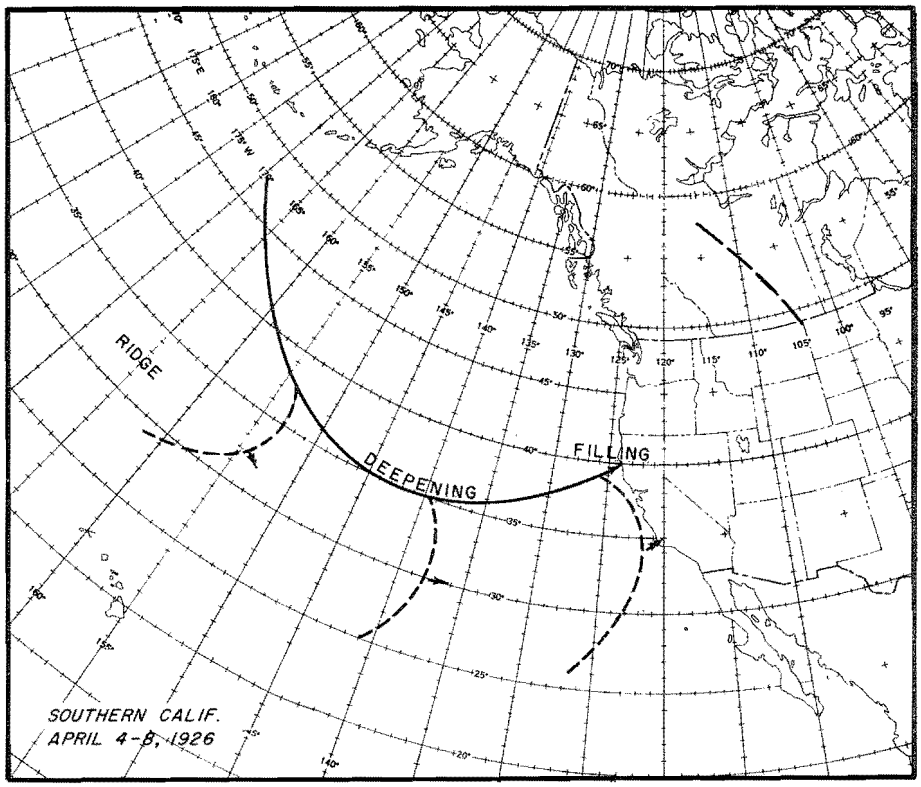

Fig. 2-10b. MID-LATITUDE SOUTHWESTERLY TYPE. SOUTHERN CALIFORNIA. For legend see figure 2-1.

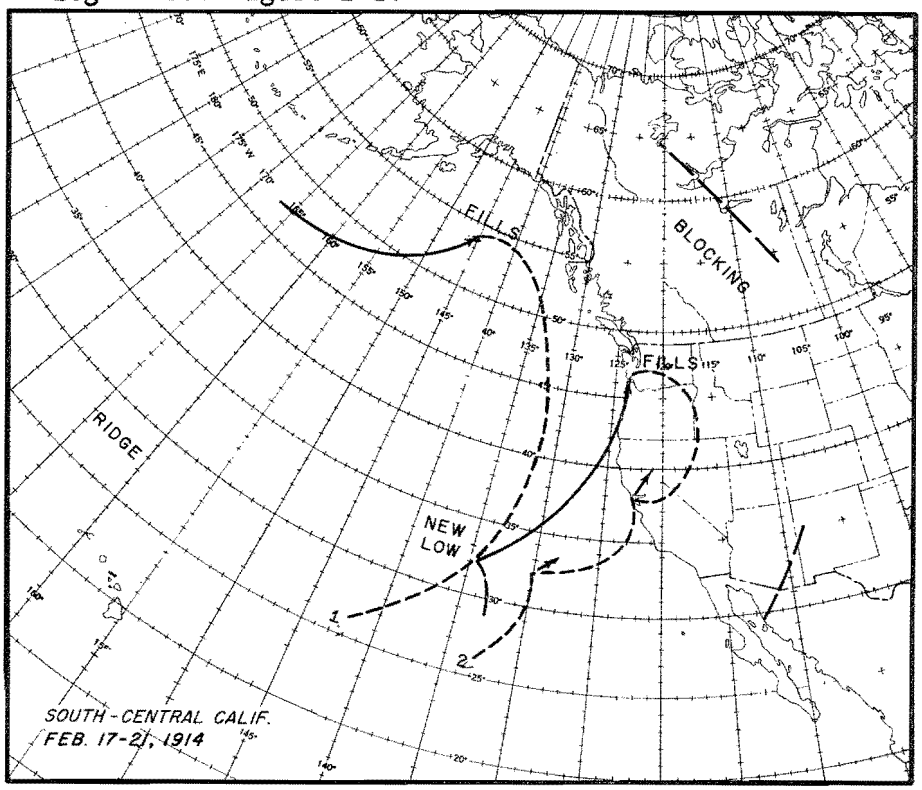

Fig. 2-10c. MID-LATITUDE SOUTHWESTERLY TYPE. SOUTHERN AND CENTRAL CALIFORNIA. For legend see figure 2-1.

Wind directions are nearly due west, except southerly a short time in advance of a frontal system. Pressure gradients are very strong near the frontal systems. The air is relatively unstable in lower layers and cold at all levels, since the trajectory and rate of movement is such that the polar air does not attain near the complete modification of the Southerly and Southwest subtypes.

This type causes heavy snowfall accumulations in mountain areas over a period of time and a low snow line. Heavy rainfall totals may occur at low levels if the storm is of long duration (March 29-April 4, 1958). Frontal rain at lower levels is a significant part of the total and, because of convective instability, local short-period intensity may be very high; but the intermittent nature of the rain controls runoff on major streams.

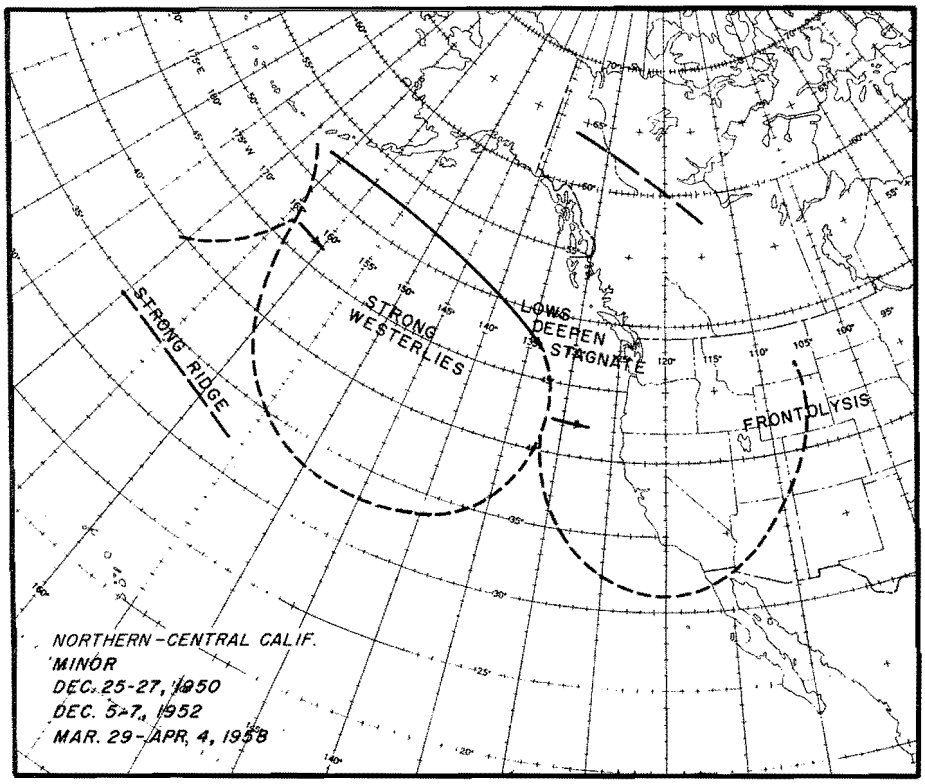

Fig. 2-11. MID-LATITUDE WESTERLY TYPE. For legend see figure 2-1.

2-B. SYNOPTIC HISTORY OF RECENT MAJOR STORMS

The synoptic history of several recent major storms is discussed. Description of various storms prior to 1943 is contained in Hydrometeorological Report No. 3 (2) for Northern California, and Hydrometeorological Report No. 21B (3) for Southern California.

2-B-1. The December 1955 Low-latitude type storm

This storm ranks high among known storms in Northern and Central California from the standpoints of large areal extent, duration and intensity of precipitation. This is evident in precipitation records and more dramatically in streamflow records. Most streams listed in table 2-1 set new peak flow records, some by wide margins; this list includes larger streams on the coast from Monterey Bay northward and all larger Sierra streams.

Emphasis in the following discussion of the storm is on depth and track of the surface Lows associated with the frontal boundary extending from a low latitude over the Pacific to the coast and their relation to the position and strength of the moist flow over Northern and Central California, which was largely responsible for periods of heavy precipitation and high streamflow. Also emphasized is the role of the Lows in the southern Gulf of Alaska in bringing cold air southward toward the tropical flow to develop or deepen waves on the frontal boundary, as well as to maintain a broad offshore trough extending to low latitudes and a strong onshore flow over Northern California. The upper-air circulation in this storm was a reflection of that near the surface except for brief periods when the surface flow became light. The upper-air Gulf of Alaska Low was somewhat more extensive and the mid-Pacific ridge somewhat narrower than the surface portions of these features.

Conditions prior to the storm were favorable to high streamflow with considerable snow accumulation above 4500 feet in the northern Sierras and 6500 feet in the southern Sierras from previous storms.

The storm was split into two periods--prior to and following the 20th, a day when precipitation was generally light while the frontal boundary from the coast to low latitudes was being re-established. The second period was by far the more important. See figure A-6 in Appendix for 24-hour isohyets.

December 17-19. The initial frontal system of the storm and associated Low, labeled (1) in figure 2-12, moved slowly south of the mid-Pacific block on the 14th to the 16th, then rapidly to the coast by the morning of the 18th and northward off the Washington coast. This Low was followed closely by an occluding wave, (2) in figure 2-12, forming on the trailing front not far offshore (figure 2-13a). Another wave forming on the trailing front (in figure 2-13a and later) occluded along the Northern California coast and weakened rapidly as it moved inland near midday of the 19th (figure 2-13b).

Precipitation in this part of the storm was confined mainly to Northern California and the Central California coast north of Monterey. Only moderate on the 17th, it was more or less heavy from late on the 18th with approach of the second frontal system until after passage of the third during the 19th. This period is labeled (1) on the 6-hourly hyetographs for selected coastal mountain and Sierra stations (figure 2-15). Some stations show a peak with each frontal system.

The first of the Gulf of Alaska Lows, (A) in figure 2-12, experienced intense cyclogenesis over the northern Gulf of Alaska on the 17th, as a cold outbreak of air across northern Siberia and western Alaska encountered the warmer Pacific water. Moving rapidly southward by the 18th, this Low stagnated about 800 miles west of Seattle for nearly 2 days, recurved northward and slowly filled. Its circulation kept the Low centers (1) and (2) in figure 2-12 and the following wave small in area and on a counterclockwise track around its periphery. It maintained a strong southwest flow over Northern California on the 20th following the first storm period. More important, as it took on a northeast-southwest orientation on the 20th, it provided a broad offshore trough (figure 2-13c) to facilitate entry of low-latitude Lows into the eastern Pacific and to establish a deep flow of moist air from near the Hawaiian Islands to the Northern California coast, not present to the same degree on the 19th.

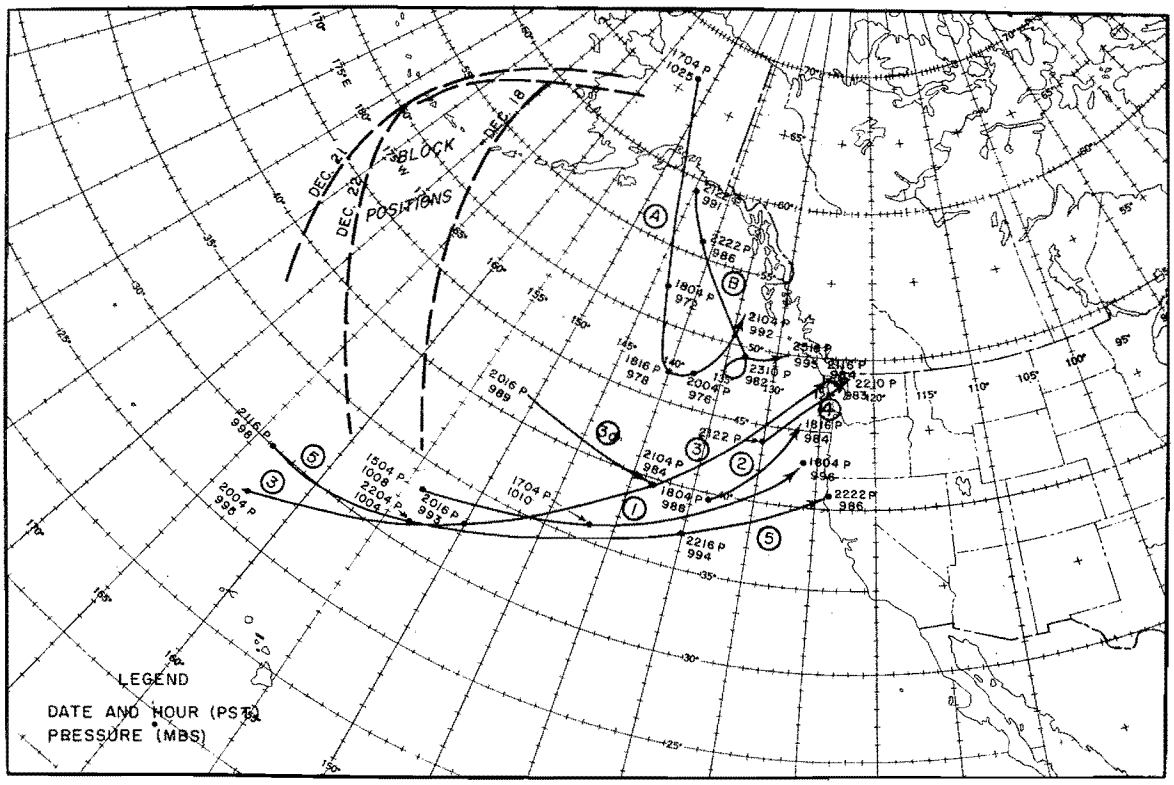

Fig. 2-12. TRACKS OF SURFACE LOWS IN THE DECEMBER 1955 STORM

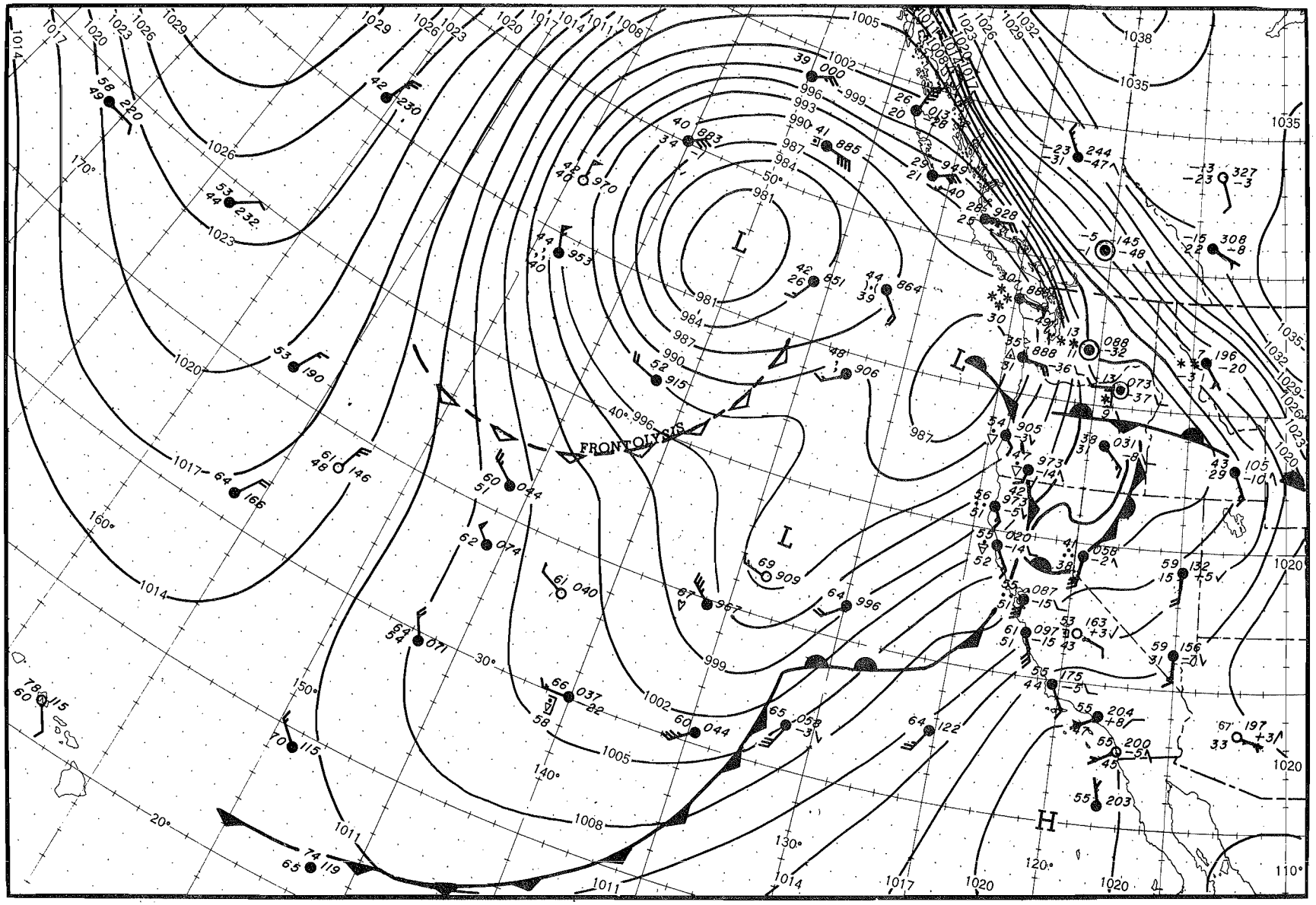

Fig. 2-13a. SEA LEVEL CHART, 1630 PST, DECEMBER 18, 1955

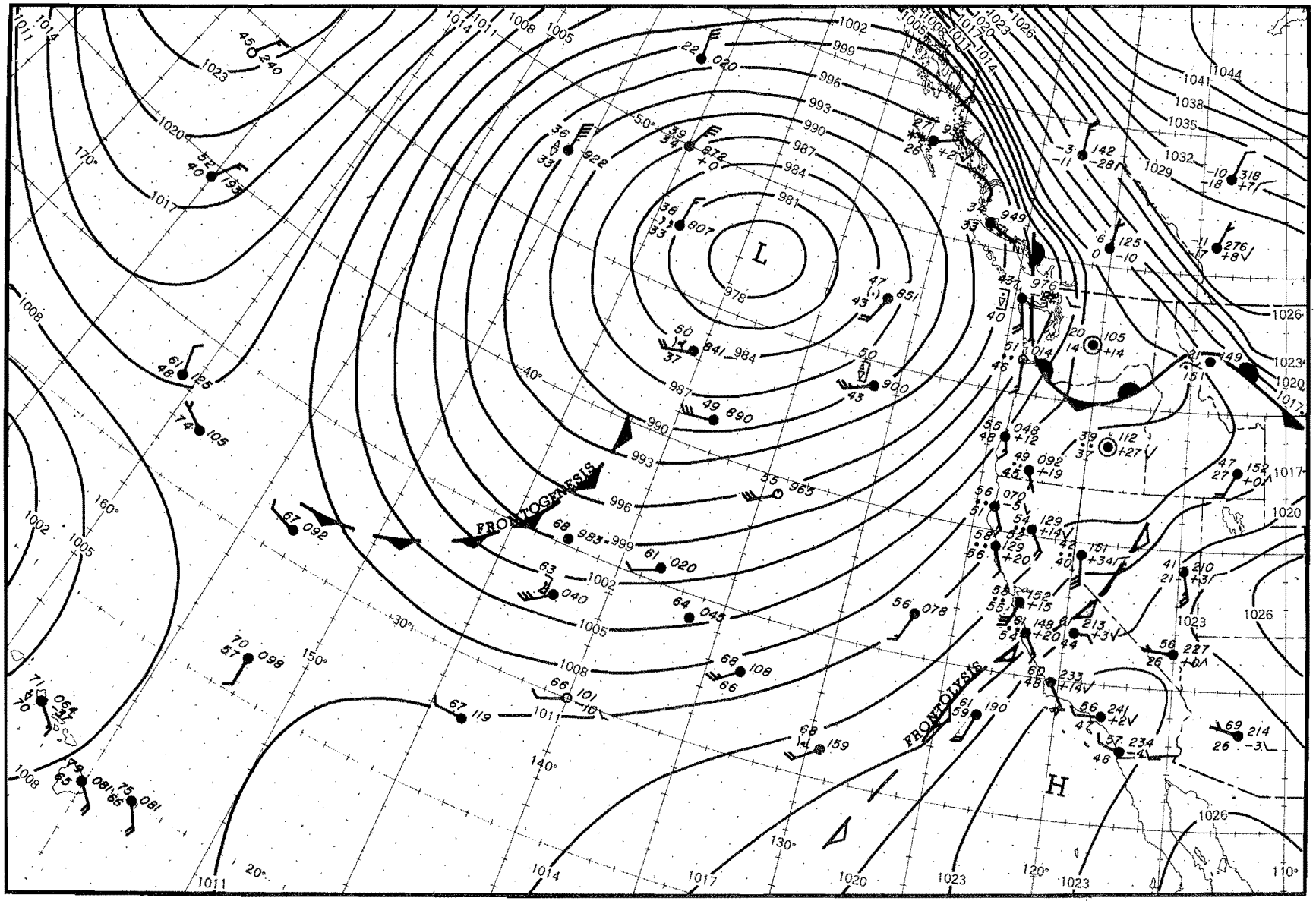

Fig. 2-13b. SEA LEVEL CHART, 1630 PST, DECEMBER 19, 1955

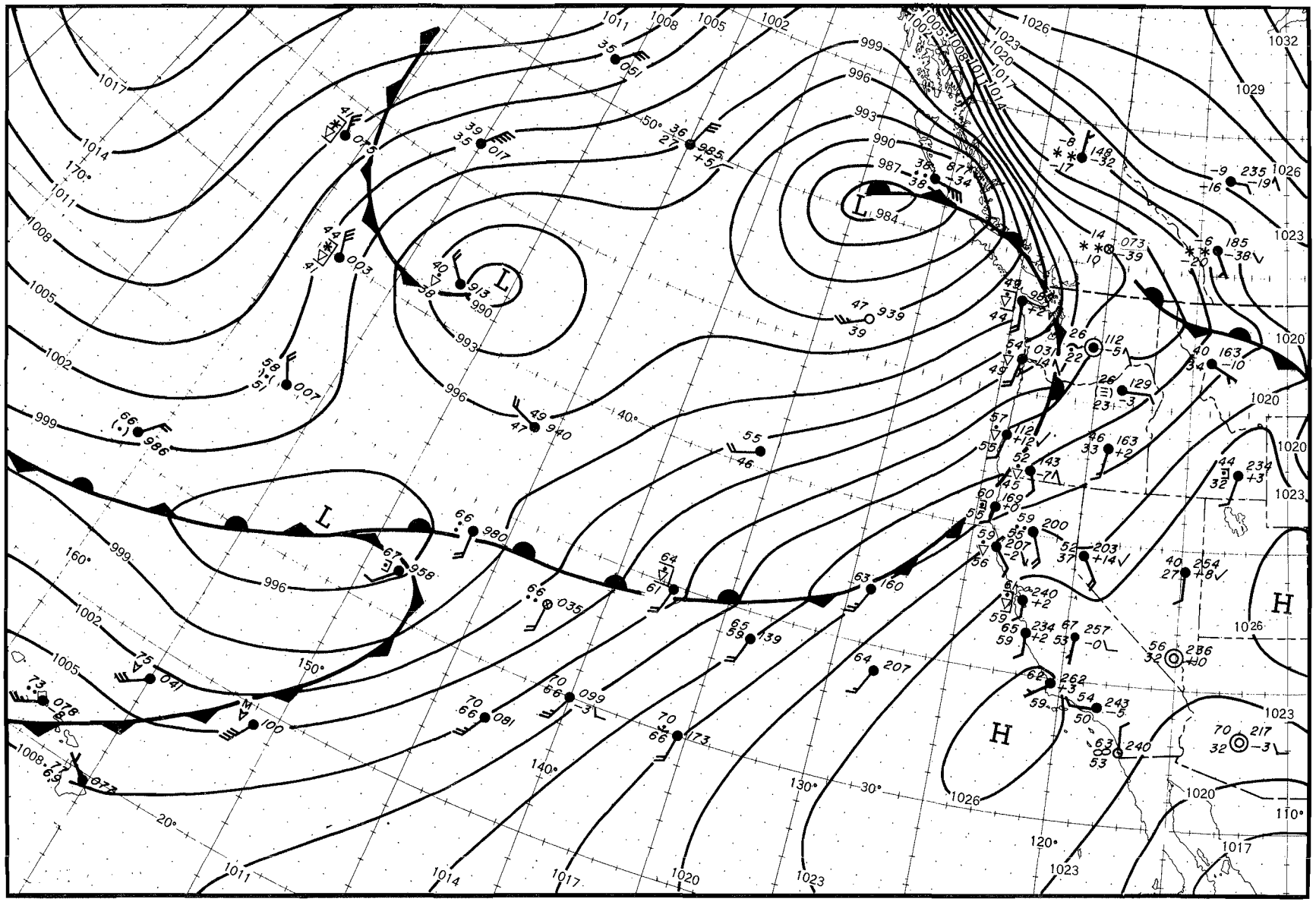

Fig. 2-13c. SEA LEVEL CHART, 1630 PST, DECEMBER 20, 1955

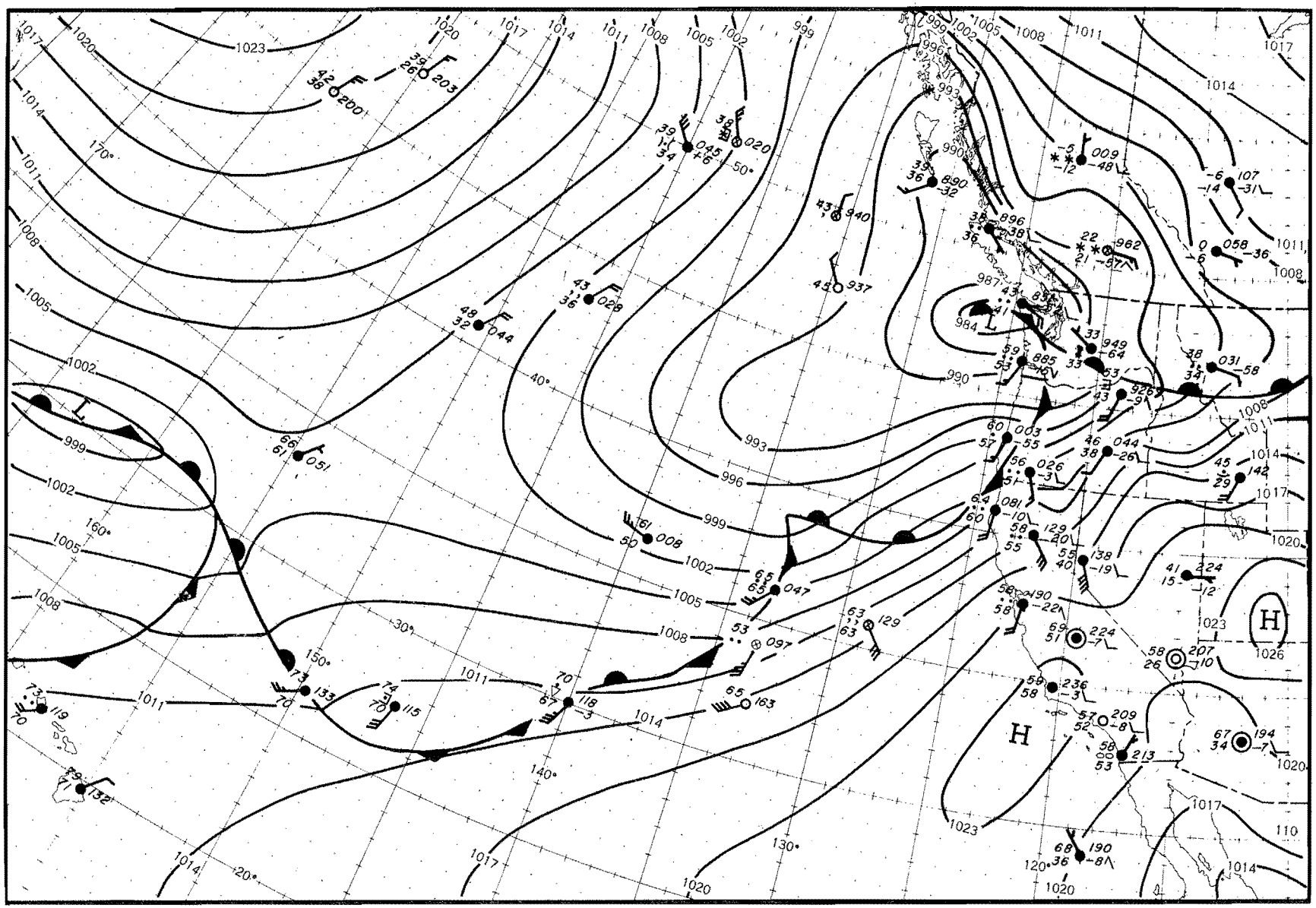

Fig. 2-13d. SEA LEVEL CHART, 1630 PST, DECEMBER 21, 1955

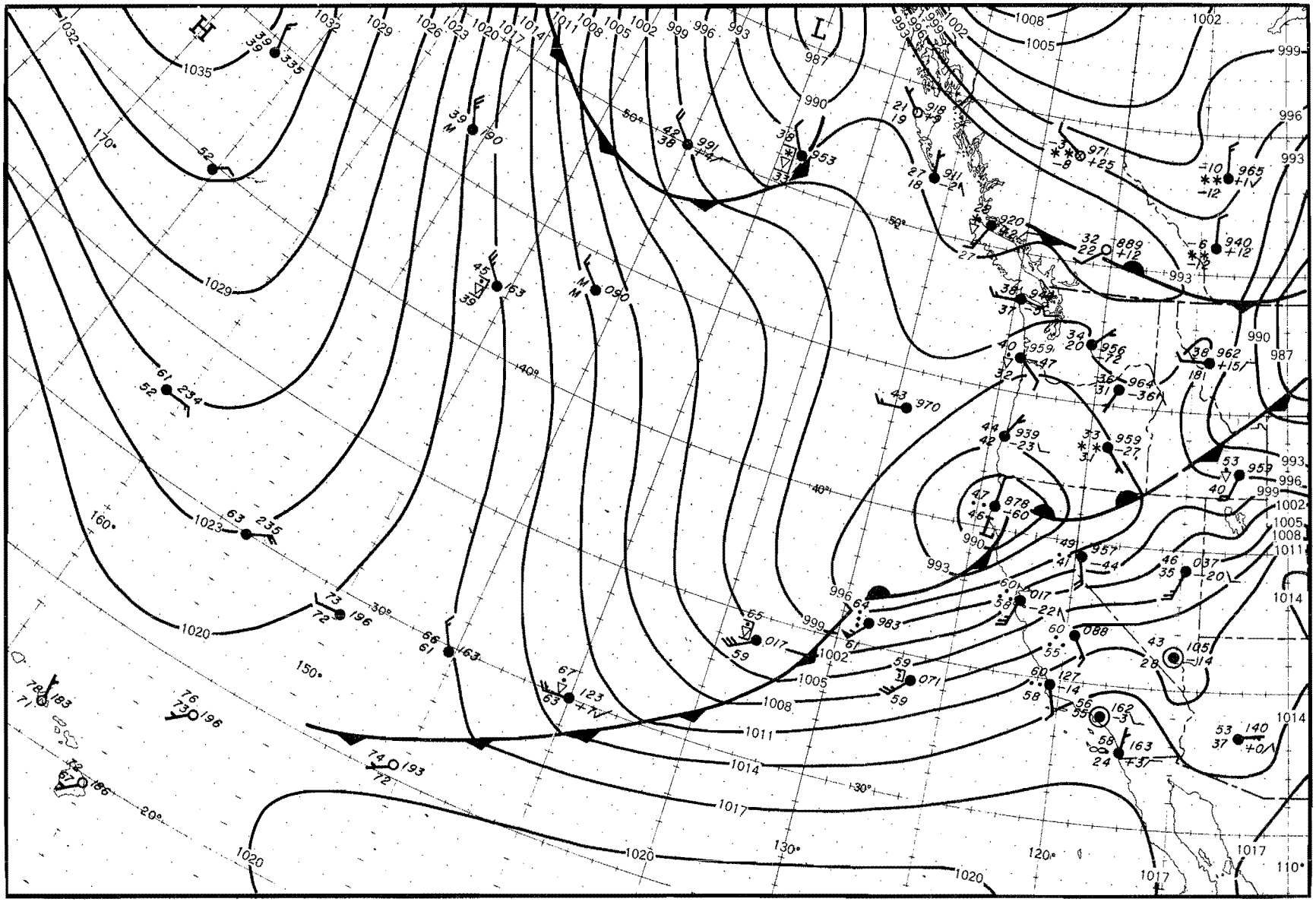

Fig. 2-13e. SEA LEVEL CHART, 2230 PST, DECEMBER 22, 1955

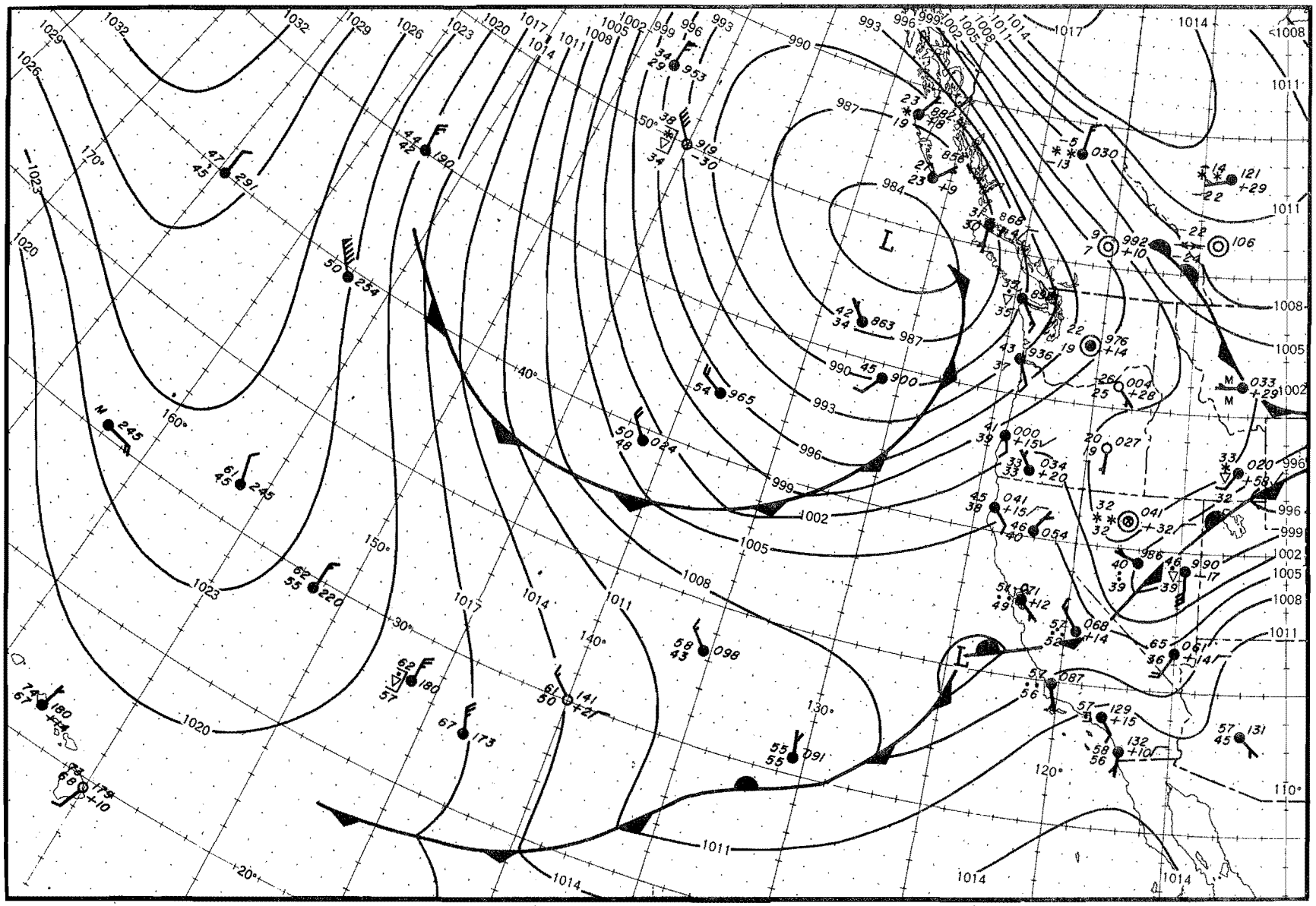

Fig. 2-13f. SEA LEVEL CHART, 2230 PST, DECEMBER 23, 1955

December 21-24. By the evening of the 20th the offshore frontal boundary extending from the coast south of the mid-Pacific block into the western Pacific (partially shown at left edge of figure 2-13c) was re-established when the southwest extension of a cold front, which had rotated around the Gulf Low to the Washington coast, joined the next system moving under the block. Open waves moved rapidly northeastward along this boundary. The first of these, (3) in figure 2-12, deepened rapidly far offshore the night of the 20th as a surge of cold air, (3a) in figure 2-12, driving southward on the back side of the Gulf Low, entered its circulation. The combined center moved quickly to the Washington coast by the evening of the 21st (figure 2-13d). A wave, forming on the trailing front just off the coast, (4) in figure 2-12, moved onshore in the same area on the morning of the 22d. This sequence resulted in a very strong flow of tropical air, especially at low levels, over Northern California for about 18 hours. It was followed by a brief lull in low-level winds and convergence precipitation as a weak surface pressure ridge passed during the afternoon; winds at upper levels continued strong from southwest, however.

The next wave,(5) in figure 2-12, moved under the mid-Pacific block, then rapidly to the Northern California coast by the evening of the 22d (figure 2-13e), restoring strong low-level flow of moist air and high precipitation intensity, this time centered over Central California. As stable waves moved along it, the frontal boundary moved slowly southeastward into south-central California by the evening of the 23d, cutting off the moist flow as it passed (figure 2-13f).

The second Gulf Low,(B) in figure 2-12, originated as cyclogenesis south of Anchorage on the evening of the 21st, then moved southeastward by the 23d to a position west of Vancouver Island where it stagnated for 2 days. Its minor role in the storm was to maintain a strong southwest flow of polar air over Northern California from the 24th to the 26th; this permitted the weakening frontal boundary to stagnate and the rain to continue in south-central California on the 24th. (The Low also caused light precipitation in extreme Northern California on the 25th and 26th.)

Extremely heavy precipitation occurred over Northern and Central California in one or both of two periods, one on the afternoon and night of the 21st, the other on and subsequent to the evening of the 22d, (2) and (3) in figure 2-15. They were associated with the strong moist flows to the south and east of the frontal boundaries shown in figures 2-13d and 2-13e, respectively. The axis of the former flow (and resultant heavy precipitation) crossed the north coast. That of the latter crossed the central coast with an orientation slightly more toward west-east. There, a minor increase in precipitation occurred later, prior to the frontal passage (4, figure 2-15).

Peak runoff and most severe flooding on north coast streams occurred on the 22d, following the first period (col. 2, table 2-1). A location map for the river basins is shown in figure 2-14. The Russian River peak was

very flat, occurring with the frontal passage on the afternoon of the 23d. South of San Francisco, coastal streams peaked during the second period and later with the frontal passage (cols. 3 and 4, table 2-1). Peak flow on the San Lorenzo River on the night of the 22d was particularly sharp, causing a flash flood in Santa Cruz. Because of the slow southward progress of the frontal boundary, rain south of Paso Robles occurred mainly on the 23d and 24th. Only the slight shift in position and orientation of the moisture flow pattern in the second period prevented a repetition of the disastrous flows from the first precipitation period on the Eel and Klamath Rivers, which far exceeded prior record flows.

The first precipitation period, on the 21st, was the more important one in the extreme northern Sierras and the southern Cascades (2 at Shasta Dam, figure 2-15). In the central Sierras precipitation was comparable during the two periods and the lull between them at midday of the 22d was brief at other than low elevations (Blue Canyon and Yosemite, figure 2-15). In the southern Sierras the short precipitation period from the first sequence almost merged with the much more intense precipitation from the latter (3 at Grant Grove, figure 2-15).

A peak in Sierra streamflow occurred on streams from the Stanislaus northward on the 22d (col. 2, table 2-1), following the first period of strong moist flow on the night of the 21st. But higher peaks (though not much higher from the American River northward), occurred on the 23d on all Sierra streams (excluding the Sacramento River north of Shasta Dam), either in the morning or afternoon or both. South of the Calaveras River a peak occurred in the morning only (col. 3); from there northward, the main peak occurred later in the day (col. 4). While the former resulted primarily from the extremely high inflow of moisture on the night of the 22d, represented by figure 2-13e, the latter resulted from the cumulative effect of this and an increase in precipitation intensity during the late morning of the 23d, prior to passage of the final frontal system. This increase is apparent at Blue Canyon (burst 4 in figure 2-15). The disastrous consequences of the flooding on various Sierra streams resulting from these record peak flows are well-known.

In the above discussion, association of runoff peaks from Sierra streams with prior rainfall bursts was possible because the sizeable contribution of Sierra snowmelt to runoff was sufficiently coincident with that of rainfall as not to obscure their relation.

With Low B in figure 2-12 filling rapidly by the 26th, a cold front moved southeastward across California, preceded by a short period of moderate precipitation in Northern and Central California on the 26th. It was followed by a ridge of high pressure on the 27th, finally terminating the storm after a prolonged anticlimax.

Table 2-1

DATE AND HOUR (PST) OF PEAKS IN STREAMFLOW (THSDS. C.F.S.) IN DECEMBER 1955 STORM

River	Gauging Station	(1)	(2)	(3)	(4)	Previous Record Date and Flow	Period of Record-From
			Sierra Streams				
Sacramento	(Shasta Dam)	2101 (119)#	2204 (200)			2/28/40 (280)	1895
Feather	(Oroville)	1922 (93)	2206 (184)		2312 (218)	3/19/07 (230)##	1902
Bear	(Wheatland)	2000 (16)	2213 (32)		2320 (33)	1/21/43 (31)*	1903
Yuba	(Smartville)	1921 (58)	2210 (140)		2314 (162)	3/26/28 (120)*	1904
American	(Folsom)		2214 (196)		2316 (218)	11/21/50 (200)*	1904
Consumnes	(Michigan Bar)		2215 (21)	2308 (34)	2318 (43)	11/18/50 (28)*	1907
Mokelumne	(Benson's Ferry)		2213 (14)	2308 (26)	2316 (28)	--	1926
Calaveras	(Hogan Dam)		2214 (16)	2306 (23)	2316 (31)	1/31/11 (50)	1907
Stanislaus	(Melones Res.)		2219 (54)	2305 (100)		1/31/11 (60)*	1903
Tuolumne	(Don Pedro Res.)			2311 (105)		11/11/50 (95)*	1895
Merced	(Exchequer Dam)			2310 (102)		11/19/50 (83)*	1922
Chowchilla	(Buchanan Dam)			2307 (31)		11/19/50 (23)*	1921
Fresno	(Daulton)			2307 (13)		3/2/38 (15)	1937
San Joaquin	(Friant Res.)			2306 (84)		12/11/37 (77)*	1907
Kings	(Pine Flat Res.)			2308 (100)		11/19/50 (91)*	1895
Kaweah	(Three Rivers)			2308 (74)		11/19/50 (52)*	1904
Tule	(Porterville)			2306 (14)		11/19/50 (25)	1901
Kern	(Isabella Res.)			2310 (28)		11/19/50 (27)*	1905
			Coastal Streams				
Smith	(Cresent City)		2204 (165)			10/29/50 (150)*	1931
Klamath	(Klamath)	2006 (160)	2213 (400)			1/18/53 (297)*	1910-26, 1950
Eel	(Scotia)	2004 (218)	2216 (500)			12/11/37 (345)*	1910
Russian	(Guerneville)	2008 (68)			2314 (89)	2/28/40 (88)*	1939
Napa	(St. Helena)	1919 (9)	2206 (13)	2300 (8)	2316 (8)	2/6/42 (12)*	1929-32,1939
San Lorenzo	(Big Trees)		2210 (7)	2301 (29)	2315 (16)	2/27/40 (24)*	1937
Pajaro	(Chittenden)				2409 (18)	4/4/41 (11)*	1939
Salinas	(Spreckles)				2503 (24)	2/12/38 (75)	1929

*December 1955 peak set new record
#Result of local instability precipitation
##Upstream storage in 1955 not existent in 1907
Source: Geological Survey Water Supply Paper 1445

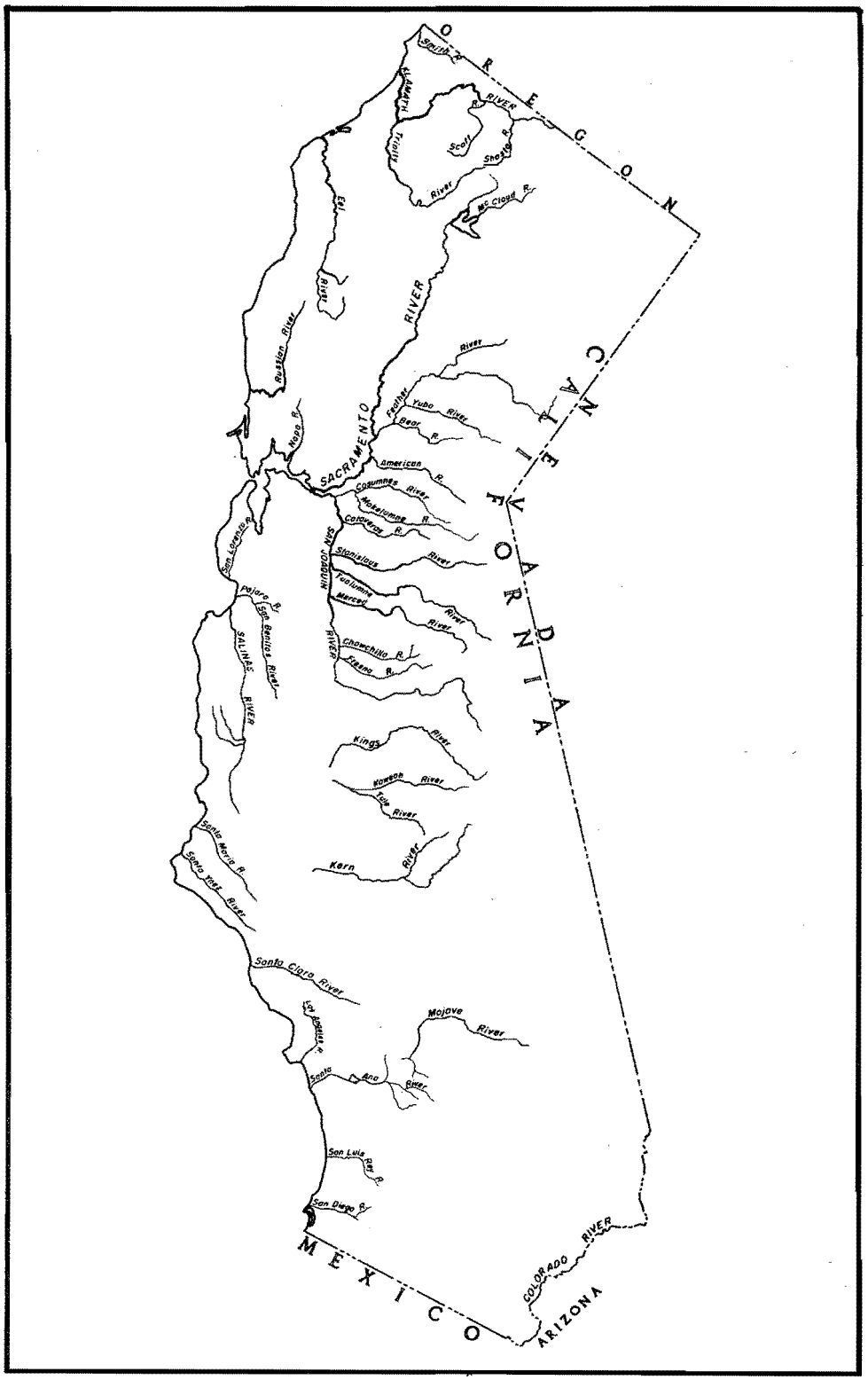

Fig. 2-14. LOCATION MAP OF CALIFORNIA RIVER BASINS

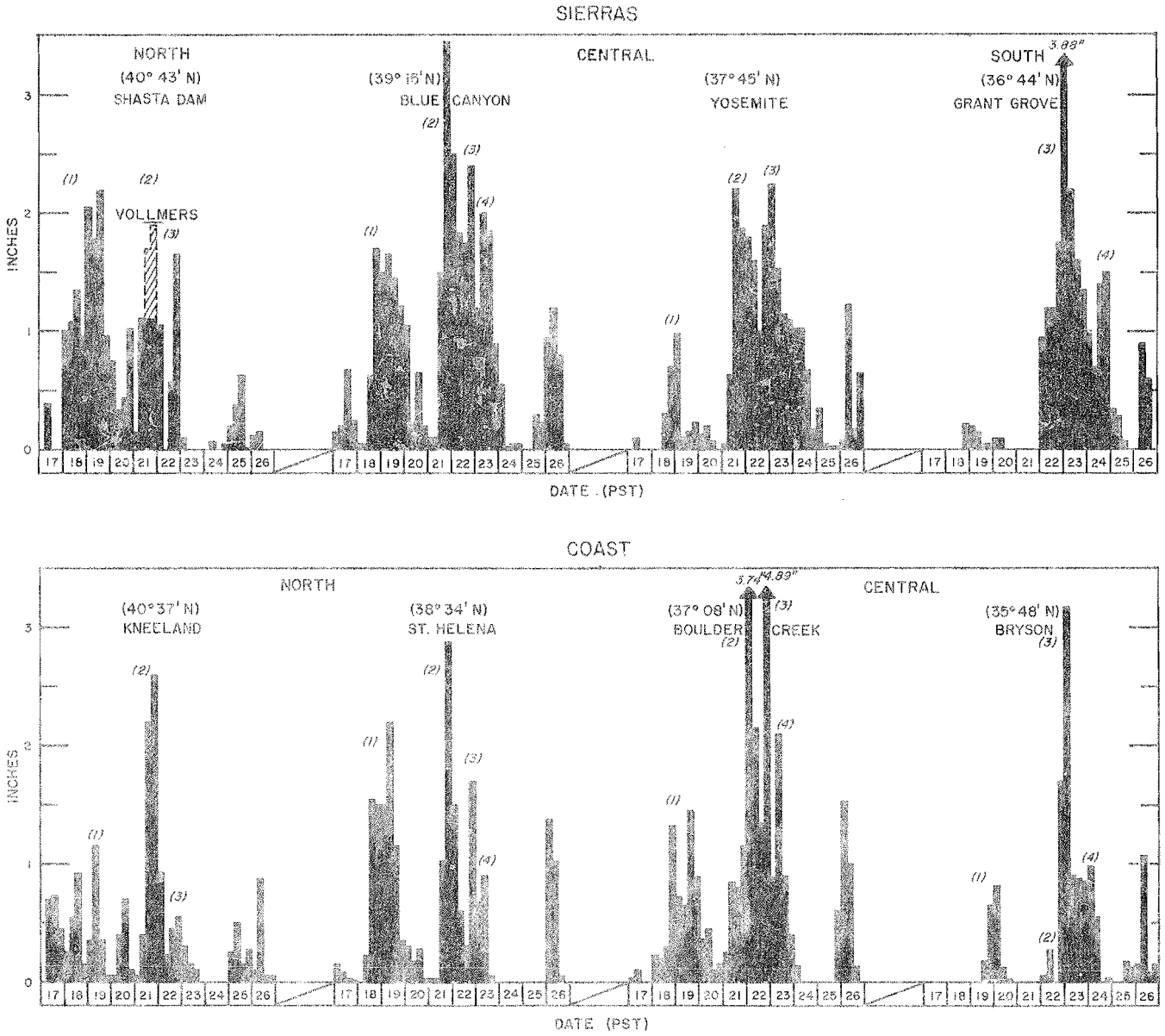

Fig. 2-15. HYETOGRAPHS OF 6-HOUR PRECIPITATION, DECEMBER 17-26, 1955

2-B-2. The November 16-20, 1950 Low-latitude type storm

This storm appears prominently in high central Sierra precipitation and streamflow records primarily as a result of inflow of tropical air from near the Hawaiian Islands, as in the December 1955 storm. But in this storm weakness of the mid-Pacific block at high latitudes more readily allowed entry of storm systems southeastward across western Alaska or the Aleutian chain. Blocking at low latitudes prevented entry there from the western Pacific and confined low-latitude Lows at the coast to development in the eastern Pacific of stable waves on the frontal boundary. The fact that Lows near the coast at the latitude of California were not deep and moved slowly somewhat limited convergence precipitation. The more important orographic precipitation resulting from a moist flow as it related to the synoptic history of the storm is best illustrated by use of 700-mb charts (figures 2-17a to e), in conjunction with the surface composite chart (figure 2-16), and 6-hour precipitation plots at coastal and Sierra Mountain stations (figure 2-18).

Antecedent conditions were less favorable to high runoff than in the December 1955 storm. There was a moderate accumulation of fresh snow in the northern Sierras above 5000 feet and considerably less to the south above 6000 feet. This fell on the 13th to 16th. Prior to the 13th nearly 2 weeks of dry weather had followed a week of intermittent rain.

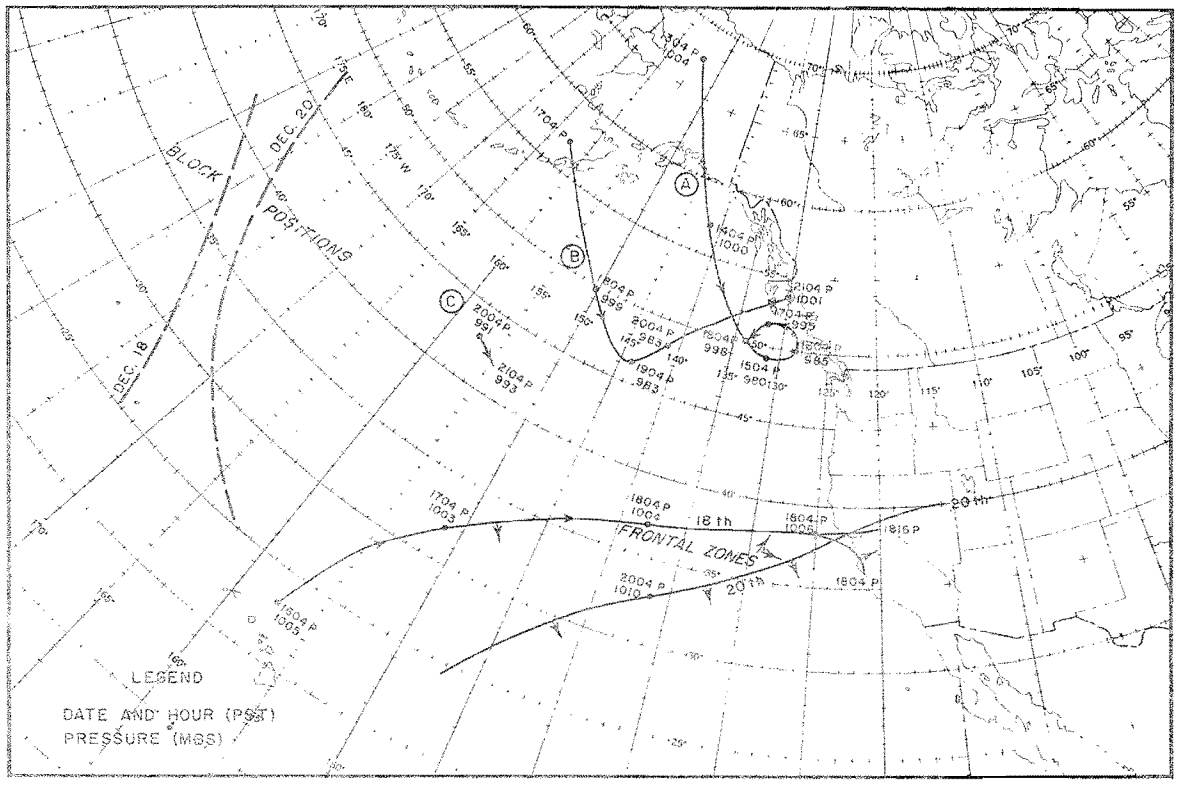

Fig. 2-16. TRACKS OF SURFACE LOWS AND FRONTAL ZONES IN THE NOVEMBER 1950 STORM

The storm featured excessive orographic precipitation in mountain areas of Central California on the 18th and again in north-central California on the 20th from moist tropical flows south of the frontal boundaries shown in figure 2-16. Earlier, heavy precipitation had fallen briefly over the northern third of the state around the 16th, mainly prior to passage of the frontal system associated with Low A in figure 2-16, which moved southeastward and deepened in the Gulf of Alaska, stagnating off Vancouver Island from the 15th to the 18th. A 24-hour isohyetal map is shown in figure A-5.

November 18. The tropical flow at the coast on the 18th resulted from a rather unusual combination of circumstances. A deep Low aloft which had stagnated northeast of Honolulu since the 10th, was drawn northeastward toward the coast, beginning on the 16th (figure 2-16), as deepening occurred southwestward from Low A. On the 17th its circulation aloft was merging with that of the Low A (figure 2-17a), permitting a fairly direct flow of air to the south of the frontal boundary shown in figure 2-16 to reach the Central California coast from a distant low latitude by the morning of the 18th (figure 2-17b). This flow was preceded at the surface by a warm front which moved across Central California early that morning (figure 2-16), remaining stationary in a west-east position at about the latitude of Sacramento that afternoon and evening while flat waves moved along it. By the following morning this front was moving slowly southward where it disappeared as surface pressure rose rapidly on either side. Drier air to the north of the front was replacing the moist flow (figure 2-17c).

Precipitation near and south of this frontal boundary was heavy on the 18th and early on the 19th in coastal mountain areas from latitudes 36.5 to 39N (figures 2-18 and 19), and in the Sierras from latitudes 36 to 39.5N. Precipitation was particularly heavy in the southern half of this Sierra area, resulting in peak flows exceeded only by the 1955 storm on most streams from the Kern northward to the Tuolumne, with a higher flow than in 1955 on the Tule (table 2-1 and figure 2-14).

November 20. By the 19th the Low A (figure 2-16) had disappeared and Low B was controlling the offshore circulation. Its position farther offshore, along with a buildup of the upper-level ridge of high pressure over the Southern Great Basin by the morning of the 20th (figure 2-17d), caused the flow of air at the coast over the northern half of the state to back. By then also the frontal system associated with Low B had crossed the Pacific Northwest and extended southwestward across Northern California; offshore it had merged with the old stationary frontal boundary and pushed it somewhat to the southeast (figure 2-16). In this way a moist tropical flow (figure 2-17d), was again restored to that portion of California just south of this front, this time as a southwesterly flow at the coast, compared to the nearly westerly flow of the 18th. As surface pressure rose on both sides of the front on the 20th, it remained stationary most of the day across north-central California. Meanwhile, low-level winds became light although with colder air to the north, upper winds remained strong. The buildup of the ridge

aloft over Southern California, begun on the 19th, progressed rapidly on the 20th with filling of the Low B and shift of the offshore circulation westward around Low C. As this ridge pushed northwestward off the Central California coast during the night of the 20th and as dry air reached Northern California from the West (figure 2-17e), the narrow moist flow to the coast was cut off.

Precipitation on the 20th was centered near the stationary front. In the Sierras it was concentrated mainly between latitudes 38.5 and 40N (figures 2-18 and 19), including drainages from the Mokelumne to the Feather. It was particularly heavy on the south fork of the Yuba (Blue Canyon, figure 2-18), and the adjoining American, whose peak flow early on the 21st approached the record flow of December 23, 1955 (table 2-1). In the coastal mountains precipitation was heavy only at higher elevations between latitudes 37 and 39N.

Precipitation comparisons. It is of interest to note differences in the relation of the nearly stationary frontal zones of the 18th and 20th to convergence and orographic precipitation areas on those dates:

On the 18th, convergence precipitation was heavy at most Central Valley stations from the front southward beyond Merced (table 2-2). From Sacramento northward most of the precipitation occurred ahead of the warm front early in the morning; further south it fell later in burst patterns moving both with and across the moist flow. Orographic precipitation was heaviest in the south-central Sierras some 100-200 miles south of the stationary front. Thus orography and moisture flow rather than position of the front determined the location of heaviest precipitation in mountain areas, while convergence rain in the Central Valley was determined to a large extent by convergence mechanisms other than those associated with the east-west stationary front.

Table 2-2
CENTRAL VALLEY PRECIPITATION IN THE NOVEMBER 1950 STORM

	November 18 (Inches)	November 20 (Inches)
Red Bluff	.25	.33
Oroville	1.12	1.78
Wheatland	2.10	2.15
Sacramento	1.75	.78
Stockton	2.13	.41
Modesto	.87	.21
Merced	2.69	.15
Fresno	.79	.09

On the 20th the effect of the stationary front was to concentrate precipitation in a narrower band, both in the valley (table 2-2) and in the Sierras (figure 2-19), resulting in sharp areal decrease in precipitation

amounts on either side of this band (figure 2-18). This was accomplished at higher elevations mainly by keeping the narrow moist flow in a nearly stationary position to accumulate heavy orographic precipitation over a relatively small area, and at lower elevations by centering convergence precipitation near the front. The percentage contribution of convergence precipitation to mountain station totals--as measured by average ratio of low-elevation/downwind high-elevation precipitation amounts--near the front showed no increase on the 20th over that for the rest of the storm.

In this storm the position of the area of heavy precipitation on the 20th further north than on the 18th is an unusual feature in major storms. It resulted from the fact that the Gulf Low B was 10 longitude degrees further west on the 20th than Low A on the 18th, along with a progressive buildup of the ridge aloft over the Southwest. It is in contrast to the position of the heavy rain further southeast on December 22, 1955 than on the 21st, as the offshore upper-air trough was displaced 5 longitude degrees eastward in the interim.

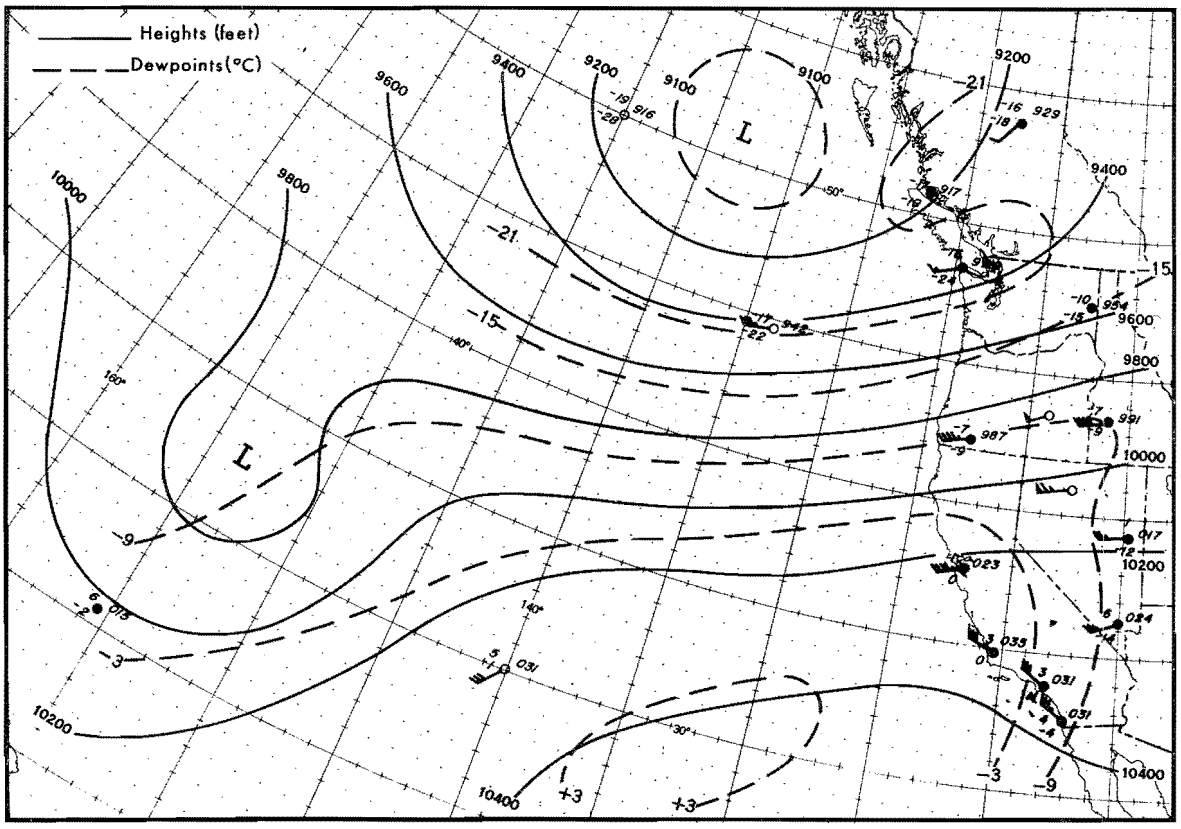

Fig. 2-17a. 700-MB CHART, 0700 PST, NOVEMBER 17, 1950

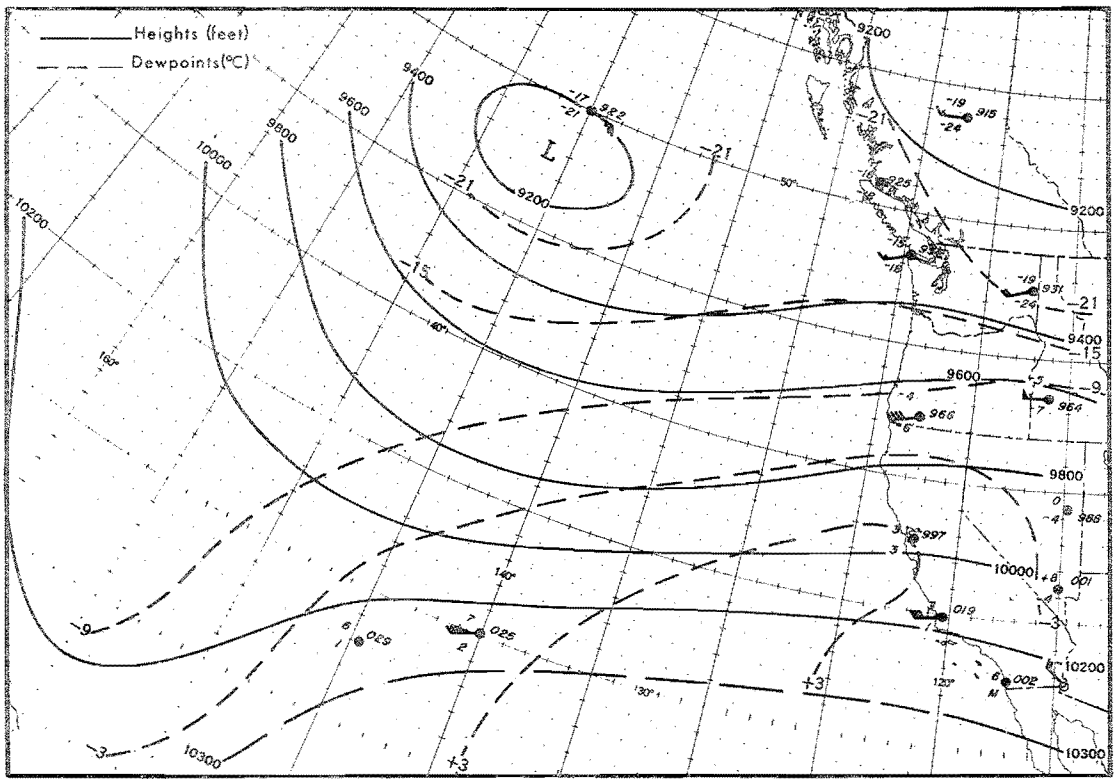

Fig. 2-17b. 700-MB CHART, 0700 PST, NOVEMBER 18, 1950

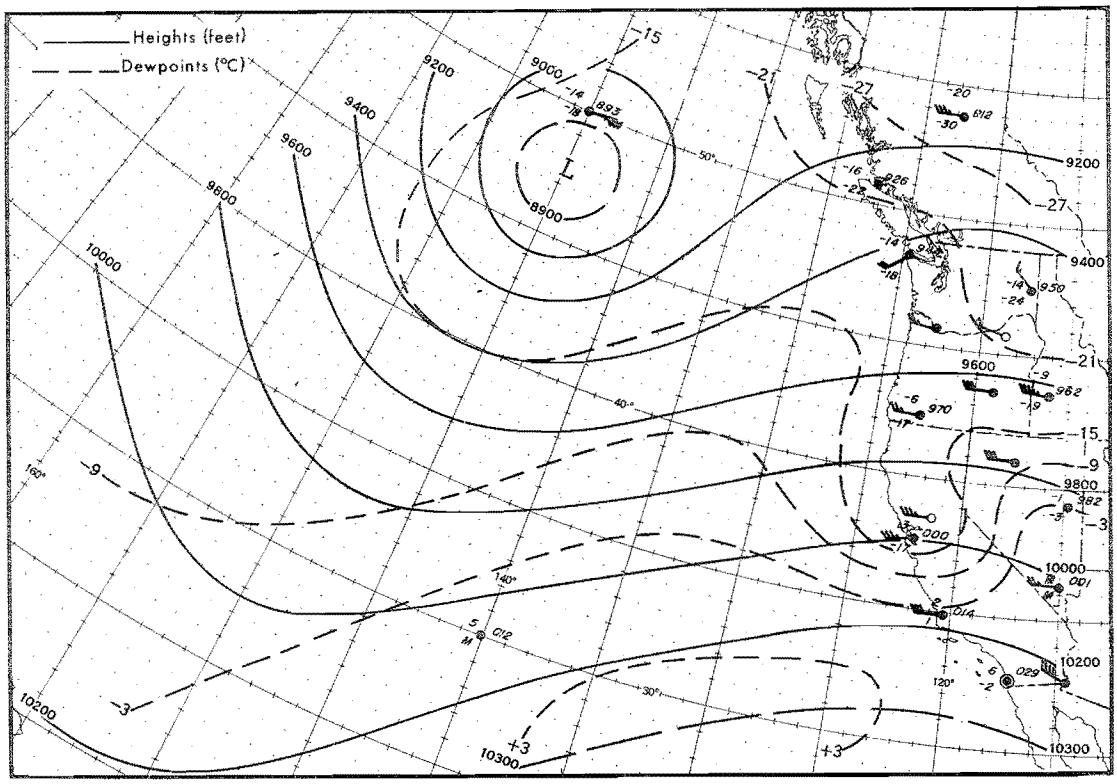

Fig. 2-17c. 700-MB CHART, 0700 PST, NOVEMBER 19, 1950

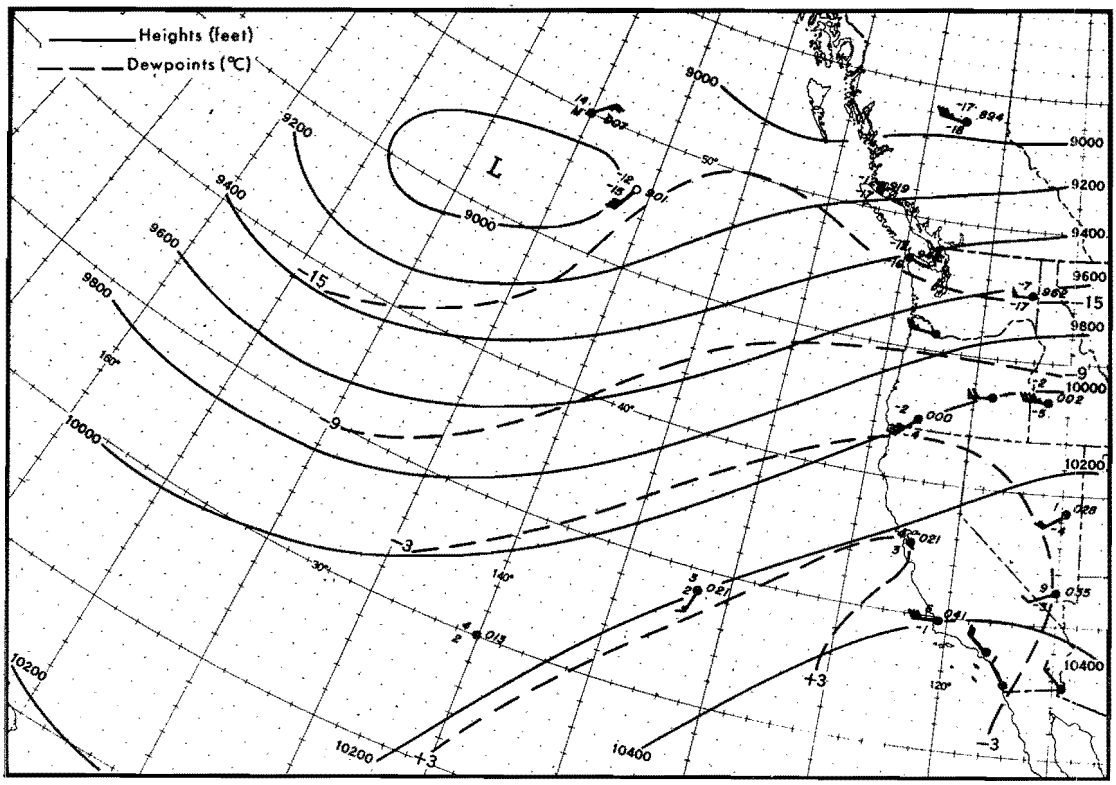

Fig. 2-17d. 700-MB CHART, 0700 PST, NOVEMBER 20, 1950

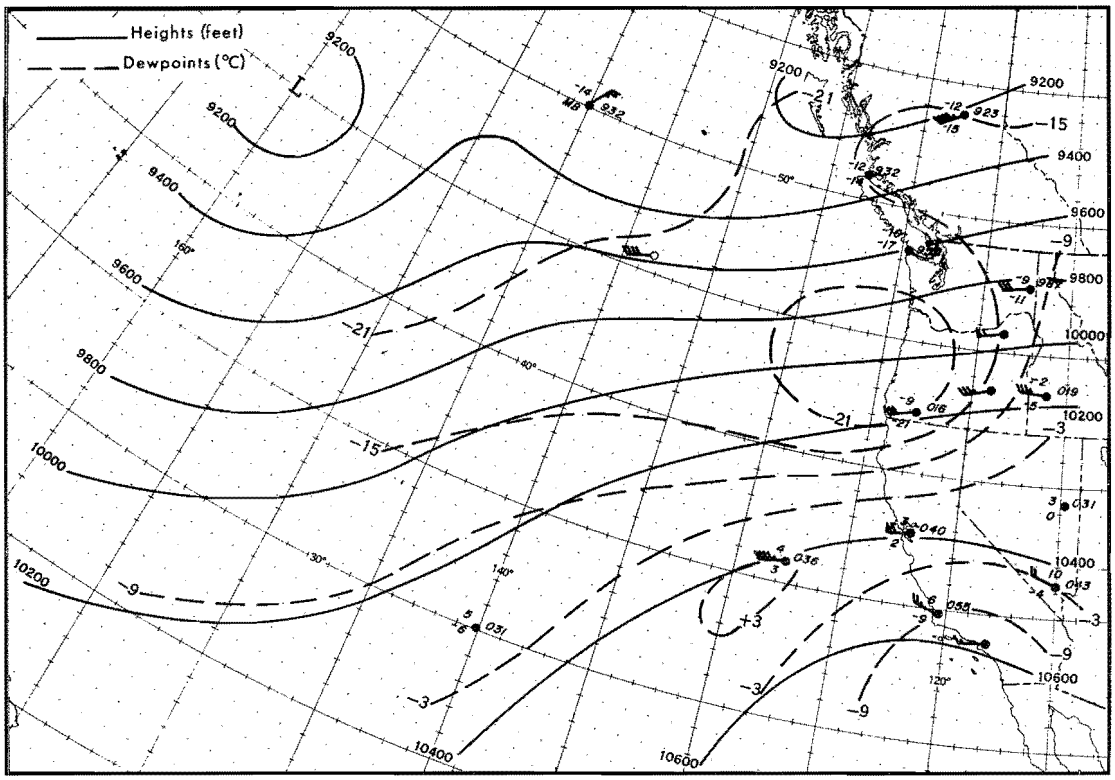

Fig. 2-17e. 700-MB CHART, 1900 PST, NOVEMBER 20, 1950

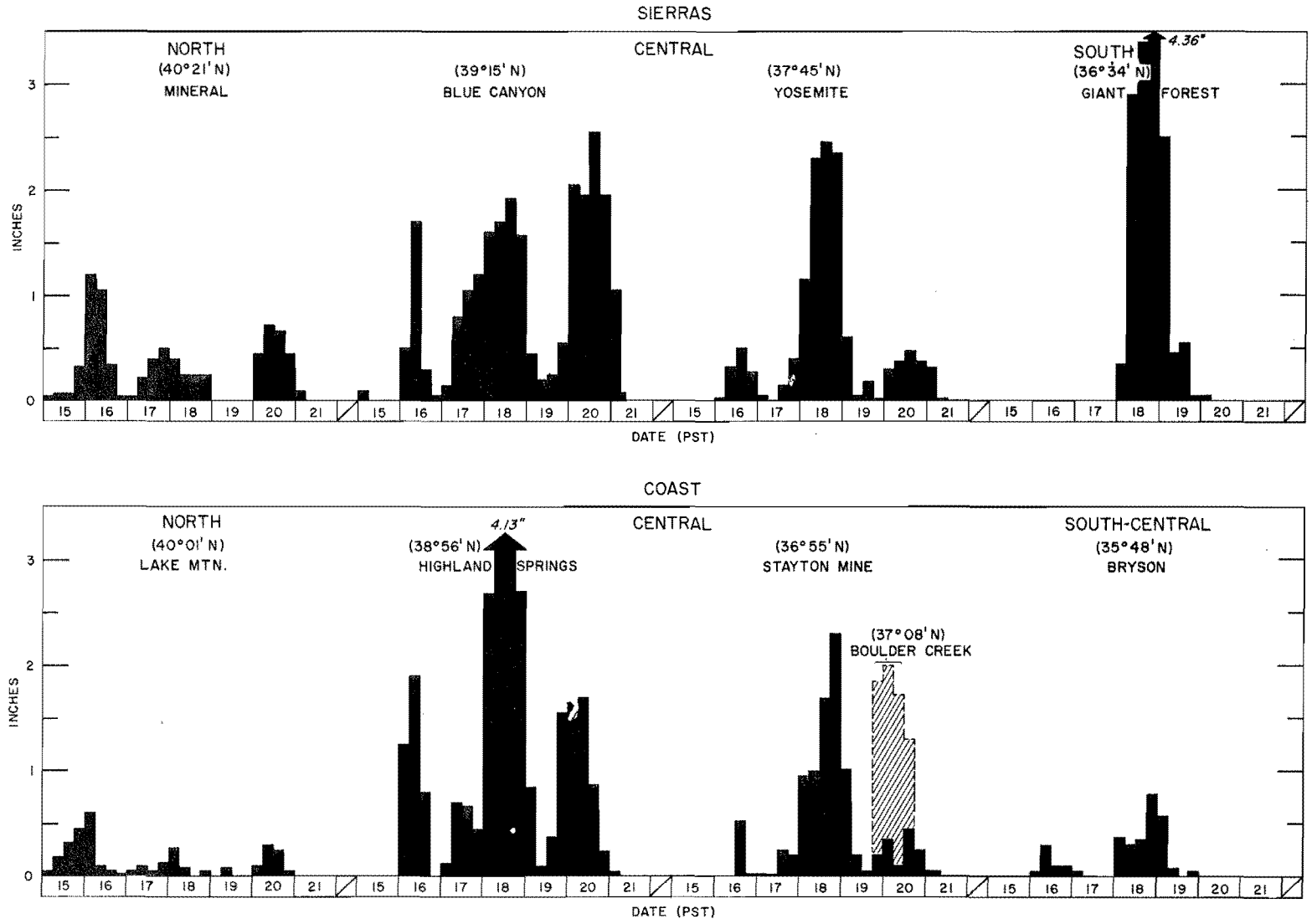

Fig. 2-18. HYETOGRAPHS OF 6-HOUR PRECIPITATION, NOVEMBER 16-21, 1950

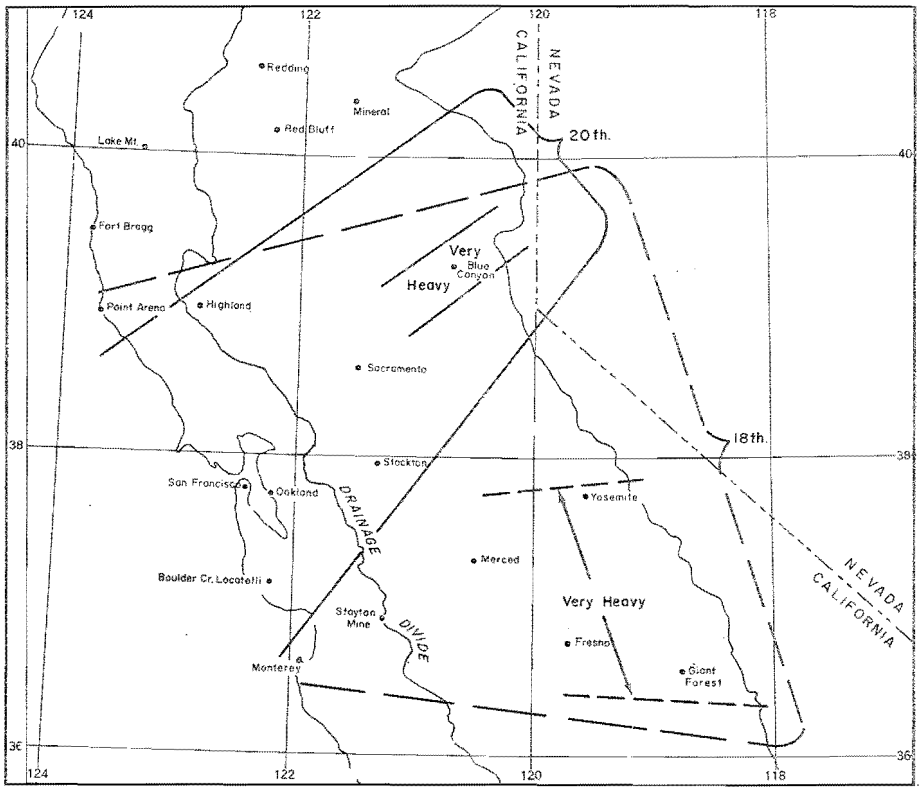

Fig. 2-19. AREAS OF HEAVY OROGRAPHIC PRECIPITATION NOVEMBER 18 AND 20, 1950

2-B-3. The January 30-February 3, 1945 Mid-latitude type storm

The main feature of this storm was the redevelopment of Low centers at middle latitudes in the eastern Pacific (or movement there from the west), with subsequent counterclockwise rotation of these Lows toward higher latitudes off the Pacific Coast so as to bring an increasingly moist flow over most of California.

Antecedent conditions were unfavorable to high runoff since January had been dry up to the 30th, except for light precipitation January 15-18. The Sierra snowpack, much below normal, was mostly above 5000 feet to the north and 7000 feet to the south. Except near the snowline, it was increased by new snow early and late in the storm.

Prior to this storm a warm ridge of high pressure, centered near the western coast of North America, effectively blocked Lows crossing eastward into the mid-Pacific at middle latitudes, forcing them abruptly northward into the eastern Aleutians. This blocking effect is seen (figure 2-20), to have been complete on Lows A and B; Low A was diverted northward on the 26th and Low B on the 27th and 28th, after forming as a wave on the trailing front. On the 29th and 30th, new Low centers 1, 2 and 3 formed on the occluded front of each of the parent Lows 1, 2 and 3 far to the southeast of

the parent Lows. These new Lows moved northeastward and northward off the Oregon or Washington coasts as shown. By the 30th, with the approach of Low 1, the upper-level ridge near the coast was moving eastward; it remained over the Midwest during the storm.

The weak occlusions extending from Lows 1 and 2 moved inland through Northern and Central California on the night of the 30th and midday of the 31st, respectively. Early on February 1 the strong occlusion extending from Low 3 passed through Northern and Central California (figure 2-21a). Low 3 had approached close to the Oregon coast before swinging northward, to be absorbed in Low 4. The much weaker occlusion associated with the intense Low 4 crossed during midday. A wave (5), forming offshore to the southwest on the trailing front, deepened and occluded rapidly as it moved northeastward off the Washington coast, its frontal system crossing Northern and Central California during the evening and night of the 1st, (figure 2-21b). This Low left a deep trough immediately offshore until the following evening as it moved northward.

The rapid succession of Lows (1 to 5 in figure 2-20), moving counterclockwise about a mean offshore position, maintained a southwesterly flow over the northern two-thirds of California from the 30th to the 3d. (Time plots of wind, moisture and moisture transport are shown in figures 3-3c and d.) It became strong the night of the 31st with approach of Low 3, continuing strong through the 2d until the offshore trough from Low 5 had weakened. This flow was fairly moist by the 1st, having traveled along the

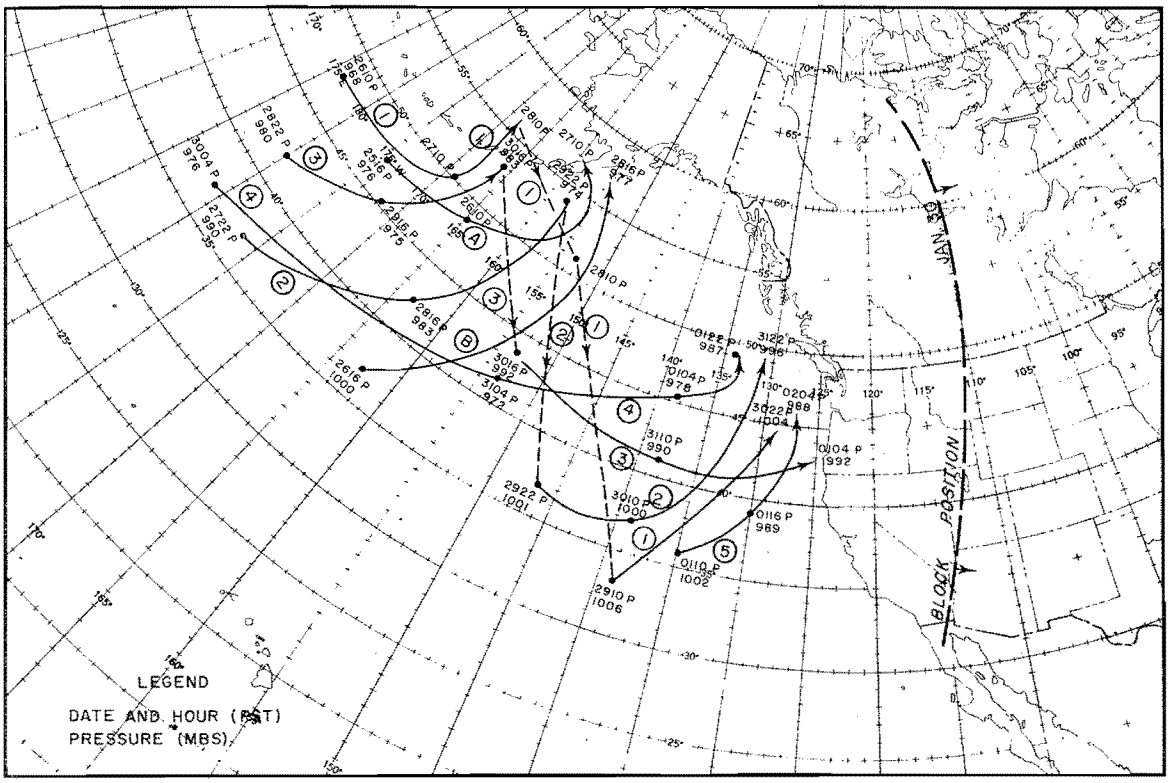

Fig. 2-20. TRACKS OF SURFACE LOWS IN THE JANUARY 30-FEBRUARY 3, 1945 STORM

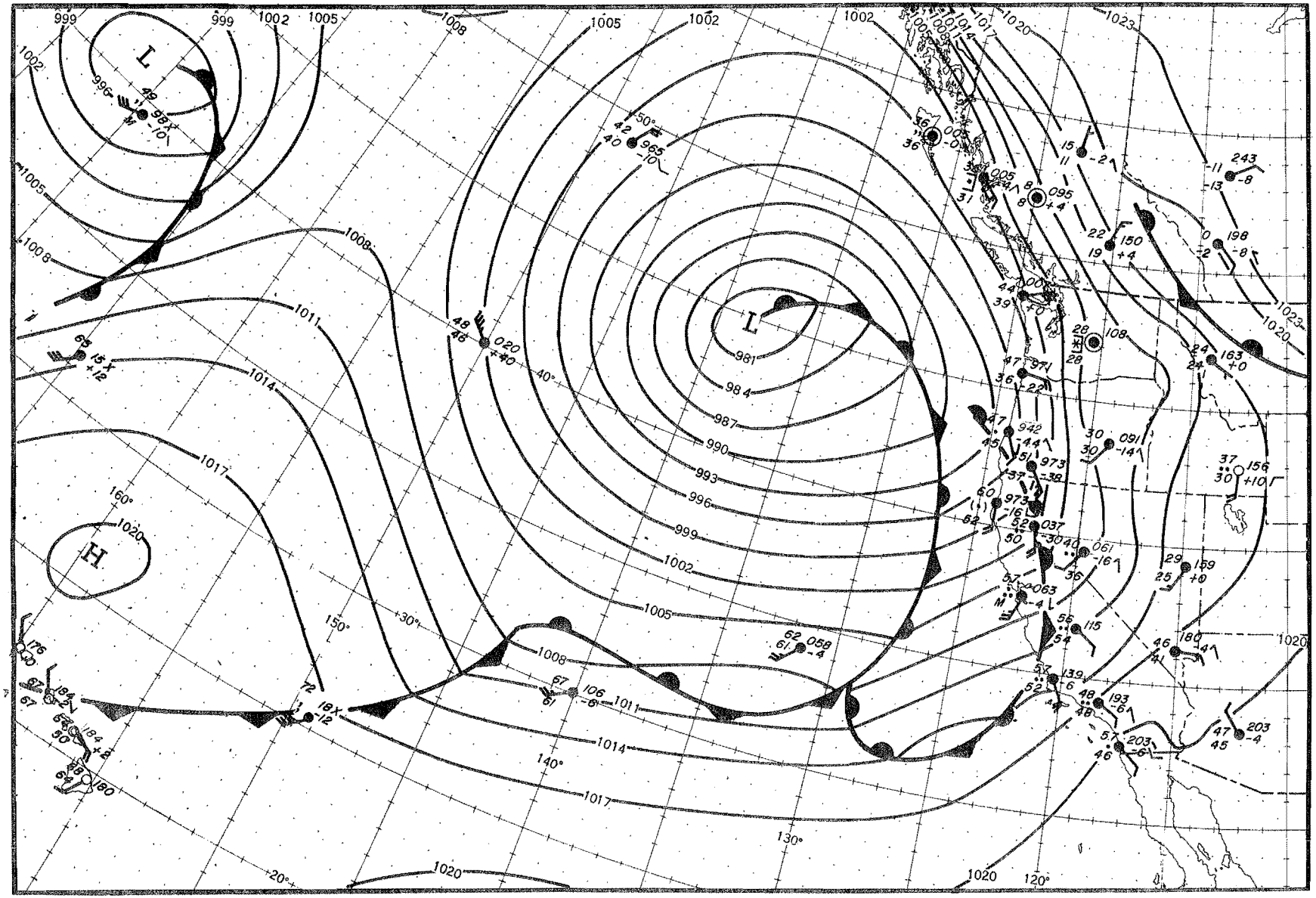

Fig. 2-21a. SEA LEVEL CHART, 0430 PST, FEBRUARY 1, 1945

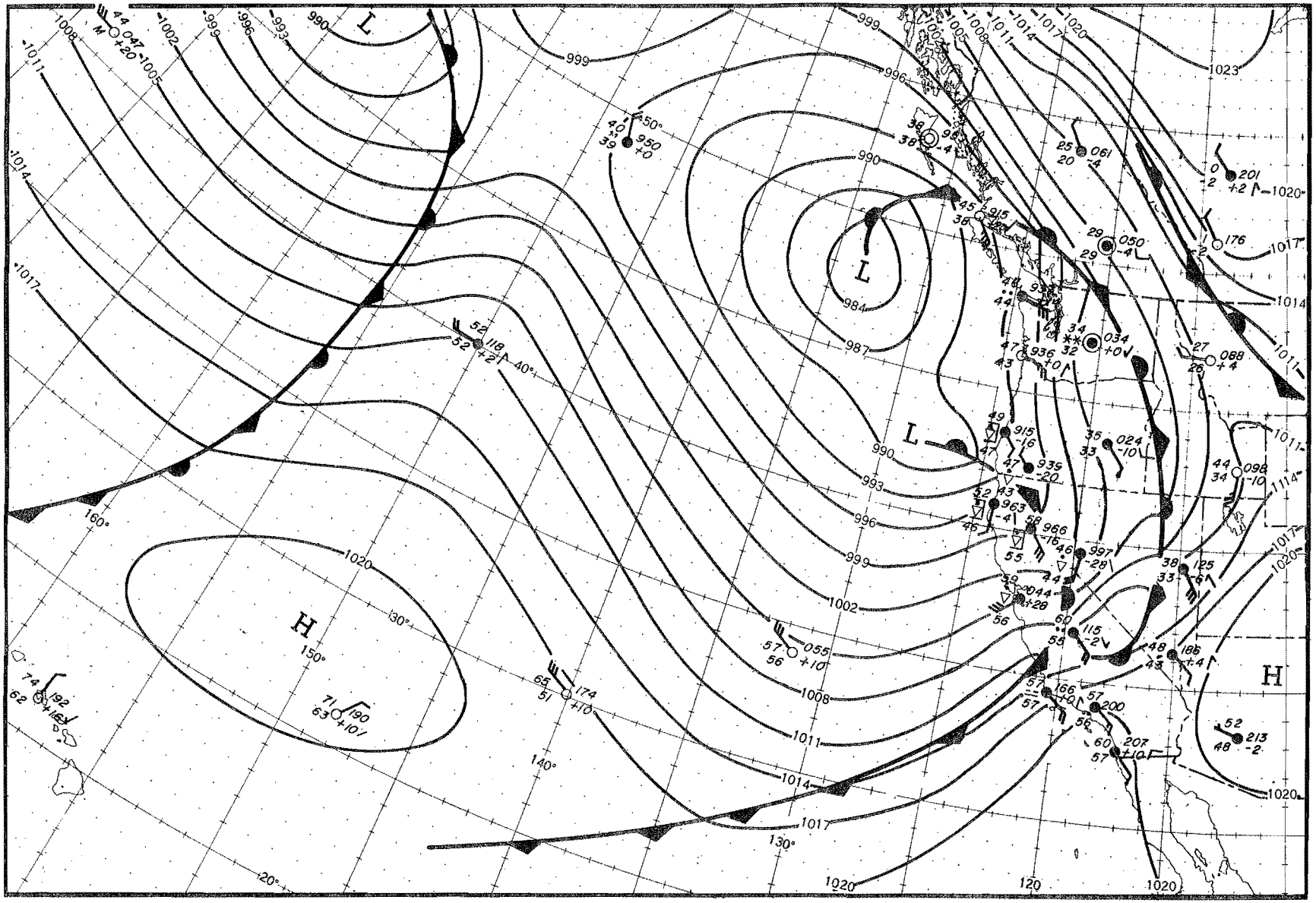

Fig. 2-21b. SEA LEVEL CHART, 2230 PST, FEBRUARY 1, 1945

southern periphery of Lows 3 and 4 across mid-Pacific at a low latitude. Its moisture content reached a peak on the morning of the 1st over Northern California and by evening further south, ahead of Low 5 which had drawn in very moist air briefly into its warm sector. This air, after upward adjustment for season, was not as warm and moist as that in the 1955 and 1950 storms. Moisture decreased sharply with ingress of cold air behind the final front, but increased again somewhat prior to eastward movement of the offshore trough on the night of the 2d.

Precipitation was heaviest in Central California, centered around February 1. Minor peaks (1 and 2 in figure 2-22) occurred mostly in central and south-central California with passage of the occlusions associated with Lows 1 and 2. Peak 3 occurred early on the 1st with the increased flow and passage of the strong occlusion related to Low 3; this peak was high at Central California mountain stations between latitudes 36 and 38N where the moist flow was especially strong and convergence precipitation at upwind coastal and valley stations was heavy. The minor increase in precipitation rate near the occlusion associated with Low 4 about 6 hours later is evident at most stations in figure 2-22 only as a broadening of peak 3. Despite the intensity and proximity to the coast of Low 5 on the evening of the 1st, its related peak 4 is not well defined in figure 2-22 at most Central California coastal mountain stations because of continuation there of rain in the afternoon. In this interim, patterns of convergence precipitation moved rapidly eastward in the continuing strong moist flow across Central California in advance of the final occlusion; also instability was evident then in reports of thunderstorms in central coastal areas. Further south, peak 4 dominated storm precipitation as the final front of the storm passed across Southern California toward morning of the 2d. Passage inland of the offshore trough during the night of the 2d resulted in a period of showers (peak 5) over most of the state.

Peak streamflow in this storm did not approach record values on any stream because of one or more of the following factors: less favorable antecedent conditions, lower precipitation intensity, shorter duration of heavy precipitation and lower freezing level. All are pertinent in comparison with the December 1955 storm. Table 2-3 compares 1945 storm peak flows with highest and second highest of record on those unregulated streams of lengthy record where the 1945 storm peak flows are among the top five of record. These Sierra streams are between latitudes 36 and 38N.

Table 2-3

COMPARISON OF HIGH STREAMFLOW IN 1945 STORM WITH 1950 AND 1955 STORMS

Stream	Location	Period Since	Date of Peak Flow	Flow in Thsds of CFS 1945	1950	1955
Merced	Bagby	1895	2/2/45	40	83	91
Tule	Porterville	1901	2/1/45	13	25	14
Kings	Pine Flat	1895	2/2/45	49	91	100

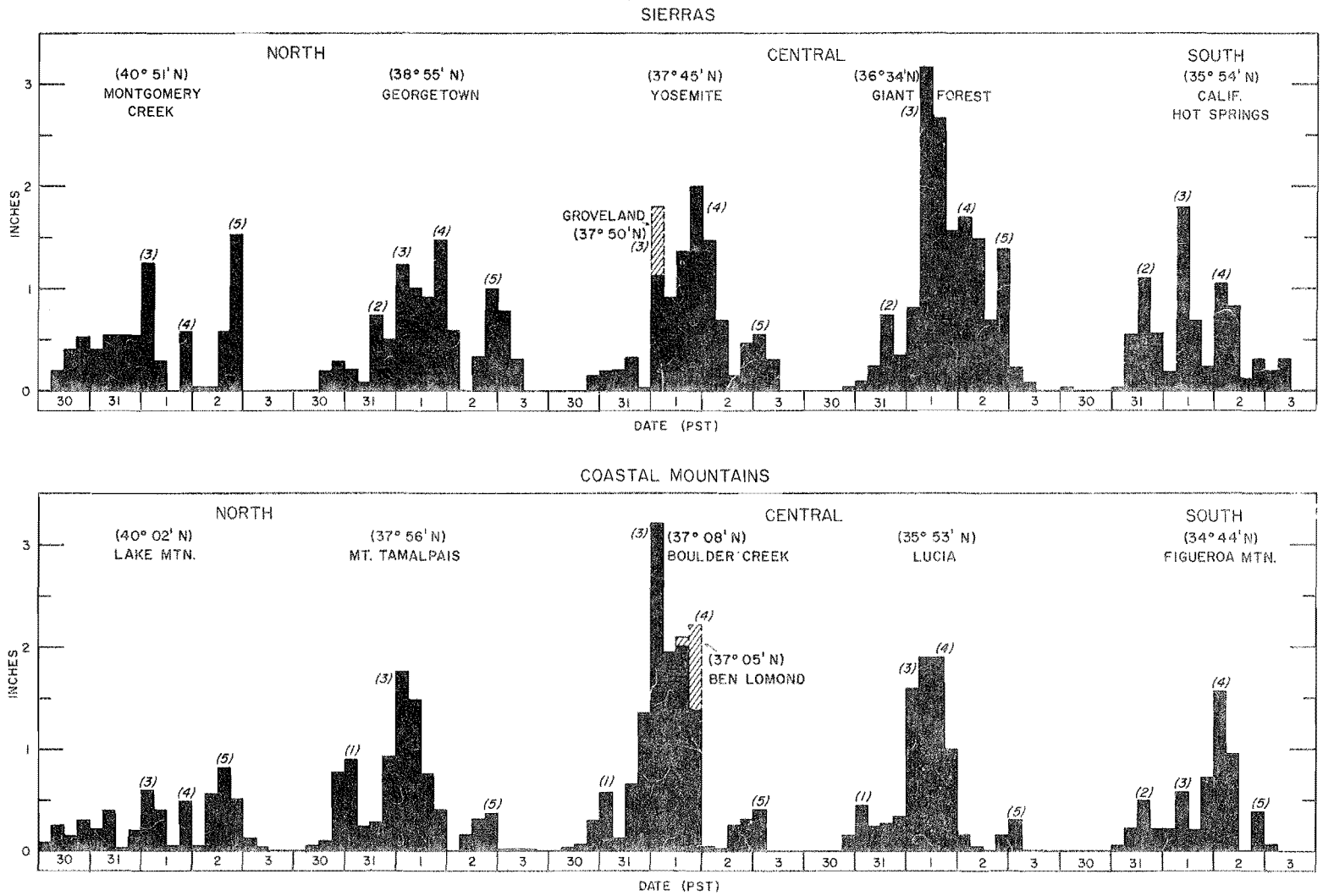

Fig. 2-22. HYETOGRAPHS OF 6-HOUR PRECIPITATION, JANUARY 30-FEBRUARY 2, 1945

2-B-4. The January 20-23, 1943 High-latitude type storm

This storm is noted both for its extremely strong winds and for its large areal extent. It was somewhat more intense in Southern California than farther north, partly because of higher average temperatures at lower latitudes. It is classified as a High-latitude type storm because of the typical crescent-shaped block surrounding an area of cyclogenesis close to the British Columbia coast in the initial period of the storm. But the track of the deepening Low on January 20 was southeastward into the Pacific Northwest (Low 1 in figure 2-23a) rather than southward along the coast, as in the typical High-latitude type storm.

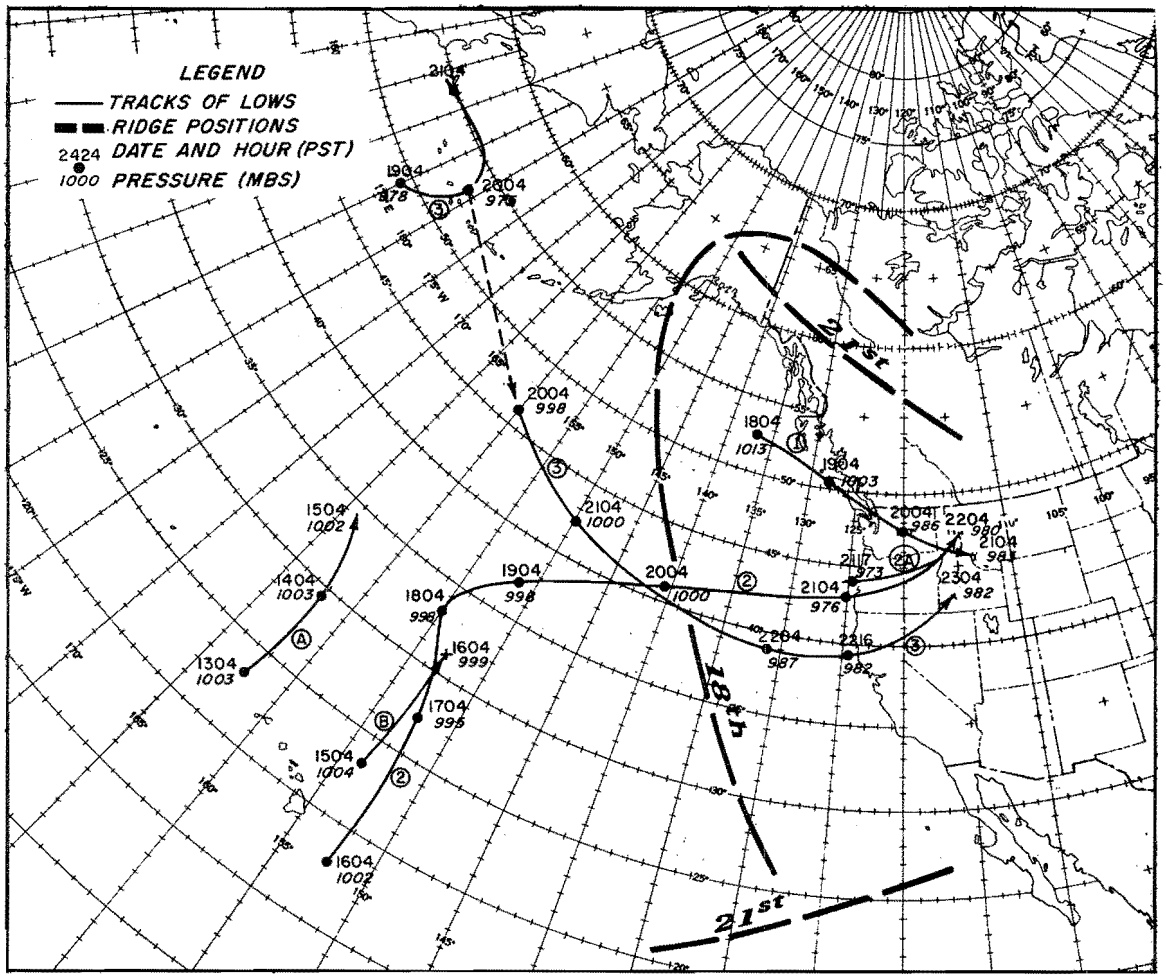

Fig. 2-23a. TRACKS OF SURFACE LOWS IN THE JANUARY 20-23, 1943 STORM

The synoptic sequence. The southeastward movement of this initial Low was concurrent with weakening of the block in the eastern Pacific at middle latitudes so as to permit breakthrough of an old Low (2 in figure 2-23a), the last of three which had moved northward from near the Hawaiian Islands along the back side of the block. Approaching the coast, this Low deepened rapidly as it encountered the southward flow of cold polar air to the rear of the initial Low moving into eastern Washington. It moved inland across the southern Oregon coast on the 21st. Low 3 in figure 2-23a formed on the occlusion extending to the southeast from a deep stationary Low in the western Aleutians. As this newly formed Low moved rapidly toward the coast it deepened in a manner similar to Low 2, entering north of San Francisco on the evening of the 22d.

A more detailed picture of the storm sequence is obtained by study of figures 2-23b through 2-23e, sea-level maps at 24-hour intervals from 0430 PST, January 20. A warm front in figure 2-23b is shown entering the coast ahead of the southeastward-moving cold front associated with Low 1 of figure 2-23a. This warm front marked the boundary of warm Pacific air replacing cold air from a prior polar outbreak over the Western States and adjacent ocean area. Heavy snowfall preceded the warm front in the extreme northern Sacramento Valley on the 20th. Rain extended southward to Santa Maria and was almost continuous north of San Francisco the entire day. The cold front progressed southward during the 20th only as far as the Oregon border where it awaited the approach of the first deep Low from the west on the morning of the 21st (figure 2-23c).

The strong westerly flow prevailing over the northern half of California from Low 1 was extended southward with approach of Low 2 by the 21st and greatly intensified as a southwesterly flow. Record surface pressure gradients for California were recorded on that date between points in both the Sacramento and San Joaquin Valleys and along the coast north of San Francisco. Persistence of these strong gradients was due not only to Low 2 with its 976-mb center as it entered the coast in the morning, but also to subsequent cyclogenesis (2A in figure 2-23a). The latter is faintly suggested as a wave in figure 2-23c forming offshore on the polar front separating the cold offshore flow from the Pacific Northwest and the mild Pacific flow behind the occlusion. This wave, entering the central Oregon coast during the evening of the 21st with a 973-mb center (deepest of the storm), is shown in figure 2-23d over eastern Idaho on the morning of the 22d. By this time the first occlusion was moving slowly across Southern California.

As with the approach of the first Pacific Low early on the 21st, the southward progress of the polar front was again delayed with approach of the second Pacific Low on the 22d (figure 2-23d), but only after cold, drier air had penetrated into the northern third of the state. This Low crossed the coast near Fort Bragg early that evening with a 982-mb center, moving into southern Idaho by the following morning (figure 2-23e). During this time the sea-level pressure gradient was particularly strong and orographic rain was

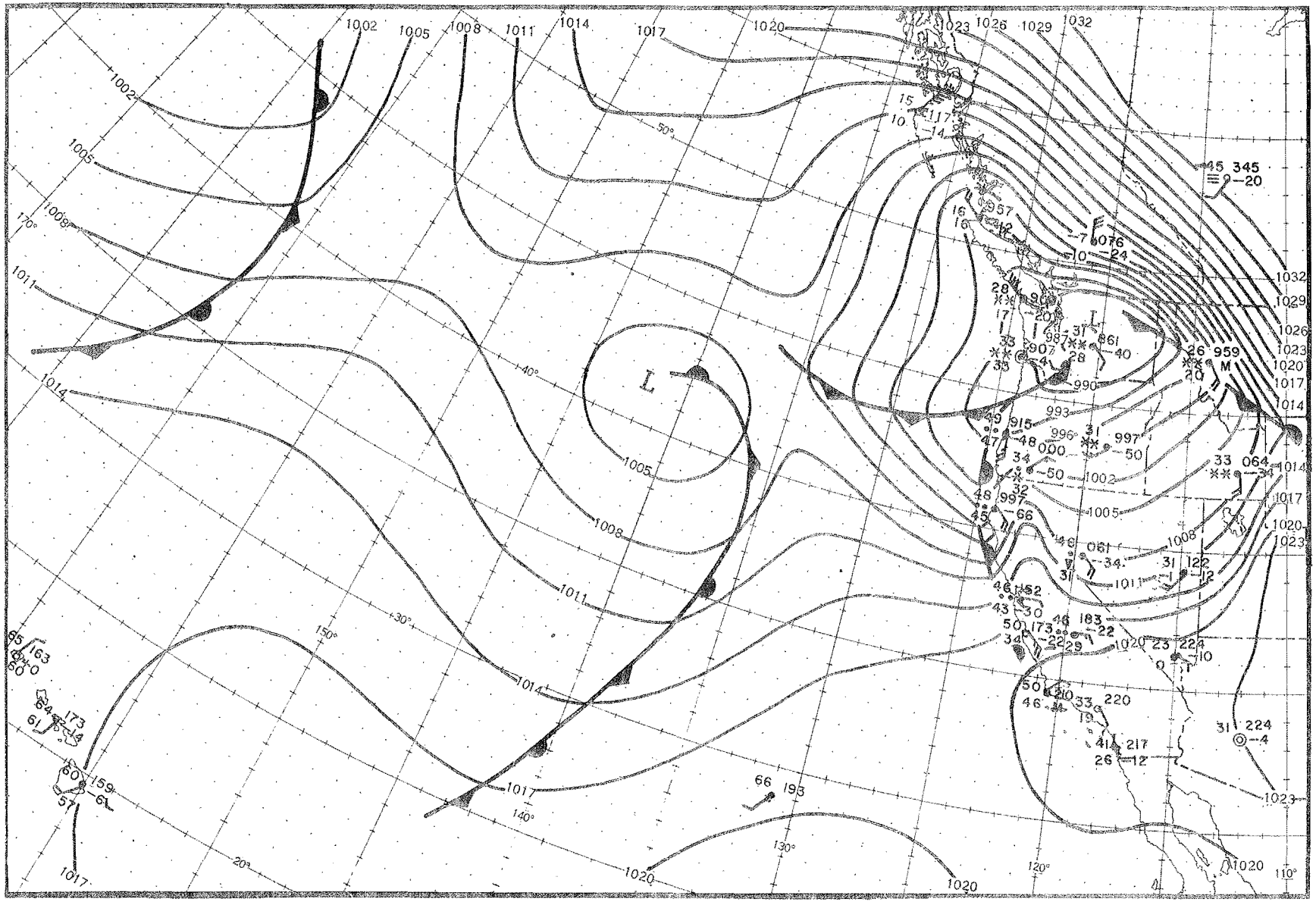

Fig. 2-23b. SEA LEVEL CHART, 0430 PST, JANUARY 20, 1943

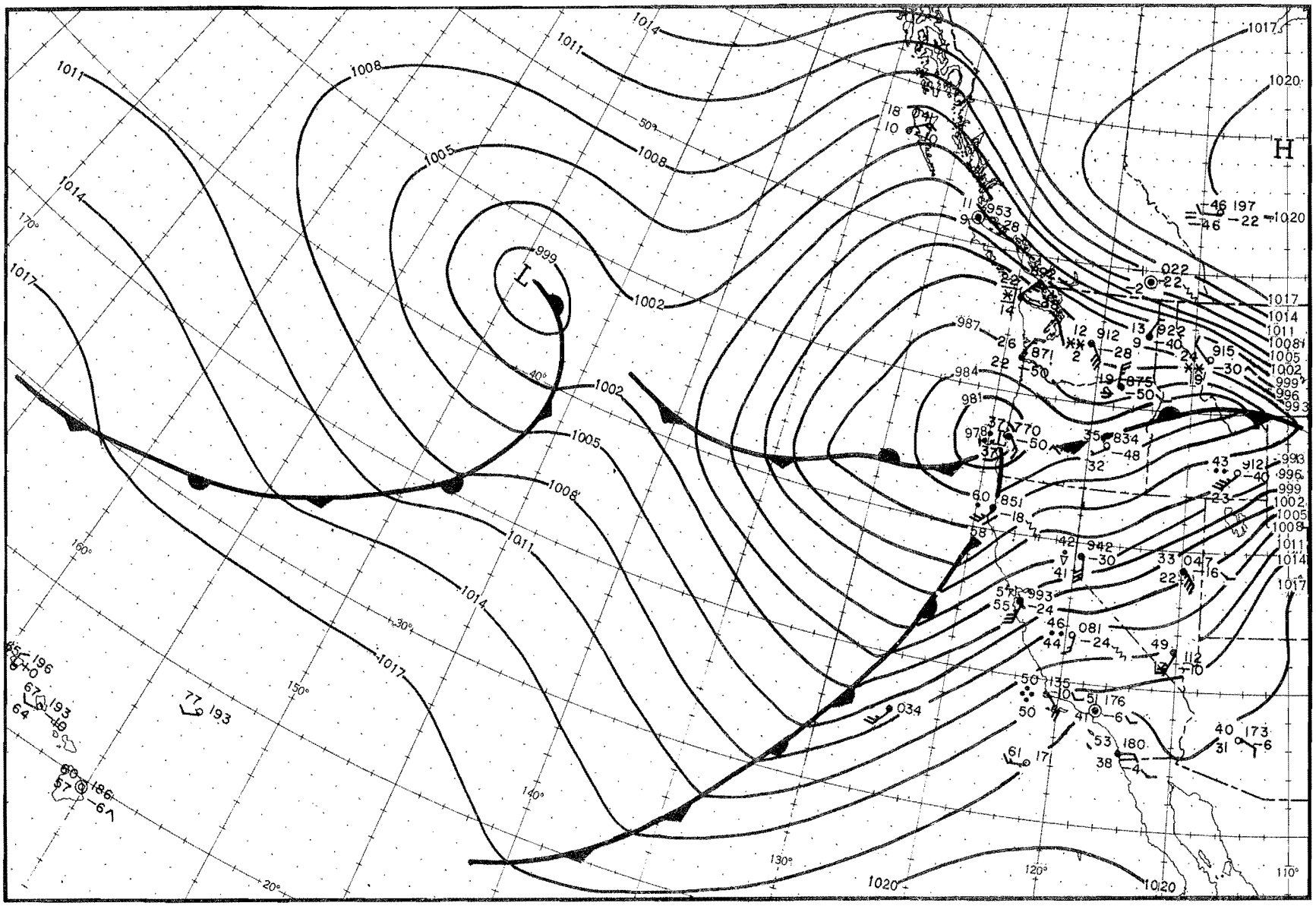

Fig. 2-23c. SEA LEVEL CHART, 0430 PST, JANUARY 21, 1943

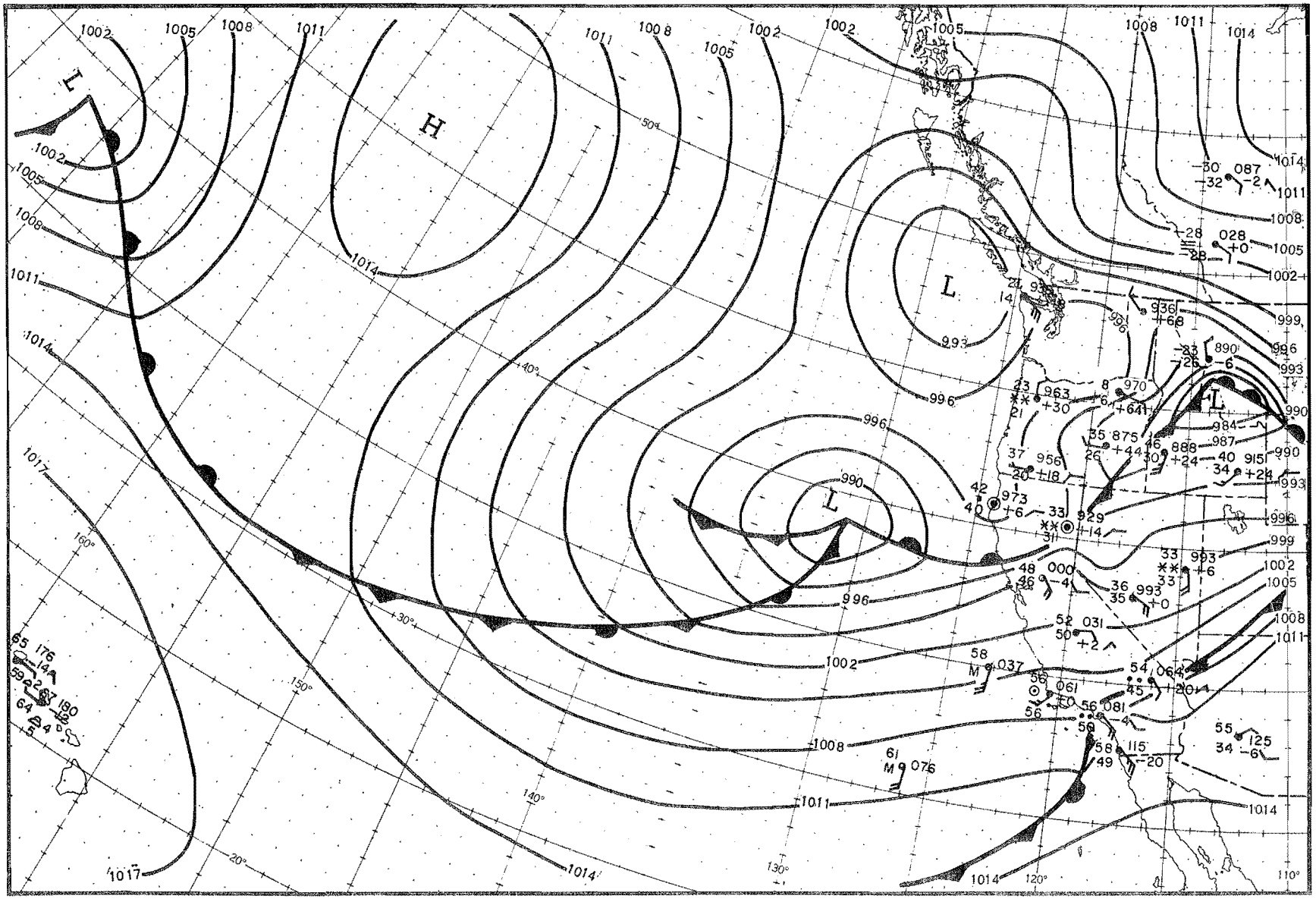

Fig. 2-23d. SEA LEVEL CHART, 0430 PST, JANUARY 22, 1943

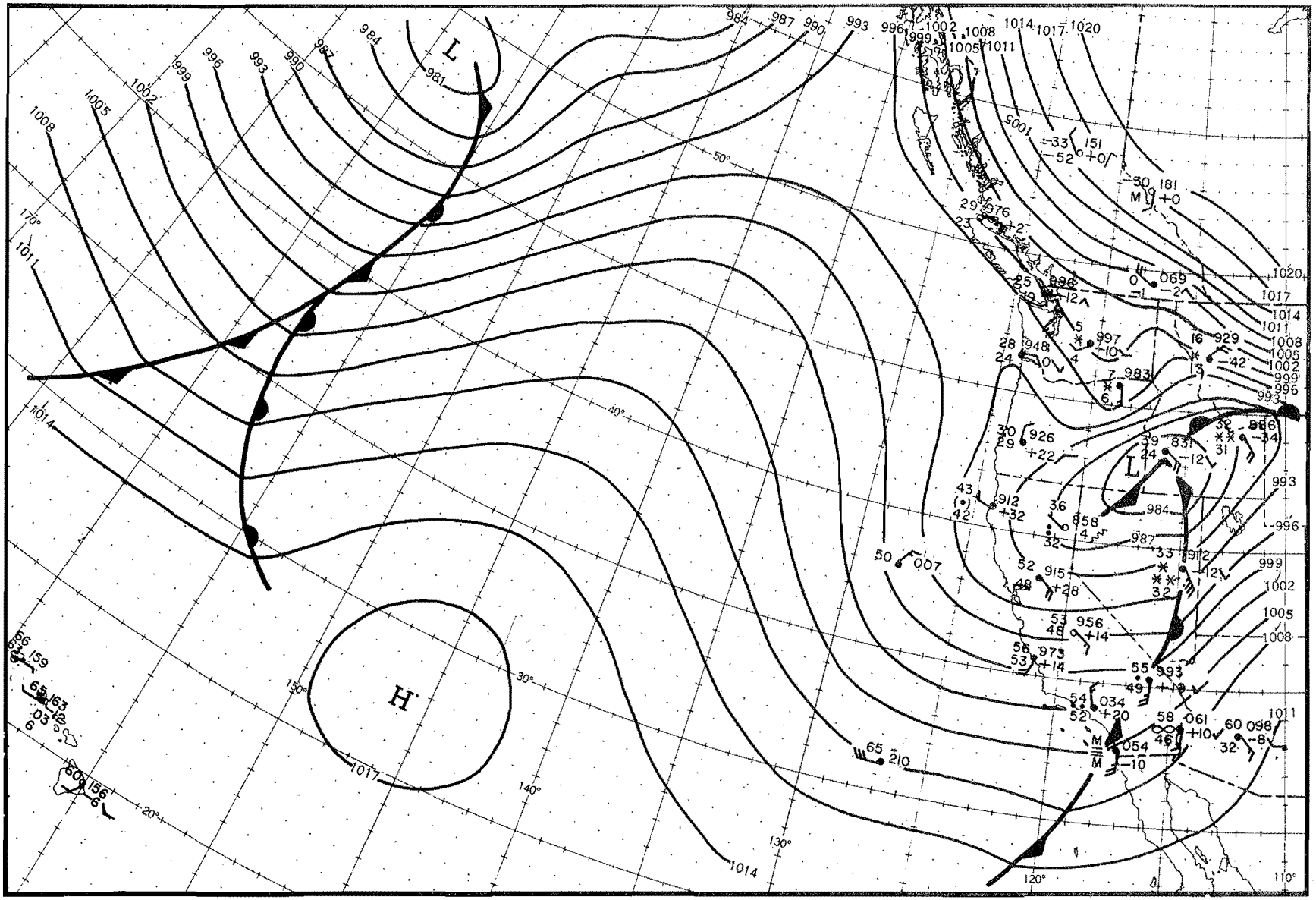

Fig. 2-23e. SEA LEVEL CHART, 0430 PST, JANUARY 23, 1943

intense over the southern part of the state. Although the occlusion is shown crossing Southern California on the morning of the 23d, a trough persisted along the south coast, continuing the showers over the southern part of the state until late that night.

Storm moisture. The tracks of the Lows suggest the moisture pattern of the storm. While pressure gradients were somewhat higher in Northern and Central California than farther south, highest moisture was centered well to the south. Table 2-4 shows average 12-hour 1000-mb dew points at 3 locations during the storm.

Table 2-4.

AVERAGE 12-HOUR 1000-MB DEW POINTS (°F) IN THE JANUARY 1943 STORM

	Red Bluff	Oakland	Long Beach
20th	39	45	--
	44	51	--
21st	52	54	--
	45	51	54
22d	46	47	57
	44	51	57
23d	--	47	54
	--	--	--

To the north, dew points were very low except on the morning of the 21st. At Oakland they were low except near time of passage of the first Pacific Low, rising again briefly late on the 22d. At Long Beach, however, dew points were fairly high throughout the 2-day period of nearly continuous rain there, especially on the 22d. This prevalence of high moisture in the southern part of the state was a logical consequence of the storm type, location and size. A strong meridional flow was present only temporarily to bring high temperatures to the north for a few hours; its persistence over the southern half of the state resulted in a strong latitudinal variation of storm moisture similar to but greater than that of sea-surface temperature.

The large range in storm dew point in the northern part of the state reflects the extreme difference in temperature between the modified tropical air reaching that area briefly in advance of the first occlusion early on the 21st (Eureka temperature 62°F), and the cold continental polar air there initially and later intermittently as a southward flow from the Pacific Northwest (Eureka maximum temperature 44°F on the 22d).

There is ample evidence of instability in this storm. Reports of thunderstorms were widespread in both coastal and mountain areas. They occurred in Northern California from the 21st to the 23d and in Southern California on the nights of the 21st and 22d.

Precipitation. The storm precipitation isohyets are shown in figures A-3 and 4 of the Appendix. The storm sequence is centered around time of passage of the two occlusions, as seen in figure 2-24. Here 6-hour hyetographs of 5 Sierra and 4 Southern California mountain stations are plotted. The Sierra plots show a minor peak on the 20th with Low 1, a broad peak on the 21st with Low 2, and a less intense peak with Low 3 on the afternoon of the 22d. The peak on the 21st has in each case a dual maximum with a slight lull near midday, associated respectively with Low 2 in the morning and with the rapidly developing wave (described above) in the afternoon.

Comparison of the Sierra precipitation of this storm in figure 2-24 with that of the November 1950 storm in figure 2-18 shows considerable similarity except to the south where only a single peak occurred in the 1950 storm. Comparison with the December 1955 storm in figure 2-15 indicates shorter duration and somewhat less frequent and less extreme intensity fluctuations in the 1943 storm.

The precipitation sequence in Southern California is shown in the lower part of figure 2-24 for 4 mountain stations located (from left to right) between Santa Barbara and San Diego. The two main Lows on the 21st and 22d are evident in their effect on precipitation. At Figueroa Mountain, north of Santa Barbara, the first peak predominates; farther to the southeast, on the slopes of the San Gabriel Mountains the two peaks at Opid's Camp are near the same intensity and tend to merge; in the Laguna Mountains to the south at Henshaw Dam the peak with Low 2 is obscured by that of Low 3, centered on the night of the 22d.

The extreme intensity of orographic rain in the San Gabriel Mountains is evident from the fact that the 24-hour precipitation of 26.12 inches at Hoegee's Camp near Mt. Wilson is a record for California. Its precipitation sequence is represented by nearby Opid's Camp in figure 2-24 with a 24-hour amount of 22.32 inches, climaxed by 6.89 inches in 6 hours near time of passage of the second occlusion on the night of the 22d.

Streamflow. In table 2-5 are shown times of peak streamflow on a number of streams that are essentially unregulated. Peaks occurred on the afternoon and evening of the 21st on most north coast and northern and central Sierra streams and during the night on southern Sierra streams. This was runoff primarily from the effects of Low 2. (Secondary peaks occurred on the morning of the 23d on most Sierra streams following passage of Low 3.) Peaks of central coastal and Southern California streams mostly followed passage of Low 3 on the night of the 22d.

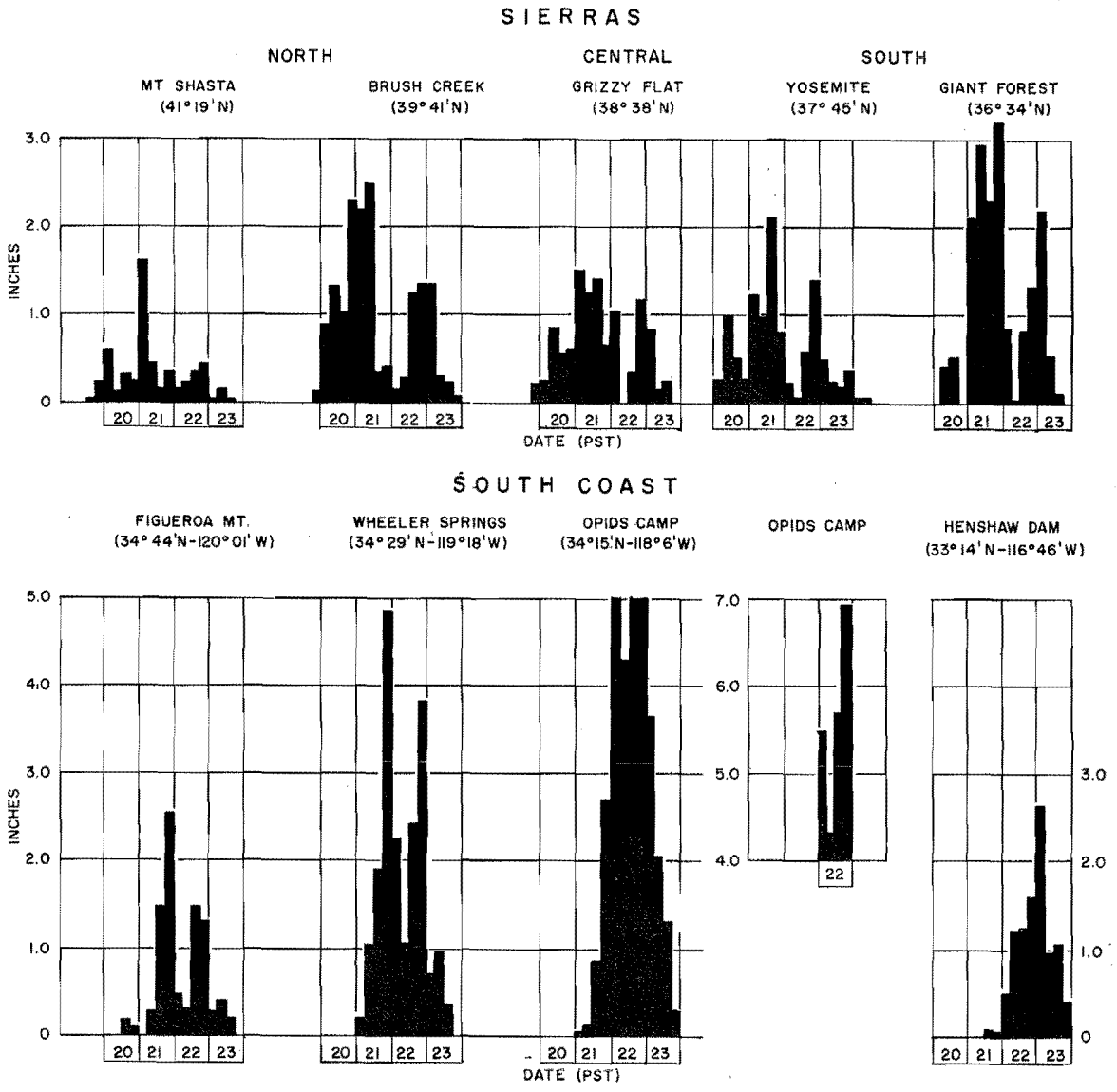

Fig. 2-24. HYETOGRAPHS OF 6-HOUR PRECIPITATION, JANUARY 20-23, 1943

Table 2-5

COMPARISON OF STREAMFLOW (THSDS CFS) IN THE JANUARY 1943 STORM WITH THE MAXIMUM OF RECORD

River	Station	Flow-Date-Time (PST)		Record Flow and Date	
		Northern and Central Coastal Streams			
Eel	Scotia	315	2122	500	12/22/55
Napa	St. Helena	5	2111	13	12/22/55
San Lorenzo	Big Trees	14	2215	29	12/23/55
Salinas	Spreckels	43	2222	75	2/12/38
		Sierra Streams			
Feather	Oroville	108	2116	230	3/19/07
Bear	Wheatland	31	2108	33	12/23/55
Consumnes	Michigan Bar	16	2119	43	12/23/55
Chowchilla	Buchanan Dam	8	2204	31	12/23/55
Kaweah	Three Rivers	17	2200	74	12/23/55
Tule	Isabella Res.	7	2204	28	12/23/55
		Southern California Streams			
Ventura	Ventura	35	2223	39	3/2/38
Santa Clara	Saugus	15	23--	24	3/2/38
Arroyo Seco	Pasadena	6	2302	9	3/2/38
Cajon Cr.	Keenbrook	11	2302	14	3/2/38
Santa Margarita	Ysidro	19	2308	33	2/16/27

Comparison of these peak flows with record flows indicates that only on the Bear River in the central Sierras and on the Ventura River in Southern California did they approach record flows. To the north both rainfall and snowmelt were comparatively low in this storm.

It is significant that in Southern California the record streamflows of the February 27-March 3, 1938 storm followed 2-day rainfall totals generally smaller than in this storm, as shown in table 2-6. (Locations are on figure 2-25.) Only in the Laguna Mountains far to the south did March 1938 2-day rainfall exceed that in this storm. This apparent anomaly was due primarily to difference in antecedent conditions. A long dry period in Southern California preceded the January 1943 storm (2.28 inches in the preceding two months at Mt. Wilson), while in the month prior to the 1938 storm, rainfall was nearly double normal amounts. Thus soil conditions and unused reservoir capacity prevented the serious flooding experienced in the 1938 storm despite heavier rainfall, especially in the San Gabriel Mountains.

Table 2-6

COMPARISON OF 2-DAY RAINFALL IN THE JANUARY 1943
AND FEBRUARY-MARCH 1938 STORMS (Inches)

Station	March 2-3, 1938	January 22-23, 1943
	Santa Ynez Mountains	
Santa Barbara	5.82	9.13
Ojai	9.83	12.39
	San Gabriel Mountains	
Mt. Wilson	15.82	22.18
Sierra Madre*	10.65	20.02
Pasadena	9.88	12.92
	San Bernardino Mountains	
Mill Creek 2	6.97	7.09
Seven Oaks	13.16	13.51
Squirrel Inn	15.67	17.85
	Laguna Mountains	
Guyamaca	10.14	9.15
Warner Springs	5.42	4.72

*3-day total

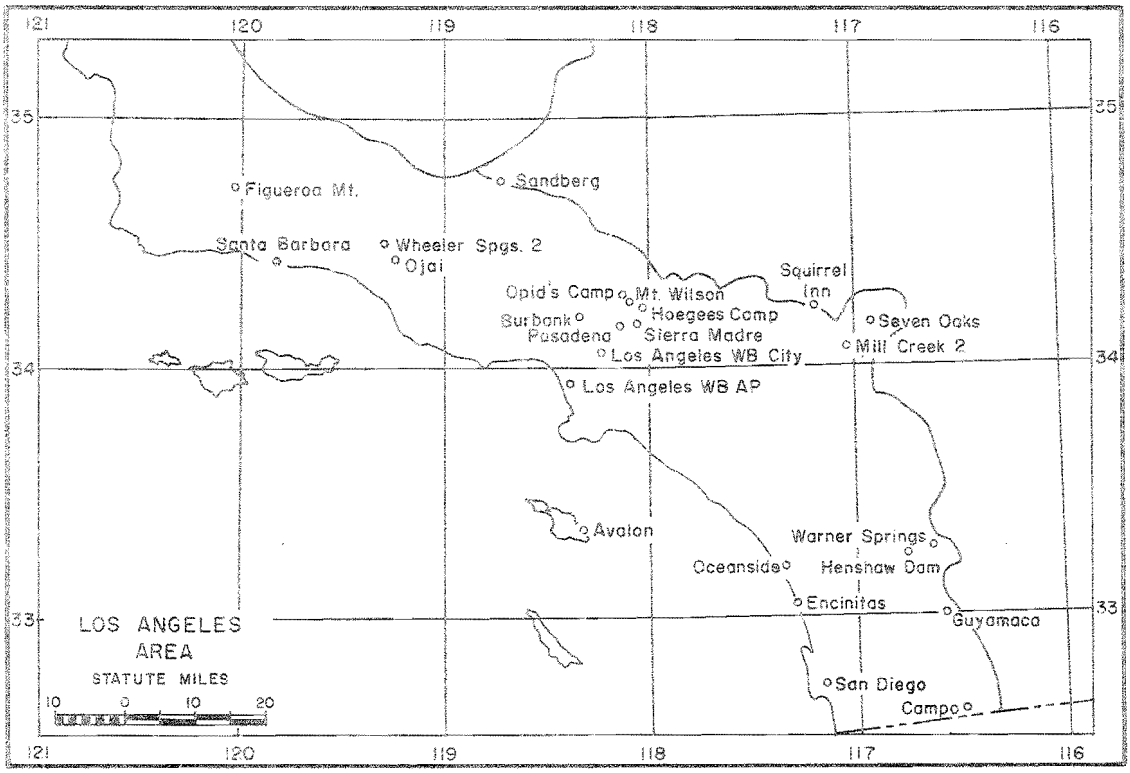

Fig. 2-25. LOCATION MAP OF SOUTHERN CALIFORNIA RAINFALL STATIONS

2-C. COMPARISON OF THE DECEMBER 1884 AND DECEMBER 1955 STORMS IN THE CENTRAL SIERRAS

Appraisal of storms on the basis of storm rainfall rather than on the basis of runoff may lead to a widely differing view of relative importance. This is largely because of differing antecedent conditions. A major precipitation storm following a dry and snowless period conceivably may not be listed in the record as a flood storm. The December 1884 storm is an example. The purpose of this section is to document the meteorological aspects of this early storm and account for the contrast in degree of flooding with that of other storms, particularly the December 1955 storm in which central Sierra rainfall was in some respects strikingly similar.

The synoptic sequence. The sequence of storms affecting the Pacific Coast from December 17 to 26, 1884 is shown by 8 daily 1200 PST maps (figures 2-26 and 2-27), part of a series drawn at 8-hour intervals. Maps for the 17th and 26th are not included. Rainfall amounts shown are for 8 hours ending at map time.

From the 16th to the 19th the polar front extended across the Pacific Northwest, thence south-southwestward offshore. Open waves on the front reached the coast and moved eastward across Oregon to the south of cold air over Washington and southwestern Canada. Passage inland of this frontal boundary on the 19th (figure 2-26) was followed quickly by an elongated occluded front which crossed the coast late on the 20th. Deepening of occluding waves to the southwest on the offshore portion of this front resulted in a series of three Lows reaching the coast (figure 2-27). The first, a deep Low, moved onshore in southern Oregon on the 22d, then rapidly eastward. Most streams in the Sacramento River Basin reached their peaks following passage of this Low. A weaker Low moved northeastward to the extreme Northern California coast on the 23d. On the 24th and 25th the third Low, a very deep one, moved northward just off the Northern California coast, thence slowly into western Oregon, maintaining a strong southwest flow of unstable air over Northern California into the 26th.

Referring to the map sequences (figures 2-26 and 2-27), it appears that the storm features were most characteristic of a southwesterly Mid-latitude type. Because the average latitude of the main polar front in this storm was relatively far south, with blocking farther north, the trend was for waves to move onshore more often than for deep occluded Lows to stagnate offshore, as is more typical of this type. The sequence from the 23d was similar to that of February 1-2, 1945 (figure 2-21).

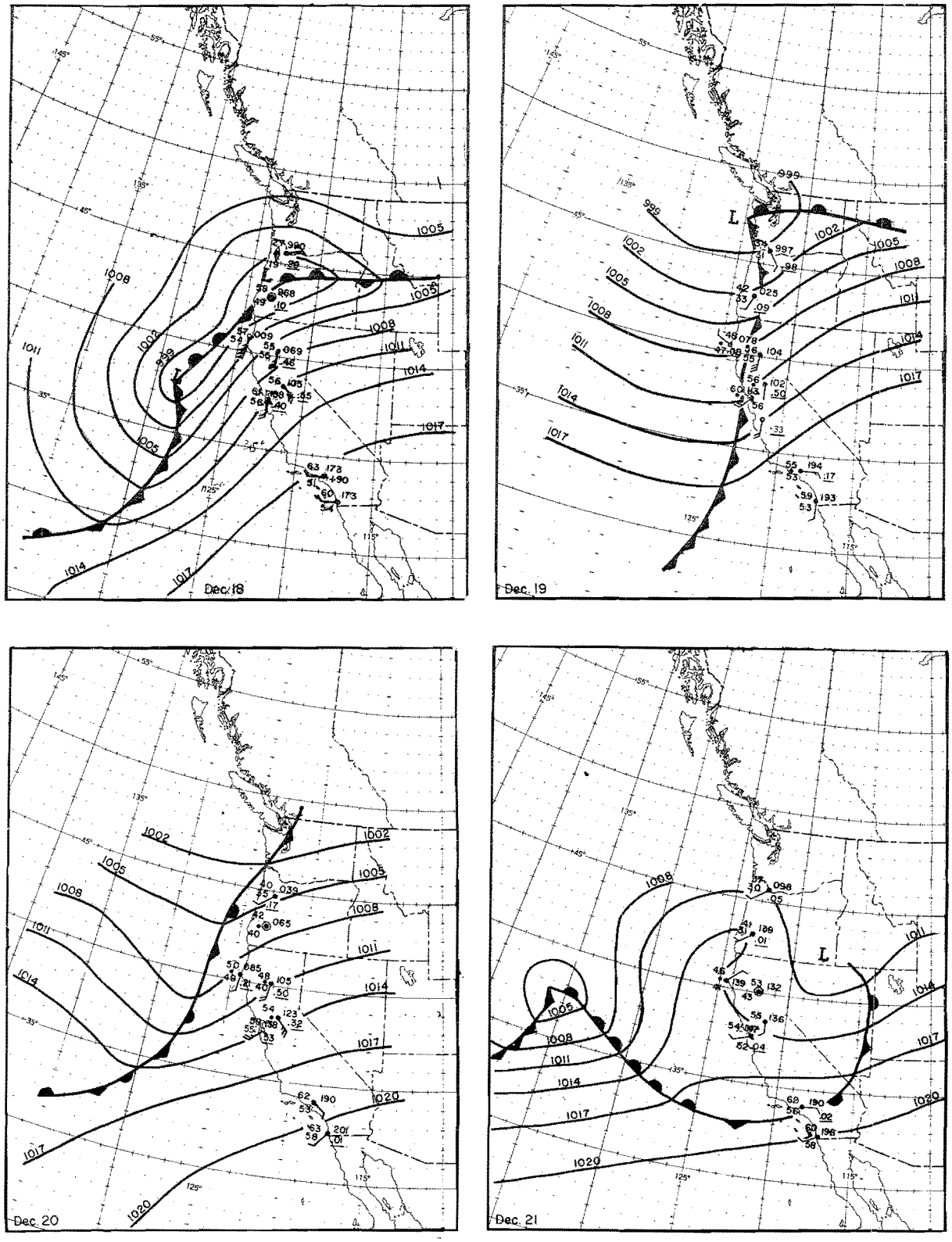

Fig. 2-26. SEA LEVEL CHARTS AT 1200 PST, DECEMBER 18-21, 1884

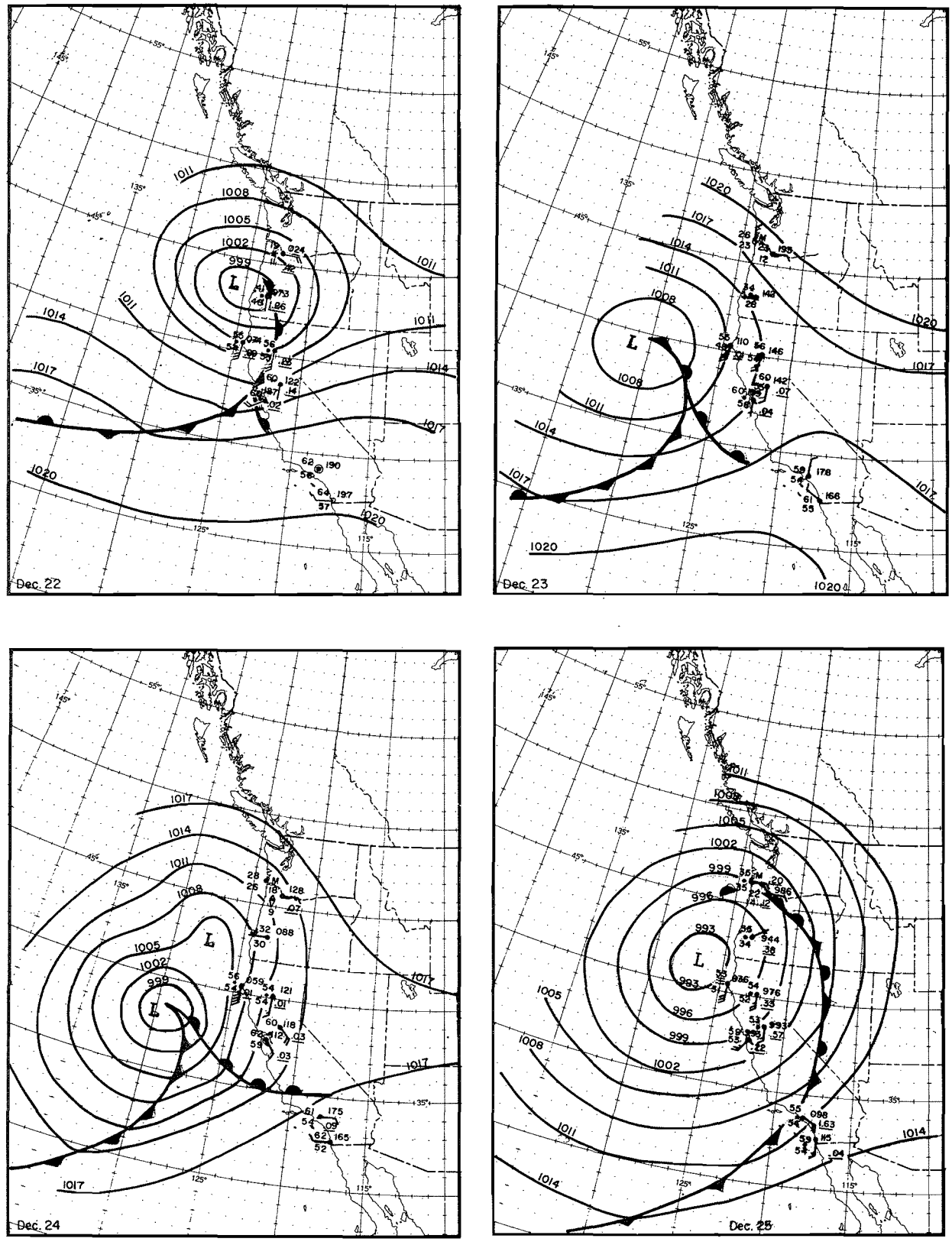

Fig. 2-27. SEA LEVEL CHARTS AT 1200 PST, DECEMBER 22-25, 1884

Rainfall comparisons. Table 2-7 compares rainfall for various durations in the 1884 and 14 other major storms at a representative moderate elevation Sierra location, Nevada City. This site is at an elevation of 2600 feet, about 60 miles north-northeast of Sacramento. The data for January 1862 were obtained by adjusting nearby Grass Valley data, using a ratio of 16-day totals at Nevada City and Grass Valley.

For 6- and 9-day periods the 1884 storm totals rank 4th and 2d, respectively. But for durations of 1 and 2 days the 1884 storm ranking is low while those of the 1862 and 1955 storms are high. For 6 days and less the 1884 storm values were roughly 2/3 of the 1955 storm values.

Table 2-7

ACCUMULATED PRECIPITATION (INCHES) AT NEVADA CITY, CALIFORNIA IN 15 MAJOR STORMS FOR 1, 2, 3, 6 and 9 DAYS AND RANKING OF THE DECEMBER 1884 STORM

Storm	1-day	2-days	3-days	6-days	9-days
Dec. 1955	5.8	9.6	12.5	22.9	26.1
Nov. 1950	4.6	7.5	9.5	16.6	17.6
Jan.-Feb. 1945	4.6	8.2	10.1	10.8	11.5
Jan. 1943	5.2	8.7	10.9	12.1	14.5
Feb. 1940	4.4	7.6	10.0	12.3	12.7
Dec. 1937	4.7	8.7	9.8	9.9	9.9
Dec. 1929	4.1	7.3	7.8	13.3	15.7
Mar. 1928	3.7	6.1	8.2	12.7	12.8
Dec. 1913-Jan. 1914	6.0	7.6	8.8	10.8	11.0
Jan. 1911	4.1	5.4	7.9	10.7	15.8
Jan. 1909	4.5	7.7	10.7	13.0	17.5
Mar. 1907	3.6	7.0	9.4	12.2	17.2
Jan. 1906	3.7	6.7	8.0	13.6	19.0
Dec. 1884	3.5	6.7	9.6	15.2	24.9
Jan. 1862	6.2	11.4	14.7	16.9	19.7
Dec. 1884 Rank	15th	12th	8th	4th	2d

Figure 2-28 compares the 1884 and 1955 storm rainfall sequences at Nevada City. While the mass curves are similar, that of the 1955 storm has a steeper slope through the 23d, an important factor with respect to peak runoff.

Representativeness of Nevada City rainfall data, in terms of area, is tested in figure 2-29 by comparison of 15-day totals for the 1884 and 1955 storms. Data are primarily from the American and Yuba Basins to the northeast of Sacramento at elevations up to 6000 feet. Nevada City is point 9. Most low-level foothill locations (points 1-4) and stations east of the Sierra summit (points 14 and 15) had greater 1955 storm totals; at windward locations above 1300 feet (points 5-13) greater 1884 storm totals predominated.

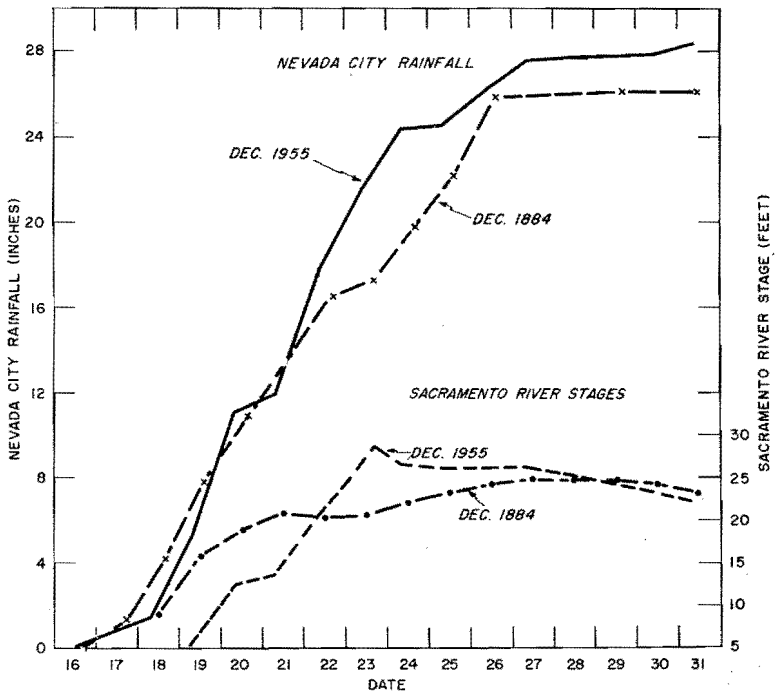

Fig. 2-28. CUMULATIVE RAINFALL AT NEVADA CITY AND RIVER STAGES AT SACRAMENTO IN THE DECEMBER 1884 AND DECEMBER 1955 STORMS

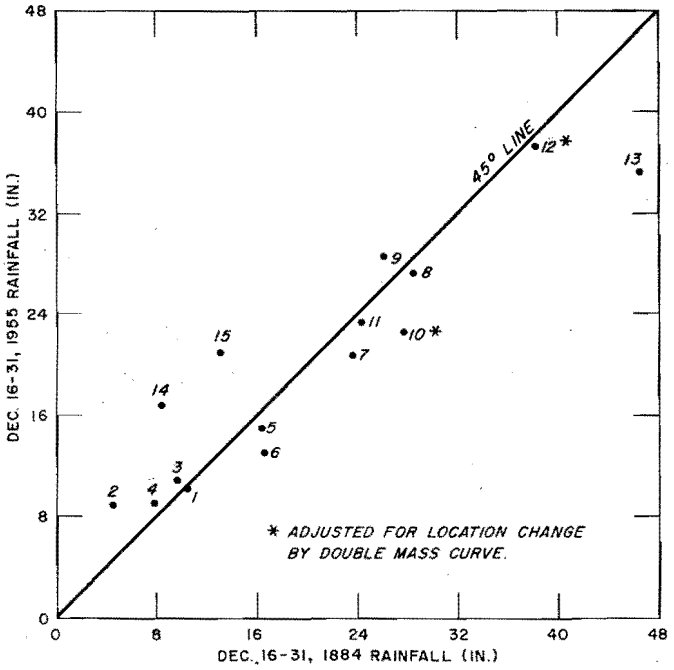

Fig. 2-29. COMPARISON OF STORM RAINFALL AT 15 CENTRAL CALIFORNIA LOCATIONS FOR THE PERIODS DECEMBER 16-31, 1955 AND DECEMBER 16-31, 1884

This trend toward higher 1884 than 1955 storm totals at higher elevations is especially evident at Bowman Dam (point 13, figure 2-29), elevation 5347 feet. Double mass curves validate the comparison. Table 2-8 shows that, even for durations of 1 to 3 days, 1884 storm amounts at higher elevations were comparable to 1955 storm amounts and rank very close to it in the list of storms of table 2-7.

Table 2-8

ACCUMULATED HIGHEST PRECIPITATION (INCHES) FOR 1, 2, 3 and 6 DAYS AT BOWMAN DAM IN THE 1955 AND 1884 STORMS

Storm	1-day	2-days	3-days	6-days
Dec. 1955	9.9	16.3	21.4	28.0
Dec. 1884	7.6	14.5	18.9	33.8

Moisture and wind comparisons. The moisture in this storm was apparently not much less than that in the December 1955 storm. The highest 3-day average dew point at San Francisco was 57°F in both storms. The component of flow normal to the Northern Sierra and Coast Ranges was less in the 1884 storm than in the 1955 storm. This conclusion is supported by a comparison of highest 3-day average sea-level pressure difference between Red Bluff and Sacramento (2-mbs in the 1884 storm versus 5-mbs in the 1955 storm) which exaggerates the actual difference in flow.

Comparison of snow behavior. Comparative data in figure 2-30 suggest that the 1955 storm snowmelt in the Yuba River Basin was about as great as in any other major storm of this century. Initial and final snow depths at approximately the 5000- and 7000-foot elevations are plotted for major Northern California storms. It can be assumed that snowmelt contributed to runoff through a considerable range of elevation in storms in which snow depth decreased at both elevations (Jan. 1909, Dec. 1913-Jan. 1914, Nov. 1950 and Dec. 1955). The initial snow depths and the high freezing level of the 1955 storm permitted the 4000-7000 foot range of elevations to contribute to runoff. This range involves a large percentage of the total area of some Northern Sierra basins.

In contrast to the 1955 storm, snowmelt did not contribute in the 1884 storm which followed a 9-week period of dry weather in the Northern and Central Sierras. Infiltration was a significant factor in the early part of the storm.

There was no significant difference in the relative contributions of snow and rain during the two storms. Comparison of temperature data at Sacramento and at several central Sierra locations in the two storms indicates that the snow level was only slightly lower in the 1884 storm.

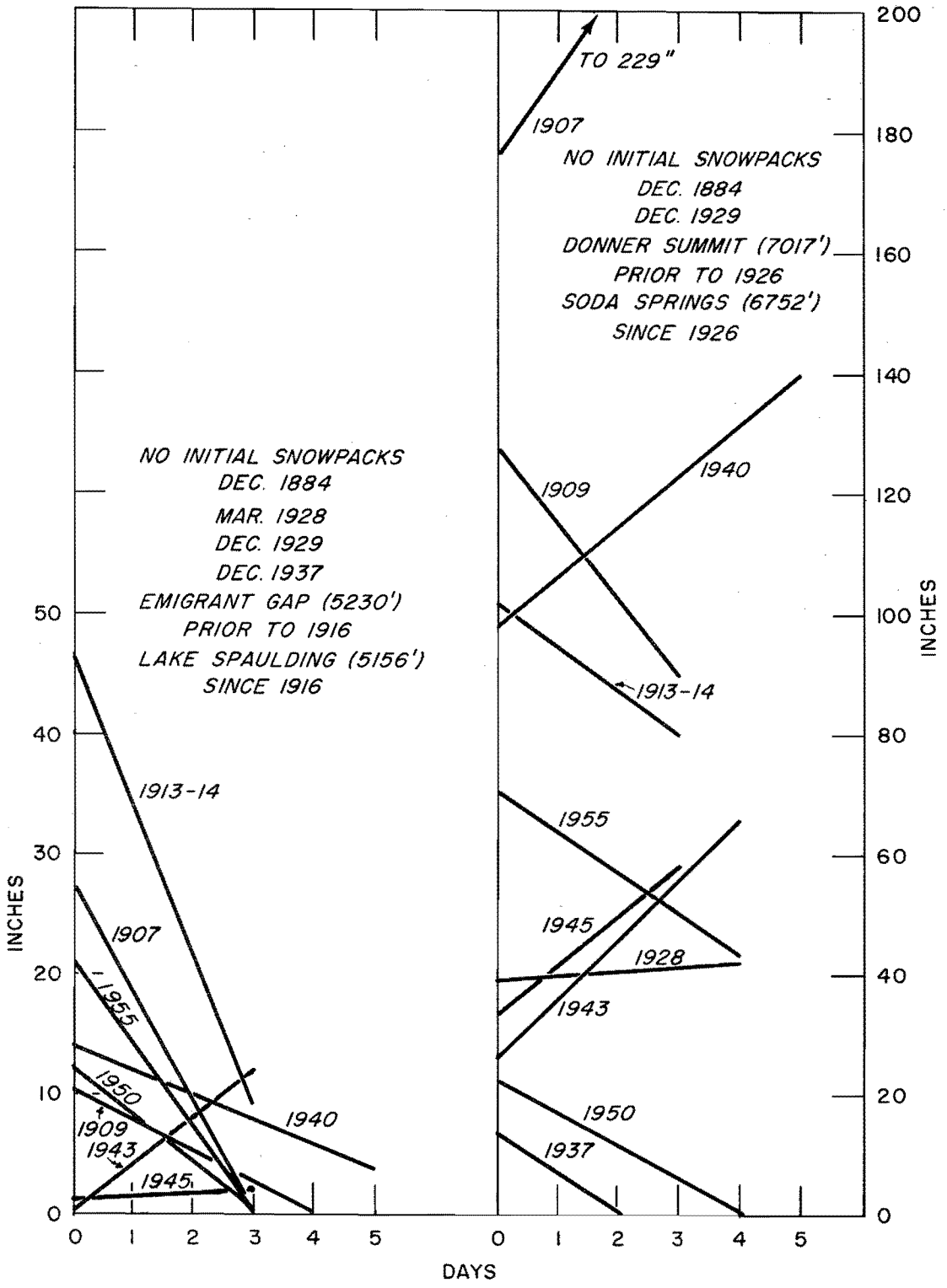

Fig. 2-30. SNOW DEPTHS PRIOR TO AND NEAR END OF MAJOR STORMS NEAR 5000-ft AND 7000-ft LEVELS ON THE YUBA RIVER BASIN

Runoff comparisons. Comparison of the December 1884 and December 1955 storm runoff is attempted, particularly on the Yuba and Sacramento Rivers. It is recognized that stage heights cannot be compared directly because of changes in channel conditions, both natural and man-made. Hydraulic mining around the time of the 1884 storm raised certain stream bed elevations, partially corrected by nature in later years. Also construction of levees in the flood plain have increased stream channel capacity and bypasses have reduced the percentage of runoff that some streams carry; on many streams upstream storage has reduced runoff in later years.

December 1884 records reveal the following information. The Yuba River at Marysville reached a stage about 1 foot below some previous high water mark but 5 feet below top of levees on the 22d and 23d. Train service was interrupted near there on the 23d. High water was reported on the American and Consumnes Rivers on the 22d, the Feather River on the 23d and the Truckee River on the 24th but no flooding of consequence was reported. The Sacramento River stage at Sacramento (figure 2-28) reached a flat peak near the end of the storm, with an earlier peak on the 21st reflecting rain early in the storm in the north part of the basin. Neither peak approached the top of levees.

In the 1955 storm, stages on the Sacramento River at Sacramento (figure 2-28) were reduced by upstream storage early in the storm and later by bypasses which just after peak flow on the 23d carried 3/4 of the total flow. Thus the 1955 storm peak flow there was far greater than indicated by peak stage, which exceeded that in the 1884 storm.

Conclusion. The December 1955 storm peak runoff far exceeded the December 1884 storm peak runoff, not only on the Sacramento but on other streams. This was due to 3 factors. Watersheds were primed by previous rains in the 1955 storm but were dry prior to the 1884 storm. Snowmelt was inappreciable in the 1884 storm compared to that in the 1955 storm. There were periods of rainfall in the 1955 storm that were more intense and more closely spaced than in the 1884 storm.

The data presented above indicate that had antecedent conditions in the 1884 storm been comparable to those in the 1955 storm, the former would have been known for serious flooding on most major central Sierra streams, though not to the extent of the 1955 flood.

2-D. SYNOPTIC HISTORY OF COOL-SEASON STORMS INVOLVING INTENSE LOCAL CONVERGENCE PRECIPITATION

Statistical analysis provides one measure of heavy convergence precipitation in California. In the areas of the state which are relatively free from orographic effects and where precipitation is thus essentially convergent, 24-hour point precipitation amounts with a 100-year return period are of the order of 4 to 5 inches (4). Most of the largest observed 24-hour amounts in such areas in the cool season during the last 100 years are in this range and are contained in the list of convergence storms with orographic storm characteristics on figure 4-7 of HMR 36. Amounts are considerably higher in two storms listed on figure 4-8 of HMR 36, at Sacramento in the April 1880 storm and at San Francisco in the December 1866 storm.

Features of the high local convergence precipitation in these two storms are explored in this section and the storms are compared with recent major orographic storms in order to make the following points: First, the similar onshore stagnation of Low centers localized 24-hour convergence precipitation in the two storms to a greater extent than occurs during storms yielding extreme rainfall up to high elevations. Secondly, this behavior was, in turn, associated with the storms' similar offshore track from northwest (and limited moisture and high instability). This track is not typical of those storms listed on figure 4-7 of HMR 36.

Warm-season storms with extreme convergence rainfall intensity for short time intervals are discussed in chapter VI.

2-D-1. The April 19-21, 1880 storm

This storm was severe over north-central California. The area with both high intensity of precipitation and lengthy duration was smaller than in most major storms and the snow level was lower. The unusually heavy convergence rain in the storm, with 7.24 inches at Sacramento in 22 hours, is the feature which is of greatest interest in relation to the synoptic history of the storm.

The general storm. A composite map of Low center tracks (figure 2-31a) and seven sea-level pressure charts at 8-hour intervals (figures 2-31b through h) illustrate the storm sequence. Observation time is 0400, 1200 and 2000 PST except at stations where the pressure is enclosed in parenthesis, where the times are 0700, 1400 and 2100 PST, respectively. Pressure change and precipitation are since the previous observation. Isallobaric centers are shown as dashed lines.

The storm under discussion was preceded by a less intense storm 2 to 3 days earlier. In both a Low reached California from the northwest. Presumably the second Low formed in or moved southeastward across the Gulf of

Alaska in a manner similar to that of major High-latitude type storms. The track of this Low was southeastward offshore to about the latitude of Central California, then northeastward toward the Northern California coast on the morning of the 20th (figure 2-31b) and inland southeast of Eureka by noon (figure 2-31c). The frontal system was then approaching Sacramento and the heavy precipitation period had begun there. Soon after the frontal passage pressures began falling again. While the Low center continued to deepen slowly, it moved southeastward during the afternoon and night to within 100 miles of Sacramento by 0400 PST of the 21st (figure 2-31e).

By this time the rain at Sacramento was becoming less intense. The Low reversed direction toward northwest and surface pressures rose over all of Northern California, rises which continued for two days as the Low filled and was replaced by a weakening stationary trough near the coast (figures 2-31f through h). Meanwhile pressure rises in the San Joaquin Valley on the 21st were relatively small. This resulted in formation there of a weak Low by noon (figure 2-31f) which moved slowly southeastward (figures 2-31g and h), causing showers over the southern third of California.

The Sacramento precipitation sequence. The mass curve of figure 2-32 is based on rain gage measurements together with descriptions of rain intensity between measurements. The 1.99 inches (burst 1), 1200-1400 PST of the 20th, was associated with passage of the frontal system. The heavy rain periods, 1800-2000 PST (burst 2) and 2340-0200 PST (burst 3), are presumed to have been due largely to ageostrophic convergence (defined in chapter 5-A-2) in a falling pressure field, indicated by both the isallobaric Low shown near Sacramento at 0400 PST on the 21st in figure 2-31e and the southeastward motion of the isobaric Low prior to this time. Local release of instability probably contributed much to the high 22-hour intensity, although the nearest thunderstorm report in this period was at Downieville, in the Sierras to the northeast. The accumulation from the "bursts" or peaks in rain periods mentioned above and rain in the interim was 4.15 inches in 8 hours to 2000 PST and 2.20 inches in the following 8 hours. Rain ended at 1000 PST of the 21st; light showers fell on the 22d.

Wind and moisture. Surface pressure gradients verify that winds were strong on the 20th over Northern California and both there and over Central California that night, weakening on the 21st. Velocity reached 32 mph at San Francisco and 40 mph at Red Bluff on the 20th. Because the initial offshore track of the Low was from a higher latitude, its moisture was quite low. The 24-hour average dew point at San Francisco during the heavy rain at Sacramento was only 50°F; it was 57°F during a comparable period in the December 1955 storm when surface dew point probably underestimated precipitable water more than in this storm. The snow level at reporting stations on the rail line from Sacramento to Reno across the northern Sierras, initially at 3500 feet, reached the 5700-foot level briefly on the morning of the 21st. At Blue Canyon (elevation 4700 feet) snow turned to rain for 13 hours. Extremely heavy snowfalls were reported from 5000 feet to the Sierra pass at 7000 feet. In the December 1955 storm the snow level was 4 to 6 thousand feet higher. Hence the elevation of greatest orographic rainfall was much lower in the 1880 than in the 1955 storm.

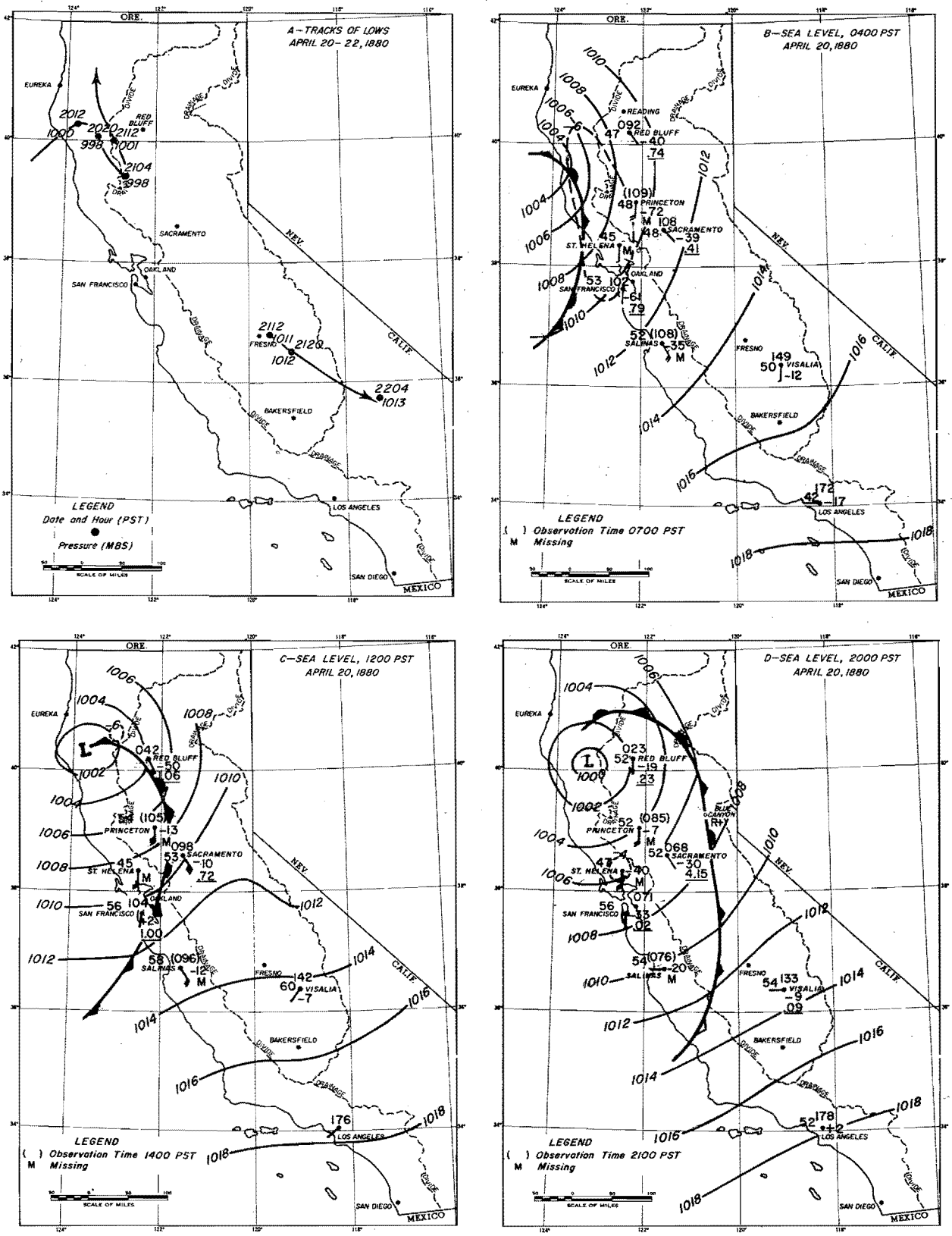

Fig. 2-31. THE APRIL 1880 STORM

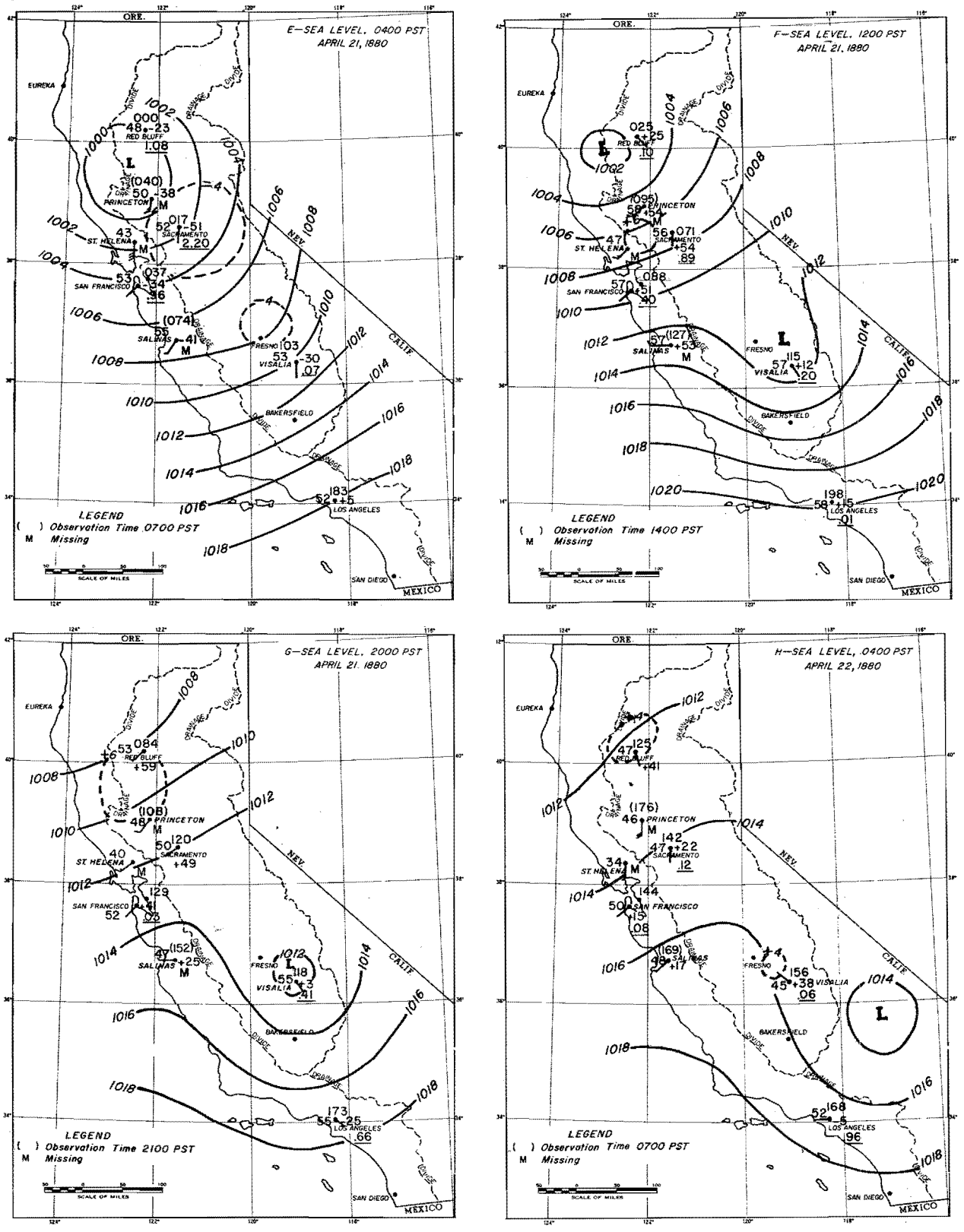

Fig. 2-31. (CONT'D.) THE APRIL 1880 STORM

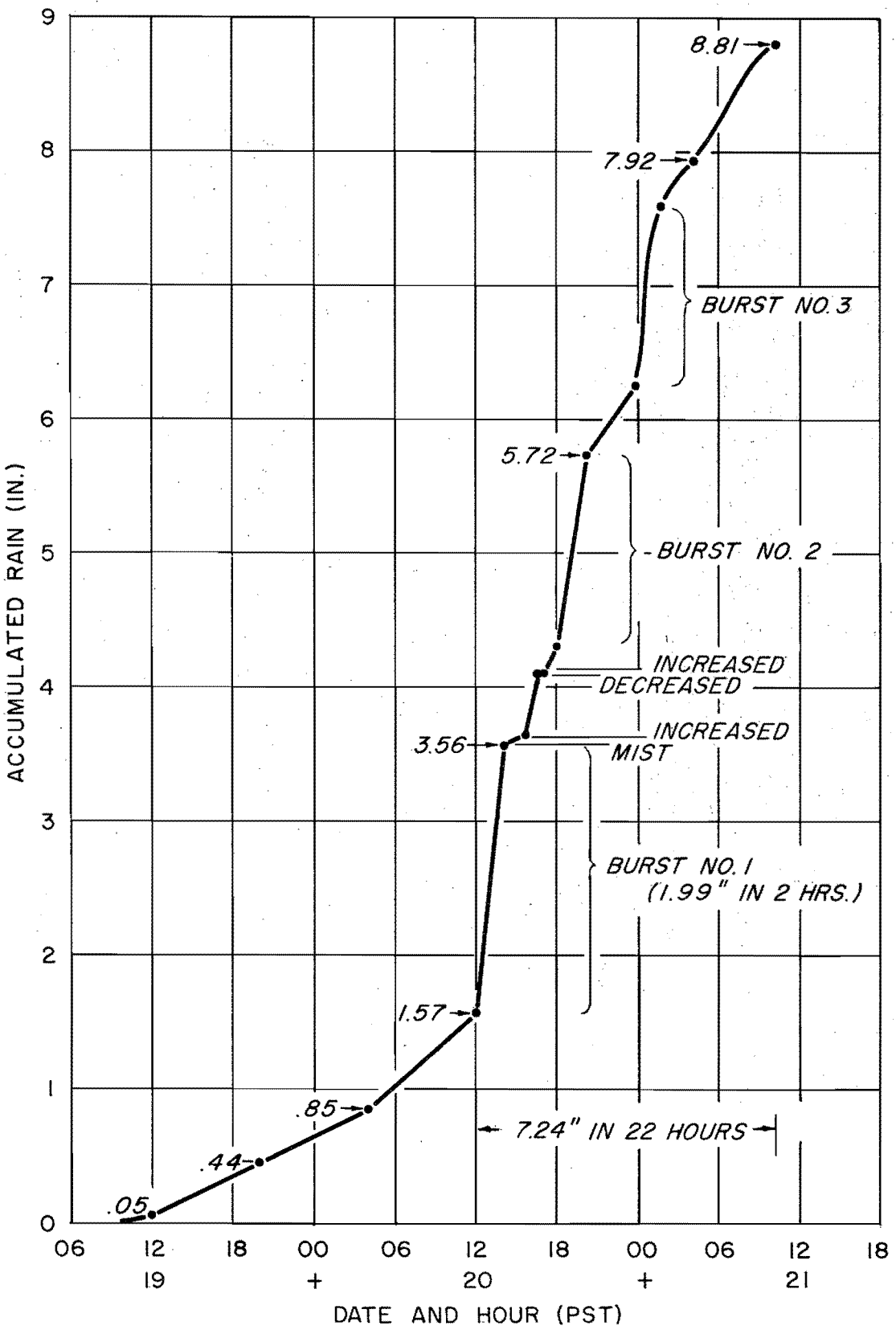

Fig. 2-32. SACRAMENTO MASS CURVE, APRIL 19-21, 1880

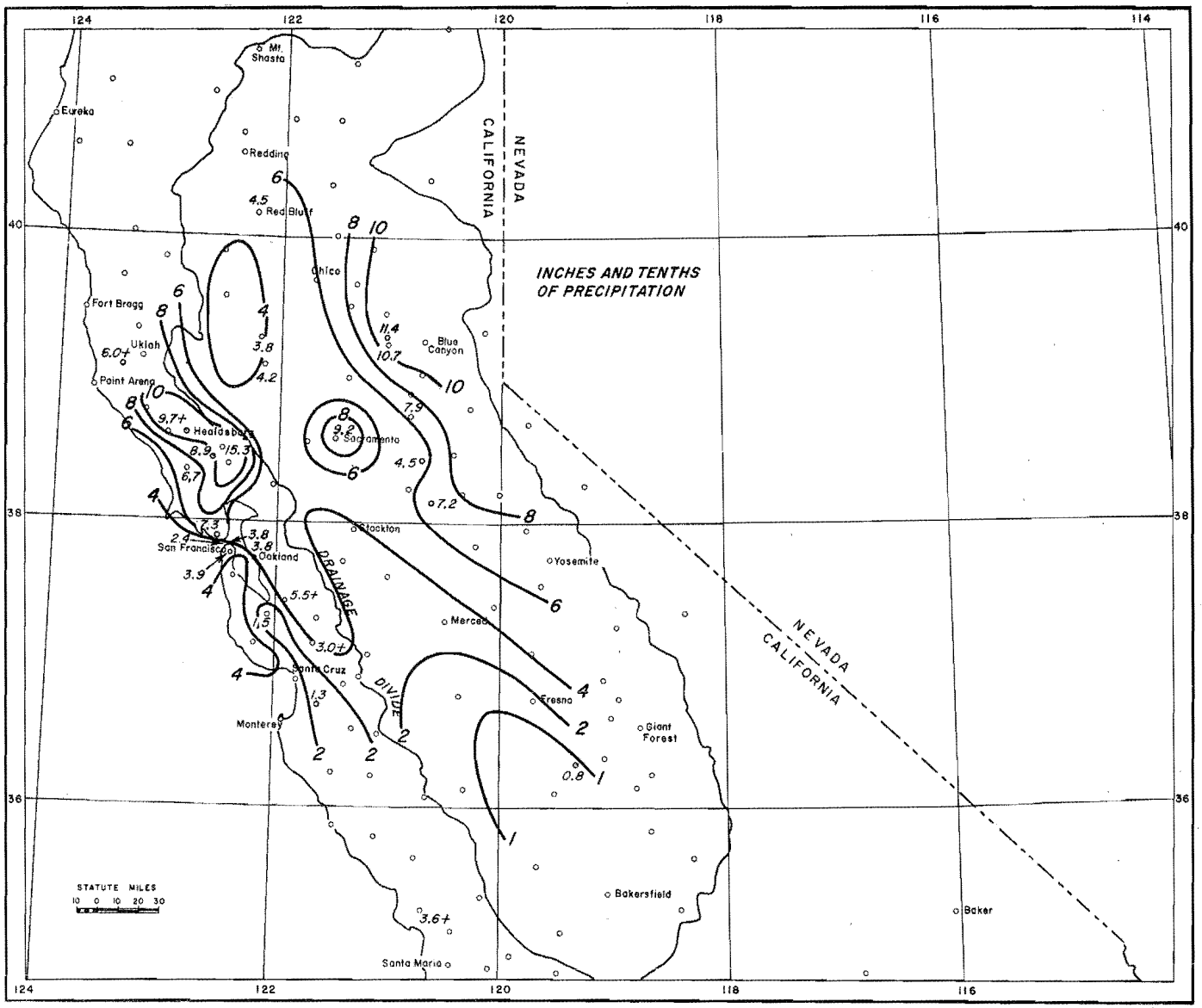

Fig. 2-33. STORM ISOHYETS, APRIL 19-22, 1880

Precipitation and streamflow. Storm isohyets are shown in figure 2-33 in areas where data are available. In addition to the local center at Sacramento, two areas of heavy rainfall attributable largely to orographic effects are shown. One is in the northern Sierras, the only observations being at about 2600 feet; the other is in the coastal mountains north of San Francisco.

Table 2-9 compares 3-day rain at the few places that determine the above two areas with 3-day rain at the same locations in the December 1955 storm. The 1955 storm values are not much larger. But this table reflects orographic rainfall at low elevations; at elevations above the average basin height in the Sierras rainfall was inappreciable in the 1880 storm, the precipitation nearly all falling as snow. (Because in the 1880 storm 3 days elapsed since its predecessor compared to 1 day in the December 21-23, 1955 storm, 6-day totals at stations in table 2-9 were much smaller in the 1880 storm.)

Table 2-9

COMPARISON OF 3-DAY PRECIPITATION (INCHES) IN THE APRIL 1880 AND DECEMBER 1955 STORMS

Northern Sierra Foothills	1880	1955
Nevada City	11.42	12.50
Grass Valley	10.28	12.89
Coastal Hills north of San Francisco		
St. Helena	8.88	9.08
Healdsburg	9.72	7.46
San Rafael	7.34	9.82

Streamflow reports indirectly verify reports of heavy rain at low elevations in the storm area. Most of the smaller low-level streams from Chico southward to beyond Merced in the Central Valley and all coastal streams from Ukiah to Santa Cruz were full or flooding. (See figure 2-33 for station locations). Most serious flooding was on streams flowing south and east from the coastal mountain area of high rainfall of figure 2-33. But main Sierra streams draining higher levels were not very full because of the heavy snow and low snow level in both this and the prior storm period. Reports of Sierra streams disappearing as snowslides filled stream beds at higher elevations indicate the effect of low temperature in reducing immediate runoff.

2-D-2. The December 18-21, 1866 storm

This storm is of interest because of its intensity over north-central California and especially in San Francisco where 7.66 inches was measured in 20.5 hours on the 20th to 21st. The hilly terrain there affected rainfall intensity. Comparison with that at Sacramento in the 1880 storm can be made only after allowing for this effect, which adds about 30 percent to average monthly precipitation. (This has been done in figure 4-8 of HMR 36.)

The general storm. As in many major storms, this storm occurred in two periods with an interlude of almost a day, except less in mountain areas. Like the April 1880 storm, the direction of approach of Lows offshore was from the northwest, as shown in figure 2-34, with a sharp change in direction near the coast.

The first Low approached the coast southeast of Point Arena on the night of the 18th with a 1008-mb center which moved northward during the 19th and filled rapidly. This track, determined from thrice-daily synoptic charts (not shown), is verified by the ending of the brief period of heavy rain

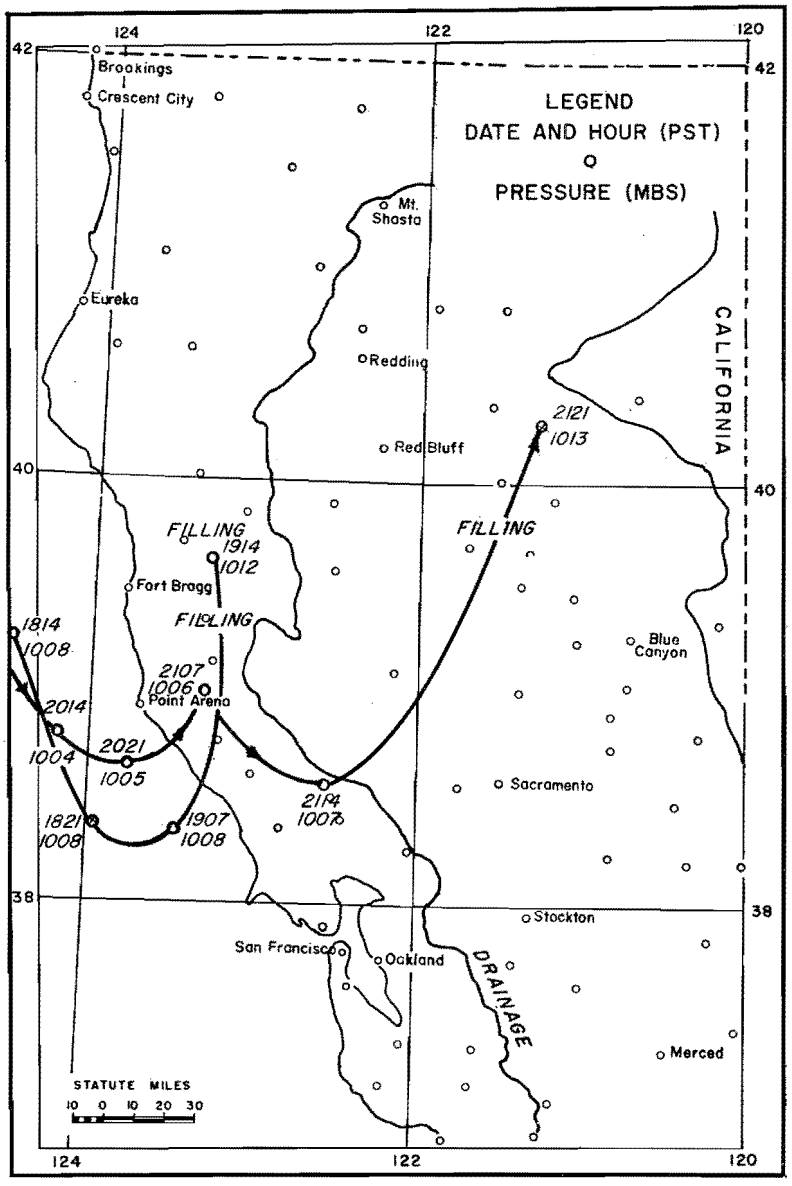

Fig. 2-34. TRACKS OF LOWS IN THE DECEMBER 18-21, 1866 STORM

along the north coast shortly after time of beginning in the San Francisco Bay region. The frontal system passed northeastward through the Bay region about 0500 PST of the 20th with gales, heavy rain and scattered thunderstorms, leaving as much as 4.28-inch 24-hour amounts.

The second Low also approached from northwest, as indicated by synoptic maps and start of heavy rain on the north coast on the afternoon of the 19th. It entered the coast southeast of Point Arena during the night of the 20th with a 1006-mb center which moved northeastward then southeastward to a point 50 miles north of San Francisco during the morning of the 21st before moving rapidly northeastward during the afternoon and filling. Rain with this Low was more widespread than with the previous Low; it lasted longer, fully two days in the extreme north. The frontal system with this Low passed through Central California on the evening of the 20th, preceded by southeast gales and heavy rain. Thunderstorms occurred both ahead of and following the front, as well as on the 21st.

The area of the storm was restricted, more than in most major storms, by the nearly identical track of the two Lows. The centering of the Lows over the coastal area resulted in winds less nearly normal to the Sierras than in most major storms. But strength of surface geostrophic winds in the Bay region approached values in the December 1955 storm. Low temperatures restricted rain at high elevations much more than in some major storms but less than in the 1880 storm. Based on 1866 storm temperatures 2° or 3°F higher, the snow level is assumed to have been about 1000 feet higher than in the 1880 storm. The role of instability in this storm reduced differences between high- and low-elevation precipitation totals since it was released with minimum orographic lifting.

Precipitation measurements were too sparse to permit drawing storm isohyets. However, some idea of storm rainfall can be obtained through streamflow reports. Little flooding occurred with the first Low. Streams receded following the break in the storm on the 19th. But on the night of the 20th and on the following day very high flows were experienced following the second Low on coastal streams from Healdsburg to Santa Cruz and low-level Central Valley streams from Chico to Sacramento (see figure 2-33 for locations). Several of these streams had flows higher than in the major storm of January 1862 (2). Also the Yuba, American and upper Sacramento Rivers approached flood stage briefly despite negligible runoff from high levels due to the low snow level and prior snowpack.

Storm rainfall in San Francisco. Six records of rainfall in San Francisco mutually substantiate the heavy rainfall there. They are shown as estimated mass curves for the second rain period only, in figure 2-35. Their shape is patterned after that of the most detailed curve (16th and Mission), along with reported beginnings and endings and incremental amounts. Except for the 16th and Mission location, all are along the waterfront on the north edge of the city or in the Bay. Wide variation in rainfall totals between stations only 1 or 2 miles apart is evidence of the large role of instability and variation in its release by the hilly terrain. But the rather continuous

nature of the 16th and Mission rainfall and the changing pressure pattern indicate that ageostrophic convergence was also an important factor. It was especially so during the most intense period of rain of the 20th when 2.27 inches fell in the 3 hours ending 1945 PST, an amount which compares with highest 3-hour amount at Sacramento in the 1880 storm. It fell prior to and during the frontal passage. Though no thunderstorms were reported in the city at this time, they were reported in surrounding areas to the south, east and northeast. On the 21st only one thunderstorm was reported in the city, briefly at the end of the rain period, although there were reports of frequent thunder to the south.

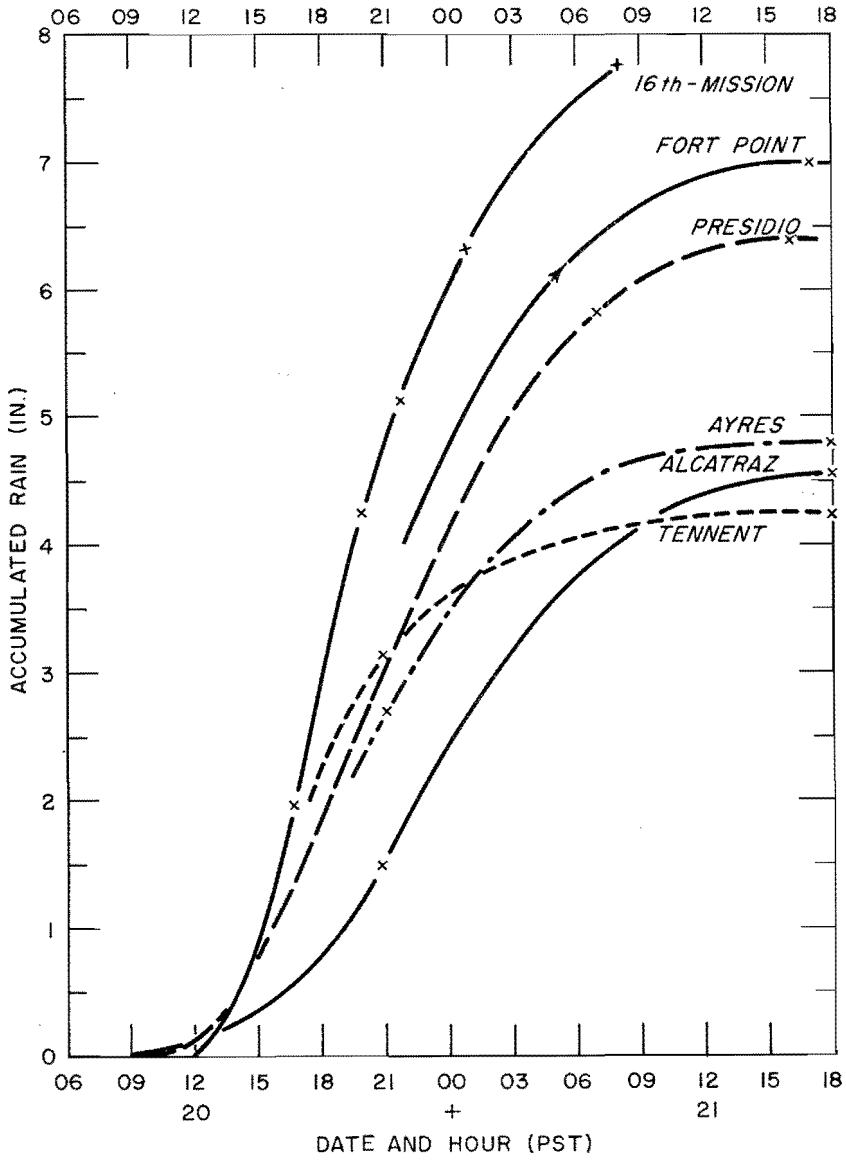

Fig. 2-35. MASS CURVES OF SAN FRANCISCO RAINFALL, DECEMBER 20-21, 1866

Information on San Francisco rainfall in figure 2-35 comes from observation forms, with the exception of the 16th and Mission curve which was listed in the December 21, 1866 issue of the local newspaper, "The Evening Bulletin", as follows:--

Date and Hour	Rainfall (Inches)
201145 - 201645 PST	1.97
201645 - 201945 PST	2.27
201945 - 202150 PST	0.85
202150 - 210100 PST	1.20
210100 - 210815 PST	1.47
Total in 20.5 hours	7.76

2-D-3. The Avalon storm of October 21, 1941

This storm is listed here because, like the prior storms, it involved unusually heavy local precipitation in a general storm whose offshore track was toward lower latitude. Unlike the other storms, heavy rain was less clearly associated with a nearby surface Low than with release of instability, in this case in a relatively much shorter interval. 5.53 inches of rain fell in 3-1/2 hours at Avalon, on the southeast shore of Santa Catalina Island.

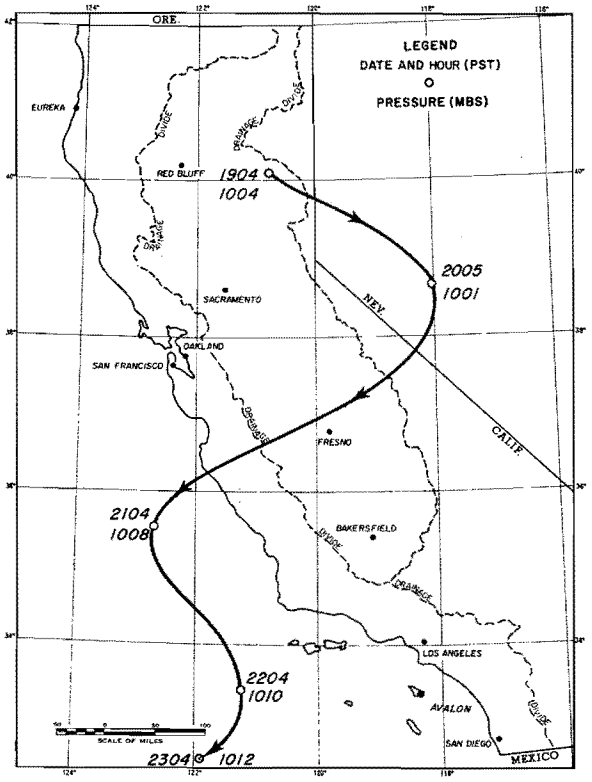

Fig. 2-36. TRACK OF SURFACE LOW IN OCTOBER 19-24, 1941 STORM CENTERED AT AVALON

The general storm. The storm took place during a prolonged shower period of 3 to 4 days' duration over the southern third of California. Storm totals in Southern California averaged only 2 to 4 inches with much less over the southeastern interior. They were not much larger in mountain than over low-level areas, indicating little orographic effect.

The shower period developed as an upper cold Low formed over Northern California and moved erratically southward from the 20th to the 23d, following passage of a weak cold front from northwest on the 19th. Positions of the reflected surface Low are shown in figure 2-36.

Relatively cool air of limited moisture content at intermediate levels in the storm is indicated by the report of a trace of snow at Sandberg (elevation 4500 feet) with a temperature of 36°F on the morning of the 21st. Evidence of instability is found in reports of hail at Lake Arrowhead and Avalon on the 20th and of scattered thunderstorms on the 22d. The offshore water temperature (normal for the date, 63°F) contributed to instability.

The local storm. Rainfall at Avalon, centered on the morning of the 21st, was as follows:

Date and Hour	Rainfall (Inches)
210300 - 210700 PST	.68
210700 - 211030 PST	5.53
211030 - 220700 PST	1.22
220700 - 230700 PST	.26
230700 - 240700 PST	.18

It is likely that a thunderstorm occurred during the heavy rain, although this is not confirmed. At this time the Low was west of Santa Maria. Surface winds near the Southern California coast were light southeasterly. Rain did not occur along the coast until later.

Surface dew point during the heavy rain is believed to have been about 54°F. (This estimate is 1°F lower than the minimum temperature, which probably occurred during the heavy rain. It is 3°F higher than the concurrent Sandberg reduced temperature and is equal to highest dew point during the day at San Diego and Los Angeles.) A 54°F dew point gives an extremely high 3.5-hour P/M ratio of 5.4. P/M ratio is an index of convergence as discussed in chapter 5-D.

Chapter III

MOISTURE TRANSPORT AND ITS COMPONENTS

Major precipitation storms at middle latitudes must be supported for the duration of the storms by a strong transport of moisture from a warm ocean region. This chapter will describe the manner in which moisture is transported from the source regions to the California coast, and will deal with the synoptic aspects of windflow and of atmospheric moisture, and of their combination into moisture transport. Illustrations are given from recent major storms.

3-A. WIND

Certain preferred directions as well as moderate or high speeds at low levels are characteristic of winds approaching the coast in major storms. These are conditions requisite to a deep moist flow from a low-latitude source region.

Discussion of wind is partly in terms of the geostrophic value over the coastal waters rather than the actual velocity since many of the facts about moisture transport can be ascertained from conventional weather maps on which isobars (or contours of equal height) are the most prominent feature. In a shallow layer near the coast the actual wind direction is essentially parallel to the coast regardless of the geostrophic direction, but the sea-level isobars indicate the predominant flow both over the open sea at all levels and at the coast above the surface layer of greatest friction and mountain impedance. Other departures of the wind from geostrophic, which are important for several reasons, will be discussed in chapters IV and V.

3-A-1. Wind direction

The most effective geostrophic inflow wind direction for moisture transport at the coast and offshore is southwest. In some of the most persistent and intense storms the southwesterly current extends for as much as two thousand miles, providing a direct transport from source region of air in which dew points may exceed the ocean surface water temperature at the coast by 10°F or more (3-B-3). December sea-surface temperatures are shown in figure 3-1. A flow directly from the south is usually less favorable for moisture transport than from southwest because this air has likely undergone subsidence or is of recent continental origin. On the other hand, the more westerly the flow approaching the coast, the greater likelihood that the air is of recent polar origin which will contain less moisture than polar air with a longer trajectory at lower latitudes.

There is some variation of direction of the axis of moist coastal inflow with storm type. The Low-latitude type most favors an effective southwesterly flow from a distant source region as pointed out in chapter II. A south-southwest direction is more typical of the Southerly Mid-latitude type

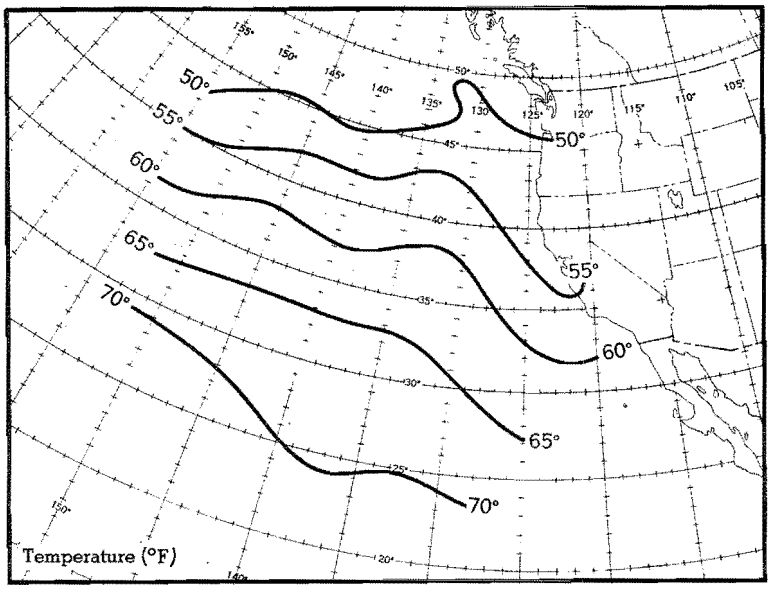

Fig. 3-1. DECEMBER SEA-SURFACE TEMPERATURES (AFTER ROBINSON)

in which occluding waves move northward off the coast, and of High-latitude type storms in which a persistent offshore trough has a north-south orientation. Relatively dry air from a westerly direction is particularly noted in Westerly Mid-latitude type storms, especially in weak ridges between individual occluding systems. In some Low-latitude type major storms a westerly direction appears temporarily at the coast without seriously restricting moisture, when deep Lows penetrate the northern plateau. Here the track of the moist flow is from a low latitude but turns anticyclonically and becomes westerly near the coast.

Variation with height. A feature of geostrophic wind direction near the coast in major storms is its relative constancy with height. Thus it is possible to discuss inflow wind direction without close specification of the level. Variation in wind direction with height is least during the main part of a major storm. There is a broad area of warm air in which the thermal wind is weak or tends to be oriented parallel to the surface geostrophic wind. What variation in direction does occur is usually a veering with height early in the storm in association with warm air advection at lower levels and a backing with height near the end of the storm as low-level cold air advection begins. This backing with height is often reduced to a minimum by persistence of a low-level trough offshore. This generalization of wind direction variation applies both to individual trough or wave passages and to the total storm period.

Height variation of wind direction is illustrated for the December 1955 storm by actual winds at various levels at Oakland in figure 3-2. Least variation is near time of heavy rain and high low-level windspeed.

3-A-2. Windspeed

Except for lowest layers subject to turning of wind by friction and terrain, high windspeeds at the coast, oriented more or less normal to the main California mountain barriers, are characteristic of major storms. This is seen in the strong onshore winds during heavy rain periods at Oakland in the December 1955 storm (figure 3-2). It is seen also with respect to the onshore component of the geostrophic wind over a broad sector of the coast several hundred miles in width in figures 3-3a to e. (In these figures are plotted average geostrophic wind normal to the coast, integrated from surface to 500 mbs and expressed as an average windspeed. Values are shown for the segments Oakland to Brookings and from Santa Maria to Oakland in the January-February 1945 and December 1955 storms and from Santa Maria to Oakland in the November 1950 storm. Also plotted are 6-hour amounts of rain at representative downwind Central Valley stations relatively free from orographic effects.) Average values of 40 mph and over are characteristic of the main parts of these storms, as indicated by the rain sequence.

To insure highest moisture content it is necessary that a strong coastal flow start offshore to the southwest at low latitudes. The extent to which this condition is met depends, in part, on storm type. It is more nearly met in Low-latitude and Mid-latitude type storms than in a High-latitude type storm, although at the latitude of Southern California the distinction is less marked than in Northern California. This is illustrated by comparison of the offshore flow in the three storms in which highest known surface geostrophic winds over California occurred (figure 5-17, HMR 36). Highest values for most distances across the stream and most durations occurred in the January 1943 storm. But because in this storm, as in other High-latitude type storms, the Lows became deep only as they approached the coast, it less nearly meets the requirements of a favorable wind sequence than do the December 1955 and January-February 1945 storms, with somewhat lower coastal gradients but with a strong flow offshore from low latitudes.

a. Variation with latitude and season. Trends in highest observed geostrophic and actual winds in storms are indicative of trends in windspeed in the average major storm, with respect to both latitude and season. Examples of trends in highest observed winds are cited below.

A latitudinal variation in high windspeed is shown in figure 5-32, HMR 36. (The surface wind relation is based on highest yearly surface geostrophic wind for 15 Januarys between coastal stations; the upper-air relation is based on a 5-year average of maximum annual observed southwest winds at Medford, Oakland, Santa Maria and Long Beach). Figure 5-32 indicates a decrease in maximum winds south of San Francisco (38N). At the surface it amounts to about 15 percent at the latitude of Los Angeles (34N) and 25 percent at the latitude of San Diego (33N). Aloft, the percentage of decrease becomes smaller with height to about half at 500 mbs.

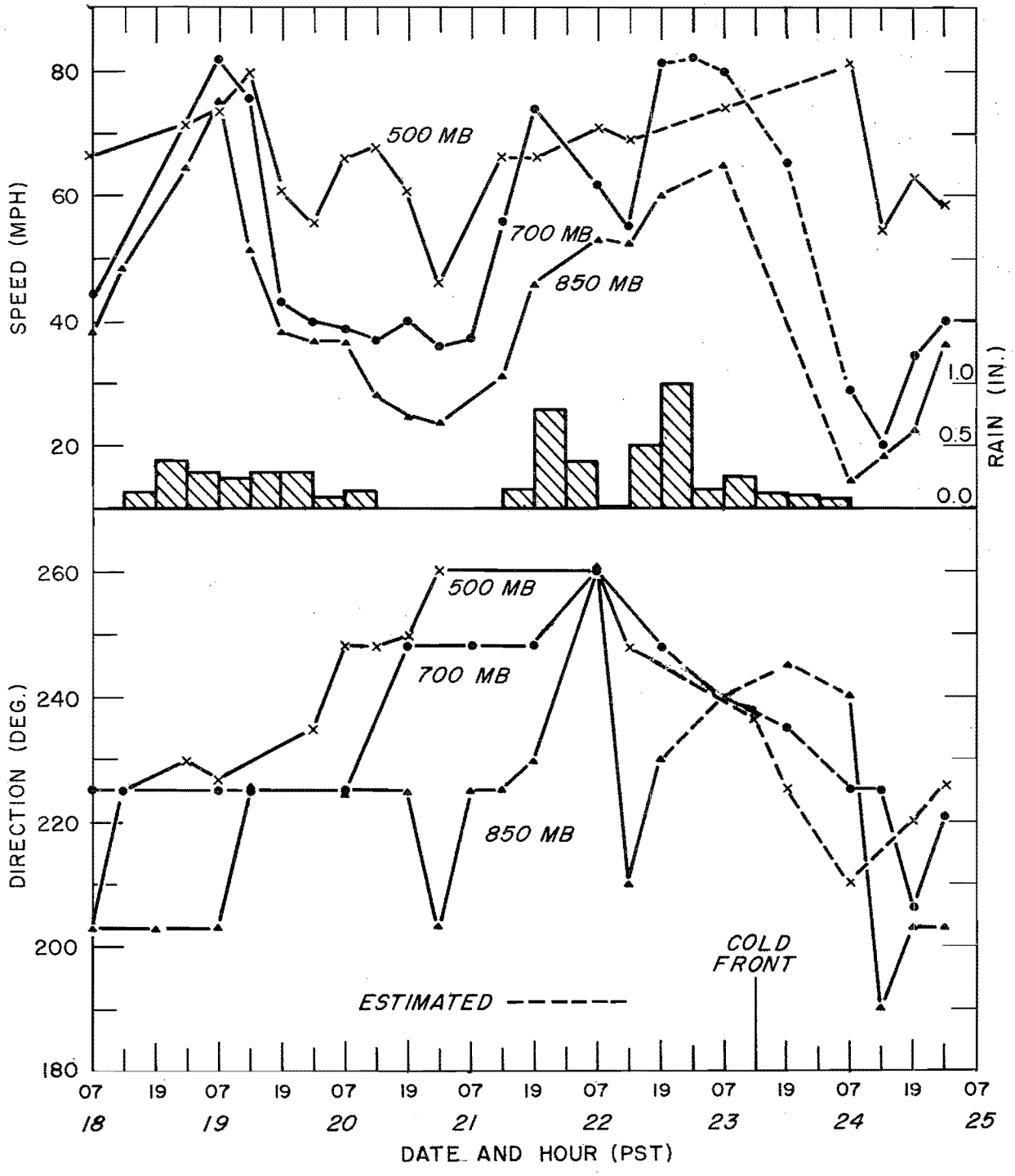

Fig. 3-2. WIND AND 6-HOUR RAIN AT OAKLAND, DECEMBER 1955

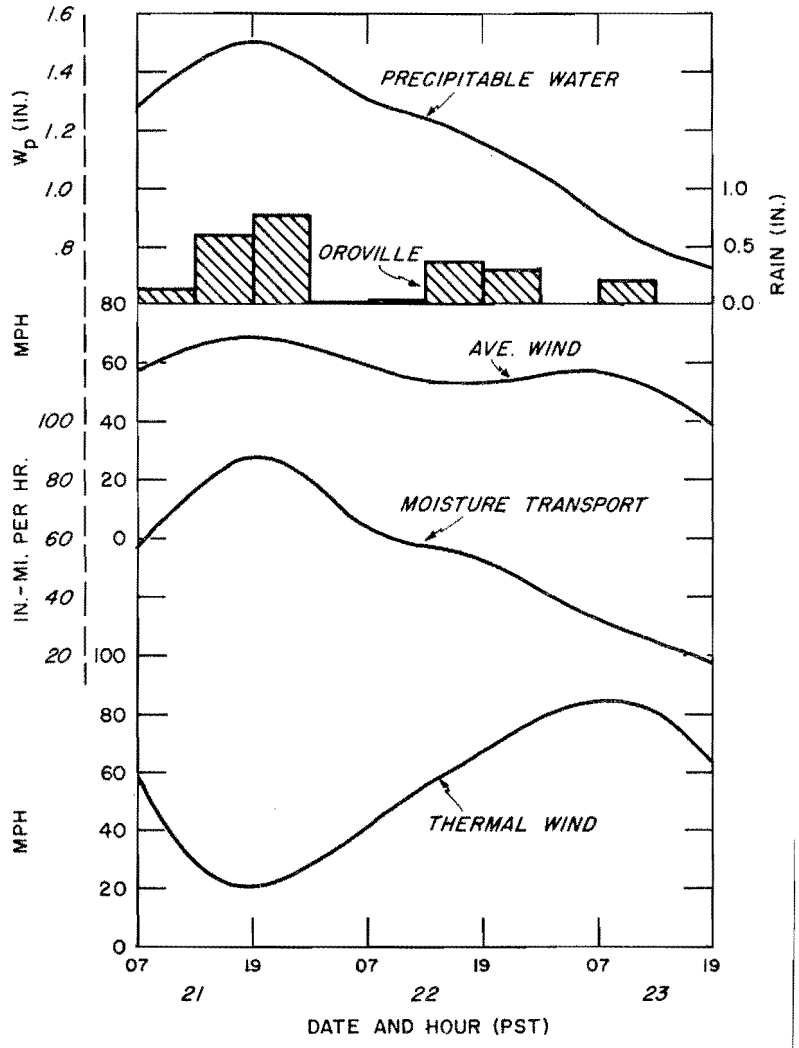

Fig. 3-3a. VARIATION OF MOISTURE TRANSPORT PARAMETERS 1000-500 MB, BROOKINGS-OAKLAND, DECEMBER 1955

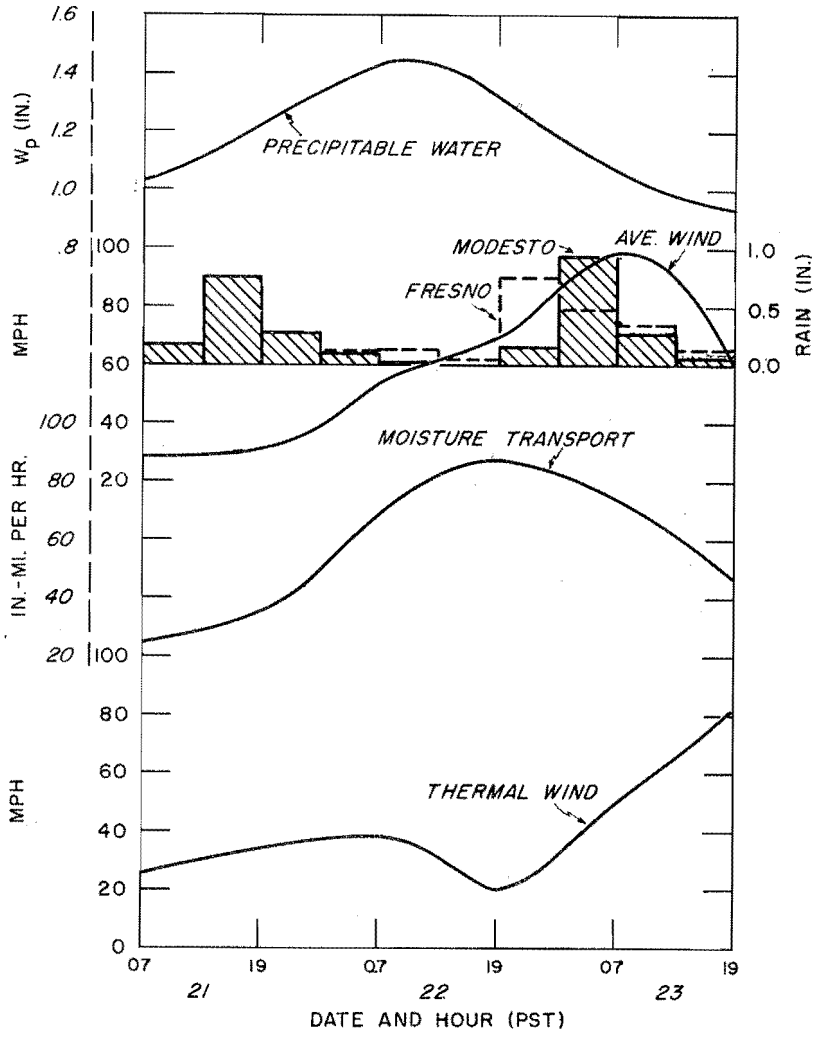

Fig. 3-3b. VARIATION OF MOISTURE TRANSPORT PARAMETERS, 1000-500 MB, OAKLAND-SANTA MARIA, DECEMBER 1955

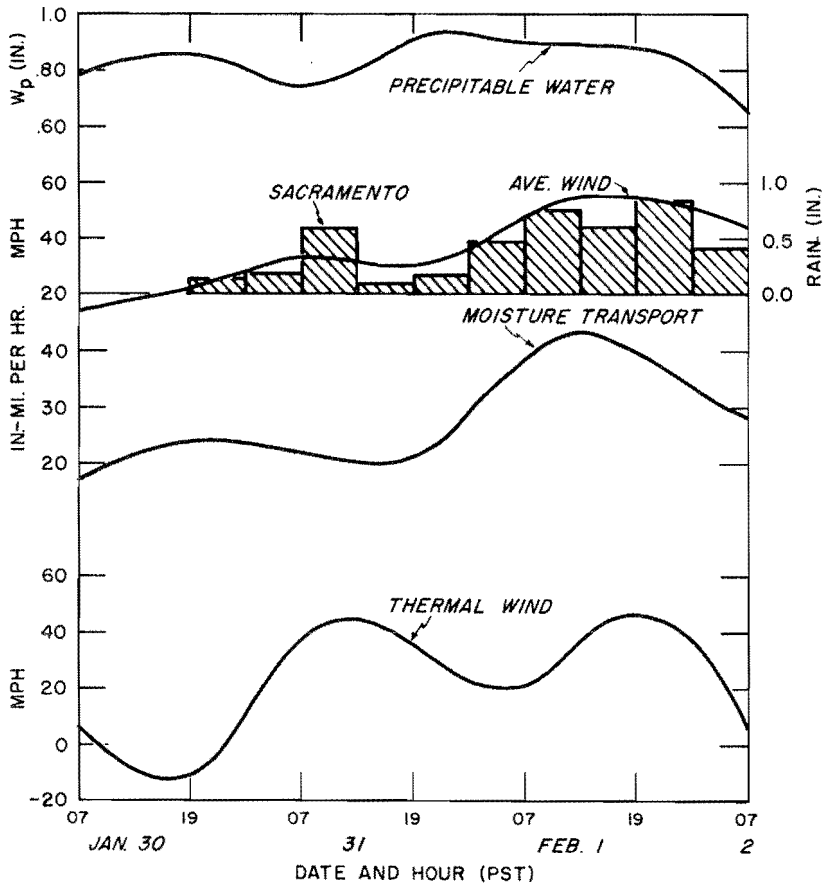

Fig. 3-3c. VARIATION OF MOISTURE TRANSPORT PARAMETERS, 1000-500 MB, BROOKINGS-OAKLAND, JANUARY-FEBRUARY 1945

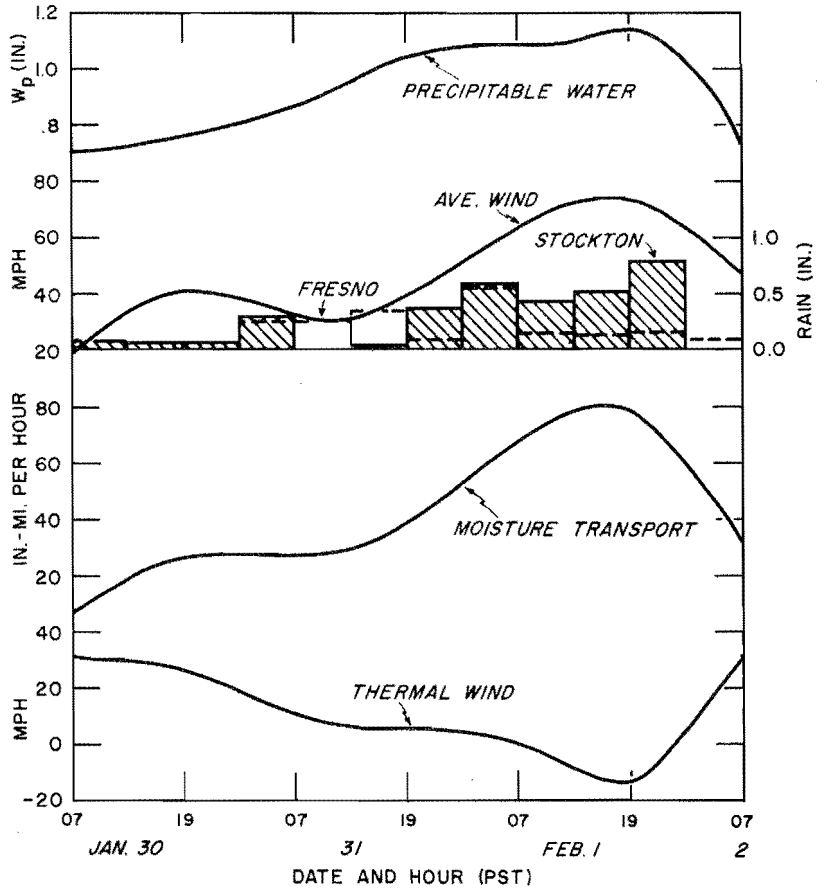

Fig. 3-3d. VARIATION OF MOISTURE TRANSPORT PARAMETERS, 1000-500 MB, OAKLAND-SANTA MARIA, JANUARY-FEBRUARY 1945

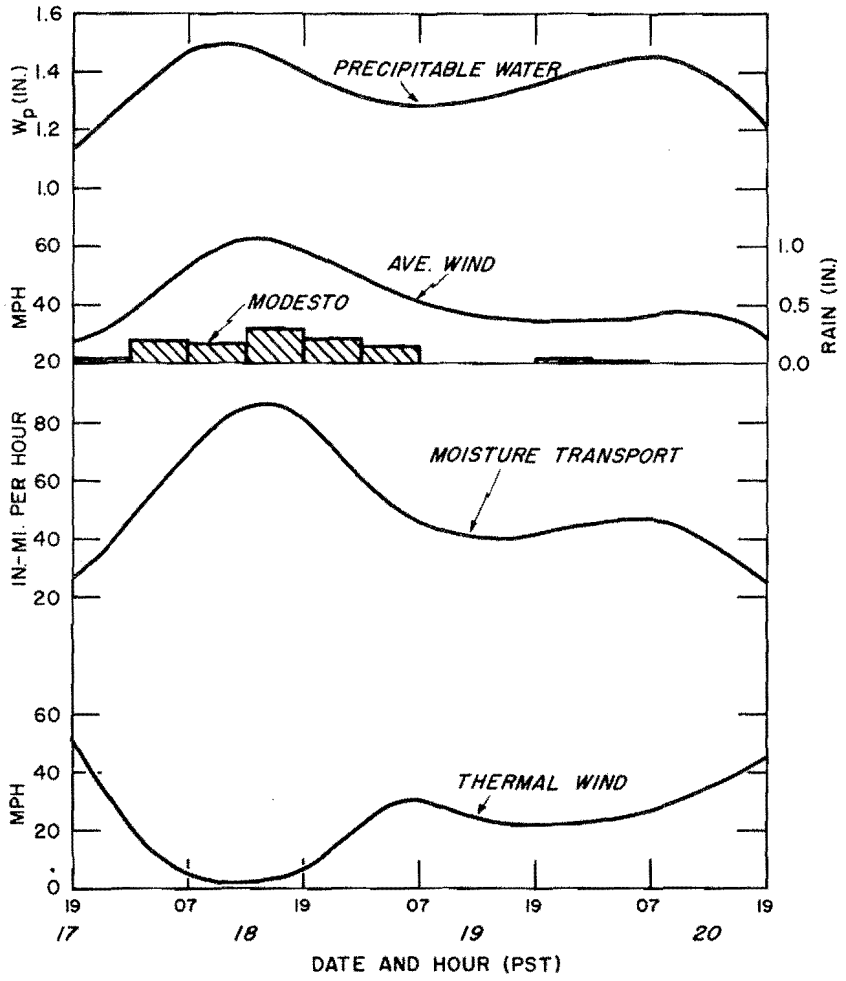

Fig. 3-3e. VARIATION OF MOISTURE TRANSPORT PARAMETERS, 1000-500 MB, OAKLAND-SANTA MARIA, NOVEMBER 1950

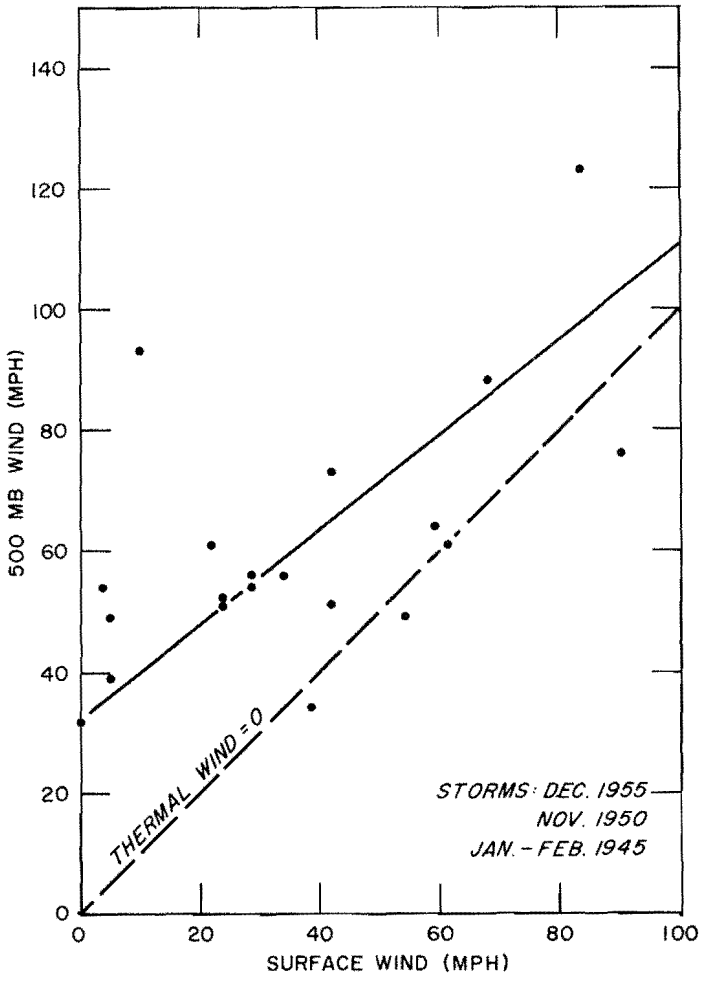

Fig. 3-4. SURFACE-500 MB GEOSTROPHIC WIND RELATION FOR OAKLAND-SANTA MARIA SECTOR

An indication of the seasonal variation of winds in major storms can be obtained from seasonal trends in maximum monthly wind data, as shown in figure 5-37, HMR 36. (Here, seasonal trends in surface winds are based on maximum monthly values of instantaneous surface geostrophic wind Eureka to San Francisco and San Francisco to San Luis Obispo, and of 5-minute, 6-hour, and 24-hour average actual wind at those stations for a 22-year period. Upper-air trends are based on a 5-year average of maximum monthly actual winds at Seattle, Medford, Oakland and Long Beach). Figure 5-37 shows highest values between mid-January and mid-February. There is a 16 percent reduction at the surface from mid-February to April 1 which decreases aloft to 8 percent at 500 mbs. A similar reduction is shown from mid-January to December 1 and from December 1 to mid-October.

b. Windspeed variation with height. A characteristic of windspeeds in the main storm area of a major storm is that when they are highest (averaged through height) there is then least variation of speed with height. This is seen in figure 3-2 at Oakland during the December 1955 storm. Variation of actual windspeed with height was least during the periods of high wind and heavy rain on the morning of the 19th, and again from the evening of the 21st to the morning of the 23d.

This relation is also seen to some extent in geostrophic wind normal to the coast during recent storms where thermal wind represents height variation of windspeed in figures 3-3a to 3-3e. In most cases thermal wind was least at times when the average 1000-500 mb windspeed (and necessarily the surface wind) was high. In table 3-1 it is noted that times of occurrence of low thermal wind and high average wind coincide in 3 of the 5 cases of figures 3-3a to 3-3e and are 12 hours apart in another.

Table 3-1

DATE/TIME OF PEAK VALUES OF 1000-500 MB MOISTURE TRANSPORT (PST) PARAMETERS IN 3 STORMS

Storm	Sector	Highest Moisture	Highest Avg. Wind	Highest M. T.*	Lowest Thermal Wind
Dec. 1955	OAK-BKS	211900	211900	211900	211900
Dec. 1955	TZM-OAK	220700	230700	221900	221900
Nov. 1950	TZM-OAK	181300 301900	181300	181300	181300
Jan.-Feb. 1945	OAK-BKS	010100	011900	011900	010700
Jan.-Feb. 1945	TZM-OAK	011900	011900	011900	011900

OAK-Oakland; TZM-Santa Maria; BKS-Brookings.
*M. T. - Moisture transport.

Increase in windspeed with height is a function of location with respect to the storm, as seen in table 3-2.

This table demonstrates the smaller increase of wind with height in the warm flow in the southern part of a storm compared to that in the area of higher north-south temperature gradient on the northern side.

Table 3-2

AVERAGE 1000-MB GEOSTROPHIC AND 1000-500 MB THERMAL WINDSPEED IN STORMS (MPH)

		Oakland-Brookings		Santa Maria - Oakland	
Storm	Date/Time (PST)	1000-mb	Thermal	1000-mb	Thermal
Dec. 1955	210700 - 231900	24	56	35	42
Nov. 1950	171900 - 201900	11	59	35	26
Jan.-Feb. 1945	300700 - 020700	29	20	42	13

Average thermal wind values of the Oakland-Brookings sector averaged considerably higher than corresponding values Santa Maria to Oakland in these 3 storms. Some increase in thermal wind with latitude across the storm area is probably typical of all major storms.

The average variation in geostrophic windspeed with height from Santa Maria to Oakland during the 1955, 1950 and 1945 storms is shown in figure 3-4 as an eye-fitted regression of 500-mb wind on surface wind. (This area was chosen because of higher average moisture flow and stronger surface wind in each of the 3 storms than in Northern California.) The relation indicates decreasing thermal wind, toward zero, with increasing surface wind.

The wide variation in thermal wind with area and time in a storm sequence and between storms, as suggested by data in figure 3-4 and table 3-2, precludes generalization of the variation of geostrophic wind with height in a major storm beyond that stated above.

Effects of terrain on wind-height relations are discussed in Chapter IV.

3-A-3. Synoptic bases for favorable wind in storm types

A wind sequence which is favorable for sustained heavy precipitation from the standpoint of orientation, strength and duration of the wind is dependent on synoptic features which are peculiar to storm type. In the Low-latitude storm type, permanence of position and strength of the Central Pacific blocking High and Gulf of Alaska Low favors stability of position of strong onshore winds at the coast. In most Mid-latitude type storms the semi-stationary Low offshore is necessary to permit successive storm centers, with their broad area of strong winds, to approach the coast at intervals frequent enough to maintain continuously strong southwest winds. Presence of the continental blocking High contributes to the maintenance of the main offshore Low and stability of orientation of the coastal flow. In the High-latitude type storm the wind strength depends on deepening of Lows near the coast, and constancy of direction depends on stagnation there.

3-A-4. Moisture restriction on optimum windflow

A thermal wind component of large magnitude coincident with and parallel to an optimum surface geostrophic wind assures optimum flow. But this condition was found to be incompatible with high values of moisture in recent major storms. In each instance in table 3-1, least thermal wind occurred at the coast near time of high moisture (as well as high convergence precipitation). Thus high surface wind and small increase with height would characterize optimum moisture flow.

3-B. MOISTURE

The amount of moisture in air reaching the coast in a major storm depends on what parts of the Pacific Ocean the air originates from and passes over and the absence or presence of convergence to destabilize the lapse rate. The moisture source varies with storm type. Sea-surface cooling enroute from source region tends to reduce moisture in lower levels, but does not greatly diminish the total in a column. The latitudinal and seasonal variation of moisture is opposite to that of wind.

3-B-1. Dependence on source region and storm type

In table 3-3 are listed highest 12-hour average coastal 1000-mb dew points in storms grouped by moisture source region and storm type, from most favorable to least favorable for high moisture. In three storms, for which upper-air data are available, the 1000-mb dew point equivalent to the observed precipitable water was substituted for the reported sea-level dew point, as more representative. (By "equivalent dew point" is meant the dew point that would prevail if the air were saturated, had a moist adiabatic lapse rate of temperature, and contained a specified precipitable water in a column). Also listed in the table are dew point values adjusted to February by use of figures 4-1a to d, HMR 36.

The effect of storm type and source region on storm moisture potential at the coast in the four groups of table 3-3 are discussed briefly in the following four paragraphs in the same order as listed in the table.

Tropical air reaches the coast most readily in Low-latitude type storms when the eastern Pacific High cell is displaced eastward close to the coast of Baja California, permitting a long flow trajectory from near the Hawaiian Islands to the California coast (Nov. 1950 and Dec. 1955). If the eastern Pacific High is absent and a north-south ridge persists over western North America, tropical air may reach California from a low latitude along a shorter, more nearly south-north trajectory, as in a Southerly Mid-latitude type storm (Dec. 1937).

Although a polar source region in the central or western Pacific is the origin of air in Southwesterly Mid-latitude type storms, heating to high

Table 3-3

VARIATION OF HIGHEST 12-HOUR AVERAGE 1000-MB DEW POINT WITH STORM TYPE AND MOISTURE SOURCE

Date	Storm Type	Location	1000-Mb Dew Point Actual	Adjusted to Feb.	Type of Air
11/19/50	Low-latitude	Monterey	62*	60	Tropical
12/22/55	Low-latitude	San Francisco	61*	60	Tropical
12/10/37	Mid-latitude Southerly	San Francisco	63	61	Tropical
12/11/37	Mid-latitude Southerly	Los Angeles	62	60	Tropical
---	---	---	---	---	
2/1/45	Mid-latitude Southwesterly	San Francisco	57*	57	Well-modified Polar
2/27/40	Mid-latitude Southwesterly	San Francisco	57	57	Polar
3/2/28	Mid-latitude Southwesterly	Los Angeles	59	59	Polar
---	---	---	---	---	
1/22/43	High-latitude with Mid-latitude break-thru	Los Angeles	57	57	
1/21/43	(Same storm)	San Francisco	54	54	Polar
12/20/21	High-latitude (trough offshore)	Los Angeles	58	57	Polar
1/17/16	High-latitude (trough offshore)	Los Angeles	57	57	Polar
---	---	---	---	---	
4/20/1880	High-latitude (Low directly onshore)	San Francisco	50	50	Recent Polar
12/20/1866	High-latitude (Low directly onshore	San Francisco	53	52	Recent Polar
1/27/16	High-latitude (Low directly onshore	Los Angeles	53	53	Recent Polar
4/2/58	Mid-latitude Westerly	San Francisco	49	49	Recent Polar

*1000-mb equivalent dew point based on upper-air data. See text.

levels enroute to the coast at low latitudes may provide a moisture supply, before return to higher latitudes at the coast, not much less that that of tropical air.

In High-latitude type storms in which the block is penetrated by storm centers from the west (Jan. 1943), modified polar air reaches the coast from a considerable distance to the southwest with moisture not much less than in some Southwesterly Mid-latitude type storms. Also in High-latitude type storms in which the Low, following southward movement offshore, recurves toward north or northeast before entering the coast (Dec. 20, 1921) or remains stationary over Northern California (Jan. 17, 1916) so as to allow a north-south trough to stagnate off the Southern California coast, there is opportunity for a prolonged flow of increasingly moist air from a fairly low latitude into Southern California from south-southwest.

In those High-latitude type storms where Lows moving south-southeastward enter rather directly into California with little offshore recurvature, air reaches the coast after having little opportunity for heating at a lower latitude (storms in group 4, table 3-3). This so limits moisture in Northern California that heavy rainfall occurs mainly in low elevation areas and locally as instability precipitation. At higher elevations, the precipitation is largely snow.

3-B-2. Latitudinal variation

The latitudinal variation in moisture between storms is similar to that of highest observed 1000-mb dew points over California, as presented in figures 4-5a and b of HMR 36. The maps show an increase in dew point values southward over Northern California, with a fairly large gradient in winter months; but over Central and Southern California dew point lines tend to parallel the coast with only a slight increase in values southward, particularly in winter.

The small latitudinal variation south of San Francisco is related to the fact that Low-latitude type storms, infrequent in Southern California, and Southerly Mid-latitude type storms tend to bring equally high moisture to Central California as to Southern California, from about the same source region. Another factor may be the nearness of Southern California to the cool-season area of subsidence dryness near the coast at low latitude.

3-B-3. Seasonal trend

Highest observed moisture in major storms decreases from October to January and rises only slightly toward spring. This is indicated in the following table of highest observed 1000-mb dew points converted to precipitable water, assuming saturation and expressed as percent of February, from data in figure 4-6 of HMR 36.

Oct.	Nov.	Dec.	Jan.	Feb.	Mar.	Apr.
121	111	106	101	100	102	104

Comparison of seasonal variation of monthly highest 1000-mb dew points at San Francisco (from figures 4-5a and b of HMR 36) with monthly normal air and sea-surface temperatures (5) (6) at San Francisco is shown in table 3-4. The seasonal range (from October to April) of highest dew point is only 3°F compared to that of normal temperature (11°F) and of water temperature (8°F).

Table 3-4

SEASONAL VARIATION OF NORMAL AIR AND WATER TEMPERATURE AND OF HIGHEST 1000-MB DEW POINT AT SAN FRANCISCO (°F)

	Oct.	Nov.	Dec.	Jan.	Feb.	Mar.	Apr.
Normal Air temperature	61.0	57.2	56.7	50.1	53.0	54.9	55.7
Normal water temperature	59.1	55.8	52.7	50.8	51.7	53.4	54.5
Highest 1000-mb dew point	64.4	63.4	62.7	61.6	61.5	61.5	61.7

The lack of a seasonal rise in highest dew point compared to normal air and water temperatures during spring months is, in part, associated with the absence (in the period of record) of spring major storms of the type which involve as strong south-north moisture advection near the coast as in earlier months.

3-B-4. Moisture distribution in the vertical

Saturation at upper levels is usually accompanied by near saturation in lower levels, except perhaps at the outset of the storm sequence. Lack of saturation at upper levels occurs at times in a major storm in air with a rather direct flow from a high-moisture source region. This is characteristic of periods of divergence during lulls in a storm as illustrated below.

In figure 3-5 are plotted 12-hourly values of precipitable water (W_p) at Oakland by 200-mb layers during the December 1955 storm; both actual values and values if the air had been saturated are shown. Near saturation, except at very high levels, occurred at Oakland when total W_p was highest during the heavy precipitation periods on the morning of the 19th, and again on and following the night of the 21st. Dry air is noted in all but low levels in the lull of the storm around the 20th. Dry air appeared at upper levels on the morning of the 23d following heavy rain, lack of saturation accounting for a reduction of about 20 percent from total possible W_p.

Effect of sea-surface cooling on lower layers is not important in reducing total moisture in the column.

3-B-5. Effect of sea-surface cooling on 1000-mb dew point

Sea-surface cooling may appreciably reduce temperature and moisture in lowest layers. It is usually a factor in those cases where 1000-mb dew point at the coast considerably underestimates total moisture. Amount of

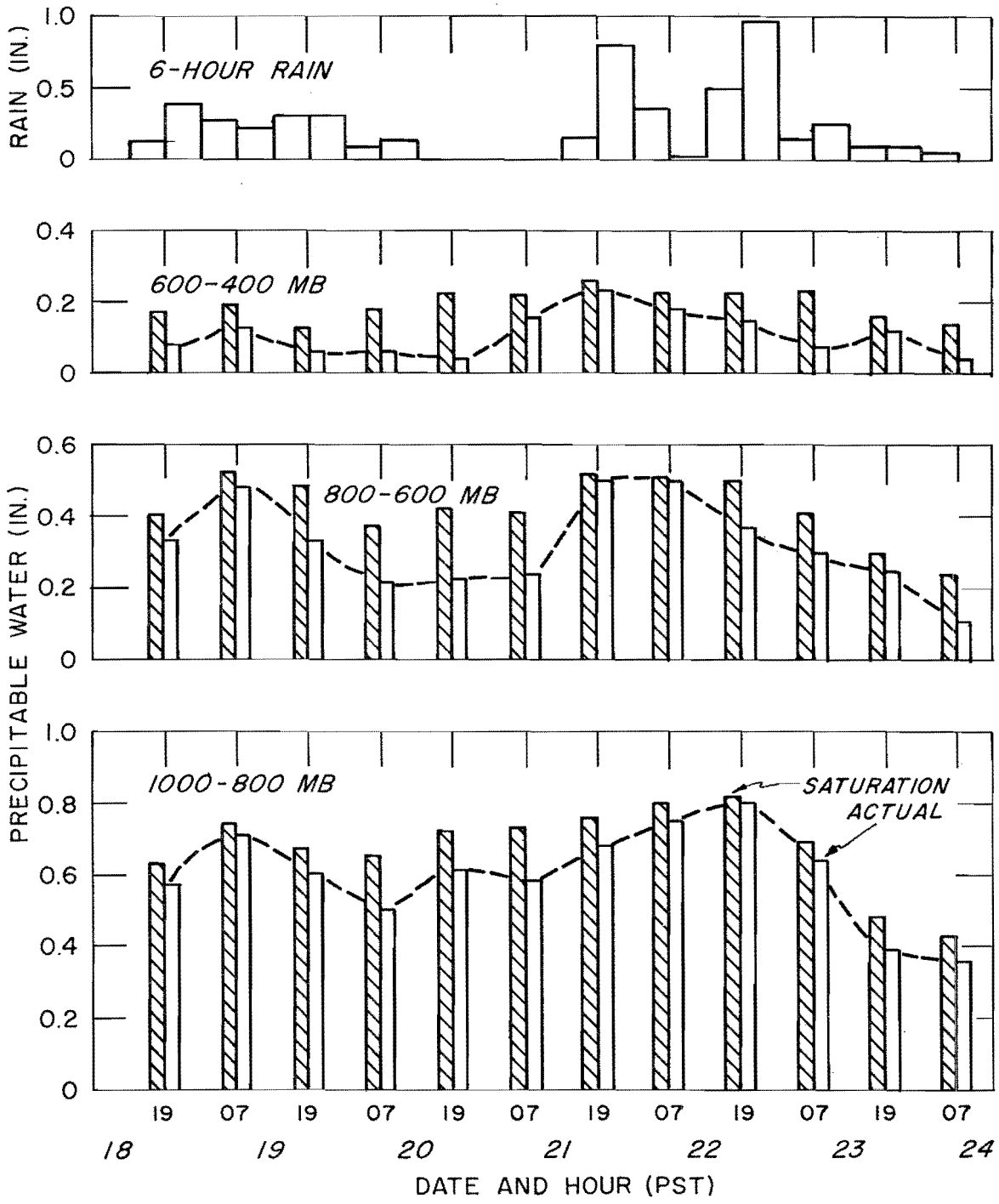

Fig. 3-5. PRECIPITABLE WATER BY LAYERS, OAKLAND. DECEMBER 18-24, 1955

underestimation in the 1955, 1950 and 1945 storms at Oakland and Santa Maria is indicated in figure 3-6. Values of equivalent 1000-mb dew points are plotted against observed 1000-mb dew points. (The amount of useful data for the 1945 storm was restricted by its shorter length, incomplete soundings, and periods of low moisture.) The dashed eye-fitted line in figure 3-6 indicates an average underestimation of about 3°F for higher moisture values.

Underestimation was considerably more in the 1955 than in the 1950 storm, largely because of stable lapse rates with and following warm advection at Oakland on December 19 and 22, 1955 (figures 5-8 and 5-11) and at Santa Maria on the 22d and 23d. The few cases of overestimation result from dry air aloft between rain periods or at the end of the storm.

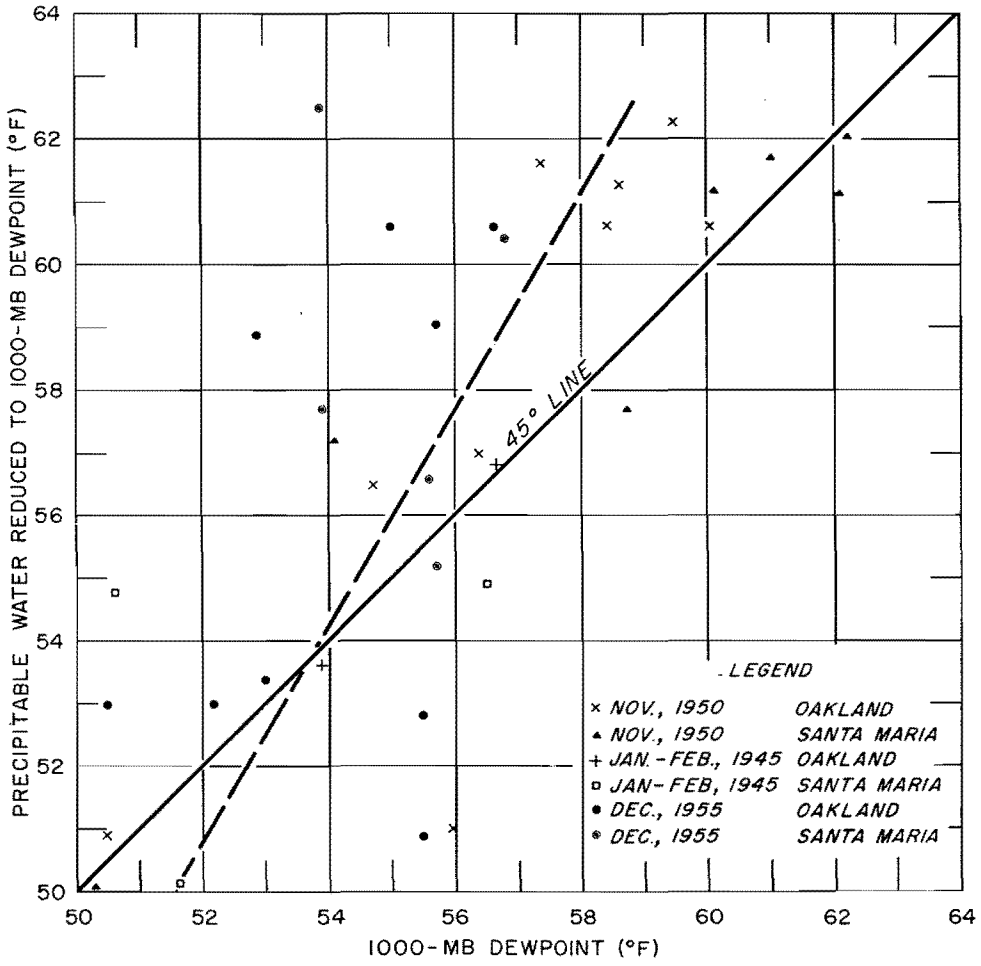

Fig. 3-6. COMPARISON OF SURFACE AND UPPER AIR MOISTURE CRITERIA

3-B-6. Synoptic requirements for optimum moisture sequence

It was pointed out in 3-A-2 that to attain high coastal moisture, high coastal winds must be part of a strong flow from a low latitude. Lengthy duration of a moist flow at the coast over the same area precludes intrusion of cooler air from a higher latitude. This requires that frontal systems reaching the coast are mostly warm occlusions or pass to the north and west of the precipitation area; further, stability of the axis of the moist flow must be maintained by frequent repetition of Low centers of similar size and depth along similar paths.

The circulation in Southerly Mid-latitude type and Low-latitude type storms best provides opportunity for realization of optimum moisture conditions, especially with respect to non-interruption by frontal passages and to stability of the moisture axis. Even in these storms the position of the axis is somewhat transitory (e.g., figure 2-19).

3-C. MOISTURE TRANSPORT

Moisture transport over a mountain barrier enters into the equations for orographic precipitation. The manner in which moisture and wind may combine influences the precipitation potential. The fact that the latitudinal, seasonal and vertical wind and moisture variations are in an opposing sense makes the optimum combination rather complex.

Values of moisture transport are expressed in terms of product of air movement and precipitable water. Across a line normal to the flow, moisture transport is expressed as inch-miles for unit width of flow, for any unit of time.

3-C-1. Time relations of high wind and moisture

a. Within storms. Time comparison of periods of highest wind and moisture in recent storms (table 3-1) indicate simultaneous occurrence in 3 of the 5 comparisons in figures 3-3a to 3-3e. This suggests the possibility of simultaneous occurrence of optimum wind and moisture (for a given season) in the same storm.

The out-of-phase moisture-wind time relation between Oakland and Santa Maria in the December 1955 storm (figure 3-3b) resulted in a flat peak in moisture transport midway between the wind and moisture peaks. Had moisture and wind peaks been in phase, moisture transport would have peaked at a value approximately 40 percent higher, assuming the same values of wind and moisture at the respective peaks.

b. Between storms. Seasonal relations of moisture transport in major storms are derived by combining the seasonal relations (based on maximum observed values) of wind (3-A-2a) and of moisture (3-B-3). Highest wind occurs in midwinter, the season of low moisture. Because of the smaller

seasonal variation of moisture than of wind, highest moisture transport occurs also in midwinter. The combined relation is shown in figure 3-7 by months in percent of January for the 1000-, 850-, 700-, and 500-mb levels. In this relation, decrease from high midwinter moisture transport to fall is about half the corresponding decrease in wind, because of high moisture in fall. Moisture transport decrease toward spring is about the same as for wind.

3-C-2. Vertical distribution of moisture transport

High onshore moisture transport is favored by small decrease of moisture with height and strong onshore wind components at low as well as high levels. The latter depends both on the thermal wind and reduction of the onshore geostrophic wind component by terrain.

In three out of five cases in table 3-1 based on the graphs of figures 3-3a to 3-3e, the maximum moisture transport is at the time of a thermal wind minimum and an average geostrophic wind maximum.

A similarly favorable distribution is shown in figure 3-8, where terrain effect and thermal wind are both included (by use of actual wind) in a comparison at Oakland during the December 1955 storm. Moisture transport values in 200-mb layers are plotted at 12-hourly intervals, with corresponding average wind and W_p to the left and right, respectively. Wind and moisture transport are components from 240 degrees.

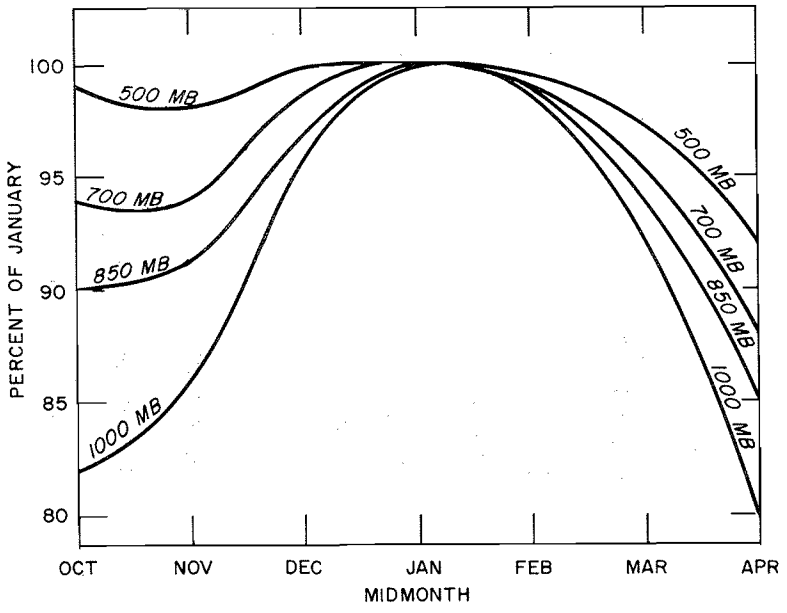

Fig. 3-7. SEASONAL VARIATION OF MAXIMUM MOISTURE TRANSPORT

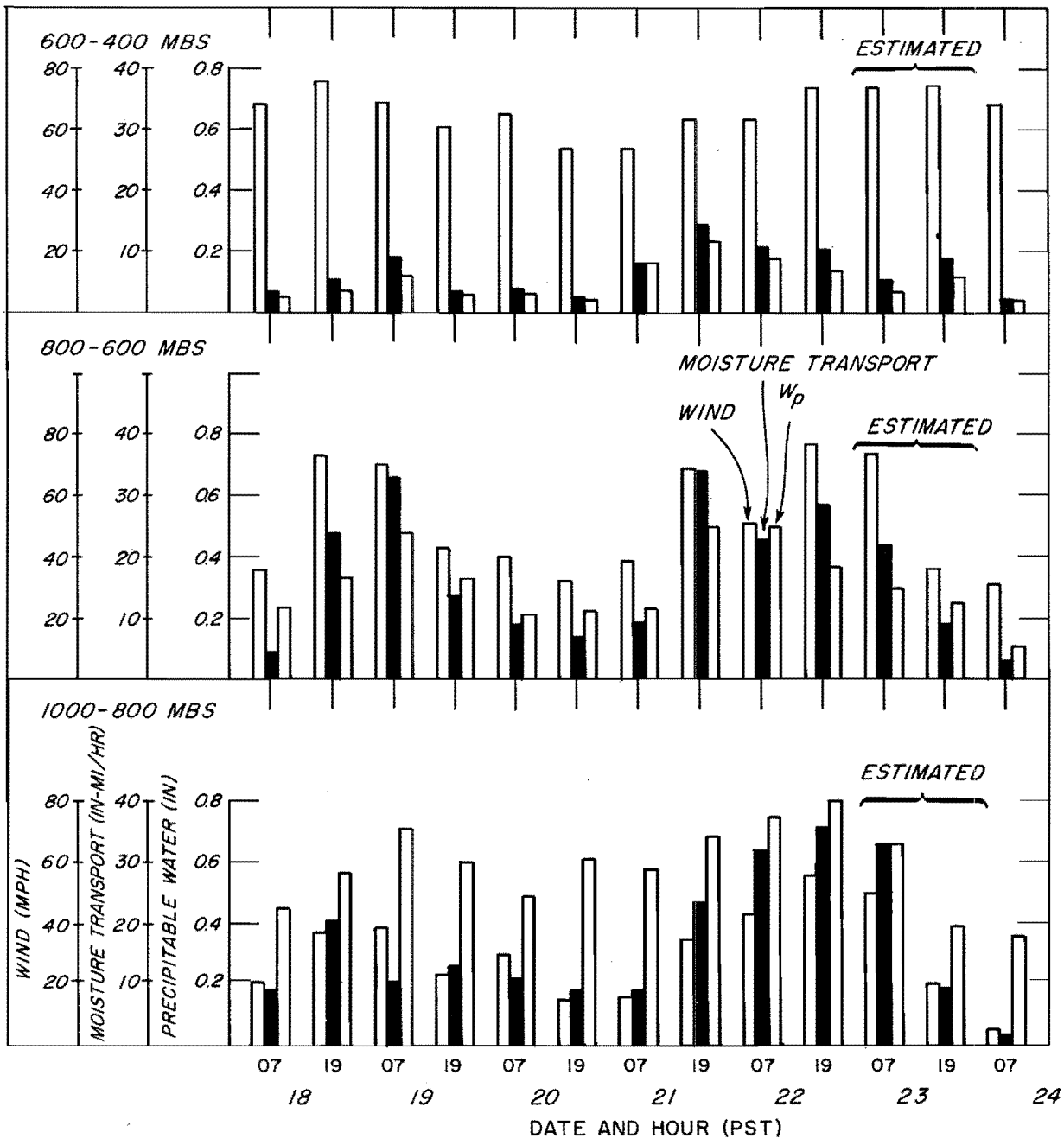

Fig. 3-8. WIND, MOISTURE AND MOISTURE TRANSPORT IN 200-MB LAYERS AT OAKLAND, DECEMBER 18-24, 1955 (COMPONENT FROM 240°)

Total moisture transport (figure 3-8) reached a peak on the evening of the 21st, time of highest W_p and least decrease with height of W_p; also on the evening of the 22d, time of highest average wind and least thermal wind. Time of highest moisture transport below the 800-mb level (221900 PST) lagged that at upper levels (211900 PST) because of a later peak in W_p. Fluctuation of moisture transport during the storm sequence was mainly that of wind in lower levels and of W_p in upper levels, since, in general, wind fluctuation decreased and W_p fluctuation increased with height.

The vertical distributions of actual wind, moisture and moisture transport at Oakland at 211900 PST are shown in more detail in figure 3-9. Moisture transport increased from the surface upward as the terrain effect on wind lessened and as geostrophic wind increased slightly. Above about 700 mbs decreasing moisture and slightly decreasing wind with height caused moisture transport to drop with height.

3-C-3. Areal relations between wind, moisture and moisture transport

a. Comparisons within storms. Latitudinal comparisons of location along the coast of highest 1000-500 mb moisture and highest onshore 1000-500 mb geostrophic wind during the December 1955 and November 1950 storms are shown in figures 3-10 and 3-11 respectively. In the December 1955 storm the axis of highest moisture crossed the coast south of the axis of highest wind, as both progressed southward during the storm. The difference was

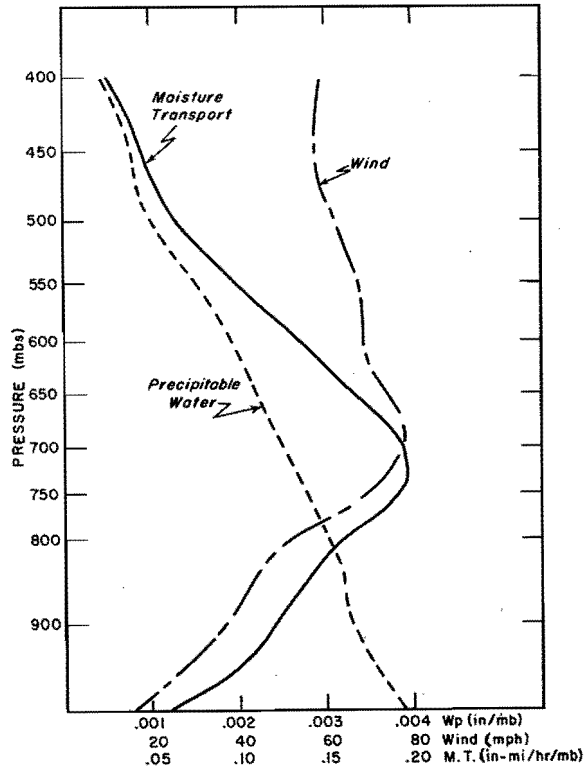

Fig. 3-9. WIND, MOISTURE AND MOISTURE TRANSPORT VARIATION WITH HEIGHT AT OAKLAND, 1900 PST, DECEMBER 21, 1955

greatest on the 22d in Central California; it accounts for the time lag there in high wind behind high moisture shown in figure 3-3b. In the November 1950 storm, the moisture axis crossed the coast at about the same latitude as did the wind axis associated with the tropical flow, both in south-central California on the 18th and further north on the 20th. (The corresponding rain areas are shown in figure 2-19).

The manner in which offshore wind and moisture combined areally in the December 1955 and November 1950 storms is illustrated in figures 3-12 and 3-13. The latitudinal and longitudinal variation in moisture and longitudinal variation in wind are shown in figure 3-12. The top figures are persisting wind as percentage of values along the coast. Bottom figures are persisting 1000-mb dew point. Data are for durations of 12, 36 and 72 hours, for 16 blocks in an area between 30 and 46 N latitude and between the coast and 140 W longitude. Longitudinal variation of moisture transport in percent of coastal values is shown in figure 3-13. Areal coincidence of axis of wind and moisture does not necessarily imply time coincidence.

December 1955 storm. In this storm the axes of surface moisture (dashed lines) and of surface geostrophic wind (solid lines) in figure 3-12 compare closely in orientation. As on the coast, position of the moisture axis is displaced slightly southeastward from the wind axis, especially for longer durations, partly because of the effect of cooler air temporarily invading the strong wind zone. (This relation of axes is typical of that in major eastern United States storms.) The closeness of the two axes favored combination of parameters of moisture transport areally in nearly optimum manner for high moisture transport. The axis of highest moisture transport (figure 3-13) does not vary with duration and lies between the wind and moisture axes of figure 3-12.

November 1950 storm. In this storm the axis of strong wind (figure 3-12) has a WSW-ENE orientation from Central California, suitable to bring moist air to the coast, but only for short durations. Another axis oriented NNW-SSE in the 135-140 W longitude strip appears because of the deep Low in the northwest quadrant of the area. The axis of highest dew point is oriented similarly to that in the 1955 storm but is closer to the coast. The axis of highest moisture transport in figure 3-13 is controlled by moisture and roughly coincides with the moisture axis of figure 3-12, despite higher winds to the northwest. (Comparisons in this storm are based on an arithmetic average of 1000-mb and 700-mb data.)

Wind and moisture in this storm did not approach optimum areal combination except far to the southwest, both because the strong flow to the northwest was not part of the tropical circulation reaching the coast and because of the absence of vigorous cyclonic systems near the coast.

b. Longitudinal comparison of moisture transport between storms. The purpose of the following comparison is to ascertain relative exceedance of coastal and offshore moisture transport in other storms, compared to that in the December 1955 storm. In it, highest moisture transport (figure 3-12) occurred near the coast at the latitude of Northern California but far offshore at the latitude of Southern California.

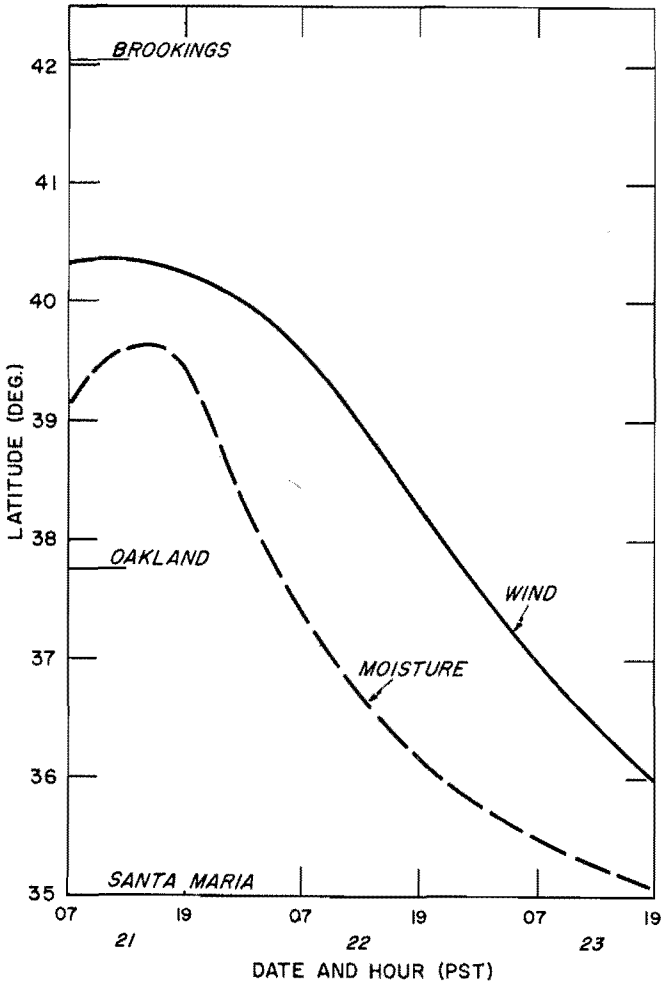

Fig. 3-10. LOCATION OF HIGH WIND AND MOISTURE AXES AT THE COAST IN THE DECEMBER 1955 STORM

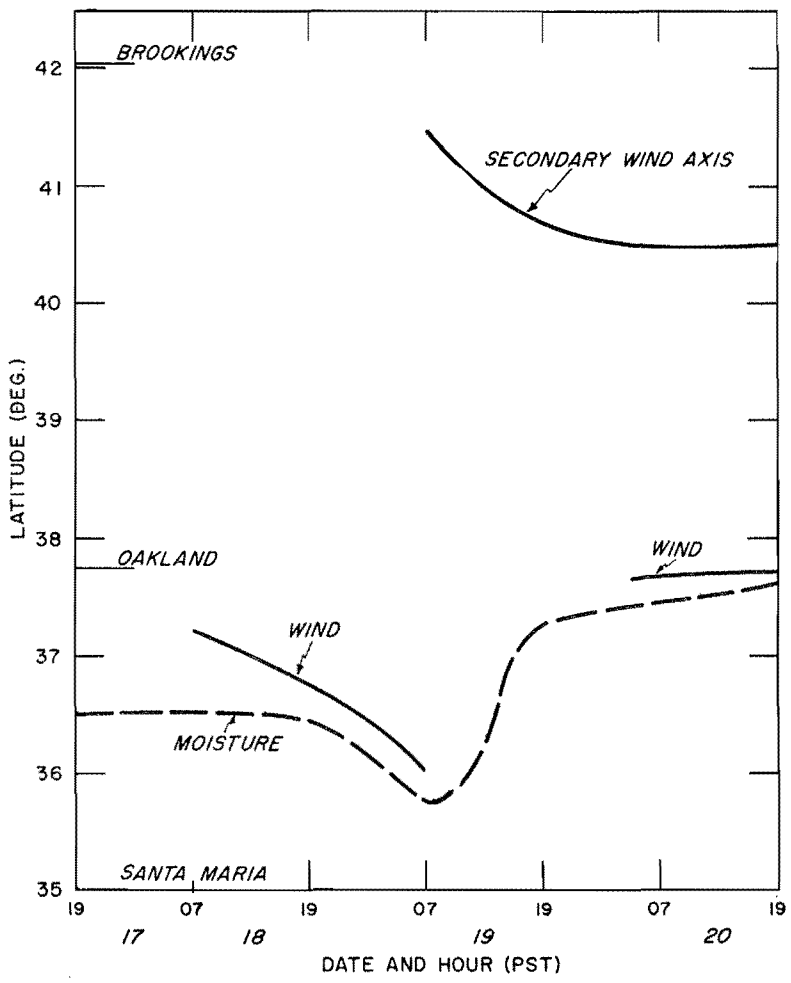

Fig. 3-11. LOCATION OF HIGH WIND AND MOISTURE AXES AT THE COAST IN THE NOVEMBER 1950 STORM

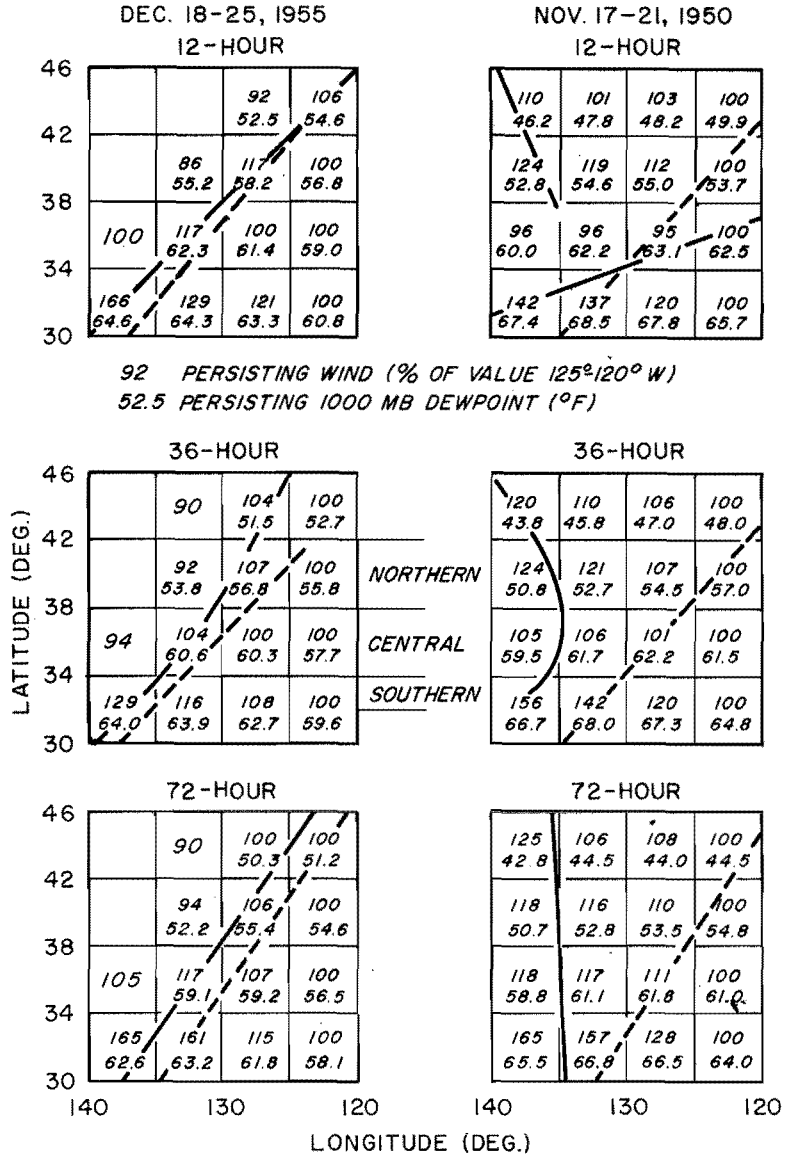

Fig. 3-12. COMPARISON OF AXES OF HIGHEST SURFACE MOISTURE (DASHED LINES) AND WIND (SOLID LINES) IN TWO STORMS

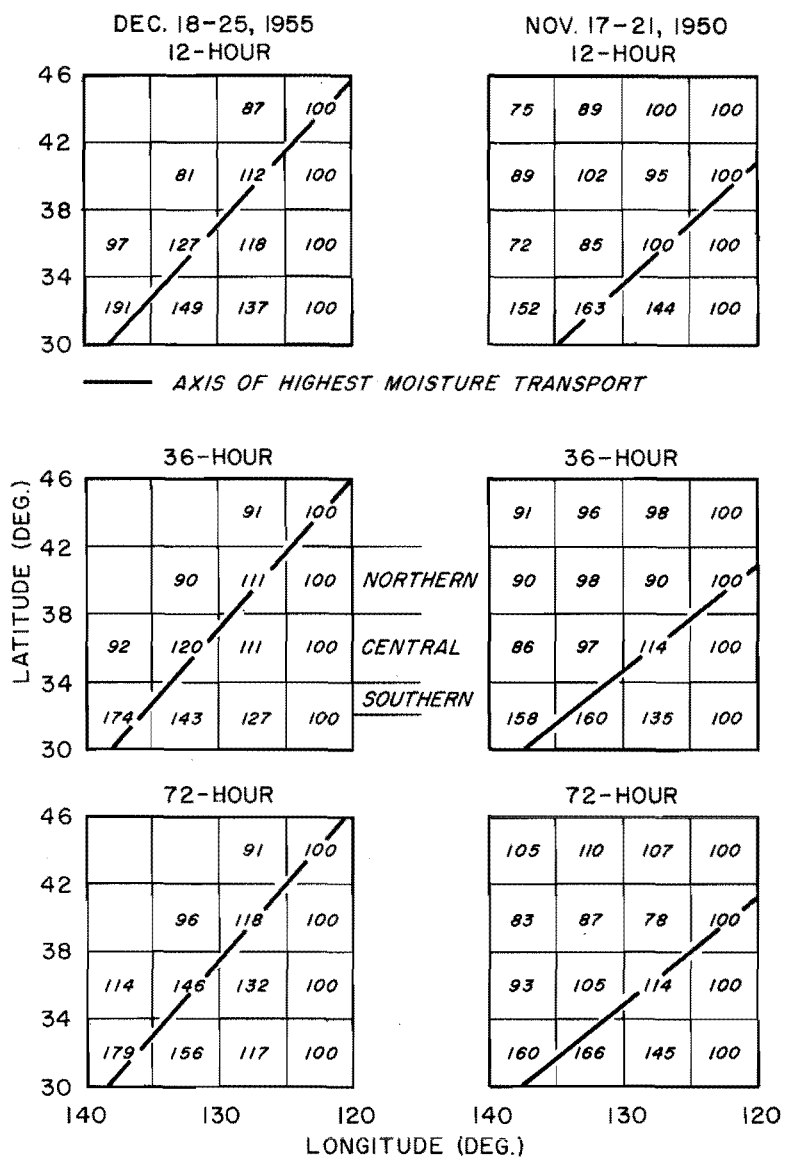

Fig. 3-13. OFFSHORE MOISTURE TRANSPORT IN PERCENT OF COASTAL VALUES IN TWO STORMS

Highest 48- and 72-hour values of persisting moisture transport in the area from the coast to 155 W and from 34 to 42 N in storms between 1910 and 1957 are compared in table 3-5 with highest values at the same latitude in the December 1955 storm. Data are based on 6-hourly surface charts subsequent to 1945 and on daily surface charts prior to that time. Values in table 3-5, expressed as percent of highest December 1955 value at that latitude, are those which exceeded 85 percent of the December 1955 values. Key to square numbers is given by the diagram at bottom of this page.

Only a few values exceeded the December 1955 values at the same latitude. Exceedances were all less than 15 percent.

Table 3-5 does not include data from some storms with higher pressure gradients west of 140 W because the synoptic situation in those storms does not lend itself to transposition to the coast. This follows from the fact that the strong gradient is associated with a strong NE-SW Plateau blocking High, which is peculiar to that area and cannot be transposed to the central United States.

It may be concluded from the above crude comparisons that moisture transport over the eastern Pacific in the December 1955 storm compares favorably with highest values at the same latitude in 1910-1957 storms of a type that could happen at the coast.

An interesting sidelight to the above moisture transport comparison is the marked similarity of the January 18-21, 1956 storm to the December 1955 storm, with the exception that the former was displaced 15 to 20 longitudinal degrees to the west relative to the 1955 storm. Transposition of its pressure field that distance eastward would have resulted in a storm similar and comparable in moisture transport to the December 1955 storm a month earlier.

16	13	10	7	4	1	42N
17	14	11	8	5	2	38
18	15	12	9	6	3	34
						30
155W			140		125	

Table 3-5

HIGHEST PERSISTING MOISTURE TRANSPORT IN PAST STORMS IN PERCENT OF HIGHEST AT SAME LATITUDE IN DECEMBER 1955 STORM

Storm	Square Number	Percent of Highest December 1955 Moisture Transport 48-hour	72-hour
	-----East of 140W-----		
Jan. 28-31, 1935	4	107	113
"	5	105	112
"	6	91	92
Dec. 27-30, 1945	7	87	91
Feb. 7-10, 1947	9	85	89
Nov. 17-20, 1954	4	90	94
Feb. 23-26, 1957	1	86	81
"	5	85	87
"	6	92	89
	-----West of 140W-----		
Dec. 21-24, 1925	12	105	106
Feb. 25-28, 1934	18	94	96
Dec. 26-29, 1945	10	108	100
"	11	102	98
"	18	113	103
Jan. 18-21, 1956	14	91	104
"	18	101	106

c. Latitudinal comparison of moisture transport between storms. The latitudinal trend in moisture transport at the California coast is indicated by combining the trends in highest winds (3-A-2a) and of highest moisture (3-B-2), namely decrease of wind toward lower latitude southward from San Francisco and decrease of moisture toward higher latitude northward from San Francisco. Figure 3-14 shows this combination of data for wind (figure 5-32, HMR 36) and coastal mid-January moisture (figure 4-5a, HMR 36). It indicates decrease of moisture transport along the coast from 38 N latitude. North of the latitude of San Francisco this trend is due to decrease in moisture; and south of San Francisco, it is primarily because of decrease in wind.

3-C-4. Comparison of observed precipitation with moisture transport

The percentage of moisture transport which falls out as precipitation is dependent on several factors, including height and slope of orographic barriers, contribution of convergence mechanisms and degree of saturation (4-C). Table 3-6 compares percentage depletion of moisture by precipitation

over a sector of the Sierra Range during the main part of the December 1955 storm, arranged in order of increasing moisture transport. The precipitation area is shown in figure 3-15. The moisture transport pertains to the foot of the range. The transport values are derived primarily from Oakland upper-air moisture and winds but with adjustment to Sacramento upper-air winds where available. Values of 6-hour precipitation, expressed as an hourly rate, are compared with moisture transport approximately midway in the 6-hour period.

Table 3-6

COMPARISON OF MOISTURE DEPLETION WITH INFLOW OVER THE CENTRAL SIERRAS IN THE DECEMBER 1955 STORM

Date and Time (PST)	Moisture Transport (Inch-miles per hour)	Observed Precipitation (Inches per hour)	Percentage Depletion of Moisture
210700	21	.02	6
221300	38	.10	16
211300	48	.18	20
211900	58	.43	42
220700	62	.32	30
221900	62	.32	30
		Average	24

In table 3-6, increase in efficiency of the orographic precipitation process, as well as increase in the convergence precipitation component of total rainfall, is suggested in the trend toward greater percentage depletion with higher moisture transport. An average depletion of 24 percent is indicated for the period.

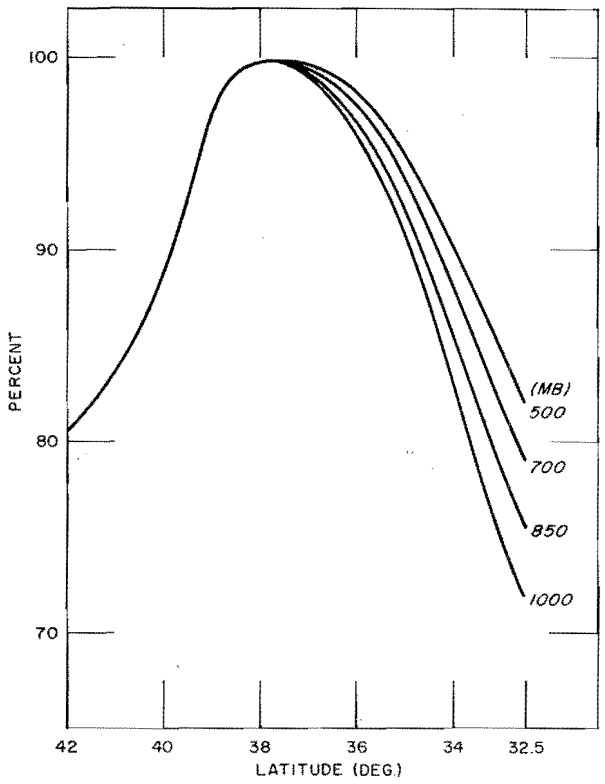

Fig. 3-14. LATITUDINAL VARIATION OF COASTAL MAXIMUM MOISTURE TRANSPORT FOR MID-JANUARY RELATIVE TO 38N

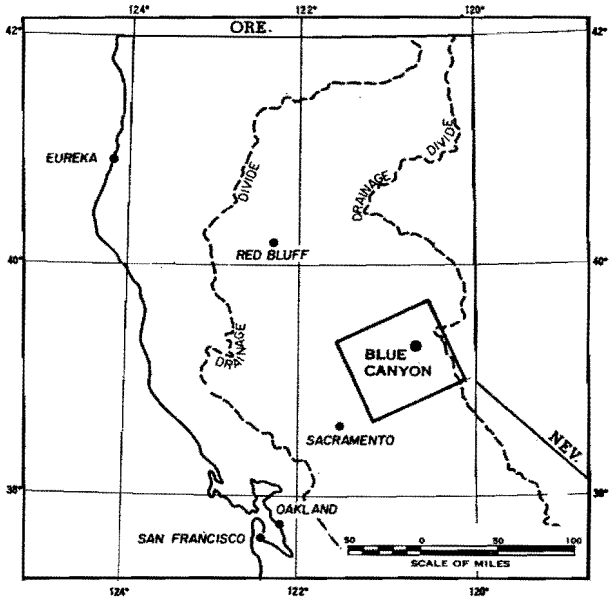

Fig. 3-15. LOCATION OF PRECIPITATION AREA, TABLE 3-6

Chapter IV

TOPOGRAPHIC EFFECTS

Introduction

Orographic precipitation is more dominant and clear-cut in California than in any other of the United States with the possible exception of Hawaii. The isohyets of mean annual precipitation, figure 4-1, readily reflect the positions of the principal mountain chains. The mountains also have a significant effect on the fields of atmospheric pressure and wind. This chapter describes some of the topographic effects on pressure, wind and precipitation.

4-A. PRESSURE

4-A-1. Effects on pressure

There are both dynamic and hydrostatic effects on the pressures in the vicinity of mountains. For the air to speed up in passing over a mountain, as it must to clear the obstruction, it must be accelerated by a pressure gradient along the direction of flow. There is also a pressure gradient directed along any valley through which the air moves against significant friction. These are the dynamic effects.

When air rises up a slope it is cooled adiabatically, while descending air is warmed. The variation of pressure with height is different in the columns of differing temperature. The horizontal pressure gradient must therefore vary with height. Thus the temperature changes due to a flow over a mountain have an effect on pressure patterns. This is the hydrostatic effect.

4-A-2. Pressure patterns

The upwind pressure wedge. When air flows over a more or less continuous ridge in great depth it must speed up in order for a given mass of air to pass above a point on the ground within less vertical space. This is usually taken for granted and has been discussed in other studies (3) (7). This acceleration can be occasioned only by a pressure gradient directed normal to the ridge. This gradient results from a wedge of high pressure on the windward side of the mountain in combination with a trough at or to the lee of the crest. This meso-scale feature is frequently drawn for on sea-level pressure charts but omitted from upper-level charts. The wedge, however, must exist in upper levels also to accelerate the flow.

The crest trough. In rising stable air the column over the crest will be colder than an inflow column above the foot of the ridge and the crest trough will increase in intensity with height.

The lee trough. The lee trough is an extension of the dynamically-induced crest trough and also has hydrostatic controls. The warm descending air tends to produce a more intense trough in the pressure pattern at low levels than at higher levels.

4-A-3. Examples

Sea level. The effects of topography can be shown most clearly by a time-average which smooths out some of the individual details of particular weather maps. Two examples are shown of 24-hour average sea-level pressure patterns. The first, figure 4-2, is for a period of relatively strong cross-mountain flow on December 21-22, 1955 in Northern and Central California. This figure, taken from another study (8), is derived from pressures obtained by indirect means at points other than observing stations as well as observed pressures. The upwind wedge and crest or lee trough are evident in the figure, both for the Coast Range and the Sierra.

Figure 4-3 shows composite sea-level pressure and mean surface winds during a 24-hour period of the January 1943 storm, when especially heavy orographic precipitation was experienced in the San Gabriel Mountains of Southern California. (See section 4-C-3). The strong gradient across the mountains appears in this case as a packing together of the general east-west isobars and is discernible in the vicinity of 34N, 118W.

700 mb. A combination of estimated thicknesses with the sea-level chart of figure 4-2 yields the 700-mb chart depicted in figure 4-4. Here the double wedge-trough pattern is in evidence. On this date there was more than usual cross-ridge low-level flow and therefore marked 700-mb troughs. Flow at 700 mb and above does not require any such perturbation of the contour lines if there is little or no cross-ridge flow at lower levels since there is then no acceleration of the air stream.

4-B. WIND

The synoptic meteorologist normally regards isobars (or contours on a constant pressure surface) as approximate streamlines. In mountain areas of California momentum, friction and stability are effective in producing quite significant departures from the geostrophic wind. These are discussed in this section, and the effects of the California terrain in modifying the wind are evaluated.

4-B-1. Low-level flow

The low-level flow at the surface and in the first 1000 feet or more is predominantly either very light or essentially parallel to the main ridges toward lower pressure. Flow in this lower layer has only a slight upslope component except where there are breaks in the general configuration of the topography, or where promontories or local ridges intercept and lift the flow.

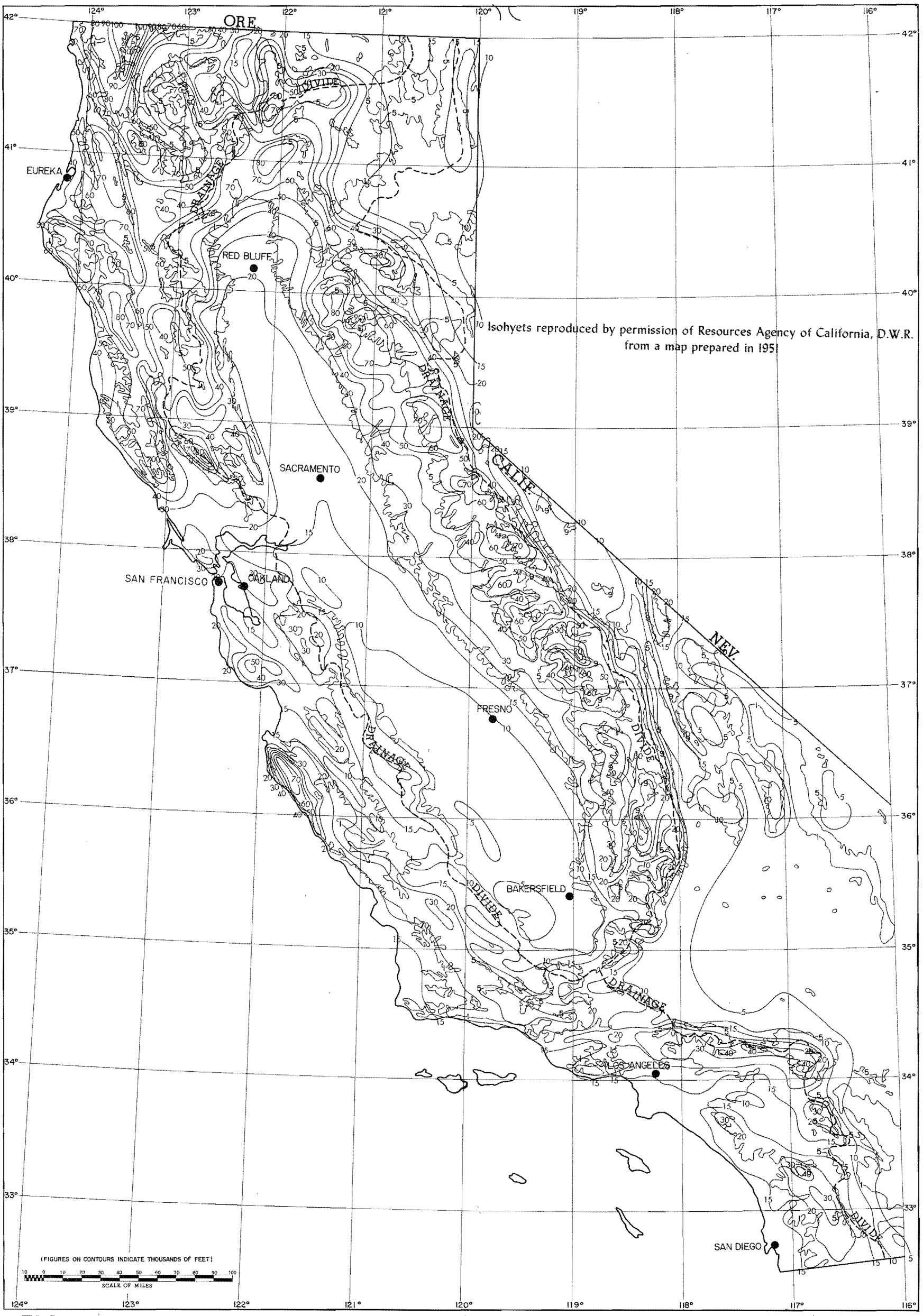

FIG. 4-1. MEAN ANNUAL PRECIPITATION (INCHES), CALIFORNIA

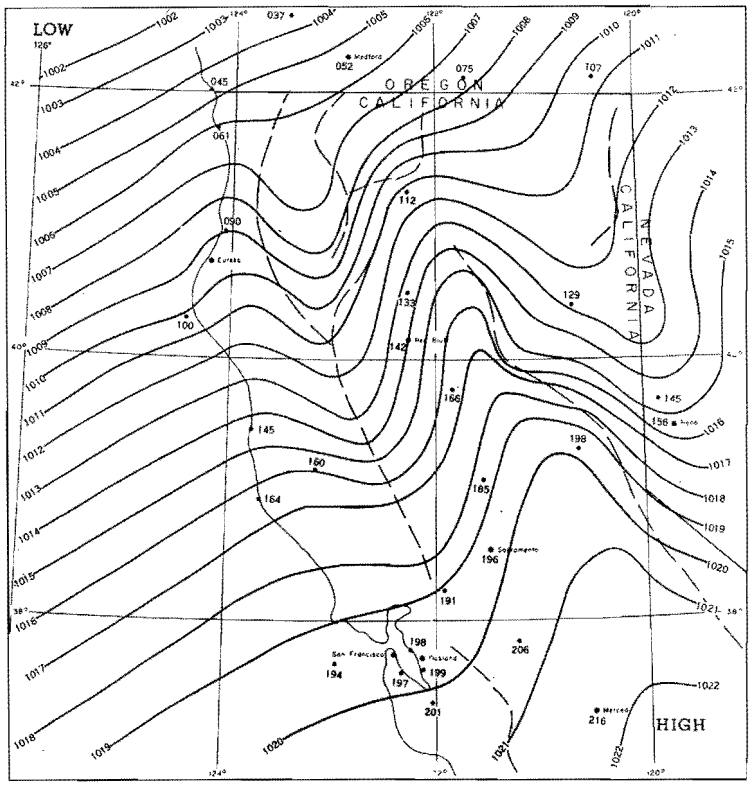

Fig. 4-2. MEAN 24-HOUR SEA-LEVEL PRESSURE (MB), 0400 PST DECEMBER 21 THROUGH 0400 PST DECEMBER 22, 1955

It would be expected that local areas with such topographic features would be centers of high precipitation, especially when stability conditions are such that some orographic lift can trigger convection. The precipitation gage network is not sufficiently dense at present to verify this effect in all regions where it may exist. Elliot and Shaffer (9) have analyzed precipitation on the Santa Ynez and San Gabriel Mountains of Southern California, which face south, and report orographic and triggering effects. These effects may be interpreted in part as interception of the general along-coast low level current. The southwesterly flow at intermediate levels below ridge top also impinges on these escarpments.

The highest mean annual precipitation shown on figure 4-1 in the Sierras is on the north fork of the Feather River. This is thought to be an effect of a bend in the general orientation of the mountain with maximum interception, for the Sierra west slope, of up-valley flow at this point.

Figure 4-5 shows mean 24-hour wind and interpolated streamlines for the same period in the December 1955 storm to which the composite pressure map

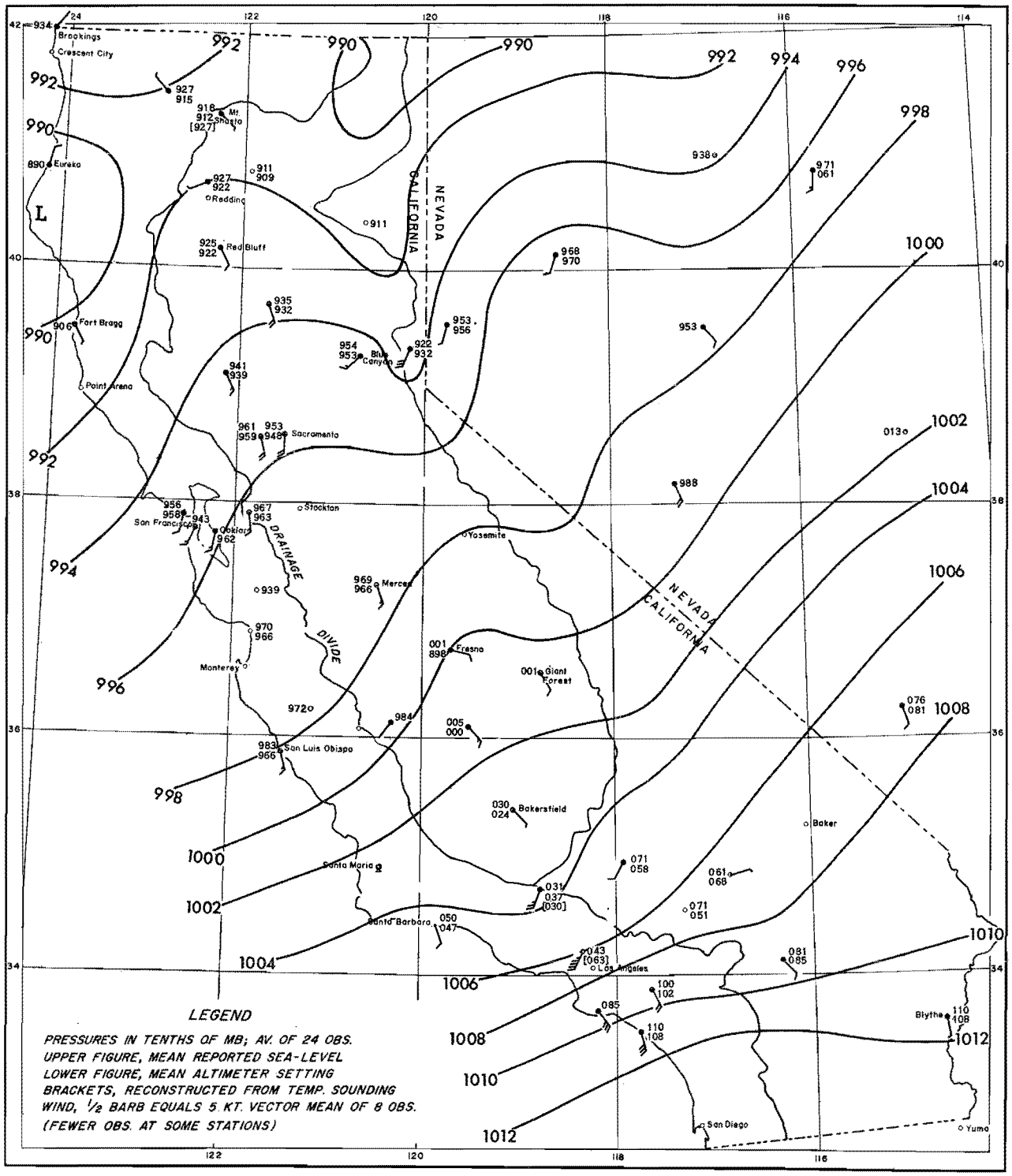

Fig. 4-3. MEAN SEA-LEVEL PRESSURE AND SURFACE WIND FOR 24 HOURS JANUARY 22, 1943 (PST)

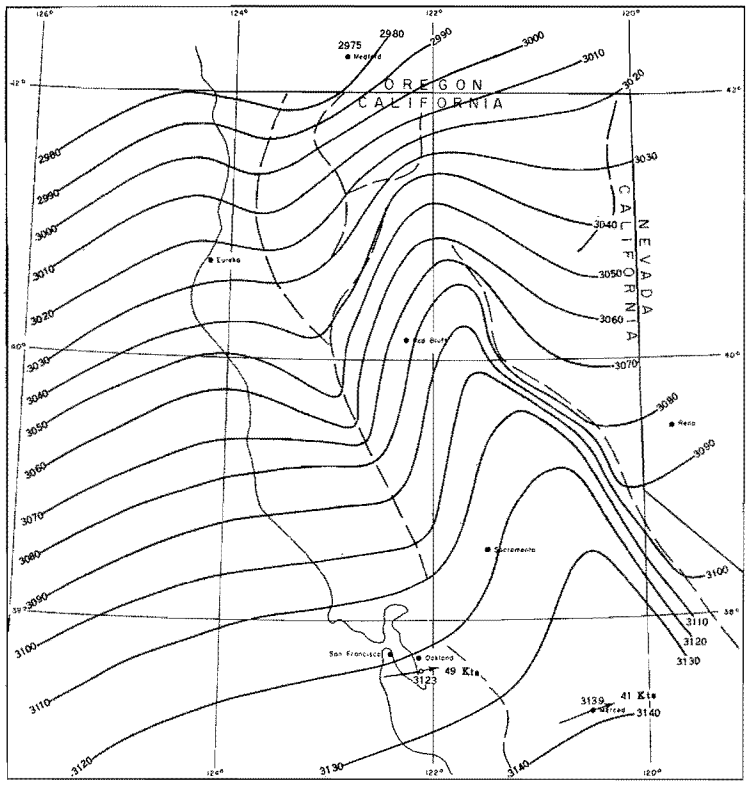

Fig. 4-4. MEAN 24-HOUR 700-MB CHART, 0400 PST DECEMBER 21 THROUGH 0400 PST DECEMBER 22, 1955

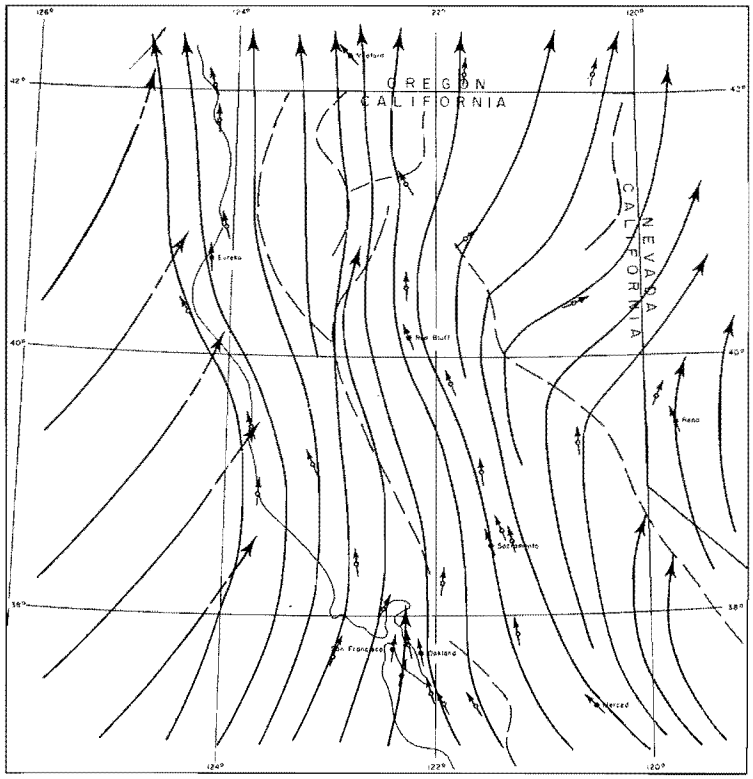

Fig. 4-5. SURFACE STREAMLINES AND WINDS, 0400 PST DECEMBER 21 THROUGH 0400 PST DECEMBER 22, 1955

of figure 4-2 pertains. The predominance of flow parallel to the ridges is evident. The surface wind at some undetermined distance offshore has the slight deviation to the left of the geostrophic wind direction that is characteristic of the open sea. This air is thought to climb above the surface alongshore current, as indicated by the dotted trajectory segments in the figure. That this must happen is deduced by considering the forces involved. There is insufficient pressure gradient directed in the proper direction to overcome the momentum of the air and to force it into a relatively sharp turn near the coast.

The gap in the Coast Range at San Francisco Bay is a significant topographic feature in admitting low-level flow into the Central Valley. Because of the predominance of a northward flow at low levels during storms this gap affects the precipitation regime far to the north but much less to the south. This appears to be one reason that there is higher mean annual precipitation at corresponding elevations in the northern Sierras than in the southern Sierras. (The increase of general storminess northward is another reason.)

4-B-2. Intermediate-level flow

The predominant characteristic of intermediate-level flow at the approximate elevation of ridge tops is that the horizontal projection of a trajectory is approximately straight or follows the general broad curve characteristic of flow at these levels. The flow does not follow the convolutions of the constant pressure height contour lines depicted in figure 4-4. This may be illustrated by computing a trajectory, by use of the equations of frictionless motion, through the contour field. Goodyear (10) describes one technique for doing this. Such trajectories (not shown) indicate that the wind speeds up and slows down depending on whether the air is moving toward lower or higher pressure but changes direction very little.

The practical consequence of the more or less straight flow is that useful results may be obtained by computing the flow across ridges as a two-dimensional problem, using wind components normal to ridge. To study orographic precipitation the windflow is needed above all elevations along the mountain. Generally, however, both surface and upper-air observations are available from only low-elevation stations representative of flow at the foot of the mountain. It has been customary to compute or estimate the flow over the rest of the mountain from these observations, by applying a two-dimensional model to the wind components normal to the mountain. Myers (7) has developed one technique for doing this which is alluded to in HMR 36, paragraphs 5.13-5.16.

4-B-3. Control of stability

The control of stability on the flow over or around obstructions deserves special mention. Elliot and Shaffer (9) have analyzed precipitation in the Santa Ynez and the San Gabriel Mountains in three stability classes; stable, unstable, and mixed. During unstable regimes lifting of the air is

facilitated and the mountain precipitation is high relative to coastal plain precipitation. During stable conditions ascent is inhibited and there is less mountain precipitation than coastal. The mixed type consists of a variation of stability at different times during the storm and produces an intermediate total storm ratio of mountain to coastal plain precipitation.

The variation in the vertical of $V_o - V_i$ (increase in windspeed from foot to crest of ridge along a streamline) in two-dimensional laminar flow according to Myers (7) is given by

$$\frac{\partial}{\partial P_i} (V_o^2 - V_i^2) = 2R(\gamma - \gamma_a) \ln \frac{P_i}{P_o} \qquad (1)$$

Here P is pressure, V speed, R the gas constant, γ the lapse rate on a pressure coordinate ($\partial T/\partial p$), with the subscripts i and o indicating inflow and outflow respectively and the subscript a denoting the adiabatic lapse rate, either moist or dry depending on the particular flow.

The stability factor is the difference in the lapse rates. A large difference means that there must be a large increase with height of the increment of velocity squared, or viewed oppositely, a large decrease of this increment with decreasing height. $V_o^2 - V_i^2$ as pointed out by Myers can even approach zero or negative values with decreasing height which means that the low level air refuses to climb the mountain. At any rate stability has a marked effect on whether the air goes around or over the mountain.

It would be expected that in general the unstable flows found with High-latitude type storms would ascend the Coast Range more readily than the more stable flows characteristic of other types.

4-B-4. Wind to geostrophic wind empirical relationships

The terrain impedes and deflects the wind to considerable heights, more than it affects the atmospheric pressure gradient. A measure of the terrain influence on the wind and its variation with height can therefore be obtained by comparing observed upper-air winds with the geostrophic wind. The resulting comparisons can be utilized, in turn, to estimate winds when observations are not available because of unfavorable weather but the pressure field may be reconstructed. This procedure was used in HMR 36 to determine winds for orographic precipitation computations. Detailed wind-geostrophic wind relations developed at ten pilot-balloon and rawin stations are presented in this section. The speed relationships are called V/V_g ratios. Direction relationships are also shown.

Two other indirect means of estimating upper-air winds are covered later in the chapter.

Geostrophic wind. The wind comparisons were restricted to dates of off-sea flow of typical rain-bearing wind direction, as categorized in detail in a subsequent paragraph. In these situations the geostrophic wind usually changes with height in a relatively simple manner. In this study the geostrophic wind at the surface, at 500 mb, and an interpolation between were deemed adequate to fix the value of the geostrophic wind, V_g, at any level to 500 mb.

The method was to determine independently the sea-level geostrophic wind, the 500-mb geostrophic wind, and the 1000-500 mb thermal wind. The three winds were then plotted on a vector diagram and modified equal amounts to make the vector sum of the 1000-mb and thermal wind equal to the 500-mb wind. These adjusted geostrophic winds were then used for plotting against observed winds.

a. Sea-level. The sea-level geostrophic wind for the above was based on three pressure readings surrounding the study station. Three pressures uniquely determine the speed and direction of the mean geostrophic wind in the area. The assumption here is that the isobars are straight and evenly spaced and that this simplification is sufficient for the purpose of characterizing the mean geostrophic wind.

b. 500 mb. The 500-mb geostrophic wind was based on the height differences between two stations generally to the north and south of the study station and the direction of the contours on the 500-mb chart.

c. 1000-500 mb. The thermal wind was obtained in an analogous way to the 500-mb wind. Thickness difference between the raob stations and the direction of the thickness contours substitute for height differences and height contour directions.

V/V_g ratios. Three sets of V/V_g ratios were developed. The choice of data, results, and purpose of each study are discussed below.

1. In the first set the geostrophic wind direction is limited to the southwest quadrant and speeds to above a certain minimum depending on station location. Figures 4-6 through 4-8 show the results of this data summary. The plot for Oakland for this and the following sets is shown on an enlarged scale with the individual observations included in order to illustrate the range and scatter of the data.

These graphs of V/V_g show a marked retardation of the wind at the surface. Oakland surface windspeed, for example, averages about 30 percent of the geostrophic speed. There is a sharp increase of the V/V_g ratio with height in the lower layers topped by a more gradual increase to near geostrophic conditions at 5000 meters.* This extension of the friction layer to

*Pibal observational data are tabulated on a height basis, while raob data are on a pressure basis. In order to compare stations all data were converted to height in km above msl using a conversion rate of 0.5 km/50 mb from sea level (1000 mb) to 500 mb.

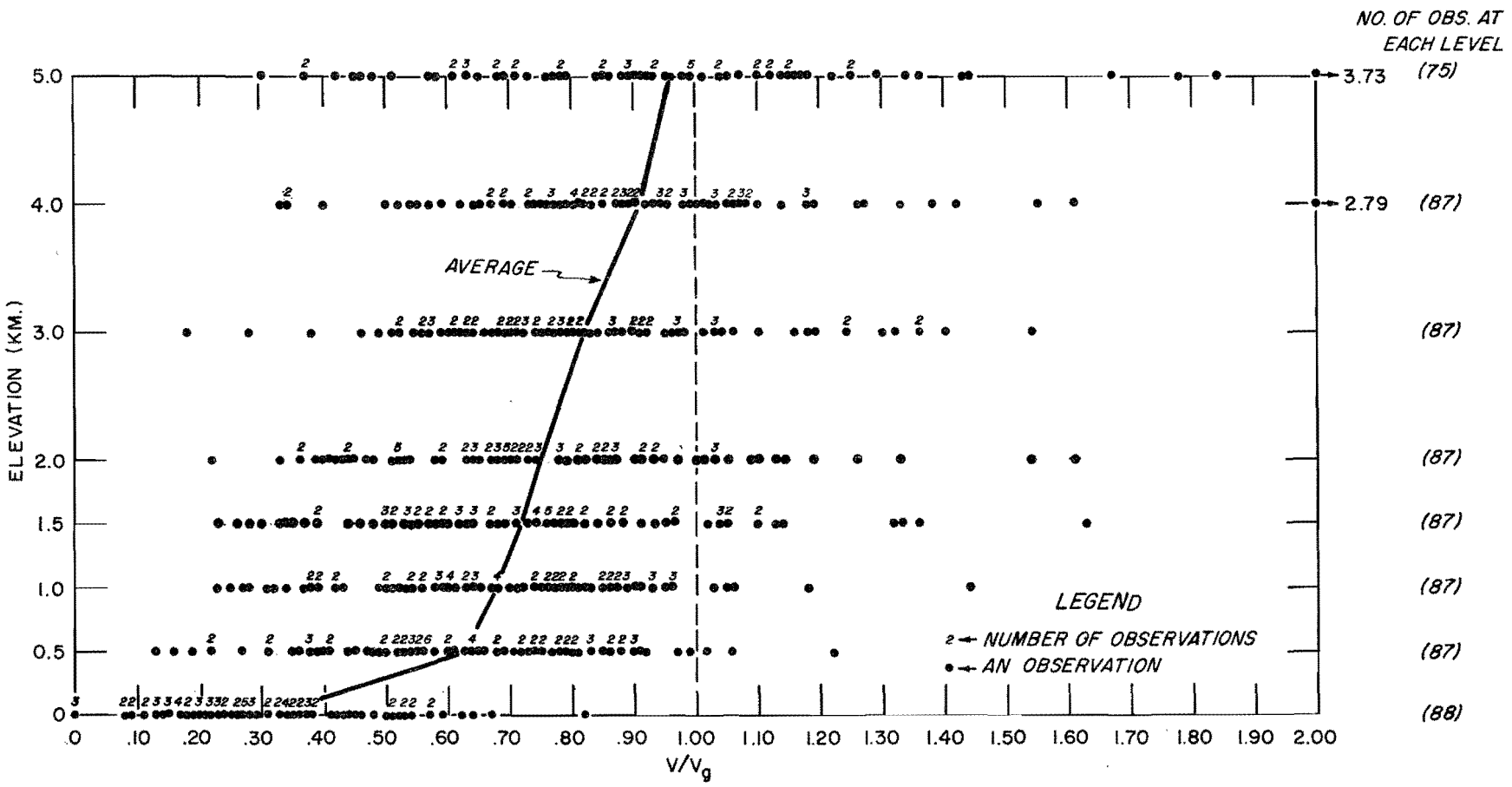

Fig. 4-6. V/V_g, OAKLAND, CALIFORNIA

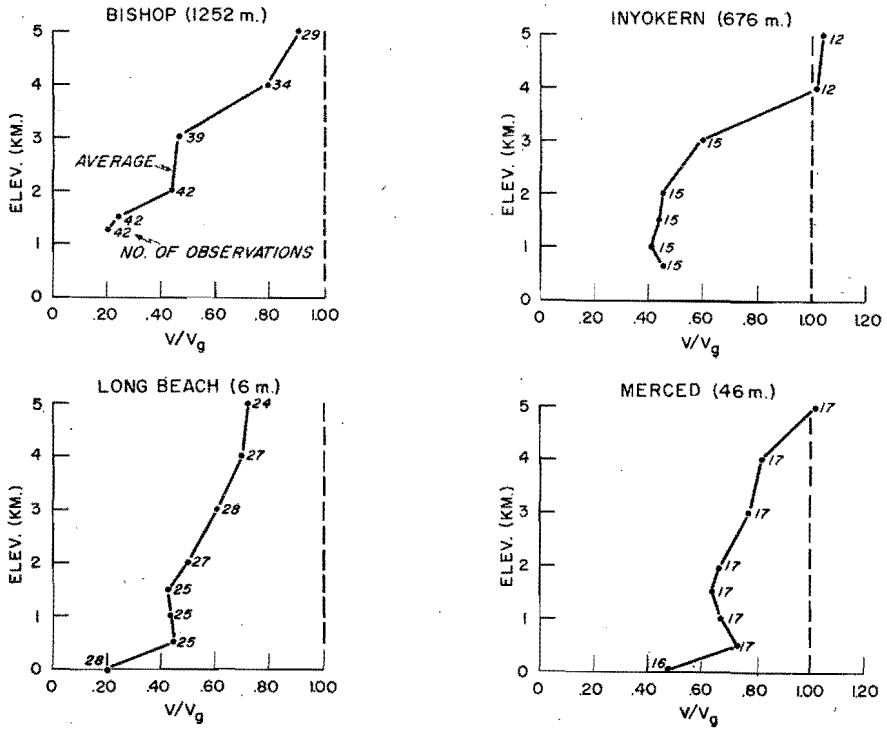

Fig. 4-7. V/V_g, BISHOP, LONG BEACH, MERCED AND INYOKERN

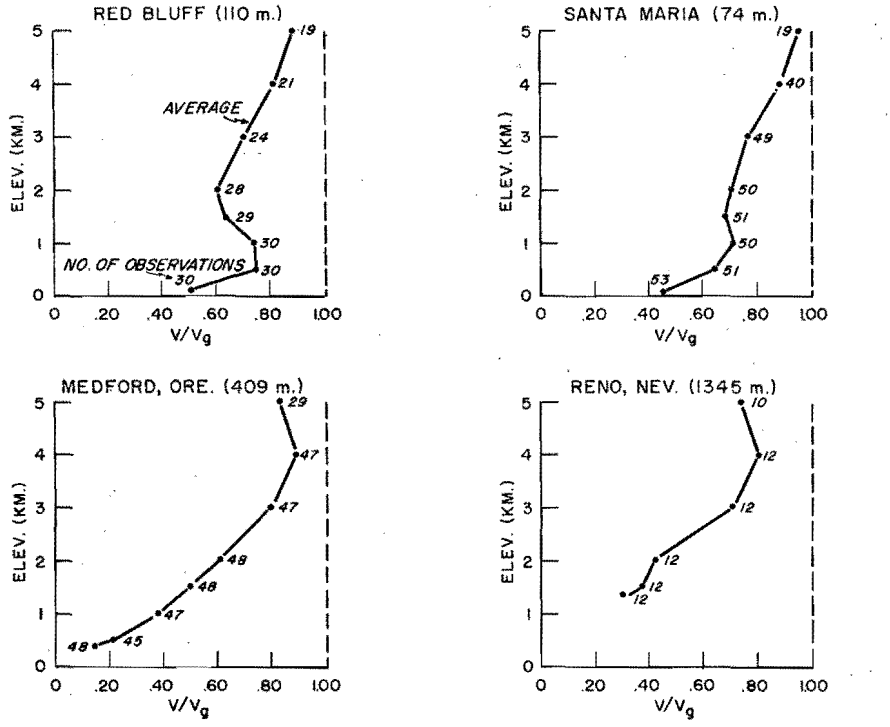

Fig. 4-8. V/V_g, RED BLUFF, SANTA MARIA, MEDFORD AND RENO

5000 meters is due to the impedence effect of the elevated land mass encountered by free ocean air. In general, the V/V_g ratios are smaller for the interior valley stations, where frictional effects are greater.

This set of V/V_g ratios was made in order to obtain a broad view of the wind-geostrophic wind relation. Since the number of observations making up the ratios is approximately three times that of any other group, the ratios are probably the most reliable.

2. The second set of V/V_g ratios is similar to the first except that the geostrophic wind direction is restricted to a 45 degree span centered on a normal to the ridge line in the vicinity of the station. This was to make the wind direction conform closest to optimum heavy orographic rainstorm conditions. The plots for 9 study stations are shown in figures 4-9 through 4-11.

This relation has been used to determine windspeeds in the free atmosphere for rainfall computations in another study (8).

3. The third wind-geostrophic windspeed set is similar to the second except that both the wind (V_c) and the geostrophic wind (V_{gc}) are components normal to the mountains in the station vicinity. (The figures showing this relation are 4-12 through 4-14). Some of these plots appear in abbreviated form in HMR 36 as the basis for average Sierra and Coastal V_c/V_{gc} relations.

The V_c/V_{gc} ratio is almost always smaller than the V/V_g ratio at the corresponding station and level. This is because the wind is usually more nearly parallel to the mountain barrier than is the geostrophic wind. The difference gradually fades with height and V_c/V_{gc} approaches V/V_g at 5 km (500 mb).

This wind-geostrophic wind relation was used to estimate the inflow winds in the test cases of HMR 36, (see par. 5.08). In addition, it was applied to the estimated maximum geostrophic winds as an approach to maximum probable winds in the same report.

Wind-geostrophic wind direction relation. The relationship between the direction of the actual wind and the geostrophic wind was investigated. Cases for study were chosen by restricting the geostrophic wind direction to a 45 degree span near normal to the mountain barrier in the vicinity of the study station. The geostrophic wind span is portrayed for each station in figures 4-15 through 4-17. The results show a tendency for the actual wind to flow parallel to the ridges at low levels and gradually to approach the geostrophic wind direction at 5 km. Exceptions to this are noted for the lower layers at Bishop and Reno where light winds may flow parallel to the ridge line from either direction but average near the geostrophic direction. The direction relationships have been found useful in studies of wind flow where accurate constant pressure charts are available but wind observations are sparse.

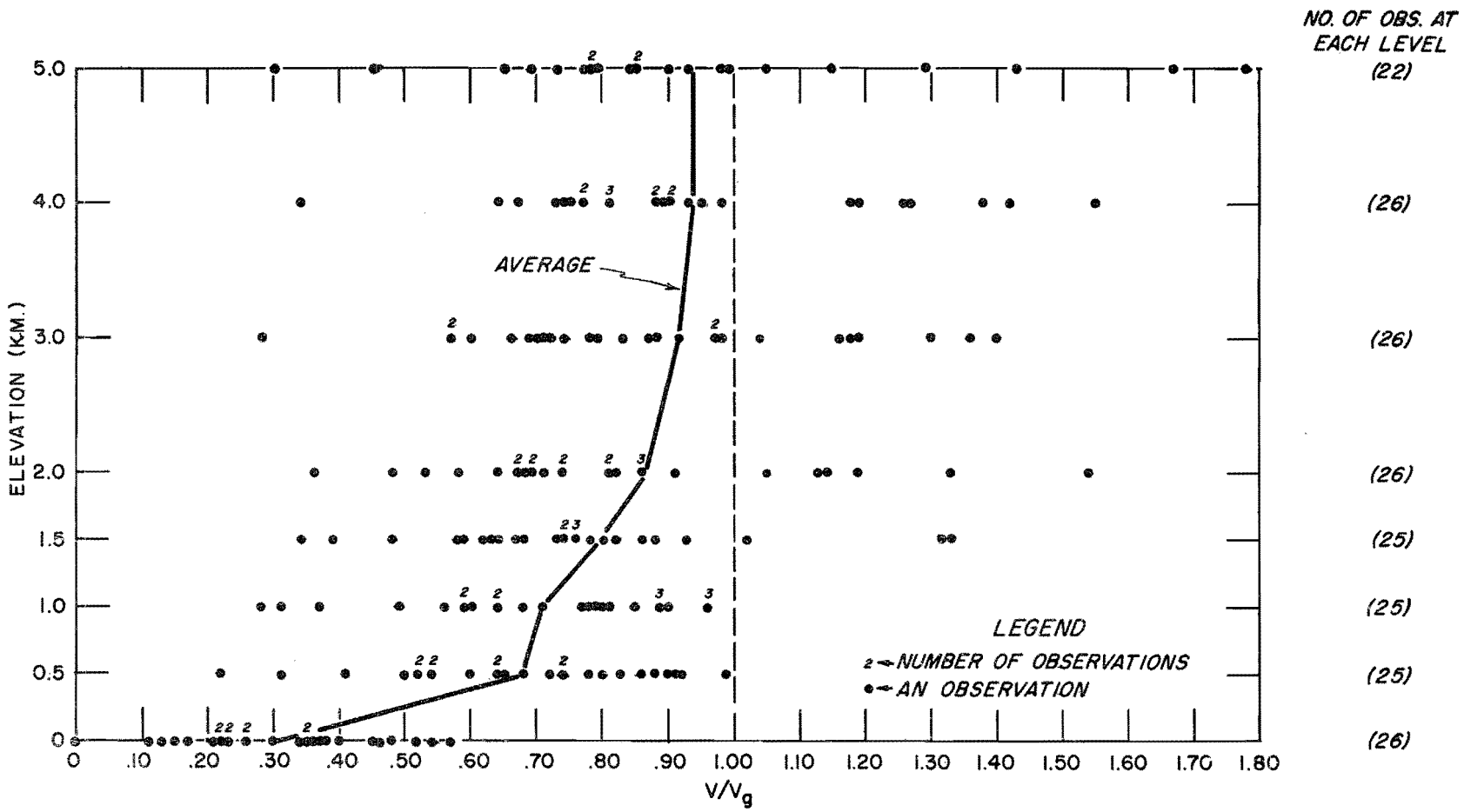

Fig. 4-9. V/V_g, OAKLAND, GEOSTROPHIC WIND SW OR WSW AT SURFACE AND 500 MB

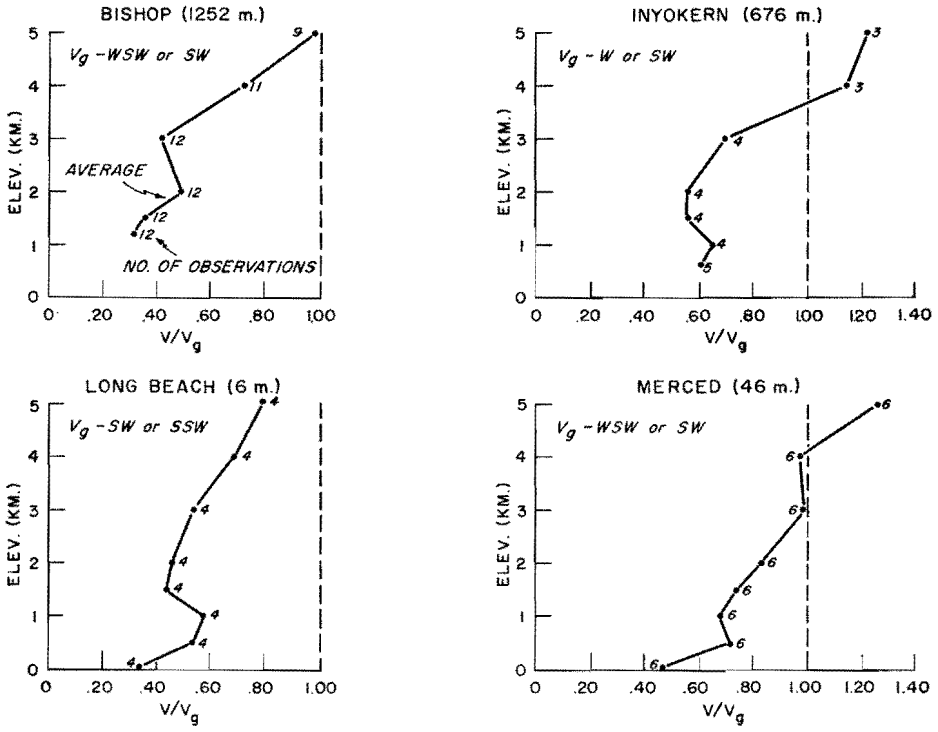

Fig. 4-10. V/V_g, BISHOP, LONG BEACH, INYOKERN, AND MERCED, RESTRICTED DIRECTION

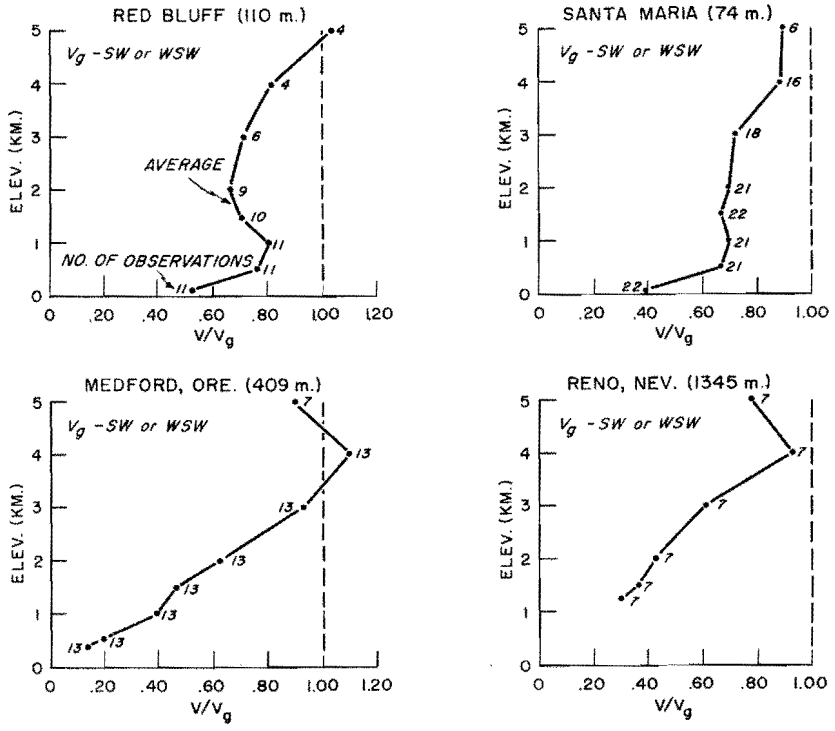

Fig. 4-11. V/V_g, RED BLUFF, MEDFORD, SANTA MARIA, AND RENO, RESTRICTED DIRECTION

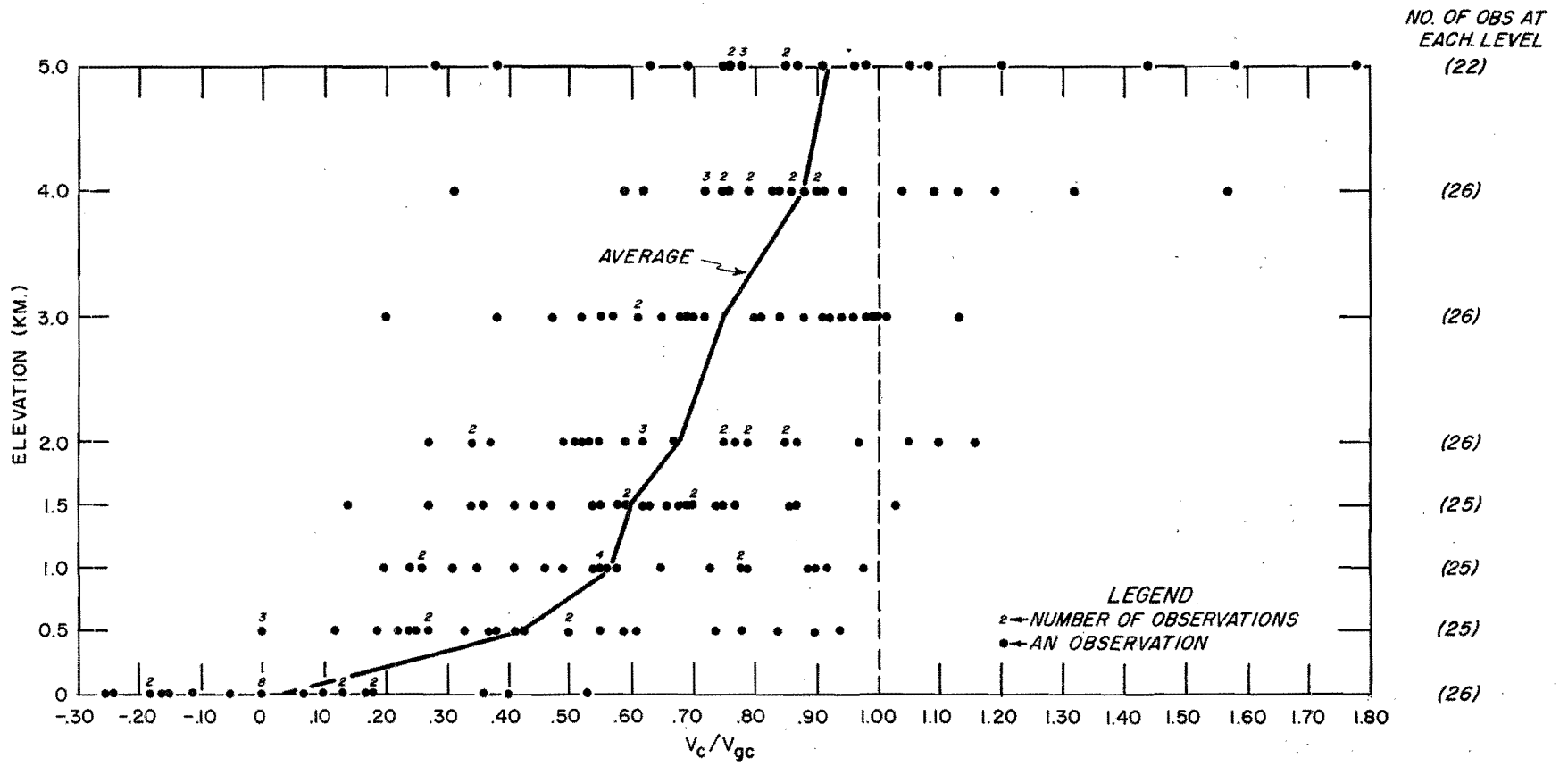

Fig. 4-12. V_c/V_{gc}, OAKLAND, GEOSTROPHIC WIND SW OR WSW AT SURFACE AND 500 MB

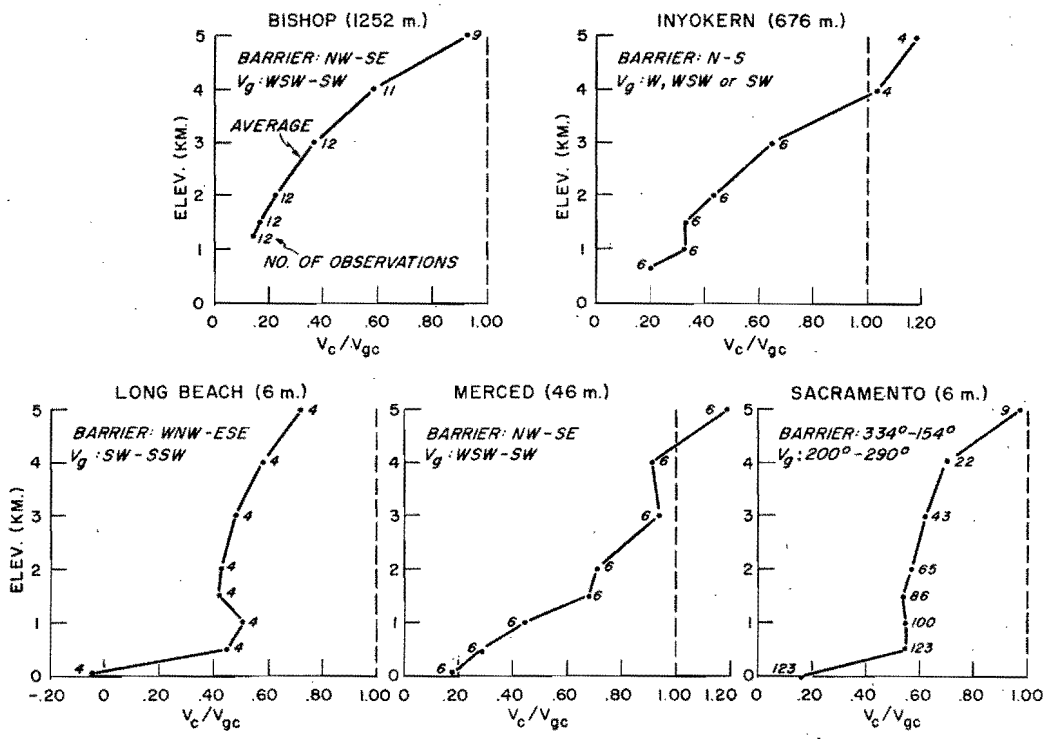

Fig. 4-13. V_c/V_{gc}, BISHOP, INYOKERN, LONG BEACH, MERCED, AND SACRAMENTO RESTRICTED DIRECTION

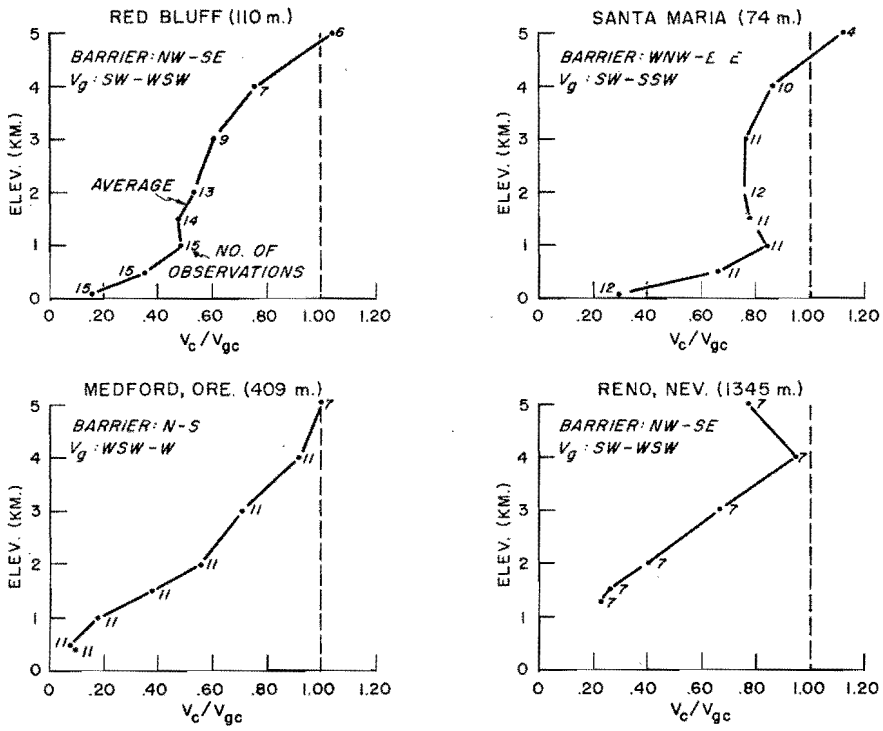

Fig. 4-14. V_c/V_{gc}, RED BLUFF, SANTA MARIA, MEDFORD AND RENO, RESTRICTED DIRECTION

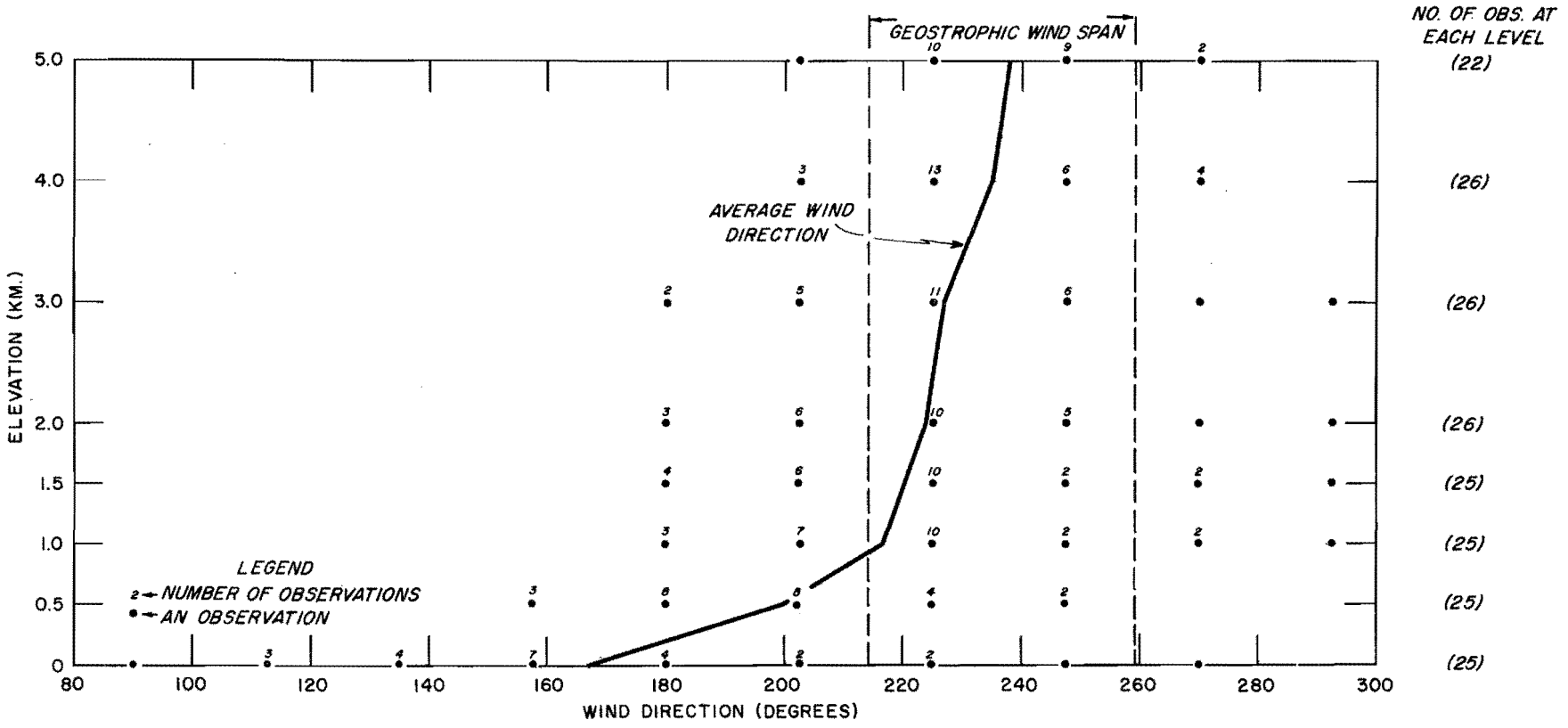

Fig. 4-15. WIND DIRECTION COMPARISON OAKLAND, GEOSTROPHIC WIND DIRECTION SW OR WSW, SURFACE AND 500 MB

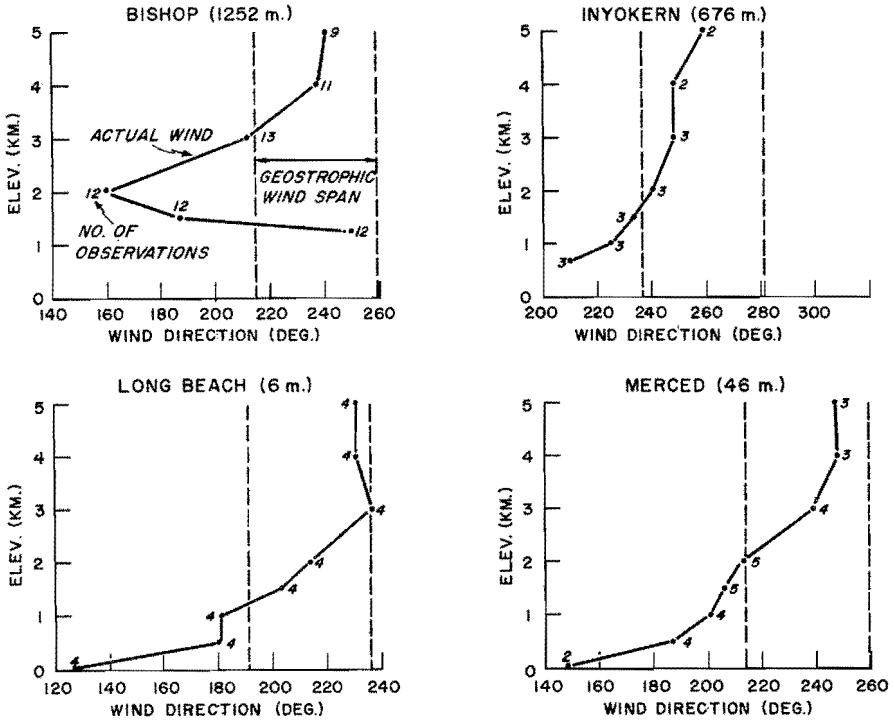

Fig. 4-16. WIND DIRECTION COMPARISON, BISHOP, INYOKERN, LONG BEACH AND MERCED

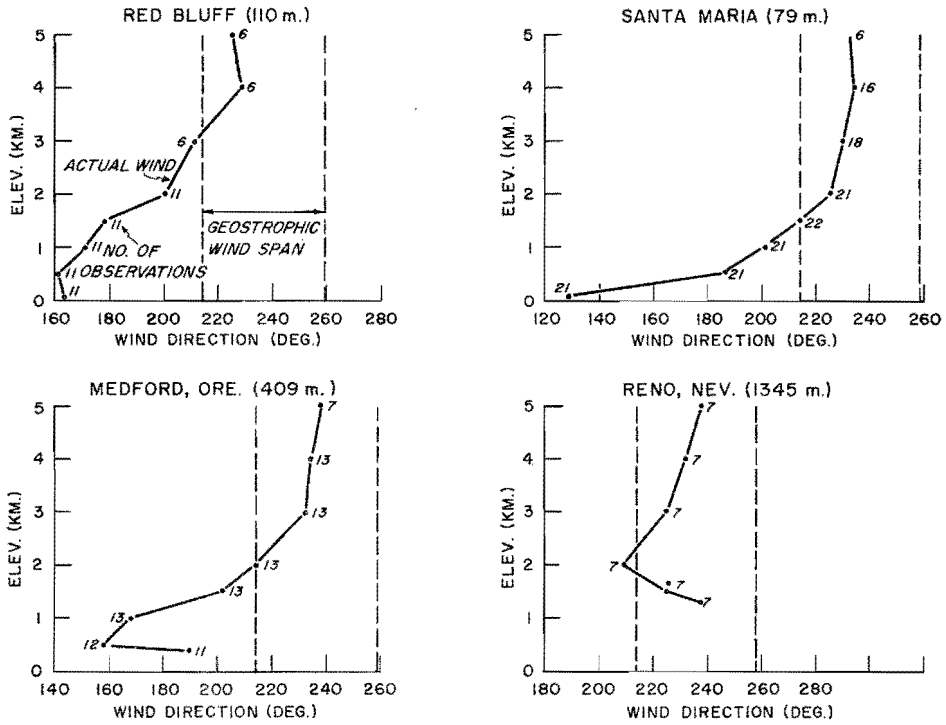

Fig. 4-17. WIND DIRECTION COMPARISON, RED BLUFF, SANTA MARIA, MEDFORD AND RENO

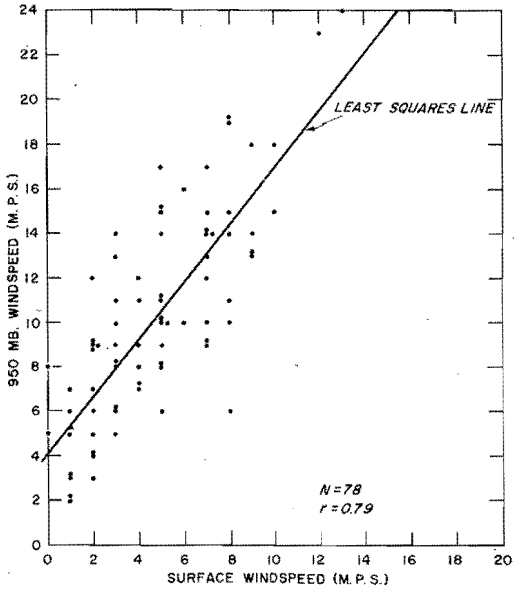

Fig. 4-18. VERTICAL WIND-TO-WIND RELATION, OAKLAND

4-B-5. Wind-to-wind relationships

Vertical. In most locations surface winds are available but upper winds are not. A useful estimate of the 500-meter (msl) (or 950-mb) windspeed and direction can be made from surface winds. Such a relation was developed from data at six land stations where 500-m winds are available, as follows:

Cases were restricted to surface geostrophic wind direction in the SW quadrant. Surface windspeed was plotted against 500-m windspeed for each station. Figure 4-18 is the plot for Oakland.

The correlations obtained between the surface and 500-m windspeed in these 6 plots are as follows:

Station	r	Number of cases
Fresno	0.72	11
Medford	0.88	40
Merced	0.75	16
Oakland	0.79	78
Red Bluff	0.78	20
Santa Maria	0.70	50

The 500-m windspeeds were then read off the six regression lines for a succession of surface windspeeds starting at 6 knots. They were plotted on a diagram with coordinates surface windspeed and station elevation. Smoothed

lines of 500-m wind were then drawn. The resulting surface wind - 500 m windspeed relation is shown as figure 4-19. This relationship can be used for isotach analysis on a 950-mb chart, since the 950 mb-500 m wind difference is usually quite small.

The turn of the wind between the surface and 500 m was also investigated. The following results were obtained:

Station	Average veer with height sfc-500 m (degrees)	Number of cases
Fresno	45	6
Medford	22	10
Merced	17	12
Oakland	29	43
Red Bluff	11	19
Santa Maria	43	37

In addition to the direction restriction, the surface windspeed was required to equal or exceed 8 kts. This was done in order to avoid including the turns associated with very low speed unrepresentative surface winds.

The wind direction results can be used as a guide to orienting streamlines on a 950-mb chart. For coastal locations such as Oakland wind veers from surface to 950 mbs about 35 degrees. In the northern Central Valley less of a turn with height occurs, down to only 10 degrees in the area north of Red Bluff.

Horizontal. Another method of supplementing upper-air observations is use of wind to wind relations in the horizontal between two pilot-balloon stations. The procedure used to develop these relations was to select pairs of wind observations with the key station having a wind within the southwest quadrant, and to compute the average of the windspeed and direction at each level. In practice, the average difference between the two is applied to the key station wind direction and speed to estimate the wind at the other station when the other observation is missing. Figure 4-20 shows the horizontal wind to wind relations.

Results of this study are useful for isotach and streamline analyses.

The Oakland-Sacramento pair (figures 4-20a and b) was chosen to establish a wind "observation" at Sacramento when weather precludes a pibal there but a rawin is available for Oakland.

The study of the San Nicholas Island-Long Beach pair was made in order to examine the change in the average wind as it passes from the sea to land. Winds between 180 degrees and 270 degrees at San Nicholas were investigated. Results of this study are shown in figures 4-20c and d. The speed relation clearly indicates higher speeds at lower levels over the sea than at the

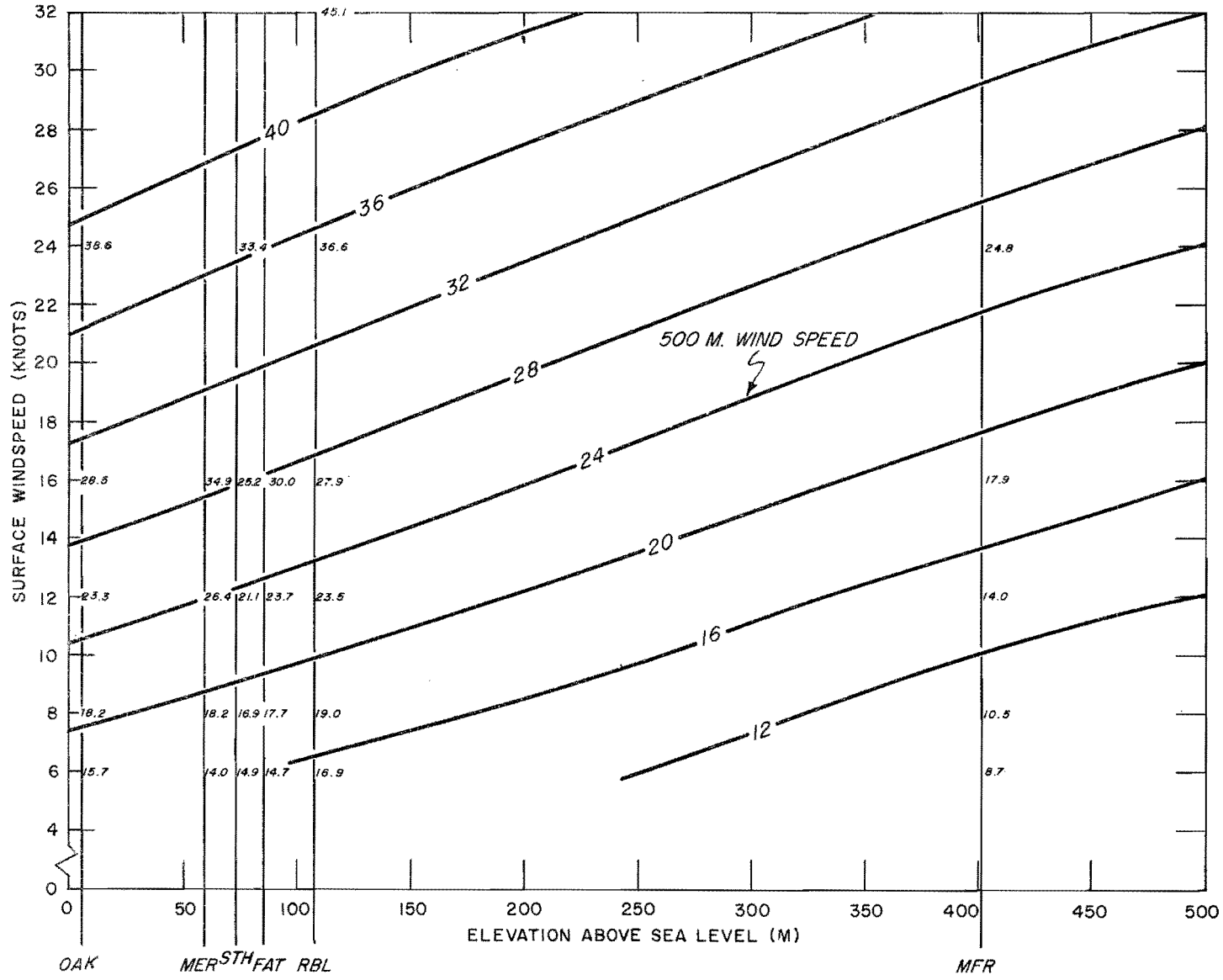

Fig. 4-19. COMPOSITE LOW-LEVEL VARIATION OF WIND WITH HEIGHT

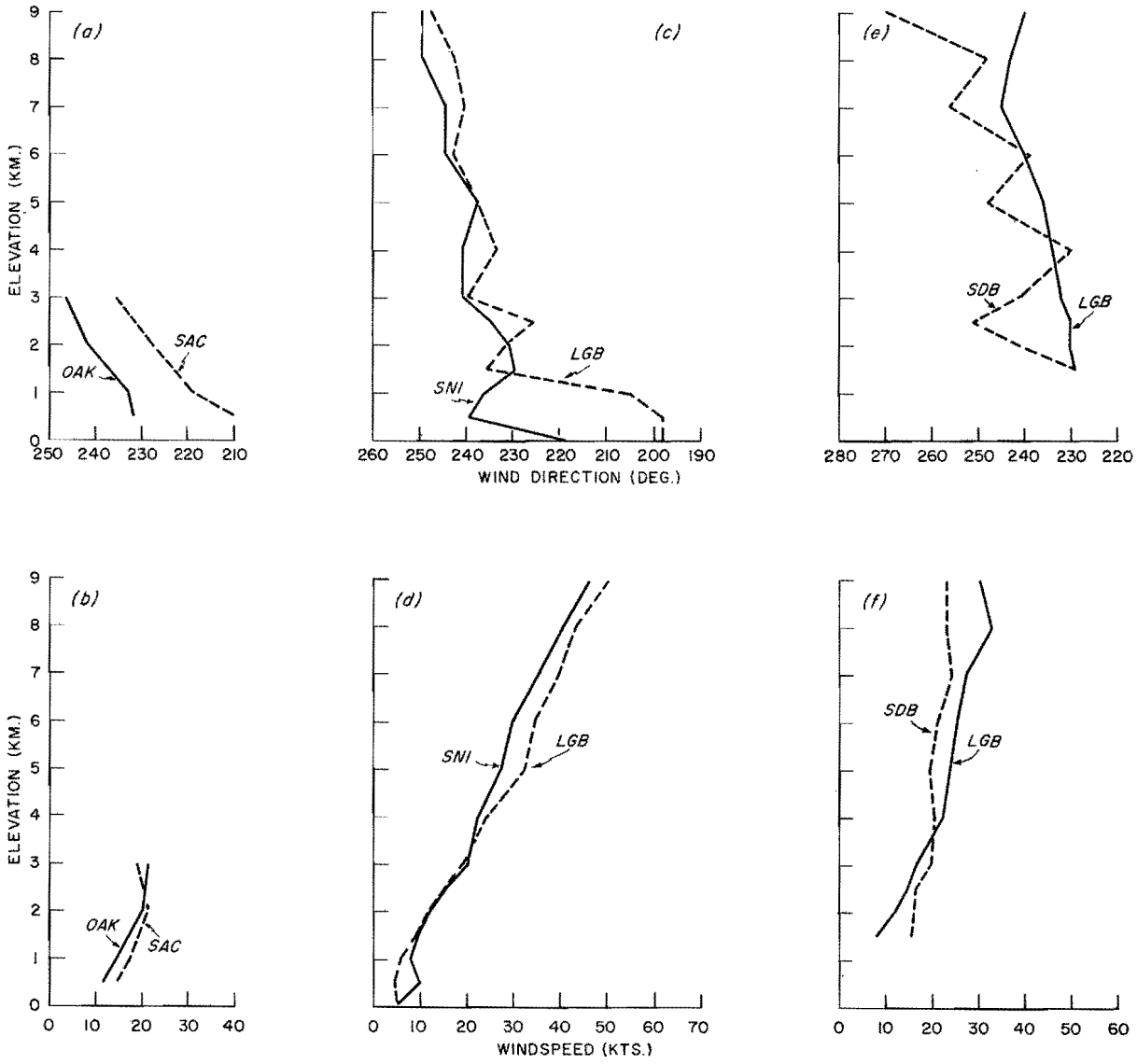

Fig. 4-20. HORIZONTAL WIND-TO-WIND RELATIONSHIPS
OAKLAND-SACRAMENTO, SAINT NICHOLAS ISLAND-LONG BEACH, SANDBERG-LONG BEACH

coast with a crossover to the reverse relation above about 3500 m. The direction chart shows the presence along the coast of the southerly air current induced by the coastal mountain barrier.

The Long Beach-Sandberg pair (figures 4-20e and f) shows the wind change caused by a substantial mountain range. Sandberg is located close to the coastal ridge line. The windspeed results indicate a speedup of the wind in the lower layers at Sandberg relative to Long Beach with a slowing down above.

4-C. PRECIPITATION

4-C-1. Factors favoring orographic precipitation

Orographic precipitation is the vertically integrated difference between the inflow mixing ratio of a stream of air (not necessarily saturated) and the outflow mixing ratio, saturated at a colder temperature, with cognizance taken of the drift of the precipitation from its point of formation to the point at which it strikes the ground. The basic formula for computing formation of orographic precipitation is

$$Y \frac{R}{t} = \frac{1}{g} \int_{\text{ground}}^{\text{nodal surface}} V_i (q_i - q_o) \, \partial P \qquad (2)$$

where R is the precipitation in time t averaged over length Y, g is gravity, q mixing ratio, P pressure, and i and o denote inflow on upwind side of area and outflow on downwind side, respectively. The nodal surface is the level at which the flow is essentially horizontal.

With length in nautical miles, precipitation in inches, time in hours, speed in knots, mixing ratio in grams per kilogram, and pressure in millibars the formula becomes

$$Y \frac{R}{t} = .0004 \int V_i (q_i - q_o) \, \partial P \qquad (3)$$

Variations of this formula are discussed in chapter V of HMR 36.

High orographic precipitation is favored, as may be seen from the formula, by the following factors:

High wind. The greater the velocity the larger the mass of air that is processed in a given time.

High topographic barrier. The higher the barrier the greater the adiabatic cooling and thus the greater the reduction in mixing ratio.

High nodal surface. The higher the nodal surface the greater the average lift for a given inflow.

Saturation. For a given inflow mixing ratio at a given level, the more nearly the air is saturated the smaller will be the outflow mixing ratio, q_o, and the greater the moisture loss. The moisture variation of lifted air before saturation is depicted by the q lines on an adiabatic chart while the variation after saturation is at the faster moist adiabatic rate. Degree of saturation also affects stability.

High temperature. There is a slight increase in $q_i - q_o$ with temperature, for any fixed relative humidity (including saturation) at inflow.

High freezing level. Snowflakes drift much farther with a given windflow than do raindrops. With other factors fixed, the higher the freezing level the less the spillover loss from a windward slope.

Stability. The less the degree of stability the more readily the lower layers ascend the mountain and the higher the nodal surface. Instability provides convective lifts in addition to the lifts associated with the laminar flow of formulas (2) and (3).

4-C-2. Variation of orographic precipitation

Some insight into the quantitative effects of the foregoing factors may be obtained by varying one or two factors at a time in equation (3) while

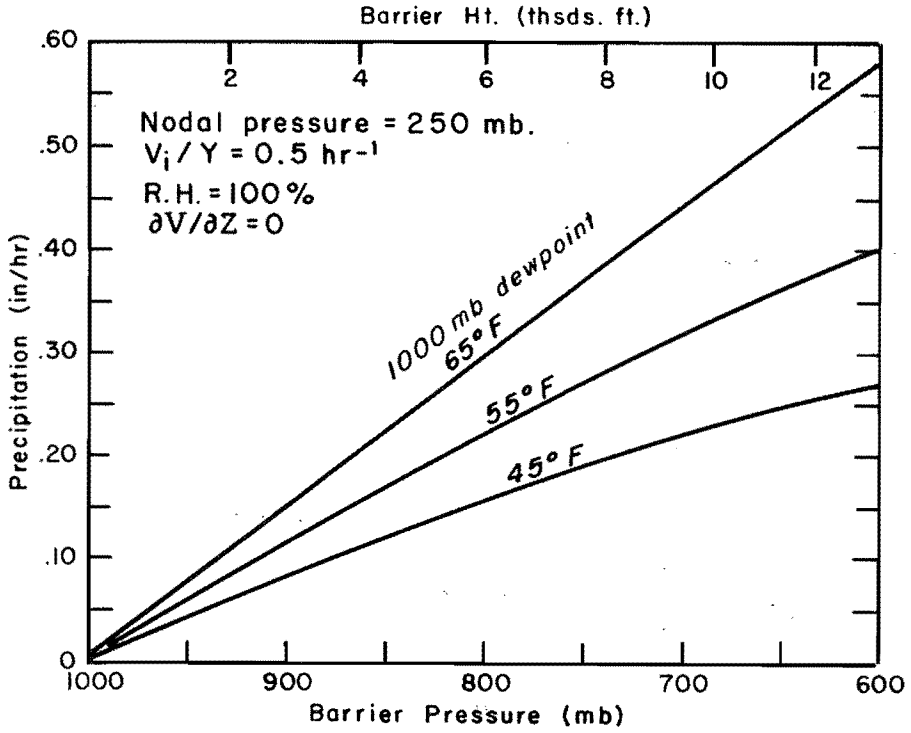

Fig. 4-21. RELATION OF OROGRAPHIC PRECIPITATION TO INFLOW MOISTURE AND BARRIER HEIGHT

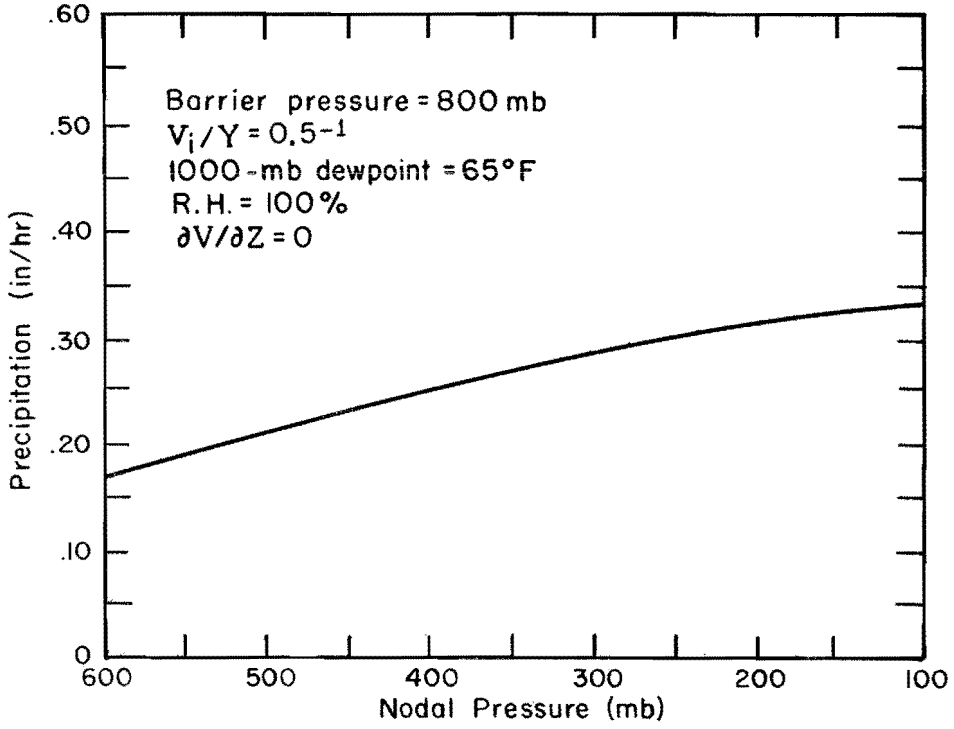

Fig. 4-22. RELATION OF OROGRAPHIC PRECIPITATION TO NODAL PRESSURE

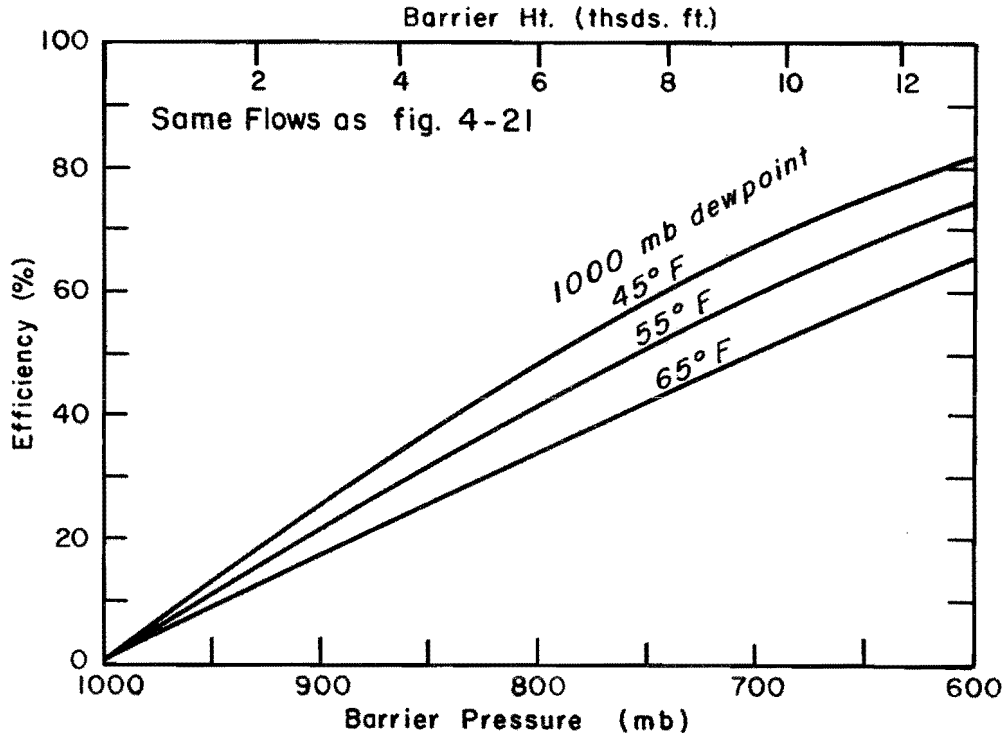

Fig. 4-23. EFFICIENCY OF OROGRAPHIC PRECIPITATION MECHANISM

holding the other factors constant and computing the resultant rate of precipitation, R/t. See figures 4-21 through 4-25. The nomograms depict the precipitation formed, considered equal to the moisture in excess of saturation, without regard to spillover and spillalong effects. The speed V_i and the distance Y are combined into a speed-distance parameter V_i/Y.

The vertical profile of q_i is taken from pseudoadiabats starting with certain dew points at 1000 mbs. The symbol T_d is used for dew point.

Barrier height. Figure 4-21 shows the effect of variation of barrier height and of inflow 1000-mb dew point. The V_i/Y ratio of 0.5 hr^{-1} means that the transit time of air from foot of ridge to crest is two hours, e.g., 30-knot wind against a 60-mile ridge.

It is seen from this nomogram that the precipitation rate from the laminar flow model is very small for low barriers of only 1000 or 2000 feet. The high mean annual rainfall on some ranges of this height on the California coast is due more to general storminess and to stimulation of convection, discussed later, than to direct orographic lift. Even for high barriers the hourly rainfall rates are modest. The effectiveness of orographic rain lies, to a considerable extent, in the persistence hour after hour in the same location.

Nodal pressure. If the air approaching the windward side of a mountain escapes over the mountain only a small distance above the crest, less precipitation will be produced than if the air is deflected to great heights, since the air will be subjected to less cooling. This effect is illustrated in figure 4-22, where the precipitation rate is graphed as a function of nodal pressure, with other variables fixed. It is seen that with the nodal pressure near the tropopause level, around 200 mb, the precipitation is about double that with a nodal pressure at 600 mb.

Percentage moisture depletion. Though a warm saturated current will yield the largest volume of rain, a cool saturated current is more efficient, if efficiency is defined as the ratio of mass of rain to mass of inflowing water vapor. This is shown in figure 4-23, which is constructed for the same inflows and barriers as figure 4-21. There is a proportionately greater escape of water vapor over the barrier in the warmer current.

Relative humidity. The less the relative humidity of the inflowing air the less the orographic rain; some of the adiabatic cooling will be accomplished without producing condensation. The effects are illustrated in figure 4-24. Here the inflow specific humidities are the same for the various relative humidities; the temperature is varied. For example at the base of the 100 percent column the temperature and dew point are both 65°F. At the base of the 70 percent column the dew point is 65 degrees but the temperature is 75 degrees. The figure reveals that lack of saturation almost eliminates orographic precipitation over low barriers and has a lesser, but not insignificant diminishing effect over high barriers.

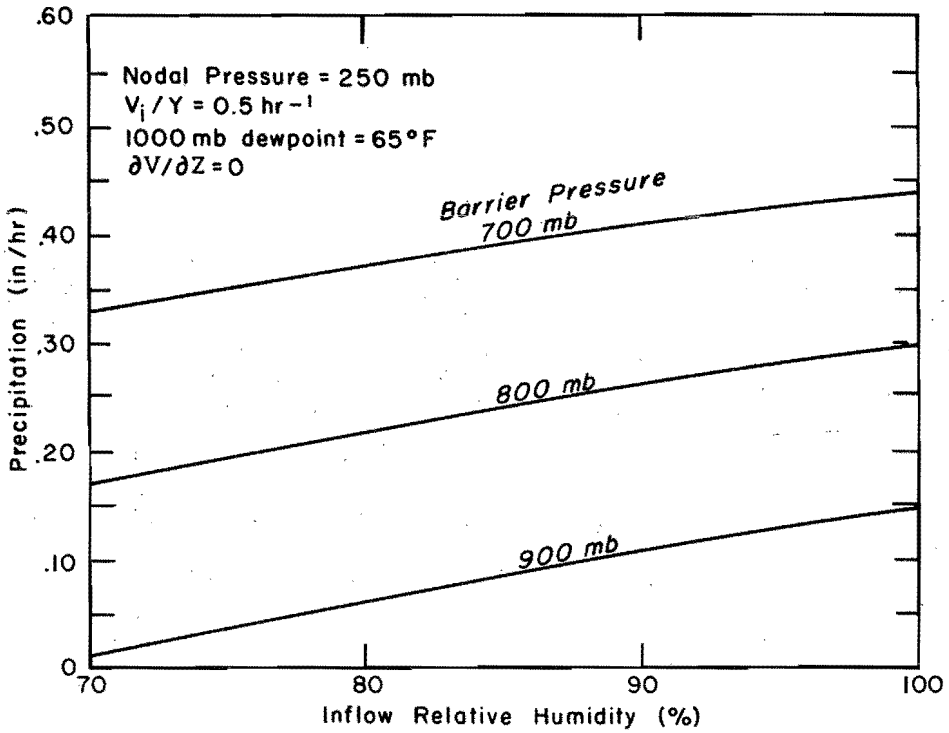

Fig. 4-24. RELATION OF OROGRAPHIC PRECIPITATION TO DEGREE OF SATURATION

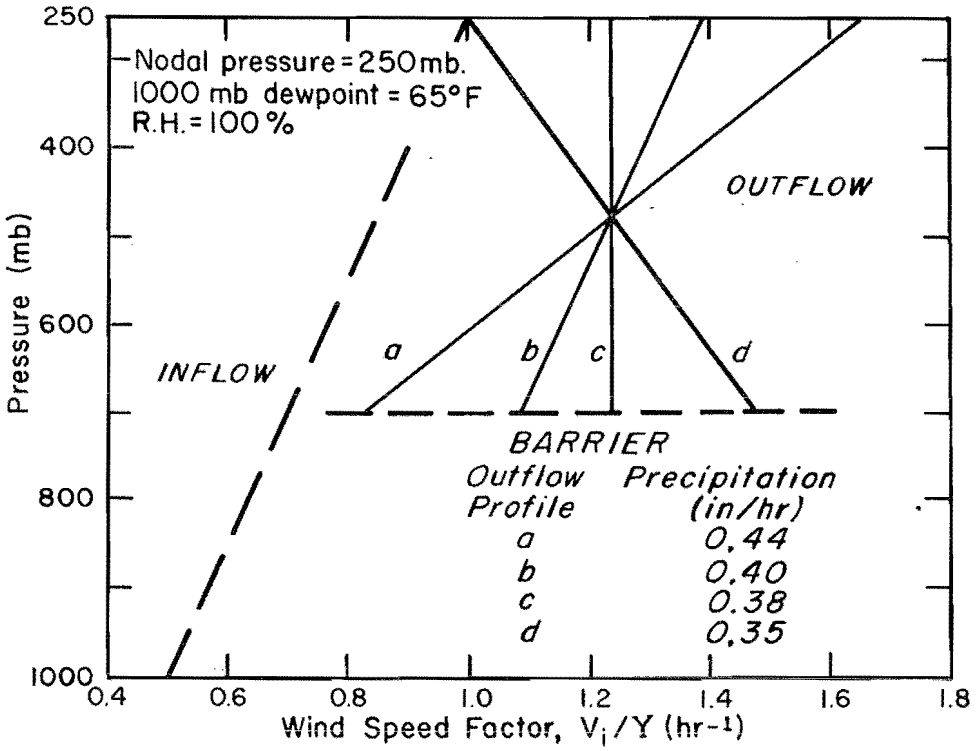

Fig. 4-25. VARIATION OF OUTFLOW WIND PROFILE AND RESULTANT OROGRAPHIC PRECIPITATION

Vertical distribution of wind above barrier. The effect of nodal pressure variations has already been illustrated. For a given nodal pressure there are also possible variations in the average lift imparted to the airstream depending on whether the greatest speedup is in lower levels or upper levels. Figure 4-25 shows a typical inflow wind profile, dashed line, and several schematic hypothetical outflow profiles, solid lines, each of which represents the same transport of air. The resulting differing computed orographic precipitation rates are tabulated on the figure. The a and b type of profile, which are the most realistic, yield more precipitation than c and d because there is more net lift of the air.

4-C-3. Test of orographic model

Block comparison in HMR 36. Numerous comparisons are given in chapter V of HMR 36 between computed laminar flow orographic precipitation and "observed orographic precipitation." The latter is obtained by subtracting an estimated convergence component from the total observed precipitation. The comparisons are for 6-hour periods in major orographic storms. In general it was found that observed precipitation exceeds the computed during periods of heaviest precipitation but is less than the computed during lighter rain periods, with an over-all average of about 1 to 1, but with quite a bit of scatter in the data. Some reasons for the variations, and the concept of a model coefficient, are discussed in HMR 36, chapter V.

San Gabriel mountains, January 22, 1943. The largest 24-hour total of precipitation recorded up to now anywhere in California was at Hoegee's Camp near the Mt. Wilson Observatory in the January 1943 storm. This storm is described in section 2-B-4, with selected hyetographs in figure 2-24. Opid's Camp, in the figure, is near Hoegee's Camp. Surface winds are shown in figure 4-3 and 24-hour isohyetal maps in the appendix. An important question is, how much of this precipitation should be classed as orographic, which would mean that it was characteristic only of this location atop a steep mountain with a south-facing slope, and how much as convergence rain, and hence transposable over a variety of topographic features.

To examine this question, the observed precipitation was compared with computed orographic precipitation along two profiles across the San Gabriel mountains, A and B of figure 4-26. The computed precipitation, in view of sparsity of data, is necessarily based on idealized schematic airflow. Further, this analysis was made early in the study and some of the dynamic checks on orographic windflow later devised were therefore not applied.

For the orographic computation average horizontal windspeeds and directions were adopted, based on the available pilot balloon observations, figure 4-27. The adopted wind direction is a function of elevation above sea level only. A and B of figure 4-26 are streamlines at 1000 ft above the ground, laid out from the adopted wind directions. For speed, winds 2000 ft and more above the ground were a function of elevation only, curve M of figure 4-27; while a reduction in speed for winds within 1000 ft of the ground

was introduced, curve N. For the vertical component of the wind, it was assumed that the wind up to 1000 ft above the ground flowed parallel to the ground along tracks A and B, with a linear decrease in vertical velocity with height from 1000 ft above ground to zero at 20,000 ft msl. (A lower effective nodal surface, such as 20,000 ft would be expected over this south-facing mountain than above the Sierra and Coast Ranges, more nearly normal to the westerlies. In the latter areas a nodal surface of 300 mb, about 30,000 ft, is more appropriate.)

Applying these vertical velocities to a saturated pseudoadiabatic atmosphere having the average sea-level dew point of the storm, 55°F, yields the profile of rain shown by the blocks in figure 4-28. No allowance is made for drift of the precipitation in the air with wind before striking the ground.

The four observed 6-hour rates of precipitation, scaled from 6-hour isohyetal maps (not shown), are compared with the computed precipitation in the figure. It can be seen that the over-all volumes of rain and distribution along the profile correspond fairly well at higher elevations, leading to the conclusion that the Hoegee's Camp value is primarily ascribable to orographic lifting. At lower elevations the observed rain exceeds the computed, suggesting orographic stimulation of precipitation in excess of that determined by assuming laminar flow.

Sierra and Coast Range slopes, December 22, 1955. Other comparisons of observed and computed precipitation are shown in figure 4-29, for selected Sierra and Coast Range slopes in the December 1955 storm. These are from HMR 36, where the details of the computations are described (p. 69). Reasonably good correspondence is found. The observed precipitation exceeds the computed at lower elevations for the Coast Range.

4-C-4. The low-level stimulation effect

The foregoing examples show a tendency for observed precipitation to exceed computed at elevations below 2000 ft. The rapid pickup of mean annual precipitation with elevation in the foothills of both the Coast Range and some parts of the Sierras as well as the Southern California mountains is at variance with the relations shown in figure 4-21 of pure orographic precipitation to barrier height, exceeding what would be predicted from that figure. The interpretation of this result is that these lower elevations in some storms stimulate the release of convection by imparting the needed initial lift. The resulting precipitation in these storms exceeds the convergence rain on adjacent plains, the orographic rain computed from the laminar flow, and the sum of these two. One can envision that under some distributions of instability this additional convection would not be released until a higher elevation was obtained; but these circumstances are probably more specialized and would tend to be masked by the higher orographic rain at the higher elevations. The possible stimulation of precipitation by very low barriers (e.g., 30-60 meters) has been discussed

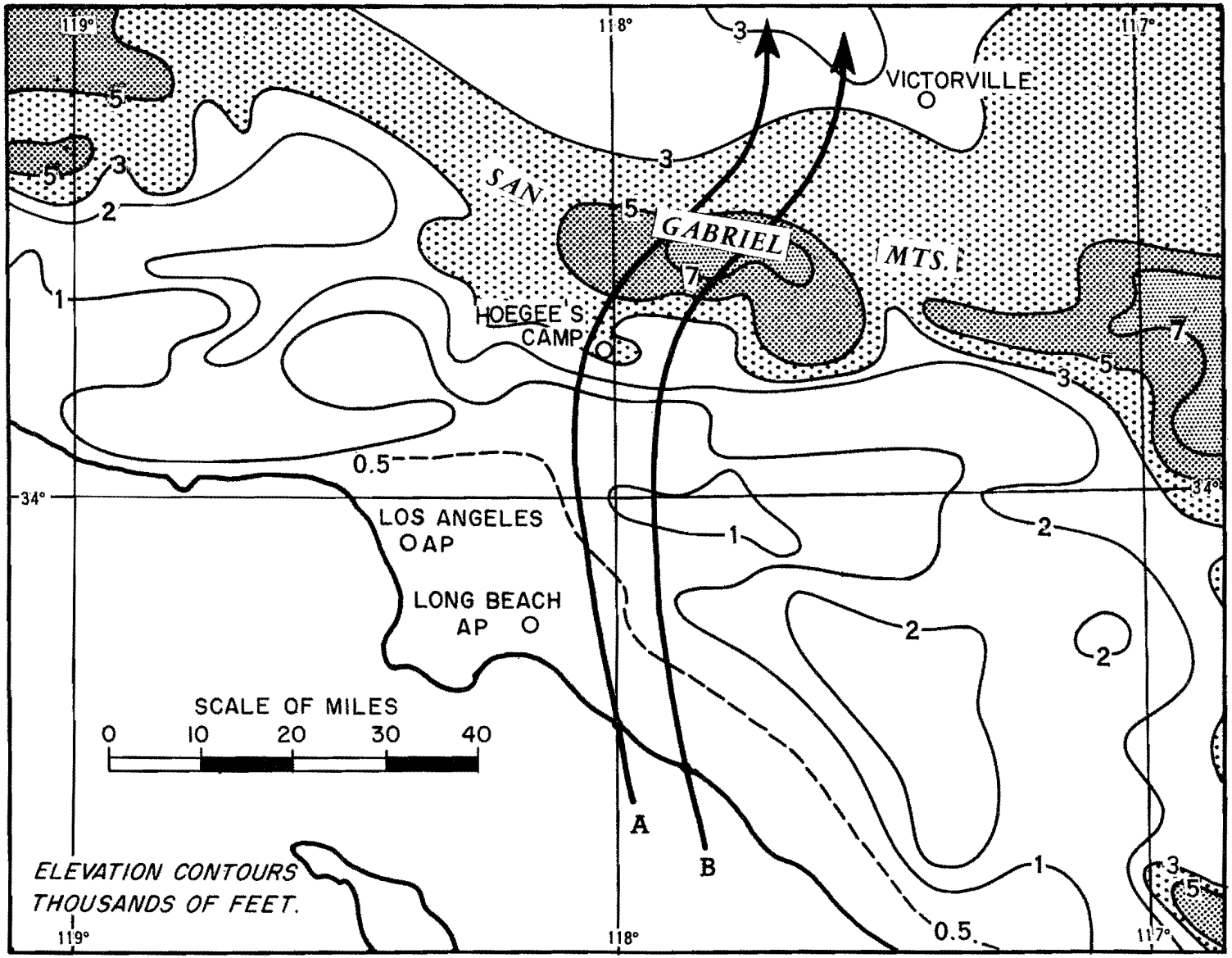

Fig. 4-26. LOCATION MAP FOR PROFILES OF FIGURE 4-28

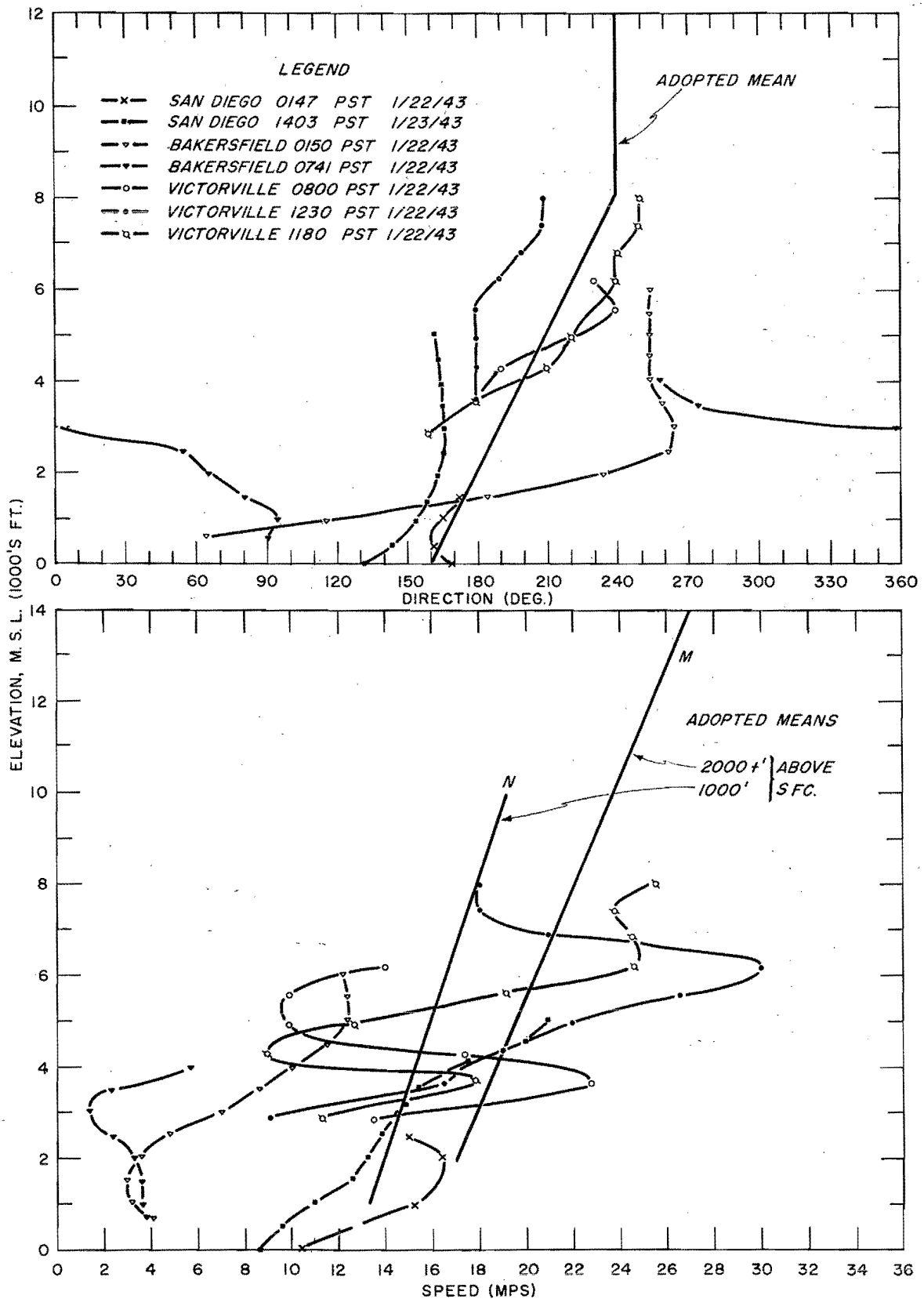

Fig. 4-27. OBSERVED WINDS AND ADOPTED MEAN FOR JANUARY 22, 1943

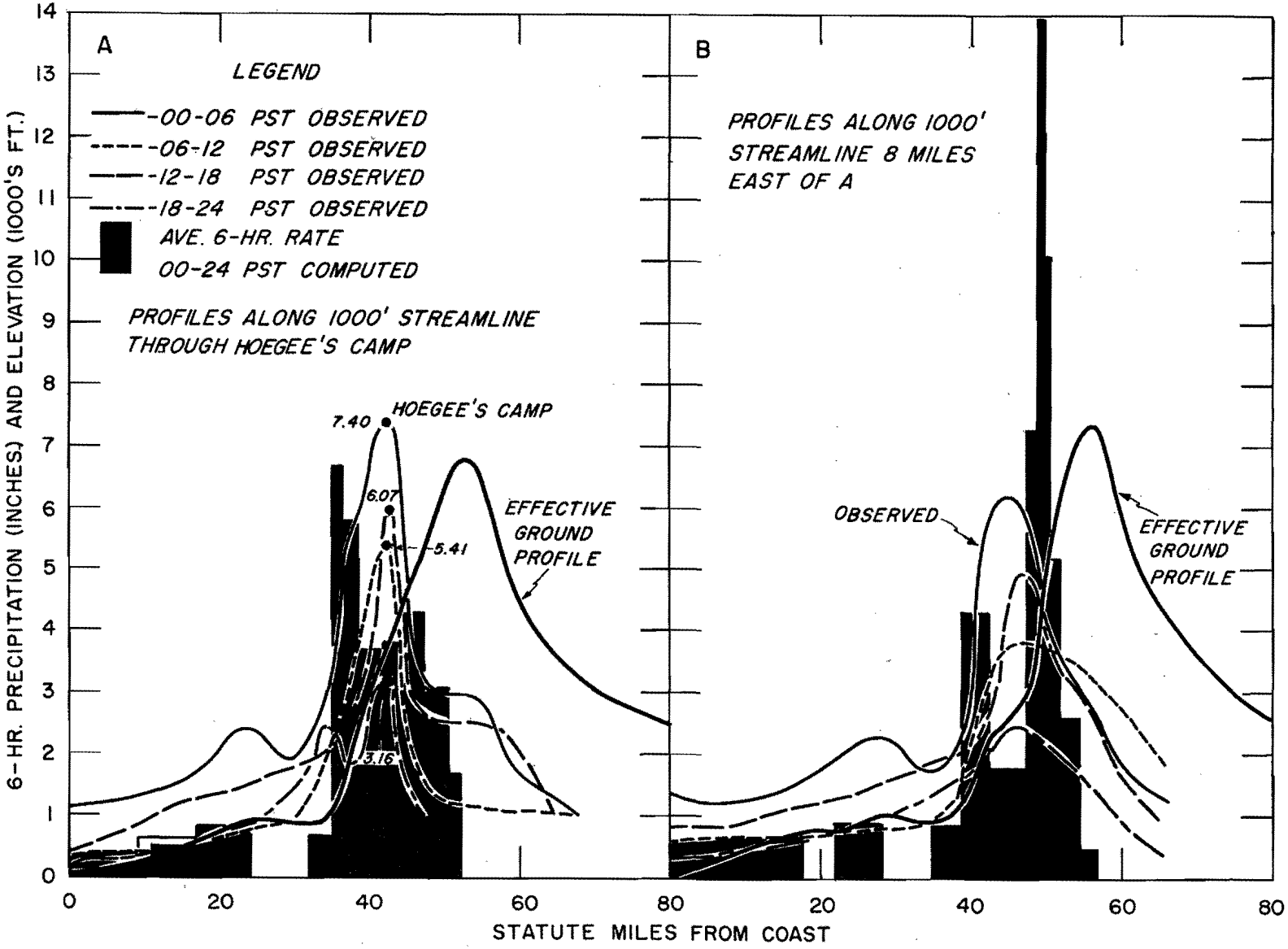

Fig. 4-28. PROFILES OF OBSERVED AND COMPUTED PRECIPITATION, JANUARY 22, 1943

by Bergeron (11). Some authorities have even suggested that the increased friction of rugged terrain of mountains or of land vs. sea is sufficient of itself to produce convergence and increase precipitation without any upslope of the surface. It is not thought that this effect is particularly significant in the California climate but the suggested stimulation of foothills effect is regarded as a significant part of the rainfall climate.

4-C-5. Lee effects

The broad-scale shielding from rainfall by the larger mountain chains in California of the areas to their lee is obvious from the mean annual precipitation, (figure 4-1), from the vegetal cover, and from the character and size of the streams. The details of the processes in the immediate lee of the mountains are not so obvious. Rainfall data in the immediate lee are very sparse and conclusions as to the rainfall regime must therefore be based largely on deduction.

First, the orographic rain formed in the rising air above windward slopes drifts with the wind before striking the ground. This drift will carry the precipitation beyond a crest. It would be expected that snow would drift much farther than rain. If the descent is marked, the adiabatic warming will increase the capacity of the air to hold moisture and some of the precipitation will evaporate. This recharge of the atmospheric moisture is proven by the surface dew points in the San Joaquin Valley during storms. These are usually about as high and sometimes even higher than coastal dew points. Attempts to evaluate these effects quantitatively are made in chapter VI of HMR 36.

Second, precipitation from meteorological causes not primarily topographic in character is inhibited but not eliminated in lee downslope areas. Intense local rains are possible but much less frequent than in more exposed areas.

Third, predominantly lee areas can at times become weak upslope areas in particular circulations, though this does not appear to be of much importance in the principal lee areas of California during major storms.

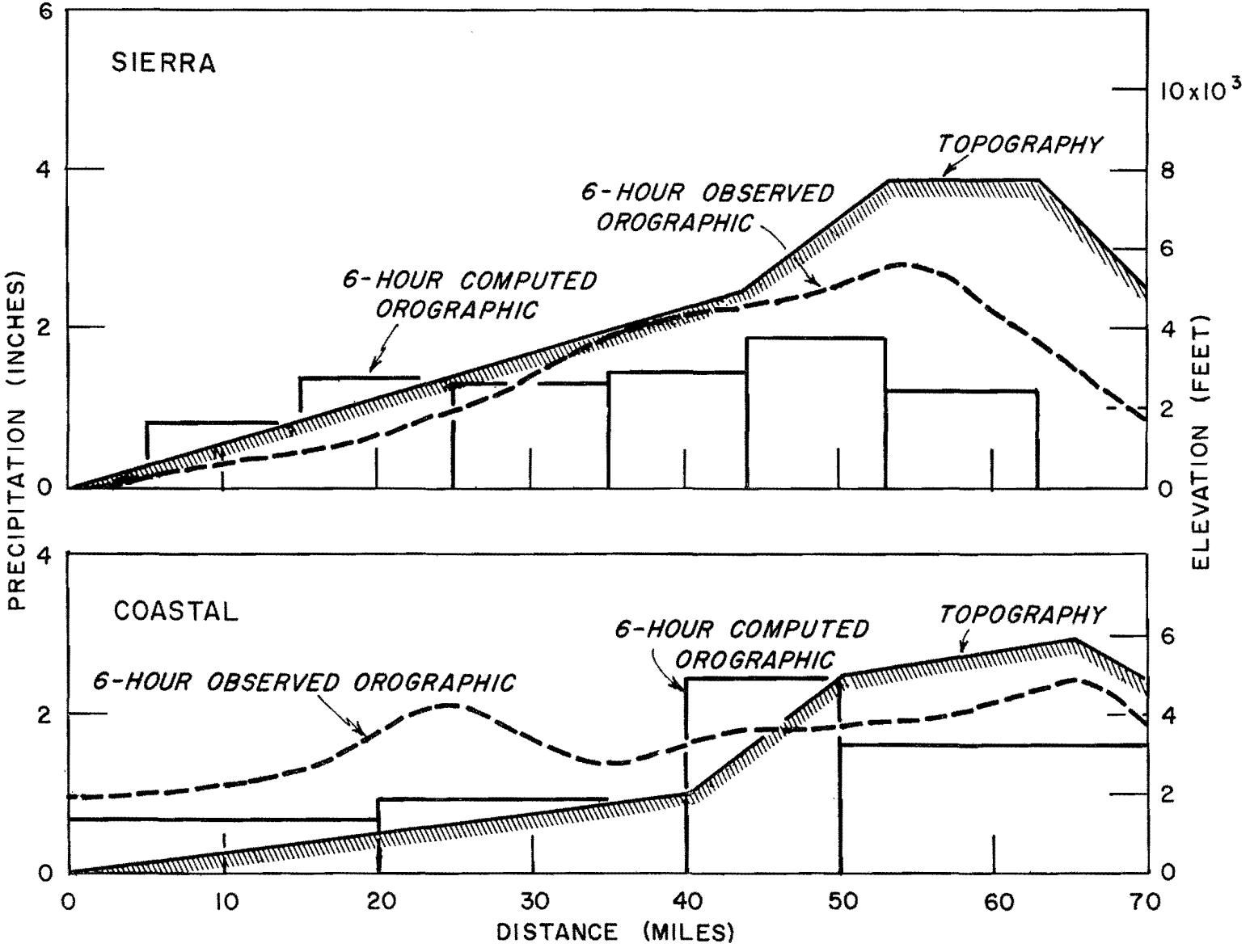

Fig. 4-29. COMPARATIVE PRECIPITATION PROFILES, DECEMBER 22, 1955

Chapter V

FACTORS IN CONVERGENCE PRECIPITATION

Vertical motion due to synoptic scale disturbances (as distinguished from that due to orography) is directly related by continuity considerations to simultaneous horizontal convergence and divergence at different levels. Horizontal convergence and upward vertical motion will be discussed under the three general headings indicative of the cause, namely, (1) non-geostrophic wind mechanisms, (2) frontal lifting mechanisms and (3) instability. They will be illustrated by examples from recent major California storms.

5-A. NON-GEOSTROPHIC WIND MECHANISMS

The assumption of geostrophic windflow loses its validity when pressure gradients change in space or time either in direction or magnitude. The inertia of the wind results in a time lag in its adjustment to changes in the pressure field. The acceleration on the wind resulting from this deviation from the geostrophic value is proportional to the magnitude of the deviation and directed at right angles to its direction in a clockwise sense (in the Northern Hemisphere).

5-A-1. Effect on dynamic trajectories

If one draws a series of vector segments of particle displacement in the horizontal as the wind is accelerated through successive periods in accordance with the above relations, a so-called "dynamic trajectory" results which defines the motion of a particle as it is acted upon by a pressure field, changing with time or distance, or both.

Effects of various isobaric configurations on dynamic trajectories are as follows (12). In a stationary pressure field, at a level where friction may be neglected, if isobars change curvature downwind toward cyclonic, the trajectory decelerates to the right of the isobars; if toward anticyclonic, the trajectory accelerates to the left of the isobars (a and b, figure 5-1). If the isobaric gradient increases downwind, the trajectory accelerates to the left of the isobars (b', figure 5-2); if the gradient decreases, the trajectory decelerates to the right (c', figure 5-2). In a pressure field changing with time, with the isobars rotating anticyclonically (a, figure 5-3) the trajectory accelerates to the left of the current isobars; if the source of the change is cyclonic rotation the trajectory decelerates to the left of the initial isobars (b, figure 5-3). Qualitatively, the foregoing accelerations are accounted for by noting that the air speeds up if moving toward, or deflected toward, lower pressure, while it must slow down if the motion or deflection is toward higher pressure. Quantitatively the acceleration vector is readily determined from the actual wind and geostrophic wind vectors (10), (13).

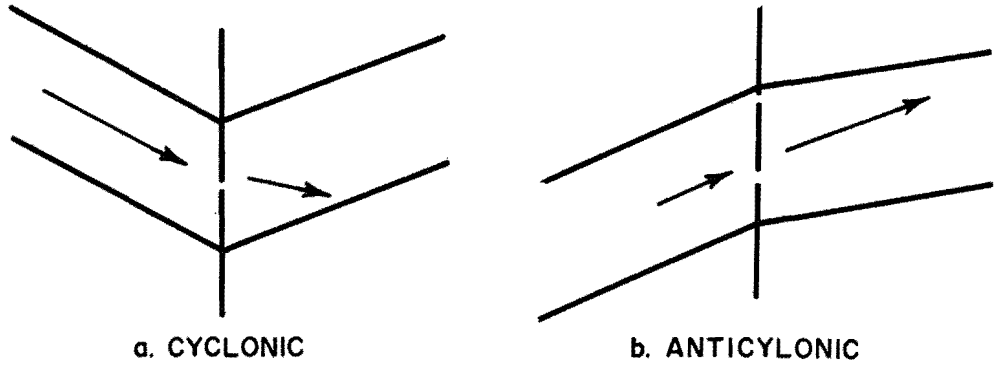

Fig. 5-1. SCHEMATIC OF DOWNWIND CHANGES IN CURVATURE OF ISOBARS AND RESULTING CHANGES IN TRAJECTORY OF AIR

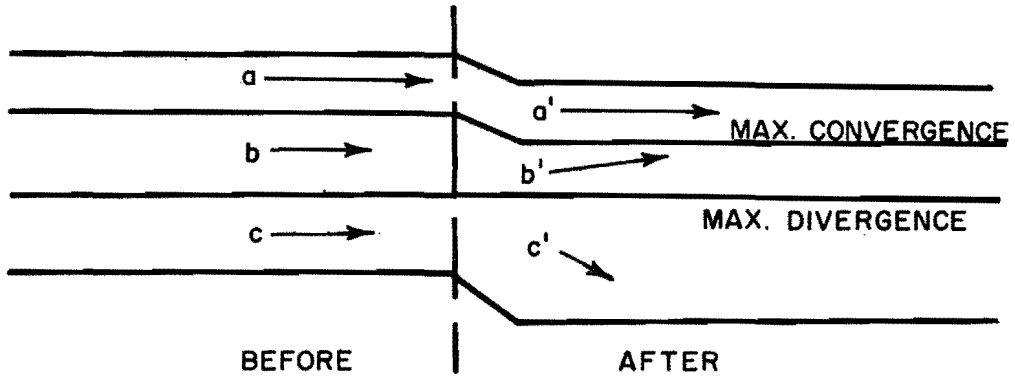

Fig. 5-2. SCHEMATIC OF TIME OR DISTANCE CHANGE TOWARD CYCLONIC AND ANTICYCLONIC SHEAR AND RESULTING CONVERGENCE AND DIVERGENCE

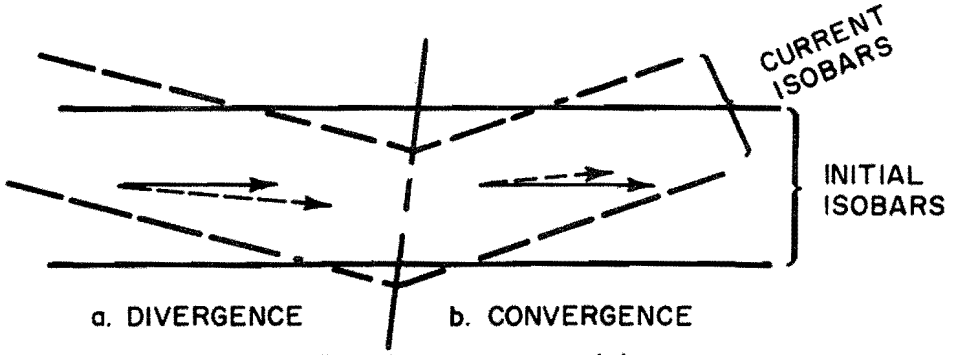

Fig. 5-3 SCHEMATIC OF TIME CHANGE TOWARD (a) ANTICYCLONIC AND (b) CYCLONIC CURVATURE IN PRESSURE FIELD AND RESULTING DIVERGENCE AND CONVERGENCE

5-A-2. Effect on convergence and divergence

Dynamic trajectories initiated at points bounding an area will at a later time bound an area the size of which relative to the original area is a measure of horizontal convergence or divergence (14). This form of convergence or divergence is referred to in this report as "ageostrophic" convergence or divergence, denoting its origin in non-geostrophic flow. It results from "cyclonicity" of the isobaric or isallobaric fields, a term which denotes concentration of cyclonic curvature or cyclonic shear.

In a stationary pressure field, convergence of trajectories and shrinkage of horizontal area result if, downwind, curvature change of isobars is toward greater cyclonic curvature and/or downwind gradient change is toward cyclonic shear; it is greatest downwind from the line of greatest cyclonic curvature (a, figure 5-1) or near the line of maximum cyclonic shear (figure 5-2) or as determined by a combination of cyclonic shear and curvature.

A pressure field changing with time toward cyclonic curvature and/or shear leads to convergence which is a maximum downwind from the instantaneous position of maximum curvature (figure 5-3) or near the line where the instantaneous cyclonic shear is a maximum (figure 5-2), or as determined by a combination of cyclonic shear and curvature.

5-A-3. Effect on vertical motion and precipitation

Shrinkage of area by horizontal convergence is compensated for by a corresponding vertical motion. This motion is upward in lower levels of the atmosphere and importantly contributes to convergence rainfall, both frontal and non-frontal. Increase in area with time, through horizontal divergence, results in downward motion (in lower layers of the atmosphere).

5-A-4. Application to typical synoptic patterns

If a, figure 5-1, is a moving trough in the pressure field, this figure and figure 5-3 together show the combined effect on horizontal convergence of changes in the pressure field with distance and time. This effect is more nearly shown by a, figure 5-1 to the extent that the windspeed exceeds the speed of the trough. Convergence is associated with the forward side of the trough; the greater the curvature, the closer is convergence concentrated near the trough line (e.g., at a front).

In a moving Low, horizontal convergence is determined mainly by combination of the effects of cyclonicity of the isobaric and isallobaric fields, effects which may tend to complement or cancel each other. Isobaric cyclonicity predominates on the forward side of a slow-moving Low with strong gradient; isallobaric cyclonicity predominates if the isallobaric shear is relatively strong or if the Low is relatively weak but is deepening or is moving rapidly.

In the synoptic scale systems discussed here, effects of variation of the Coriolis parameter with latitude in producing convergence are typically an order of magnitude smaller than the above ageostrophic effects and may be neglected.

The time lag between the imposition of isobaric or isallobaric cyclonicity to an area and occurrence of the greatest convergence of the same air parcels (downwind from this area) becomes greater as the magnitude of the cyclonicity becomes less pronounced. Thus a fast-moving isallobaric Low center of small magnitude may precede by several hours the resulting field of convergence, which, in the meantime, tends to move with the wind field (14). This time lag feature is apparent in the synoptic sequences discussed below.

Cyclonicity in the pressure field is frequently difficult to detect in mountainous areas when the gradient is strong, partly because of the problem of reducing pressures to a common level. Then, use of isallobaric fields, which require no reduction, more readily serves to locate convergence-producing time changes in the pressure field. For example, a weak isobaric trough may be located to the rear of falls and ahead of rises in the instantaneous pressure field. Similarly, elongated Lows or cols in the isallobaric field with axes oriented along the isobars indicate increasing cyclonic shear in the pressure field, concentrated near this axis on the high pressure side.

5-A-5. Examples of isallobaric cyclonicity and convergence in the December 1955 storm

During the latter part of the December 1955 storm, a small, fast-moving deepening wave entered California near the northern border on the night of the 22d (figure 2-13e). Two isallobaric Low patterns (dashed lines of 2-hour pressure change in figures 5-4a to 5-4d) entered Northern California in advance of the wave about 4 hours apart. They became elongated as they moved southeastward toward higher pressure and faded out in Central California. Thus the initial cyclonic curvature of the isallobars was later replaced by cyclonic shear, as the isallobars became oriented parallel to isobars. During this time there was little cyclonicity apparent in the isobars except far to the north near the path of the wave (figure 2-13e).

In figures 5-4a to 5-4d axes of maximum pressure fall associated with the two isallobaric patterns are shown as solid lines. The isallobaric ridge lines (not shown) followed about two hours behind the isallobaric troughs. The positions of the isallobaric trough patterns are compared with positions of zones of peak convergence rainfall downwind three hours later (broken lines). For example, in figure 5-4c cyclonicity about the two isallobaric trough lines at 1930 PST is related to convergence rain centered on the two burst lines at 2230 PST. The choice of a 3-hour time lag furnishes a reasonable 3-hour convergence of trajectories from the cyclonitic axis in a prevailing WSW flow. The exact locations of the axes of maximum convergence (dependent on both the correct time lag and trajectory behavior) are not

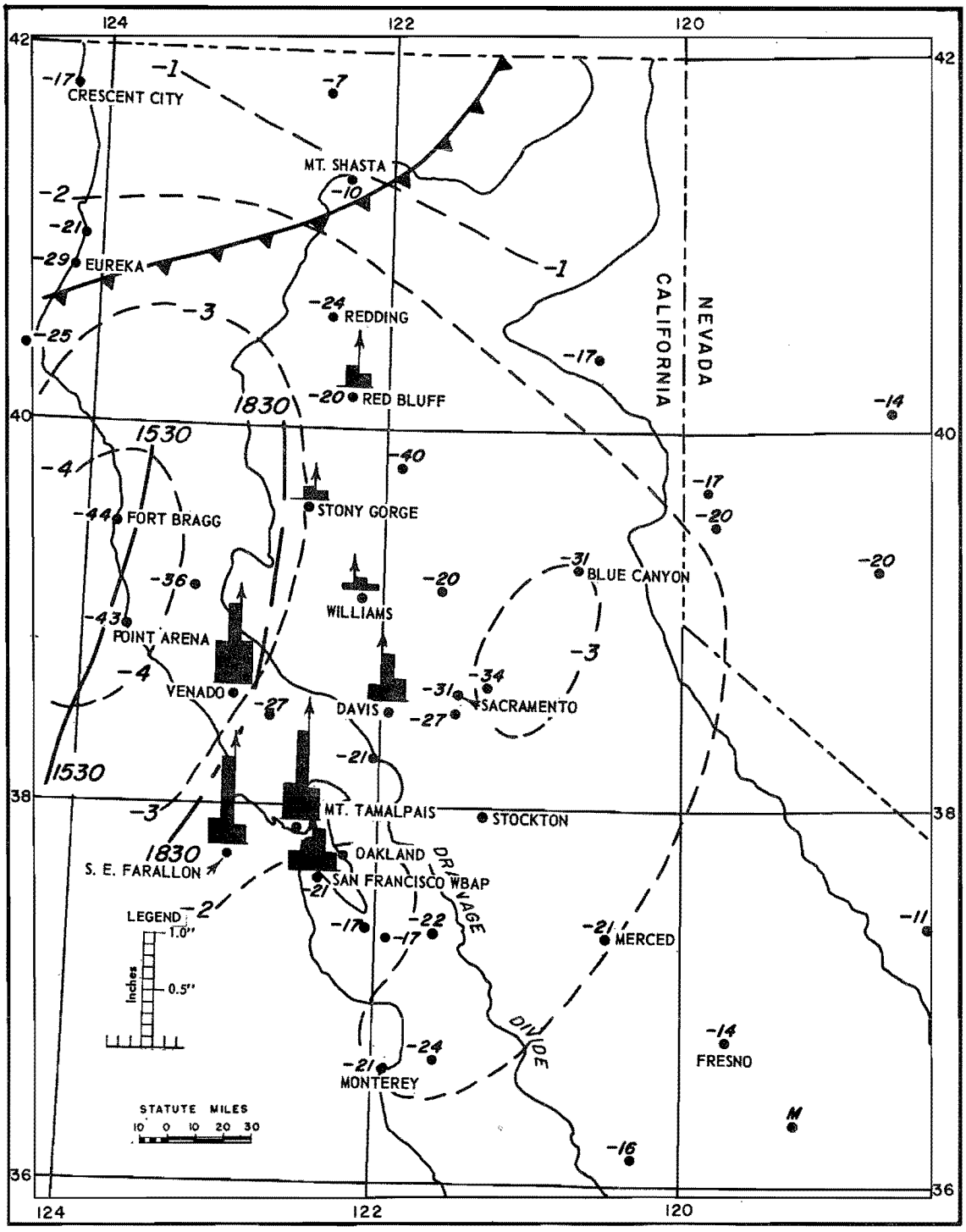

Fig. 5-4a. RELATION OF 1530 PST AXIS OF ISALLOBARIC TROUGH (SOLID LINE) TO 1830 PST AXIS OF CONVERGENCE RAIN BURSTS (BROKEN LINE), DECEMBER 22, 1955. DASHED LINES ARE 2-HOUR PRESSURE CHANGE (MB) CENTERED ON 1530 PST. BLOCK DIAGRAMS SHOW HOURLY RAINFALL BEFORE AND AFTER 1900 PST

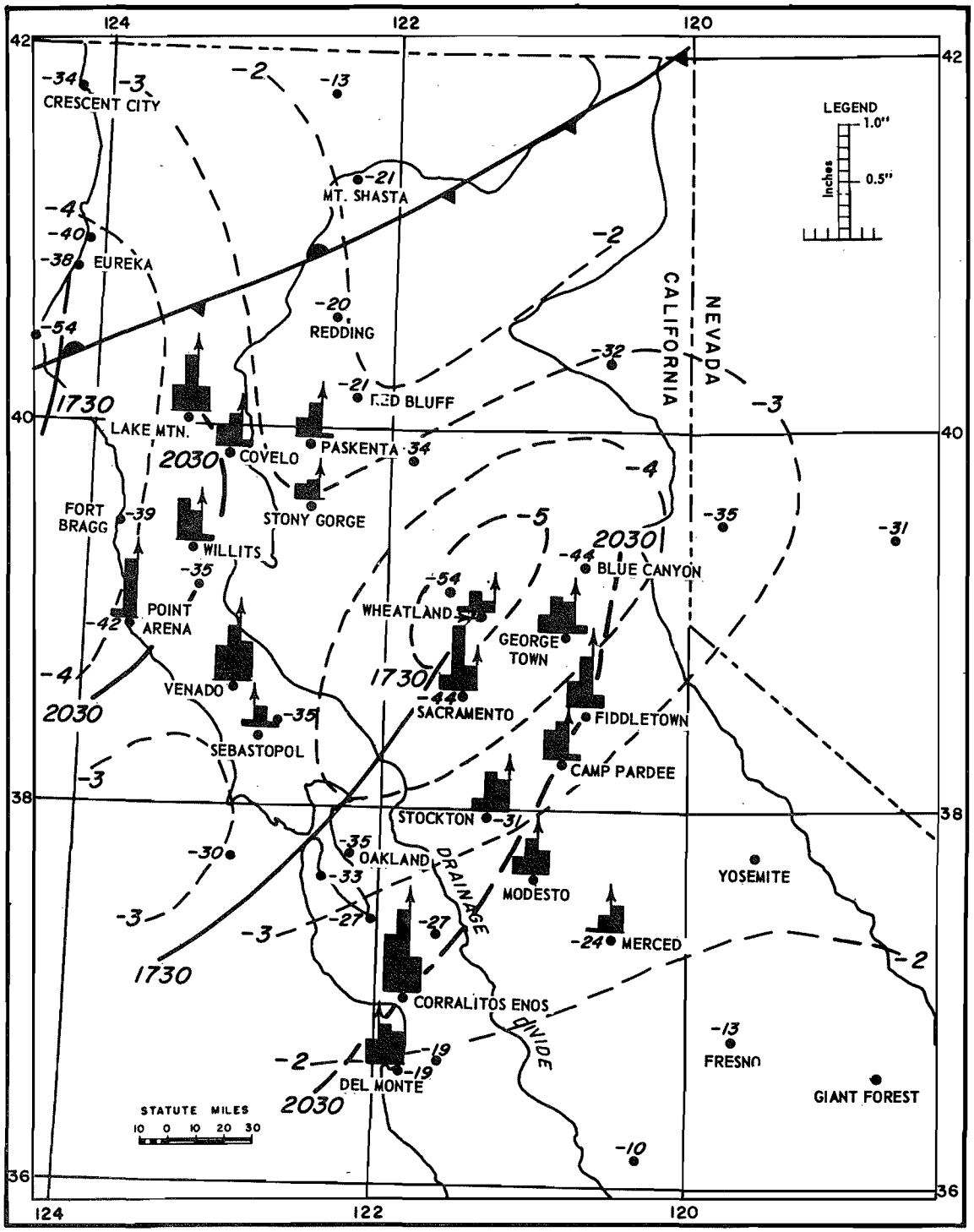

Fig. 5-4b. RELATION OF 1730 PST AXIS OF ISALLOBARIC TROUGH (SOLID LINE) TO 2030 PST AXIS OF CONVERGENCE RAIN BURSTS (BROKEN LINE), DECEMBER 22, 1955. DASHED LINES ARE 2-HOUR PRESSURE CHANGE (MB) CENTERED ON 1730 PST. BLOCK DIAGRAMS SHOW HOURLY RAINFALL BEFORE AND AFTER 2100 PST

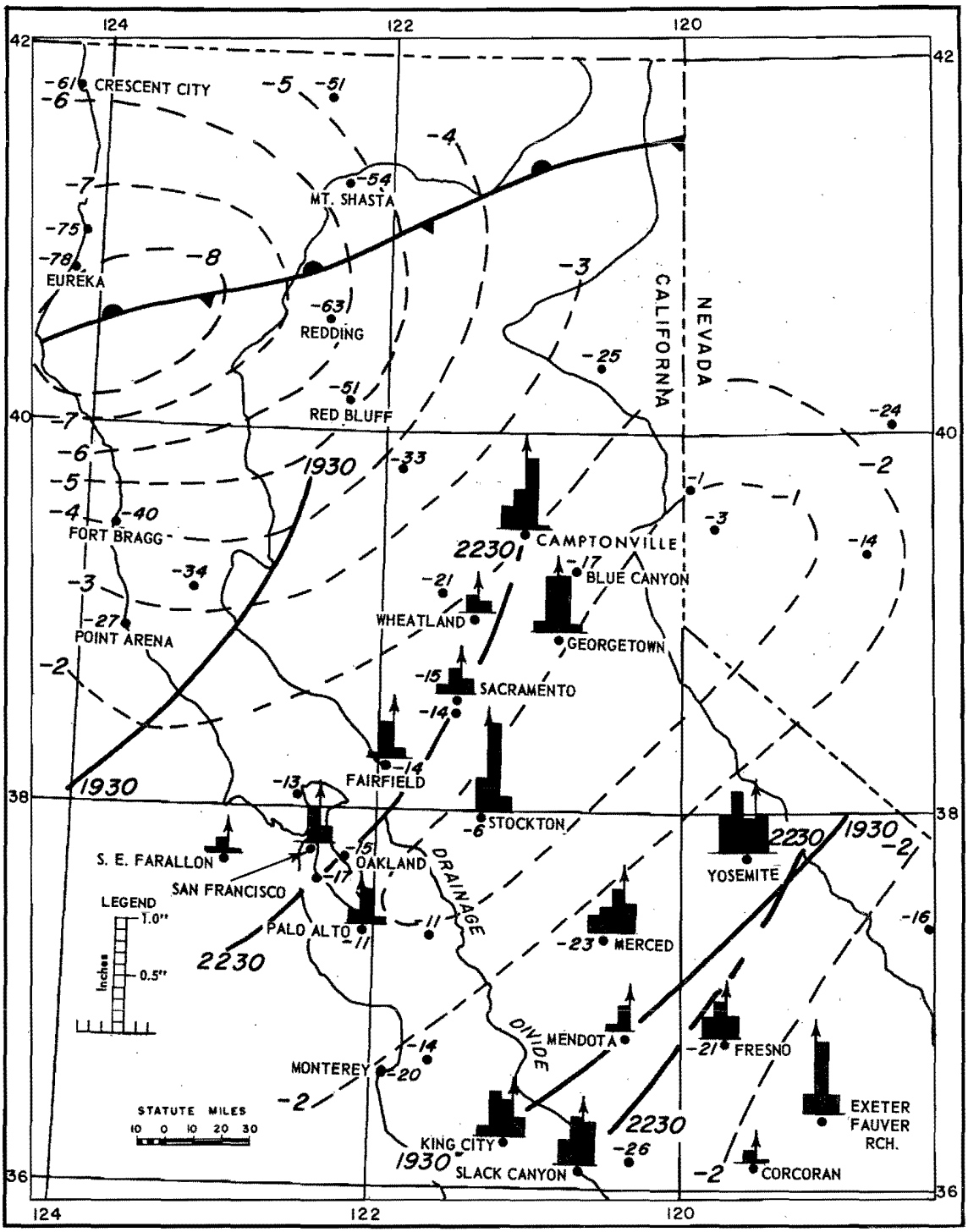

Fig. 5-4c. RELATION OF 1930 PST AXIS OF ISALLOBARIC TROUGH (SOLID LINE) TO 2230 PST AXIS OF CONVERGENCE RAIN BURSTS (BROKEN LINE), DECEMBER 22, 1955. DASHED LINES ARE 2-HOUR PRESSURE CHANGE (MB) CENTERED ON 1930 PST. BLOCK DIAGRAMS SHOW HOURLY RAINFALL BEFORE AND AFTER 2300 PST

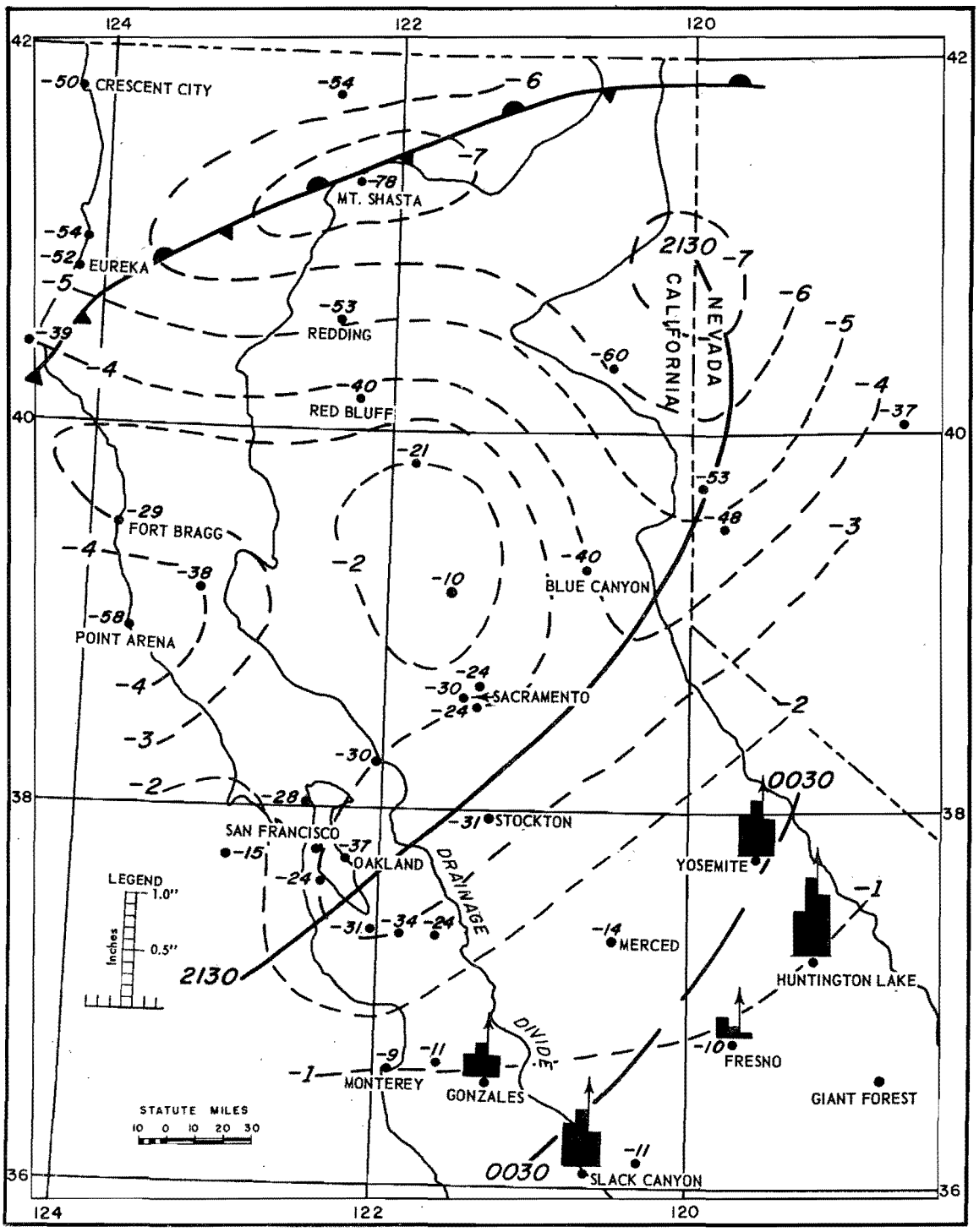

Fig. 5-4d. RELATION OF 2130 PST AXIS OF ISALLOBARIC TROUGH (SOLID LINE) TO 0030 PST AXIS OF CONVERGENCE RAIN BURSTS (BROKEN LINE), DECEMBER 22-23, 1955. DASHED LINES ARE 2-HOUR PRESSURE CHANGE (MB) CENTERED ON 2130 PST. BLOCK DIAGRAMS SHOW HOURLY RAINFALL BEFORE AND AFTER 0100 PST

known because of lack of the detailed information necessary to construct the required dynamic trajectories. Their locations are assumed to be identified with convergence rainfall patterns. There is evidence for this assumption in the similarity in orientation, rate of movement and path of the cyclonitic axes to that of the subsequent rain burst lines.

The reality of the "burst lines" as moving zones of peak rainfall intensity is indicated in figures 5-4a to 5-4d by hourly station hyetographs, centered about the interpolated time of passage of each burst line at the station. (The sharpness is obscured at some stations by timing of the peak rainfall rate relative to hourly observation time so as to distribute it more or less equally over two hours. It is obscured at most mountain stations by the concomitant orographic contribution there; at some, it is accentuated, probably by a coincident instability contribution.)

The December 1955 storm featured convergence rain not associated with fronts in which several burst lines of peak convergence rain intensity can be followed across a large portion of the storm area. Similar patterns of less definite character appeared in other recent major storms for which there is a network of hourly rainfall data. Convergence-producing fields of cyclonicity can be implied as an essential feature of storms; they are more easily recognized near fronts.

The above examples of cyclonic patterns in the isallobaric field and related subsequent burst lines illustrate on a synoptic scale the preceding theoretical presentation of cyclonicity as a cause of precipitation through convergence of trajectories in a non-geostrophic moist flow.

5-B FRONTS

Much of the precipitation in California, as elsewhere, falls near fronts. It is helpful to classify precipitation as "warm front," "cold front," or "occluded front." These designations hint at the manner of the lifting of the air and relate particular precipitation to a familiar, if complex, combination of clouds, wind, temperature, pressure, and other phenomena.

Fronts are less adequate as a concept on which to explain in a quantitative way the lifting of the air necessary to release heavy precipitation. The diffuseness of the fronts and slight temperature contrasts between air masses usually found in major California storms would render it difficult to determine frontal slope even if this were a useful thing to do. Correlation between frontal intensity or frontal slope and precipitation intensity is generally poor. Among the reasons for this, it can be deduced that air does not merely ascend a frontal slope as a parallel stream but that the motion is complicated both by release of instability and by the kind of interactions of changing wind and pressure fields discussed in the preceding section. The latter should be especially prevalent in frontal zones, though not limited exclusively to those areas.

Table 5-1

LOCAL SYNOPTIC PATTERNS INVOLVING WARM FRONTS IN MAJOR STORMS

Group, Date and Storm Location				
1	2	3	4	5
12/31/33 Srn.	1/20/43 Cntrl.	12/21/21# Cntrl.	12/18/55 Cntrl.	12/9/37 Cntrl.
4/8/26 Srn.	12/25-26/21 Cntrl. Srn.	1/18/16 Cntrl.	2/27/40 Cntrl.	2/25/40 Cntrl.
3/26/28 Nrn.	1/29/11 Cntrl.	1/26/56* Srn.		
2/15/27 Srn.	2/19&20/14# Cntrl.	11/18/50 Cntrl.		
3/2/38 Srn.	1/16-17/16 Cntrl.			
2/13/37 Srn.	1/1/14 Nrn.			

\# Warm front rain largely to north of storm center.
* In some respects not a major storm.

1. Warm front extends southeastward along the coast from a nearly occluded system. Most common in Southern California and with Mid-latitude type. Brief warm front rain as front passes.

2. An intense wave develops just offshore, usually off the Central California coast. Precipitation is more nearly related to the Low center than to the warm front.

3. More or less stable waves on a stationary east-west polar front near the coast.

4. Quasi-stationary front joining an occlusion with next wave development. Large differences in rainfall amounts across the frontal zone, little of which is due to frontal lifting.

5. An apparent warm front, the frontal boundary in an old occluded Low originating far to the southwest and later more or less absorbed in the forward part of the main storm.

Fronts are discussed in this section in accord with the usual synoptic practice as locators of precipitation with respect to other features of the weather map and as partial qualitative explanations of the cause of the precipitation.

5-B-1. Warm fronts

The frequency of occurrence and relation to convergence precipitation, of warm fronts reaching the California coast in major storms are discussed below from the standpoint of latitude, storm type and local synoptic pattern. Also the effect of terrain on warm fronts as they move inland from the ocean is discussed and illustrated by examples.

a. Variation with latitude and storm type. In general, the more southerly the latitude the less likely that a frontal system will be occluded at the coast. Hence, a smaller percentage of warm fronts in major storms reach the coast of Northern California than Southern California.

The frequency also varies with storm type. The farther offshore a wave develops, the more likely that it will be occluded at any latitude upon reaching the coast. Hence warm fronts are least important in the Mid-latitude southwest and westerly types in Northern California, where well-occluded systems usually arrive after wave development has taken place some distance offshore. On the other hand, features of some storm types tend to suppress occlusion of waves reaching the coast, as discussed later in chapter 5-B-2a.

b. Variation with local synoptic pattern. The more important synoptic situations involving a warm front along the California coast in major storms have been classified in table 5-1. Groups 1 and 3 occurred mainly in the southern half of California, and Groups 2, 4 and 5 in the central or northern part. The extreme north and south parts of the state were seldom involved. Each group is described briefly.

c. Effect of topography on warm fronts. The frontal surface in advance of a surface warm front approaching the California coast is replaced by the terrain itself as the surface front approaches the coastal range. In the Central Valley the underlying cooler air between the coastal range and the Sierras then acts as a rather flat warm front surface over which the warmer air rises only slowly. An exception is the southern Sacramento Valley where limited access of warm air at the surface by the way of the Bay region may permit a surface warm front to retain its identity. Over the Sierras the warm front slope is replaced by terrain. Thus the area over which a warm front slope serves as a lifting mechanism is limited mainly to the coast. This is illustrated in the next section by an example of a warm front approaching the Central California coast.

In major storms involving warm fronts in Groups 3 and 4 of table 5-1, warm front orientation was sometimes roughly east-west across Northern California as a part of the polar front. Over the mountains the front is more or less fictitious; its identity on synoptic maps is often obscure even in the Central Valley, and dependent on continuity between positions of the polar front over the Plateau and offshore.

d. Rainfall pattern associated with a warm front in Central California. The heavy rain period in mountain areas of Central California on November 18, 1950 was preceded by movement of a warm front through a portion of that area. Its passage at coastal stations was noted by a marked wind shift but little surface temperature change, although 12-hour temperature increase to 0700 PST at Oakland was 2°C at 900 mb and 4°C at 800-700 mb. After moving onshore about 0300 PST, oriented parallel to the Central California coast and bending westward from the San Francisco Bay region as a stationary front, it became obscure as it moved eastward and northward. Figure 5-5 shows 2-hourly positions (PST), based on hourly synoptic maps. The front is shown in a

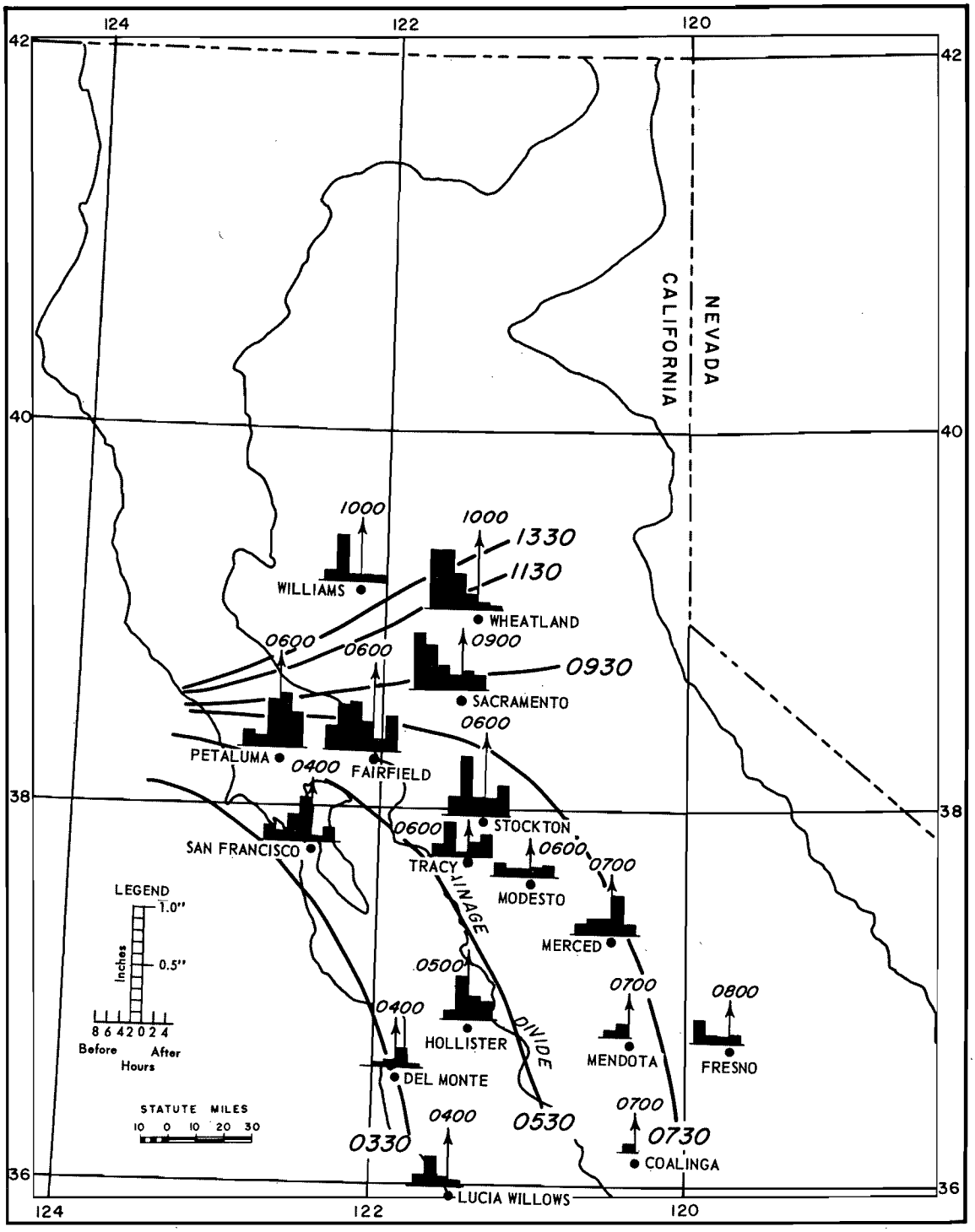

Fig. 5-5. RELATION OF RAINFALL TO WARM FRONT, NOVEMBER 18, 1950. SOLID LINES SURFACE POSITION OF WARM FRONT AT INDICATED TIME, PST. BAR GRAPHS BI-HOURLY RAINFALL

stationary WSW-ENE position through the North Bay and Sacramento Delta area by midday where, following steadily falling pressure during the morning, it was then surrounded by an elongated 1002-mb surface Low.

A peak in precipitation intensity (as indicated by the bar graphs of 2-hourly precipitation at essentially non-orographic stations in figure 5-5) preceded the front at most stations near the coast but less clearly at those in the northern San Joaquin Valley, in some cases by several hours. In the Sacramento Delta area and northward little rain occurred near the frontal trough but heavy rain fell early in the morning far in advance of the front. Cause of this early period of heavy convergence rain remains unexplained.

e. Rainfall pattern associated with a warm front in Southern California. The precipitation sequence described below is of particular interest since it is the essential part of a 24-hour high-intensity storm which influences the envelope of convergence rain/moisture ratio (figure 4-7, HMR 36) regarded as applicable to the probable maximum storm. With respect to orographic precipitation and areal extent it was not a major storm.

Beginning about midnight and continuing through noon of January 26, 1956, unusually heavy rain fell over the Los Angeles Basin presumably in connection with a nearly stationary warm front lying along the Southern California coast (figure 5-6a). The front was the trailing end of an occlusion which had passed eastward the previous day with Low A of figure 5-6a. By noon of the 26th a cold front was approaching from the northwest in connection with Low C which had formed to the southeast of the parent Low B.

Before studying the convergence precipitation pattern associated with this warm front it is necessary to trace the position of the approaching cold front to estimate its effect on the convergence rain area. Figure 5-6b shows 6-hourly positions of the cold front along with highest hourly amount of precipitation near time of passage. This front was extremely weak in Central California as it moved out of an offshore trough. But as it approached the moist southerly flow over Southern California, precipitation intensity near the cold front increased somewhat along the coast and greatly in mountain areas where the upslope flow was increasing. Highest intensity in the storm occurred at the cold front only at higher mountain stations around the perimeter of the Los Angeles Basin and in the Santa Ana Mountains where orographic lifting was most effective. This is seen by comparing in figure 5-6c time of highest intensity with time of frontal passage.

By considering only the period from 0000 to 0900 PST, the effect of the cold front is eliminated over the Los Angeles Basin except for the gradual increase in orographic precipitation in and near mountain areas as the gradient increased. Isohyets for this 9-hour period, shown in figure 5-6d indicate a 3-inch center near the coast in the Los Angeles Airport area; this rain may be regarded as "warm front" rain, as defined earlier, with no other appreciable effects. Considering its magnitude, upward motion due to

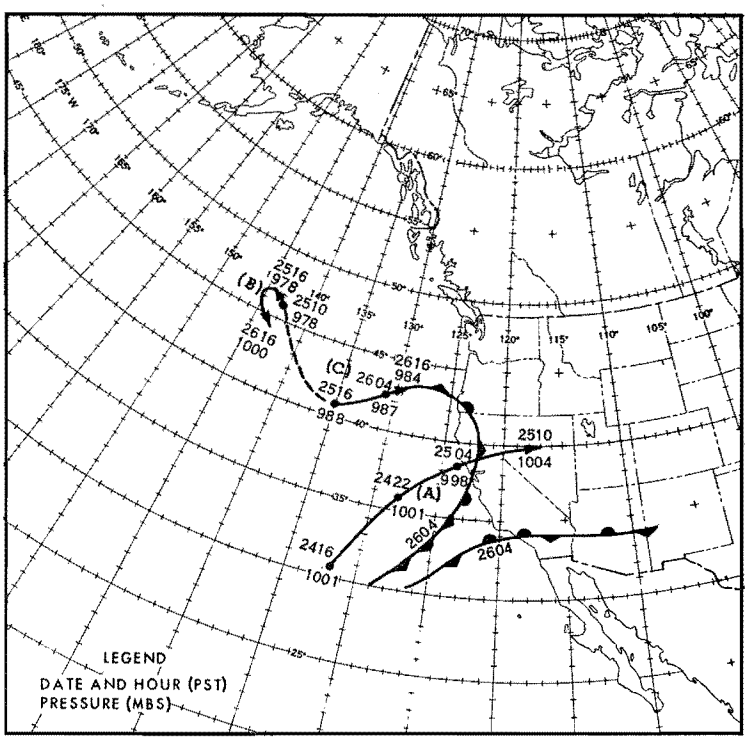

Fig. 5-6a. TRACKS OF LOWS JANUARY 24-26, 1956 AND FRONTAL POSITIONS AT 0400 PST, JANUARY 26, 1956

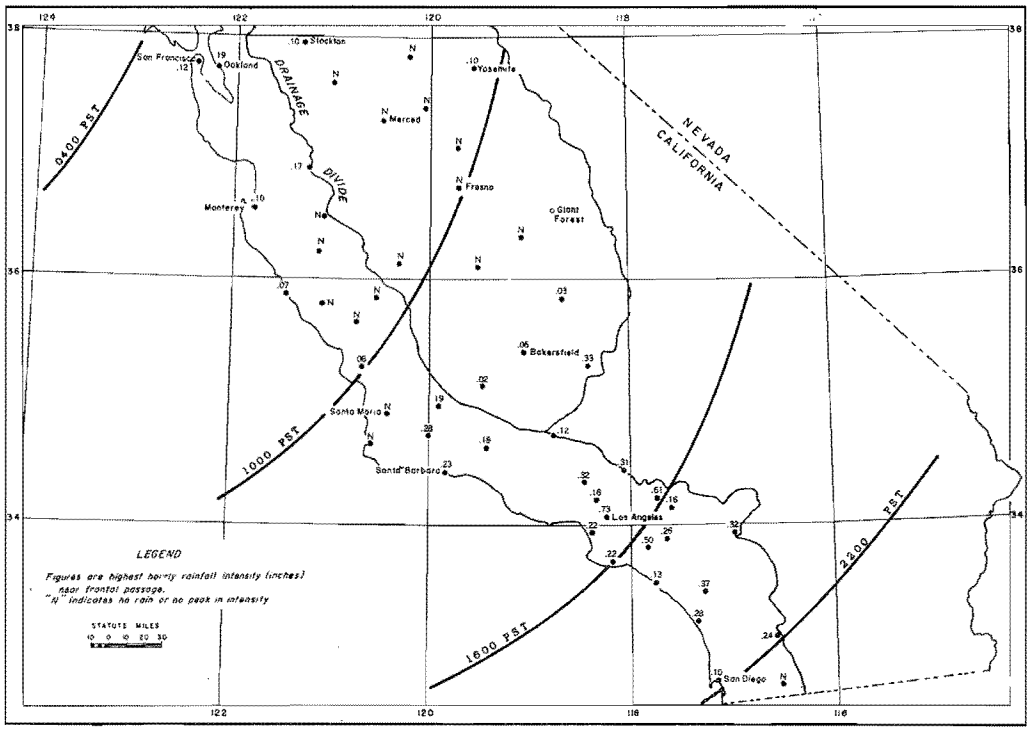

Fig. 5-6b. POSITIONS OF COLD FRONT, JANUARY 26, 1956

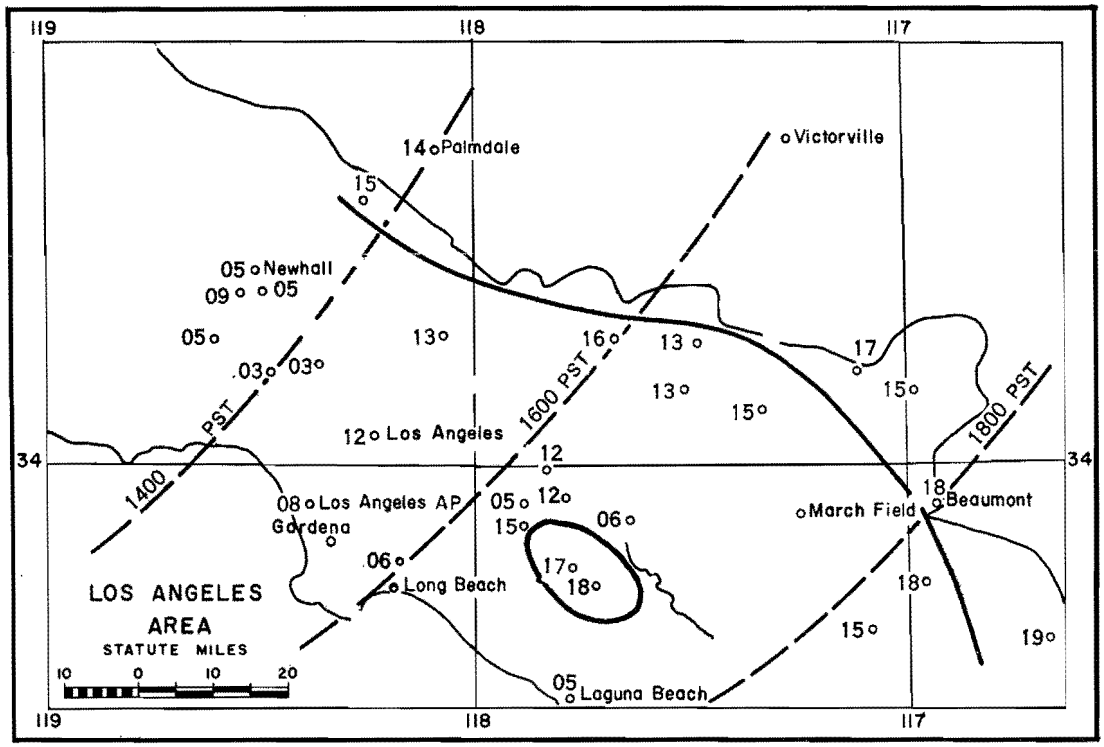

Fig. 5-6c. TIMES OF HIGHEST HOURLY PRECIPITATION (PST), FRONTAL POSITIONS (DASHED) AND AREAS OF APPROXIMATE COINCIDENCE IN TIME (SOLID), JANUARY 26, 1956

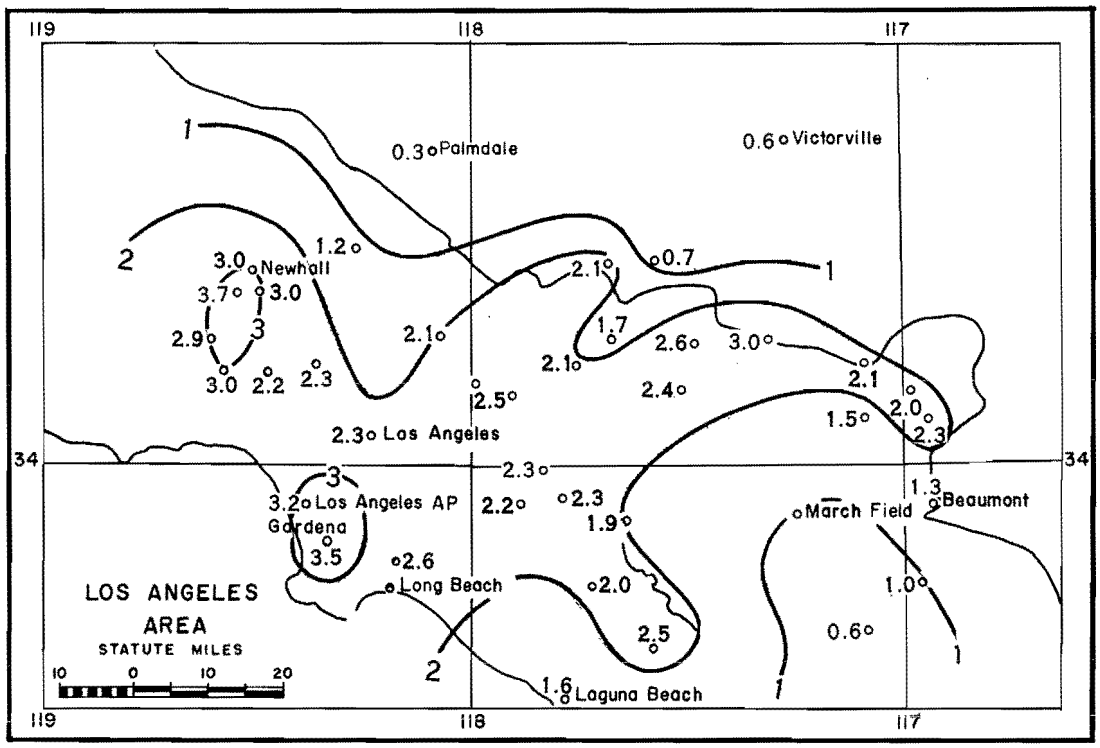

Fig. 5-6d. ISOHYETS (INCHES) FOR PERIOD 0000-0900 PST, JANUARY 26, 1956

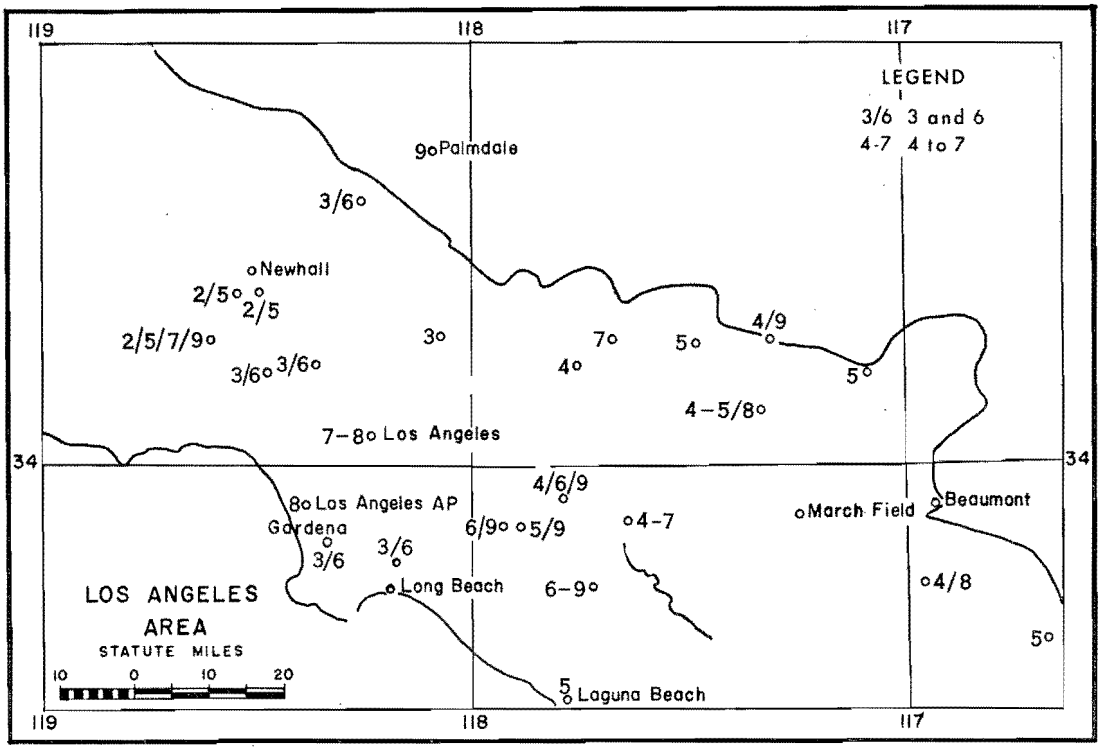

Fig. 5-6e. TIMES OF PEAK HOURLY PRECIPITATION FOR PERIOD 0000-0900 PST, JANUARY 26, 1956

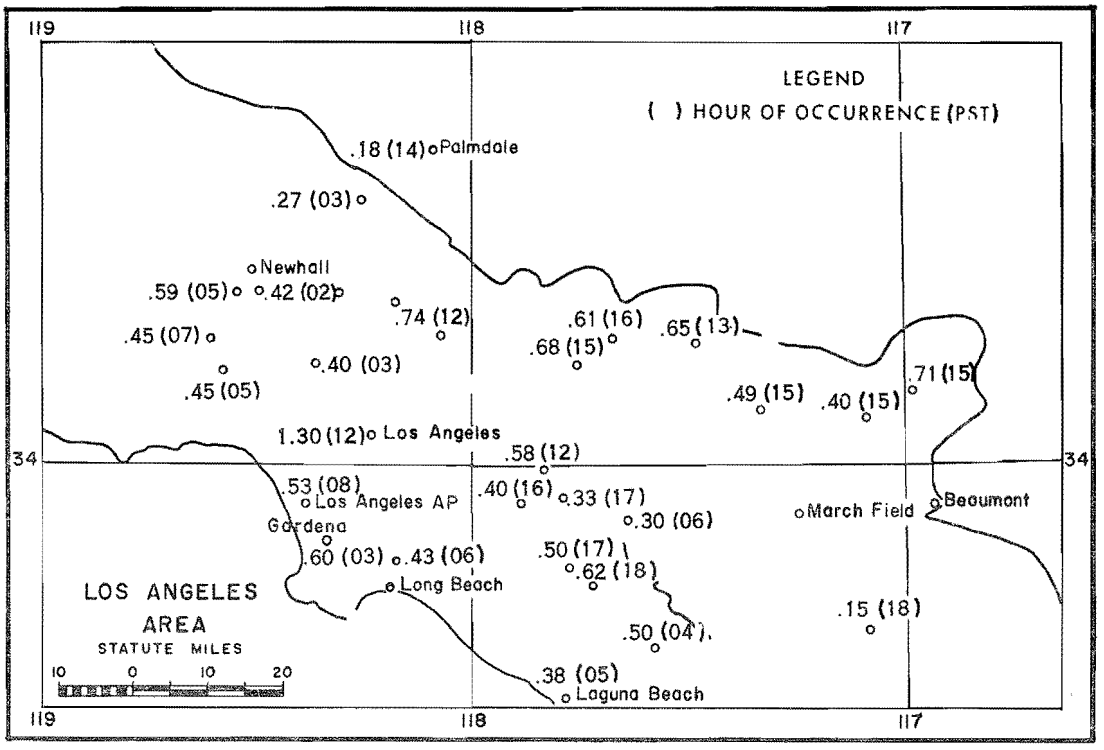

Fig. 5-6f. HIGHEST HOURLY PRECIPITATION INTENSITY (INCHES) JANUARY 26, 1956

ageostrophic convergence was a far more important factor than upslope motion at the front. Another 3-inch center in the upper San Fernando Valley is partly orographic in a southerly flow. Rainfall amounts in the western two thirds of the area decrease with elevation some distance upwind of the mountain crest rather than at the crest, indicating that dropoff in convergent precipitation from the coast more than offset the increase with elevation in orographic precipitation.

A surprising fact in regard to this convergence rain is that high intensity was recorded along the coast around Long Beach from 0200 PST even though the Long Beach raob at 0100 PST showed fairly low humidity above 850 mb.

Areal patterns of time-intensity are not well defined during this 9-hour period in figure 5-6e, a plot of hour or hours of peak intensity, although there is some agreement between peak periods at nearby stations.

Highest recorded hourly intensities on January 26 are shown in figure 5-6f, with times in parentheses. In the 9-hour period prior to 0900 PST over areas with little orographic effect the highest recorded hourly value was .60 inch near Gardena to 0300 PST. (Near midday, hourly intensities reached 1.30 inch in downtown Los Angeles and nearly an inch at foothill stations to the northeast, all subject to an orographic effect. Although this occurred three hours prior to the cold front passage it is not logical to divorce this rain entirely from the convergence rain in advance of the cold front. The evidence that instability was also a factor is given in chapter 5-C-5.)

f. Warm front precipitation intensity. Comparison of the value of .60 inch per hour near Gardena in the January 1956 storm is made in table 5-2 with hourly amounts in various types of warm front situations at San Francisco, Sacramento and Los Angeles (City) in major storms. All are considerably smaller than the Gardena amount except cases involving an occluding system. Comparison of 3- or 6-hour amounts in the same storms shows even larger differences.

5-B-2. Cold and occluded fronts

The typical behavior of cold and occluded fronts in major storms is surveyed in this section, along with variation in their role in convergence precipitation with distance from storm center and position in the storm sequence.

a. Typical frontal behavior in storm types. The following statements relate storm type with behavior of fronts at the latitude of the precipitation center of the storm, as they approach the coast. They amplify chapter 5-B-1a.

In Mid-latitude type storms, common to all of California, most fronts are occluded at the coast. This is true of a larger share of fronts in

Table 5-2

WARM FRONT PRECIPITATION HOURLY INTENSITY IN RECENT MAJOR STORMS

Station	Highest Amount (Inches)	Dew Point (°F)	Date	Time of Ending (PST)
Gardena	.60	56	1/26/56	0800
San Francisco	.34	59	11/18/50	0300
Sacramento	.19	53	12/18/55	0300
Sacramento	.35	57	2/27/40	0600
San Francisco	.29	56	2/25/40	0800
San Francisco	.16	61	12/9/37	2100
San Francisco	.24	57	3/23/28	1600 (an occluding system)
Los Angeles, City	.29		2/13/37	
"	.77		3/2/38 (an occluding system)	
"	.48		12/31/33	
"	.47		2/15/27	
"	.67		4/8/26 (nearly occluded system)	
"	.31		12/21/21	
"	.17		1/18/16 (.83 with cold front on 17th)	
"	.30		1/28/11	

Northern than Southern California-centered storms. The percentage of occlusions is high mainly because the great distance offshore at which most occluding waves form provides ample opportunity for occlusion to take place; also because in this type large individual storm centers readily develop on the southern periphery of the long-wave trough.

In the Low-latitude type storm there is more often a cold front rather than an occlusion involved, and then only toward the end of the storm, across the area of highest storm intensity. Up to that time waves moving inland along the ENE-WSW polar front are kept small in amplitude and only partially occluded by the deep Low in the southern Gulf of Alaska to the northwest of the wave chain. This was shown in chapter 2-B-1 as typical of the December 1955 storm. Occlusion of the final wave becomes more complete at the coast if the Gulf of Alaska Low acquires a stronger zonal component of motion so as to permit injection of colder air to the rear of the final deepening system.

The High-latitude type storms typically involve a cold front except when there is a breakthrough of an occlusion across the block to the west. The cold front tends to stagnate off Southern California as waves move along it,

because of persistence of an offshore trough; it becomes obscure in Southern California if it moves inland ahead of the offshore trough.

It is often difficult to classify occlusions as warm or cold as they reach the coast because of the small temperature difference across them. They are more often cold in Southern than in Northern California. The last one of the storm is usually cold, the first is sometimes warm; the majority in major storms are cold even in Northern California. Those moving northeastward are more likely warm, especially if there is a remnant of a previous outbreak of polar air over California. (On February 1, 1945 the increase in temperature at 700 mb and below, as 2 occlusions moved onshore that morning indicates they were warm occlusions; a sharp drop in temperature aloft accompanied the cold occlusion that evening.)

b. Variation of importance with distance southward from storm center. Percentage of convergence precipitation occurring near the front usually increases with distance southward from the precipitation center of the storm. This is the case for several reasons:

1. Less adequate moisture to the south for precipitation except where the strongest convergence exists (i.e., near the front).

2. Weakening of ageostrophic convergence mechanisms other than those associated with fronts on the southern periphery of the storm, because of less intense pressure gradients, less cyclonicity, and lighter winds.

3. In Mid-latitude type storms, more marked frontal troughs with passage of fronts on the southern storm periphery. This is so because of less dominance of cyclonic flow on the perimeter of a large-scale pressure system than near the storm center.

Thus in a Northern California-centered storm, rain in Southern California is usually confined to a brief period near the fronts, although it may be intense.

c. Variation of precipitation near cold and occluded fronts in major storms. The mean distribution of precipitation about time of passage of cold fronts or occlusions at the coast in major storms is indicated in the following study. Table 5-3 lists hourly precipitation and wind data in connection with cold and occluded frontal passages at San Francisco in both Northern and Southern California major storms. (In storms centered in Southern California, frontal passages usually occurred at San Francisco as well as in Southern California.) Time of frontal passage at San Francisco to the nearest hour was estimated both by positioning on synoptic maps and through study of effect on local wind, temperature, and pressure at San Francisco, along with miscellaneous recorded data. Data were omitted for a few weak fronts whose effect on local data was too obscure to permit an estimate of time of frontal passage, even though the accompanying precipitation was not necessarily negiligible.

Table 5-3

HOURLY PRECIPITATION INTENSITY BEFORE AND AFTER FRONTS AT SAN FRANCISCO

Date	(PST) Time	Type Of Front	Storm Type	Hourly Precipitation (inches) Hours Before Front Passage 4	3	2	1	Hours After 1	2	3	4	Wind Direction Before	After	Highest Hrly. Wind (mph)
				Northern California										
4/2/58	1200	Occln	M	.06	.07	.14	.14	.95	.10	.04		SW	W	14
12/23/55	1200	Cold	L	.18	.14	.07	.14	.05	.05	.04	.04	SW	SW	27
11/18/50	2200	Cold	L	.05	.05	.04	.02	.05	.02	.01	T	SW	W	17
2/1/45	0400	Occln	M	.02	.16	.23	.16	.25	.12	.04		SE	S	17
2/1/45	0900	Occln	M		.04	.08	.16	.09	.05	.07		S	SW	18
2/1/45	1800	Occln	M	.01	.19	.06	.10	.13	.04	.01		S	SW	25
1/21/43	1300	Occln	H	.35	.14	.25	.13	.01				SW	SW	26
1/22/43	1600	Occln	H		T	.08	.28	.13	.35	.10	.03	SE	SW	23
2/28/40	0500	Occln	M	.07	.08	.06	.03	.62	T			SE	SW	24
12/10/29	0200	Occln	M			T	.01	.35	.01	T		S	S	21
3/23/28	1700	Cold	L	.15	.17	.24	.06	.13	.10	.02		SE	SW	12
3/26/28	1600	Cold	L		T	.02	.19	.19	.14	.11	.03	S	W	25
1/13/09	1400	Occln	M		T	.07	.14	.07	.03	.01		SW	SW	24
12/19/55	1100	Cold	L	.05	.03	T	.03	.10	.01	.01	.02	S	SW	29
1/30/11	1400	Cold	H	T	.07	.09	.10	.09	.06	.01	.01	SW	NW	7
1/2/14	0400	Cold	M	.04	.03	0	.01	.32	.14	.07	.03	S	SW	16
	Average of 16 cases			.06	.07	.09	.11	.23	.08	.03	.01			
				Southern California										
1/25/56	0300	Occln	L		T	.10	.05	.09	.09	.06		SE	SW	21
2/28/38	2100	Occln	M	.07	.16	.24	.19	.01	T	.03		SE	SW	19
3/21/38	0400	Cold	M		.07	.03	.03	.09	.02	.02	.01	SW	SW	16
2/14/27	0900	Occln	M	.04	.01	.01	.07	.18	0	.01	.01	SE	S	19
2/18/27	0000	Occln	M	.15	.04	.22	.16	.27	.01	T		SE	SW	18
4/4/26	0900	Occln	M	.05	.10	.13	.39	.22	.15	.06	T	NE	SE	16
4/5/26	0700	Occln	M	.16	.01	.04	.24	.05	.03	.01	T	SE	SW	13
4/7/26	0700	Occln	M			0	T	.38	.08	.04		SE	SW	29
4/8/26	0200	Occln	M	.01	.12	.06	.16	.09	.19	.25	.04	S	SW	18
12/20/21	0600	Cold	H			0	.02	.04	.06	.06	.02	S	SW	19
12/26/21*	1700	Cold	H	Warm front rain			0	0	.04	.27	.02	S	SW	25
12/25/21*	1000	Cold	H	Warm front rain			0	0	0	0		SW	SW	45
1/27/16*	1400	Cold	H	Warm front rain			.05	.10	.02	0		SW	NW	19
2/20/14	1600	Cold	M	.04	.05	.02	.06	.15	.13	.07	.01	S	S	28
	Average of 11 cases			.05	.05	.08	.13	.14	.07	.06	.01			

*Omitted from average

M-Middle latitude type, H-High latitude type, L-Low latitude type

The distribution of rain about time of frontal passage varied widely. In contrast to the predominance of the pre-frontal rain in an average winter storm (15), in these major storms intensity tended to center about the frontal passage; in 19 of 27 cases the frontal passage occurred during the hour of highest precipitation intensity. Rainfall amounts for the 2 hours prior to frontal passage in Northern California storms averaged lower than for the following 2 hours, namely .20 and .31 inch; this difference is biased by the April 2, 1958 and February 28, 1940 cases in which large hourly amounts occurred following the frontal passage, much of which may have been due to instability. Larger 2-hour amounts occurred slightly less often prior to than following frontal passages. On the average, precipitation dropoff following the front was more rapid than increase prior to the front.

Two-hour rainfall intensity in Northern California-centered storms averaged higher with passage of occlusions than with cold fronts and much higher near fronts in Mid-latitude type storms than in Low-latitude type storms.

In general, largest hourly amounts occurred in storms with a noticeable wind shift at the front (table 5-3). Precipitation was more concentrated at the front with larger wind shift than with little or none. A scatter diagram (not shown) gives no indication of higher 2-hour intensities near the front with strong winds than with weak winds.

d. Effect of topography on cold and occluded fronts. The windward coastal and Sierra slopes provide a barrier to progress of a cold front or cold occlusion which locally distorts the frontal surface as the front at the ground tends to conform to the shape of the elevation contours. On lee slopes the downward motion of air inhibits frontal precipitation. Precipitation in lee areas depends primarily on spillover and ageostrophic convergence above the barrier level. In special circumstances, an upslope circulation contributes to precipitation in some normally lee areas; then normally windward areas may become lee slopes temporarily.

e. Example of an occluded front in California during a major storm. Between 1900 PST of the 1st and 1200 PST of the 2d February 1945 an occluded front passed across California. Offshore it was a distinct fast-moving front (figure 2-21a) the last one of the storm, having become occluded only as it approached the coast as part of a deepening wave in a broad offshore trough. This example is typical of the onshore behavior of many occlusions moving out of an offshore trough in major storms. Also there were available a good network of hourly surface reports, hourly precipitation records and upper air data.

Figure 5-7 shows frontal positions (solid lines) as the front moved inland. They are based on analysis of hourly surface synoptic charts. Also shown are hyetographs of 2-hour precipitation centered on the front. At the coast the front is oriented in a manner typical of that in Mid-latitude type storms. The front bulges northeastward from the San Francisco Bay area through the southern Sacramento Valley because of the strong flow through this area, with retardation over the coastal mountains north of San Francisco. Retardation is indicated also near the Tehachapis.

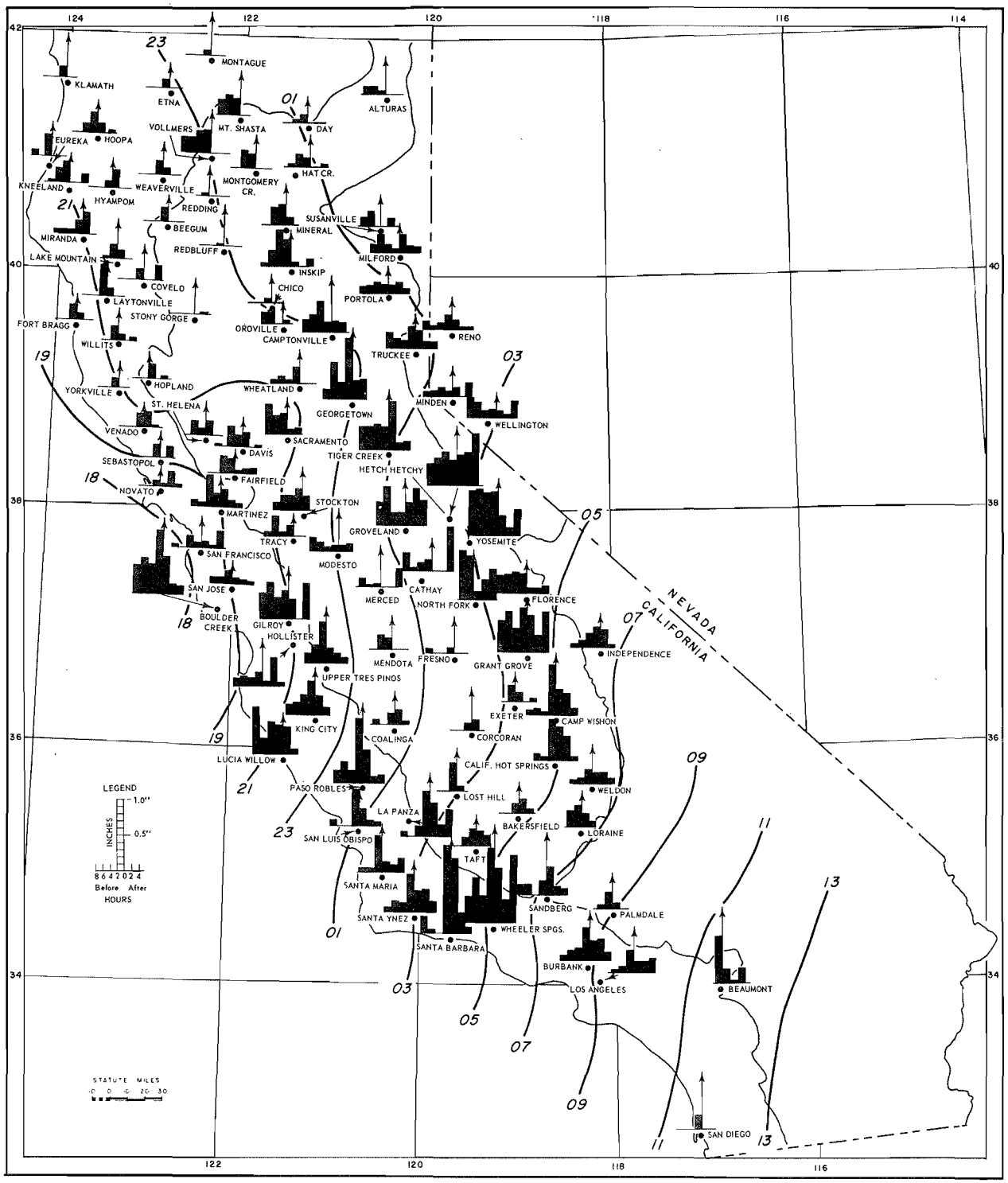

Fig. 5-7. ISOCHRONES OF FRONTAL POSITIONS (PST) AND HYETOGRAPHS ABOUT TIME OF FRONTAL PASSAGE, FEBRUARY 1-2, 1945

The precipitation sequence in figure 5-7 centers around the frontal passage in a symmetrical manner in some areas, particularly along the coast and in the north and south ends of the state. But in some areas its peak tends to precede and/or follow time of frontal passage. From San Francisco northeastward toward the Delta and in the Central Valley from Fresno northward to Oroville heaviest rain tends to precede the front by a few hours; this is the case elsewhere at scattered locations such as Gilroy and Lucia Willow. This pre-frontal rain was marked by precipitation burst lines south and east of San Francisco; in the Delta area it was associated with development of a Low to the northwest of Sacramento. Instability was evident at this time in scattered thunderstorms. Post-frontal showers dominate the precipitation sequence at scattered locations, particularly in the central part of the state; the air flowing around the persistent offshore trough was becoming increasingly unstable (figure 2-21b). In the Sierras convergence precipitation near the front tends to be obscured in the orographic precipitation which is only approximately and rather broadly oriented about time of frontal passage.

This example points up the effect of topography in distorting frontal configurations. It illustrates the addition of a large orographic component over windward areas and the robbing of the convergence component of precipitation over lee slopes. Further, it illustrates the minor role in the precipitation sequence of a typical front in comparison with other convergence-producing synoptic features in major storms.

5-C. INSTABILITY MECHANISMS

5-C-1. Instability defined

Definitions of instability are reviewed briefly below:

Conditional instability. Temperature lapse rate is between the moist and dry adiabatic rates. With reference to vertical displacement of an air parcel, the air is unstable if saturated but stable if not saturated.

Convective instability. The temperature and moisture lapse rates are such that a layer, if lifted sufficiently would be unstable. Convective instability depends on an initial more or less steep lapse rate of both temperature and moisture, the one complementing the other.

Absolute instability refers to a temperature lapse rate greater than the dry adiabatic.

5-C-2. Factors affecting stability in major storms

The following factors affecting stability in major storms are discussed: moisture source region, surface cooling or heating, vertical difference in temperature or moisture advection, and vertical motion. The effect of stability on precipitation in recent major storms is discussed in 5-C-4.

a. Moisture source region. A necessary part of the history of an onshore flow the moisture content of which is typical of the high values found in some major California storms, is that there has been opportunity for penetration of heat and moisture to high levels through surface heating in a low-latitude source region. This is of necessity followed by stabilizing of lower levels through passage over a cooler ocean surface. This moisture penetration requires (1) stagnation at low latitudes or a lengthy zonal transit at a low latitude and (2) a minimum of stabilizing and drying effect through divergence while in the moisture source region. Both can be attained on the western periphery of the Pacific anticyclone at times when it is displaced far to the southeast (as in Low-latitude type storms) or in a strong zonal flow on its north side at times when it is displaced southward to a low latitude into a narrow ribbon (as in most Mid-latitude type storms). A source region farther east at the same low latitude does not permit adequate moisture penetration into upper levels because of the stabilizing effect of horizontal divergence in those areas. More northerly latitudes cannot provide comparable moisture. Thus air reaching California with optimum moisture must have been stabilized in lower layers through surface cooling after the moisture requirement had been met.

b. Advection over a water or land surface. The destabilizing effect of heating of air by a water surface is a maximum during winter months when large differences are possible between air temperature and sea-surface

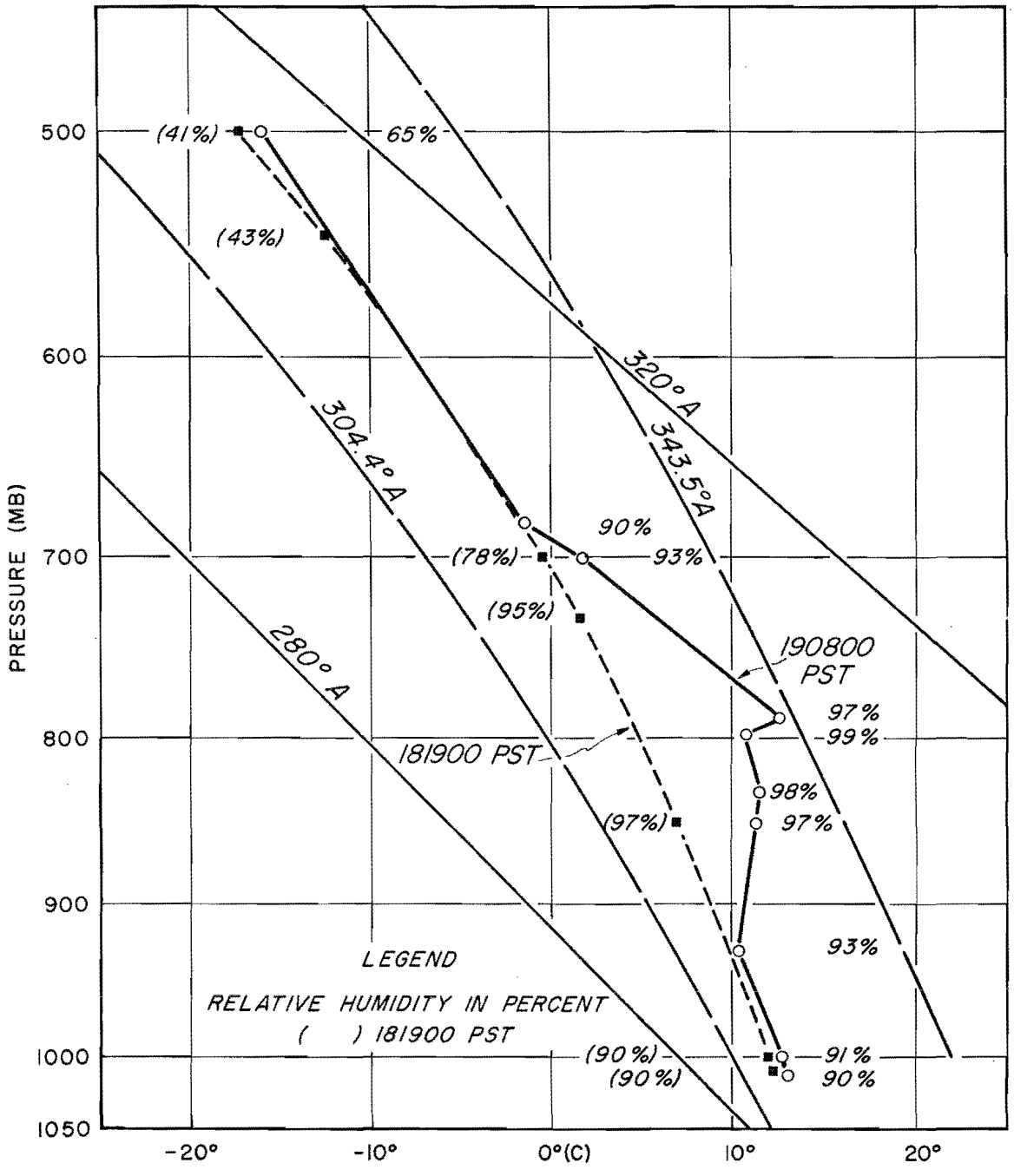

Fig. 5-8. OAKLAND SOUNDINGS - 1900 PST DECEMBER 18, AND 0800 PST DECEMBER 19, 1955

temperature along portions of the West Coast of North America. An extreme example of this occurs when cold Arctic air flows off the coast and southward over the eastern Pacific Ocean from Alaska, western Canada or the Pacific Northwest in connection with a coastal Low. The lapse rate in the air as it moves southward becomes moist adiabatic to increasingly high levels through convection, if not restricted at some upper level by the stabilizing effect of downward motion resulting from divergence.

In major storms, however, the opportunity for recent addition of heat in lower levels in a coastal flow is limited primarily to the final sequence, since at other times the relation between high moisture and source region (chapter 5-C-2a) has imposed lengthy travel from a lower latitude. Referring to the 4 groups of storms in table 3-3, it follows from this relation that there is a trend from a destabilizing influence through considerable depth on a flow to the coast in storms in the 4th group, toward a marked stabilizing influence at lowest levels in storms in the first group.

Daytime surface heating over California is most effective in steepening temperature lapse rates under the following conditions; in Pacific air from a higher latitude behind the final front of a storm, when upper cloud layers are at a minimum and during spring or fall months. Evidence of this is the more frequent daytime thunderstorm occurrence under these conditions. During the season of major storms when the role of surface heating is restricted, orographic lifting is the important destabilizing factor; but daytime surface heating of lower layers in transit northward through the Sacramento Valley in some cases also contributes to the intense convective storms in the foothills of the Northern Sacramento Valley, especially in spring and fall.

c. Vertical difference in temperature-moisture advection. In a layer, positive advection of temperature and/or moisture at one level relative to others above and below results in increased stability below and decreased stability above that level. It depends primarily on opportunity for wind direction variation in the vertical (which decreases as moisture at all levels approaches optimum values). Following are examples. On the night of December 18, 1955, in advance of an occluded front moving onshore from WSW, relatively large positive temperature advection occurred in the intermediate levels. By 0800 PST of the 19th this, along with surface cooling, resulted in great stability below the level of greatest warm advection (figure 5-8) but a steep temperature lapse rate above that level. A similar situation occurred on the nights of December 21 and 22, 1955. Advection of dry air near and above 700 mb at Oakland on the 20th in the same storm contributed to convective instability in the layer below 700 mb, as described in chapter 5-C-3.

Although advection of potentially warmer faster-moving superior air over a cold or occluded frontal surface, along with descent down the frontal slope, suppresses precipitation by stabilizing the air near and following the front in sharp troughs, as suggested by Elliot (15), this effect is less typical of fronts in major storms when the principal trough remains offshore and the frontal trough is slight.

d. Vertical motion in convectively unstable air. Orography or convergence mechanisms may lift convectively unstable air sufficiently to release the instability.

Examples of release of instability through vertical motion due to orography are given below, first in a major storm and also in lesser storms.

Between 1900 PST, January 20, 1943 and 0200 PST the next day at the height of the storm lightning was reported at Donner Summit, elevation 7189 feet. It is deduced that there was a release of convective instability following lifting of a strong moist southwest flow by orography to a high level. This occurred in advance of a rapidly deepening Low, far ahead of a surface front. The absence of thunderstorm reports from other California stations during this period suggests that orographic lifting to a considerable height was necessary for release of the convective instability.

On December 20-21, 1866, thunderstorms in the San Francisco area were severe and contributed to a record 20.5-hour rainfall of 7.76 inches in San Francisco (chapter 2-D-2). It is concluded that this case represents extreme convective instability in a winter storm approaching major proportions, in that only slight lifting by the coastal hills was sufficient for marked instability release.

At least 18 inches of rain fell at Ft. Ross (on the coast about 60 miles north of San Francisco) on November 21-22, 1874 in 24 hours during a general storm. In view of the relatively small amounts in nearby coastal areas with less steep slopes, it is likely that a large part of this rain was due to instability released by orographic lifting.

Examples of extreme local release of convective instability primarily through orographic lifting occur most frequently and with greatest violence in the foothills of the northern Sacramento Valley. This fact emphasizes the importance of orographic lifting on a low-level flow into the narrowing valley and on a superimposed onshore flow in a southwest current which has been lifted to as much as 7000 feet over the Trinity Mountains immediately to the west. (The seasons of occurrence of these storms, mainly in spring and fall, point up in some cases the additional role of land heating in increasing the lapse rate in lower levels). There is evidence from upper-air data in the more recent of these storms that the air was to some extent convectively unstable at some levels prior to entering the coast.

Release of convective instability through vertical motion due to convergence is believed to have occurred at Sacramento on April 20-21, 1880 when 7.24 inches fell in 22 hours (chapter 2-D-1). In the absence of orographic or land heating effects, ageostrophic and frontal convergence must have provided the lifting. The localization and intensity of the storm center (indicated by the nature of reports of flooding and of 24-hour isohyets) is the evidence for local release of instability.

5-C-3. Typical variation of stability with storm sequence

The typical veering of the wind with storm sequence produces related effects on the stability. These effects can be seen partially through effects on lapse rate of temperature.

Relations between surface geostrophic wind direction and departure from the moist adiabatic lapse rate are shown in figure 5-9 for Oakland during the period December 16, 1955 to February 1, 1956, a period involving repeated storms approaching the Pacific Coast from the southwest (including the major storm of December 19-25, 1955) as well as brief periods of fair weather. Data are grouped into two surface windspeed classifications for both the 1000 to 700-mb and 700 to 500-mb layers.

The following points are brought out by the relations of figure 5-9:

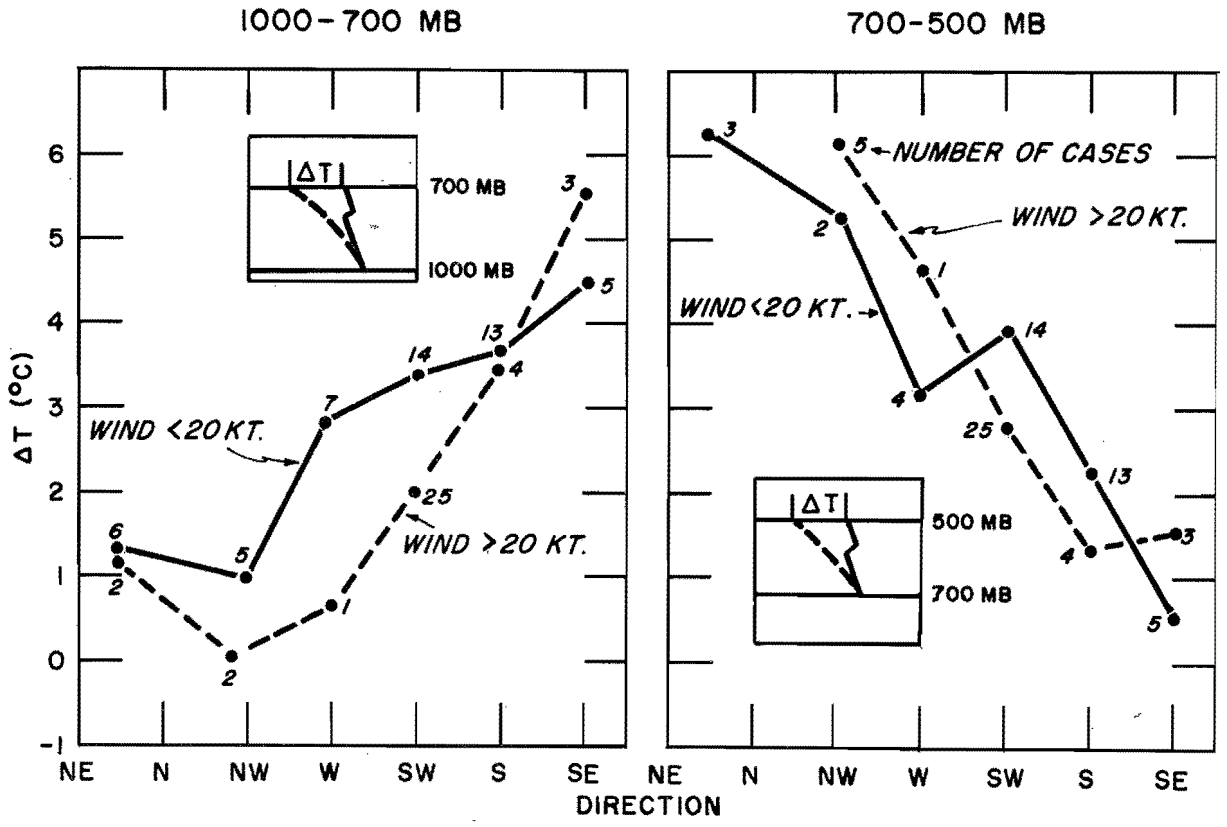

Fig. 5-9. STABILITY VS. SURFACE GEOSTROPHIC WIND DIRECTION, OAKLAND, DECEMBER 16, 1955 - FEBRUARY 1, 1956. (ORDINATE IS ΔT IN INSET)

1. The average temperature lapse rate in the 1000 to 700-mb layer is least steep for wind direction east of south, intermediate for southwest winds and steepest with wind west to northwest, as would be expected from 5-C-2b above. This implies an increase in average lapse rate below 700 mb with storm progression, to the highest value near the storm conclusion.

2. Average lapse rate in the 1000 to 700-mb layer is steeper for strong than for lighter southwest surface windspeeds.

3. Average lapse rate in the 700 to 500-mb layer has a reverse correlation with surface wind direction to that of the 1000 to 700-mb layer.

5-C-4. Comparison of stability in selected storms

The following method was used to obtain a numerical value to represent graphically the relative degree of conditional instability for comparison in storm sequences and between storms. The difference was obtained between 700-mb temperature and that resulting from lifting the 1000-mb parcel adiabatically to saturation and then along the moist adiabat to 700 mb. This difference is the width of the positive or negative area at 700 mb. Similar values were obtained using the 700-mb level as the lower level and 400 mb as the upper level. These two sets of data are plotted for Oakland as broken and short dashed lines, respectively, for 4 storms in figures 5-10, 5-12, 5-13, and 5-16 and labeled "conditional instability" with the special meaning as defined above.

Numerical values to represent "convective instability" in the 1000 to 700-mb layer were obtained as follows: It was assumed that each 100-mb layer to 300 mb was contracted to a 64-mb layer on being lifted over a 750-mb barrier, equivalent to about 8000 feet or the average height of the Sierras. The flow thus becomes horizontal at 300 mb. A value of conditional instability is then obtained for this compressed layer in the manner described above. This value represents the "convective instability" of that layer before lifting. Values for the 1000 to 700-mb layer are plotted as a solid line.

The above stability indices are plotted with stability decreasing toward negative values. The degree of stability indicated by these values is generally higher than that obtained by comparison of lapse rate of temperature with the moist adiabatic rate (figure 5-9) because of lack of saturation at the base of the layers. Temperature lapse rate comparisons within and between storms may be made by noting width of spacing between levels in the plots of 1000-, 700-, and 400-mb temperature.

December 18-23, 1955. The 1000 to 700-mb conditional and convective instability values at Oakland are compared with temperature changes and 6-hour rain (figure 5-10) and with tracks of Lows (figure 2-12, p. 17). Greatest stability in this layer occurred in the early part of the primary storm period of December 21-23; at the same time, a falling trend in 700 to 400-mb conditional instability is indicated.

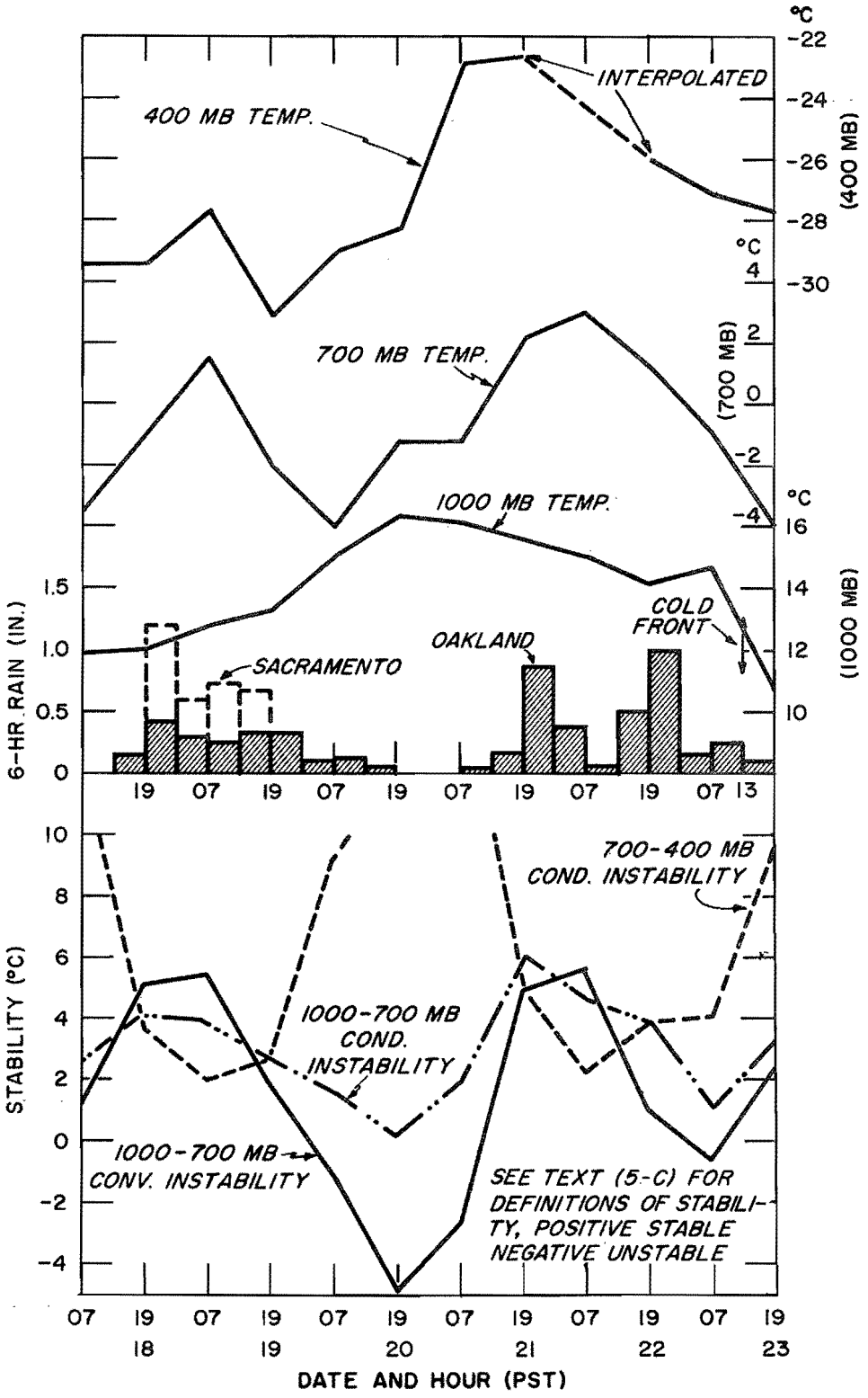

Fig. 5-10. INSTABILITY DATA, OAKLAND - DECEMBER 18-23, 1955

On the 18th, as the Low (1) and following wave (2) in figure 2-12 moved northward, warm advection at intermediate levels (figure 5-10) increased low-level stability (1000 to 700 mb) and decreased upper-level stability (700 to 400 mb). By the 20th, the 1000 to 700-mb layer was least stable following a decline of 700-mb temperature with veering of wind at that level while 1000-mb temperature rose with increasing southwest surface flow around Low (A). Moisture decrease with height in the layer resulted in a high value of convective instability. Evidence of release of this instability is found in the report of extremely heavy rain at Lakeshore for the 24-hour period ending at 2000 PST on the 20th and in the resulting inflow peak at Shasta Lake (table 2-1). Elsewhere during this period amounts were generally light.

On the 21st the rapid rise in low-level stability and decrease in upper-level stability is related to the advection of warm air over Oakland at intermediate levels with approach of Low (3) from the distant southwest. The more nearly west-east orientation of the storm track of Low (5) on December 22d brought cooler air aloft and lower stability over Central California in both the 1000 to 700-mb and 700 to 400-mb layers.

The above comparison of stability within layers of 300-mb thickness tends to obscure narrow layers of conditional instability within one or more 100-mb layers (190800 PST, figure 5-8 and 222000 PST, figure 5-11). Both observations were made during heavy convergence rain. Negative values in the left column of table 5-4 represent conditional instability, measured for that 100-mb layer in the manner described for the 300-mb layers. (These data are more sensitive to raob error than data for the 300-mb layers.) In each case conditional instability appears in one or more 100-mb layers at a time when figure 5-10 indicates a stable 1000 to 700-mb layer. Instability resulted from concentration of advectional warming at certain levels with a steepened temperature lapse rate above the level of most pronounced warming. The shallow unstable layers in these two soundings were made slightly more unstable by lifting (right column of table 5-4), because of decrease in relative humidity with height.

It is concluded that release of instability was an important factor in precipitation locally during the lull in the storm on the 20th. It contributed also during the main part of the storm, but only through layers of limited thickness, principally in mountain areas essentially above the level of the stable layer.

November 17-21, 1950 storm. The presence of a nearly stationary frontal boundary in this storm (figure 2-16, p. 29) resulted in a persistent warm flow aloft into Northern and Central California from a nearly constant WSW direction. Except for the brief and rapid rise in 700-mb temperature on the night of the 17th (figure 5-12), there is no evidence of advectional warming in middle layers comparable to that in the December 1955 storm. Thus the small range in 1000 to 700-mb stability values from the 18th to the end of the storm depended mainly on constancy of low-level circulation. The average value of the 1000 to 700-mb stability in both this and the 1955 storm was about 3°C.

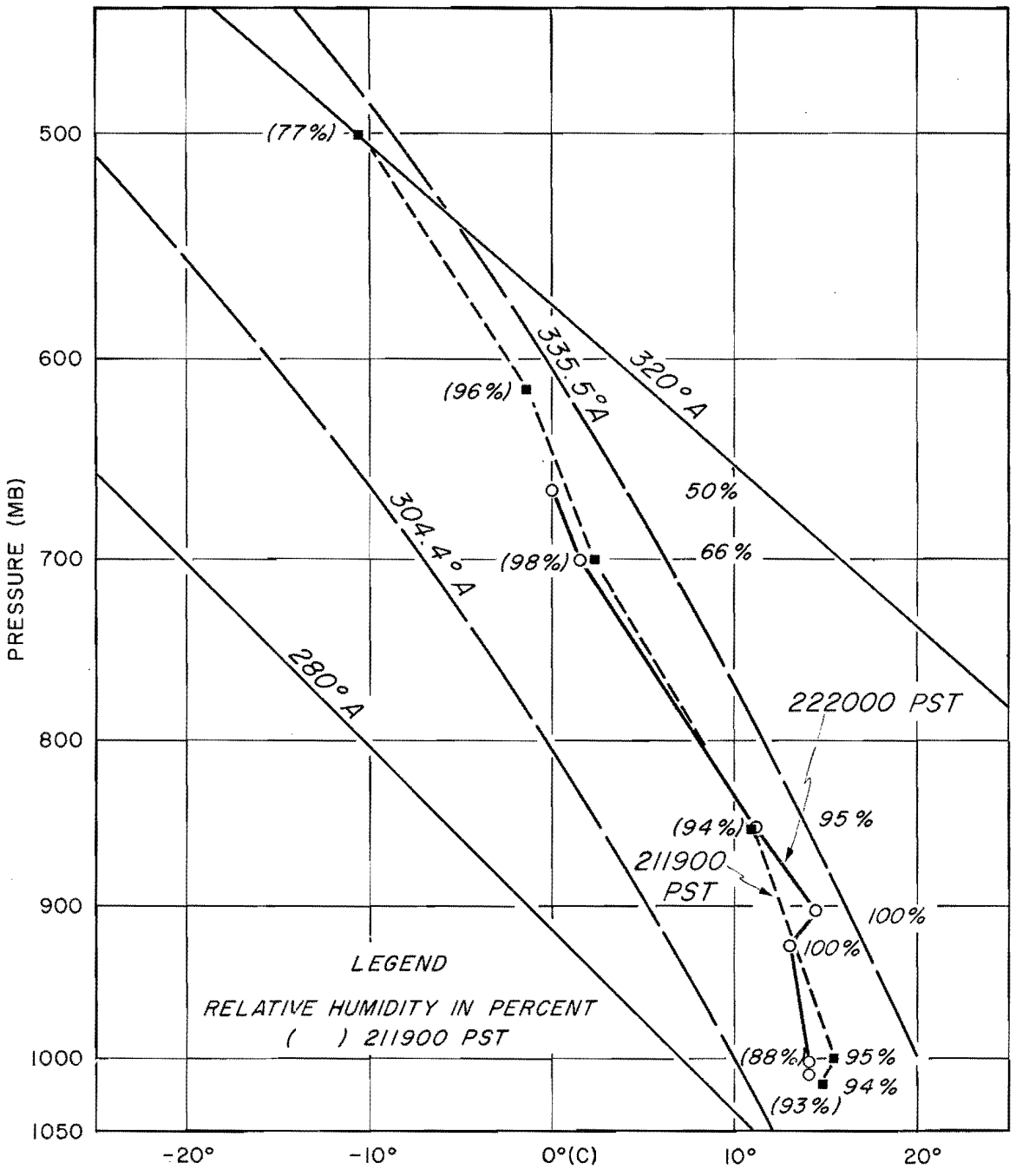

Fig. 5-11. OAKLAND SOUNDINGS - 1900 PST DECEMBER 21 and 2000 PST DECEMBER 22, 1955

Table 5-4

CONDITIONAL AND CONVECTIVE INSTABILITY WITHIN 100-MB LAYERS

(°C PER 100 MBS)

(Negative Values Indicate Instability)

Mbs	Conditional	Convective	
	0800 PST December 19, 1955		
1000-900	+3.3°C	+4.4°C	Oakland
900-800	+5.8	+6.1	
800-700	-5.0	-6.1	
	2000 PST December 22, 1955		
1000-900	+5.1	+6.0	Oakland
900-800	-1.4	-3.0	
800-700	-0.7	-2.0	
	1900 PST November 19, 1950		
1000-900	+1.0	+0.3	Oakland
900-800	-0.9	-1.9	
800-700	+2.7	+1.7	
	1300 PST January 26, 1956		
900-800	+1.9	+2.1	Long Beach
800-700	+0.5	+0.6	
700-600	-3.8	-6.5	
600-500	+2.0	-0.7	

The persistence of stability near the end of the storm depended on stagnation of Lows (B) and (C) in figure 2-16 far enough offshore in the Gulf of Alaska to permit northwestward movement of the warm ridge over Central California, maintaining high temperature aloft. This feature of increasing stability with retrogression of pressure systems is not characteristic of the end of most major storms; usually stability decreases prior to passage of the final front, increasing again only after low-level cooling becomes appreciable.

Table 5-4 shows slight instability within the 900 to 800-mb layer at 1900 PST of the 19th during the lull in the storm.

January 30-February 2, 1945 storm. In this storm instability became important near the end of the storm, as described below. The instability curves for Oakland are shown in figure 5-13.

Stability decreased at high levels from time of beginning of rain on the evening of the 30th, as the temperature from surface to above 700 mb

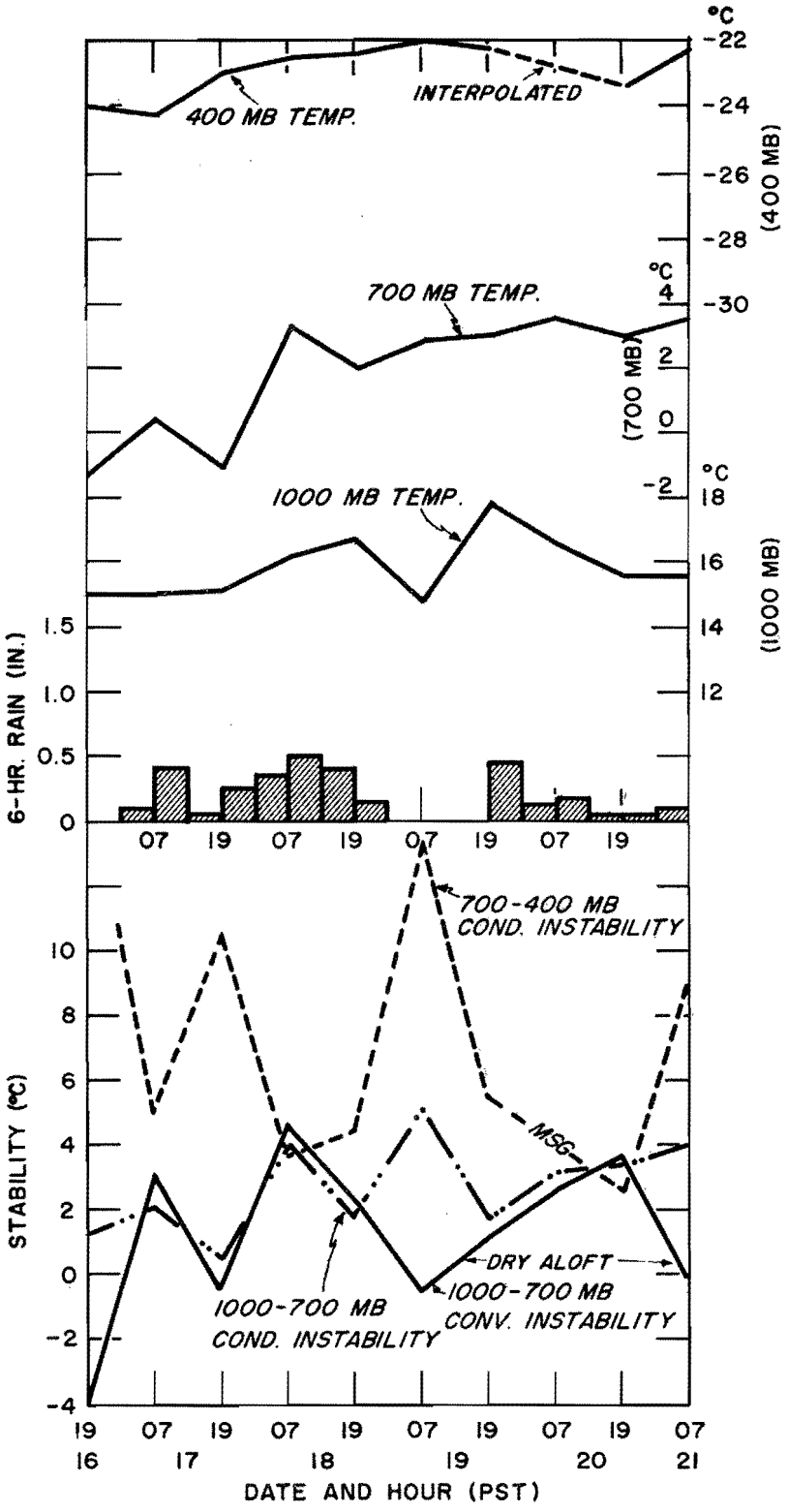

Fig. 5-12. INSTABILITY DATA, OAKLAND - NOVEMBER 17-21, 1950

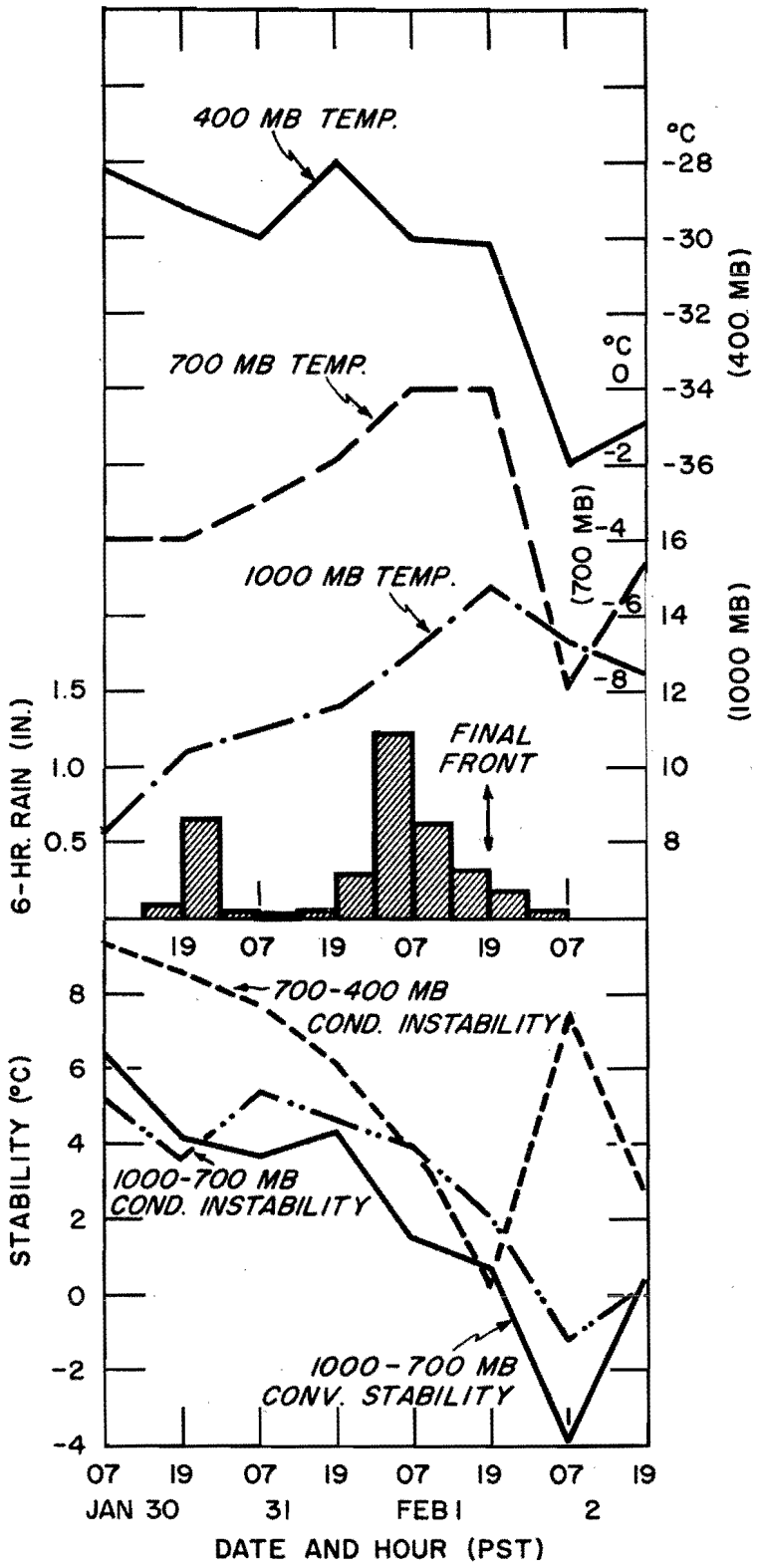

Fig. 5-13. INSTABILITY DATA, OAKLAND - JANUARY 30-FEBRUARY 2, 1945

began a prolonged rise with advection of warm air by the shallow Lows (1) and (2) in figure 2-20, p. 37). The trend toward decreasing stability at all levels on the 1st was accelerated in the afternoon as warm advection in advance of the deepening wave (5) was confined to lowest levels. Scattered thunderstorms were reported in the central coastal mountains and in the Central Valley during the late afternoon, a few hours in advance of the final occlusion, apparently coincident with non-frontal convergence patterns. Instability increased further in lower layers on the night of the 1st as fresh polar air invaded the entire California coast following passage of the frontal system associated with Low (5). This increase was due to extreme temperature drop in all layers except near the surface, which had been heated in transit through the stagnating offshore trough. Scattered thunderstorms continued in Central California on the night of the 1st and 2d as the surface trough remained offshore. Along the Southern California coast thunderstorms were limited to the time of the frontal passage on the morning of the 2d.

Despite this evidence of local instability release, largest hourly precipitation amounts at stations in non-orographic areas where thunderstorms were reported (such as .47 inches at Oakland) were no larger than highest amounts at similar locations during the December 1955 storm, when instability was apparently of comparatively minor importance.

January 25-27, 1956 storm. The possible role of instability in this Southern California storm, described in chapter 5-B-1e, is of particular interest. The heavy convergence rain in the Los Angeles Basin on the morning of the 26th is the main part of a high 24-hour value near Gardena. This value influences the envelope for California of ratio of convergence rain to water vapor of orographic storms (figure 4-7, HMR 36). There is evidence that instability became an important factor only toward the end of the heavy rain period, as follows.

With approach of the cold front extending from Low (C) of figure 5-6a on the morning of the 26th, 700 to 400-mb stability (figure 5-14) was decreasing. The rate of decrease accelerated between 0900 and 1300 PST as warm advection (figure 5-15) took place rather uniformly between about 900 and 650 mbs. By 1300 PST the conditional instability value in the 700 to 600-mb layer alone was -3.8°C (table 5-4). Following the cold front passage (mainly aloft about 1500 PST, figure 5-14), the 700-mb temperature dropped sharply with continuing high surface temperature in a southwest flow from a stagnant offshore trough. As a result low-level stability dropped and upper-level stability increased sharply in a manner similar to that in the February 1945 storm.

Most of the heavy rain at the Gardena center (similar in time distribution to precipitation at nearby Los Angeles Airport in figure 5-14) fell prior to 0900 PST, early in the period of decline in 700 to 400-mb stability (figure 5-14). Thus little of it is attributed to release of instability. At Los Angeles (city), however, most of it occurred after 1000 PST or close to the time of highest 700 to 400-mb instability so that precipitation intensity there was likely much more affected by instability.

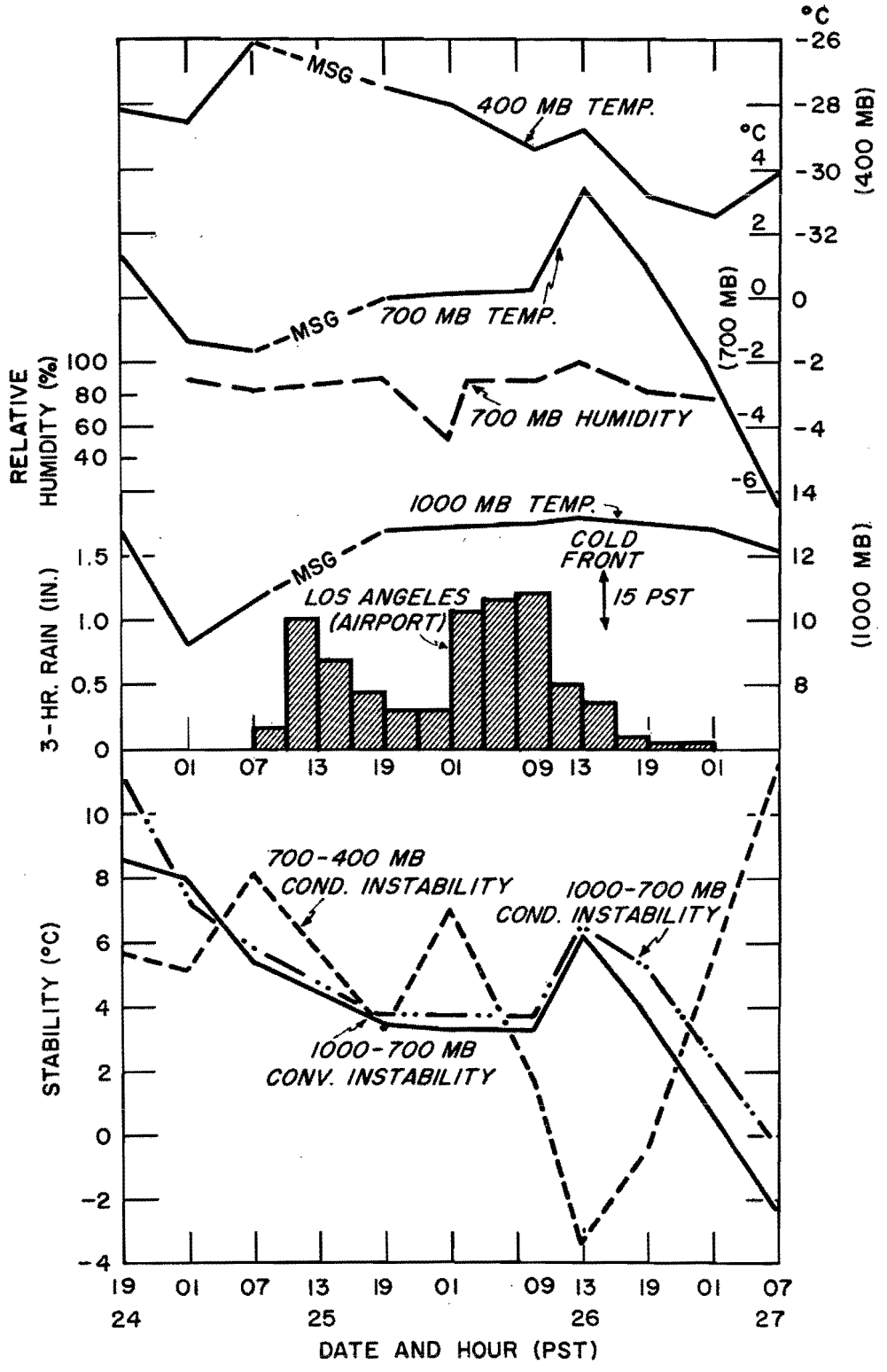

Fig. 5-14. INSTABILITY DATA, LONG BEACH - JANUARY 24-27, 1956

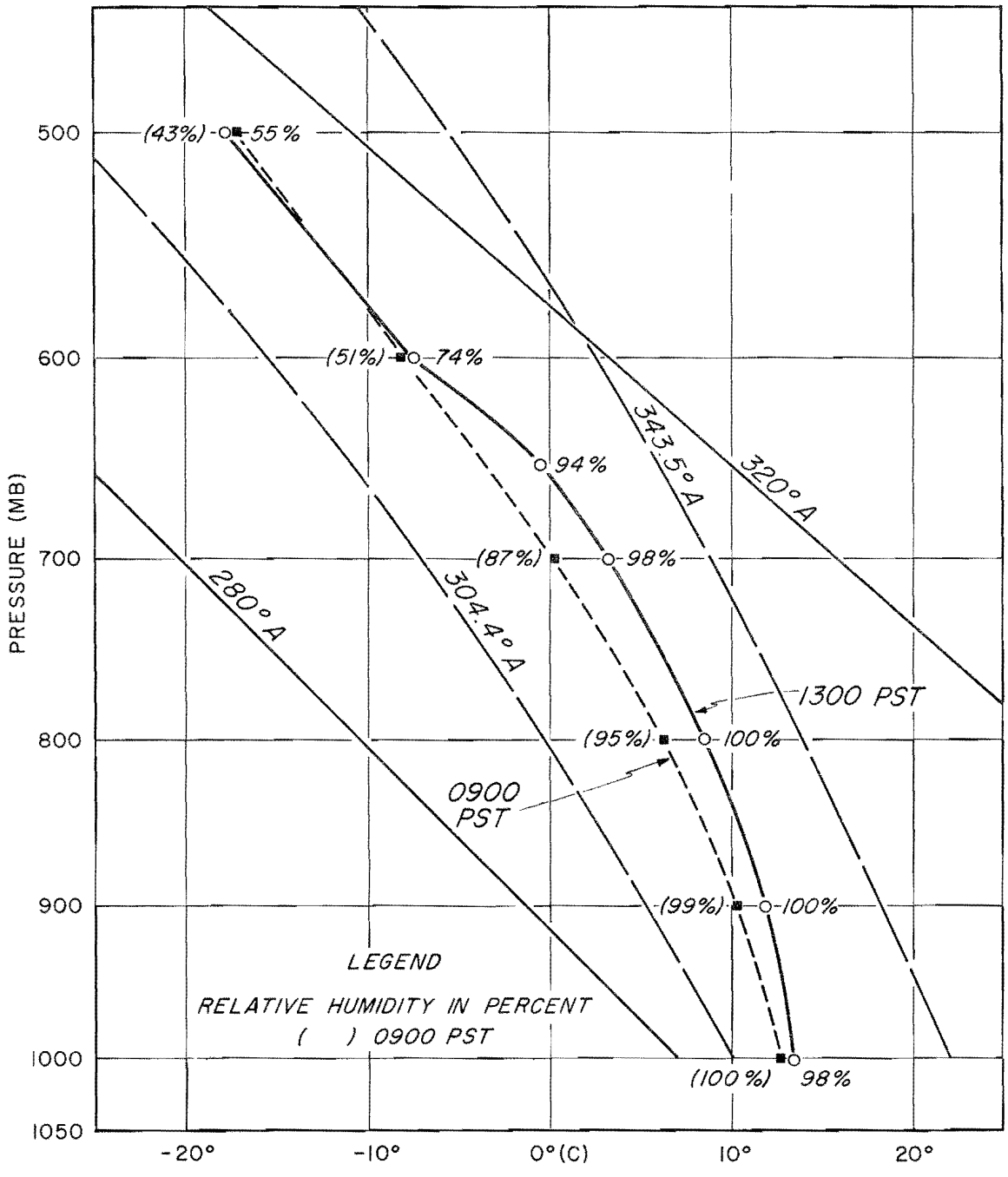

Fig. 5-15. LONG BEACH SOUNDINGS - 0900 AND 1300 PST, JANUARY 26, 1956

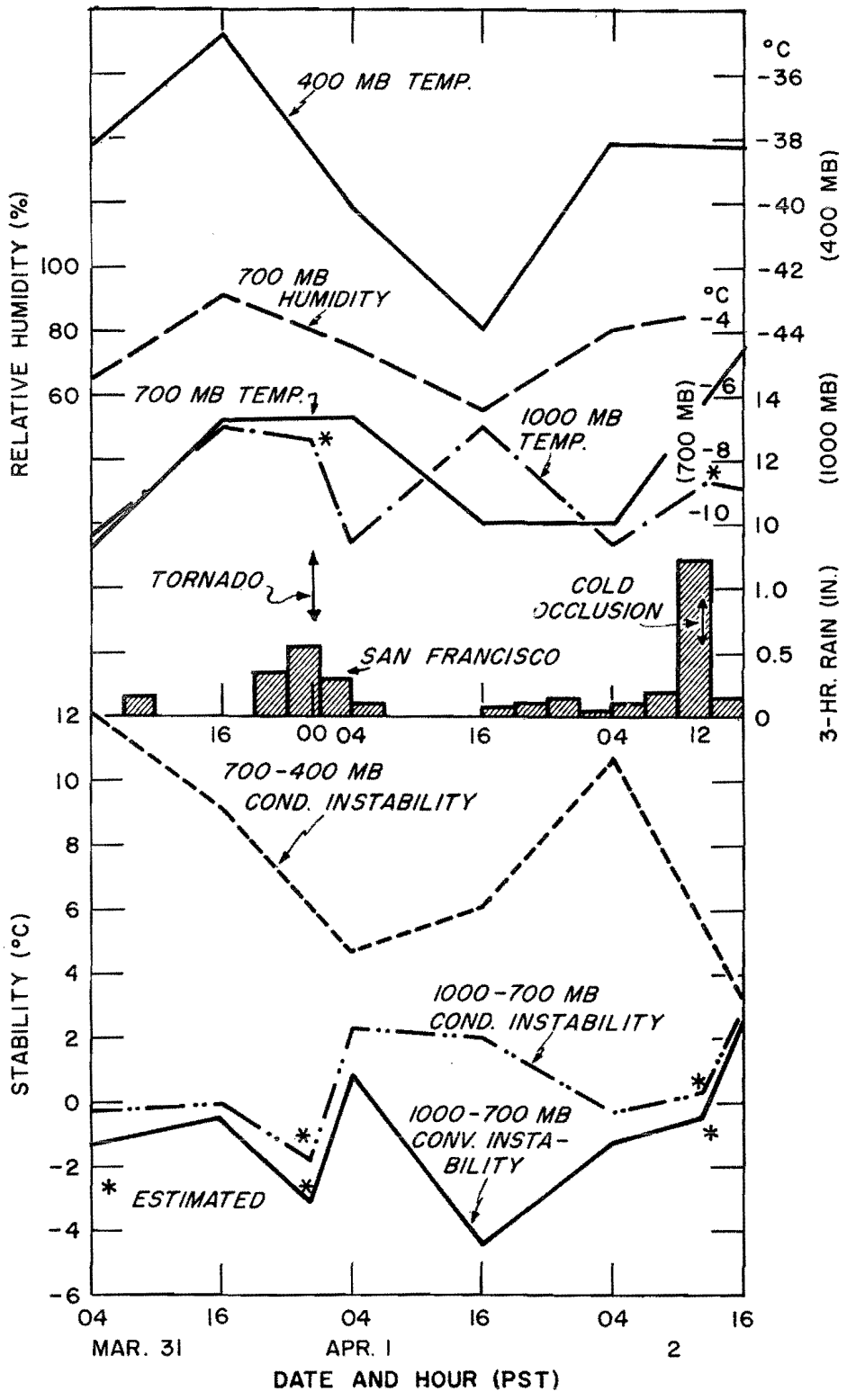

Fig. 5-16. INSTABILITY DATA, OAKLAND, MARCH 31 - APRIL 2, 1958

March 31-April 2, 1958. This period, part of the prolonged Westerly Mid-latitude type storm of March 30-April 5, 1958, is of interest from the standpoint of stability because of two unusual events (1) the occurrence of a tornado at San Francisco Airport with passage of an occlusion on the night of the 31st and (2) the extremely heavy precipitation in downtown San Francisco (.96" in one hour) with passage of an occlusion near noon of the 2d. Both suggest instability near the fronts. The 1000 to 700-mb instability values shown in figure 5-16 at these times are based on linear interpolation of 700-mb temperature in combination with the estimated 1000-mb temperature.

The tracks of the deep Lows in the Southern Gulf of Alaska, and the occlusions as they approached the coast, were essentially toward SE or ESE (figure 5-17). The more nearly direct trajectory of air from a higher latitude accounts for the crowding of temperature plots and the greater average 1000 to 700-mb instability in this storm (figure 5-16), compared to those previously discussed. Highest conditional instability value was near time of the tornado which accompanied passage of a strong cold occlusion. This front was associated with the parent Low A in figure 5-17 and the secondary Low A which later developed off the Oregon coast far to the southeast from the parent Low.

The heavy rain at San Francisco near 1200 PST April 2 occurred with passage at the surface of a strong cold occlusion, extending south-southeastward from Low B in figure 5-17. The 1000 to 700-mb conditional stability value was then near zero, lower than in storms previously discussed.

No large values of conditional instability in 100-mb layers were found in this storm; rather a uniformly steep lapse rate of temperature was more typical of the unstable periods.

December 9-11, 1937 storm. In the storm of December 9-11, 1937 average stability comparable to that in the 1950 and 1955 storms might be inferred (since upper soundings are not available) by comparison of the ratio of 3/24-hour rainfall intensity at San Francisco during the period of highest 24-hour intensity; namely .27 in this storm compared to .29 and .31 in the 1950 and 1955 storms, respectively. (Low ratio is usually indicative of absence of high local short-period intensity due to instability.)

Fairly high average stability can also be inferred from the position and orientation toward high latitude of the tracks of the deep Lows in this storm (figure 2-7, p. 11) which precluded ingress of cold polar air at any level.

December 20-21, 1866 storm. The instability characteristic of this storm, described in chapter 2-D-2, is an extreme contrast to that in the 1955 and 1950 storms. It is an example of the association of convective instability with offshore northwesterly flow. The track of the main Low brought air southeastward from a great distance, then northeastward only a short distance before entering the coast. This air was cold (and probably not very moist) above the level where a large amount of heat and moisture had been added by the ocean water during its southeastward journey. Apparently conditions for convective instability were ideal.

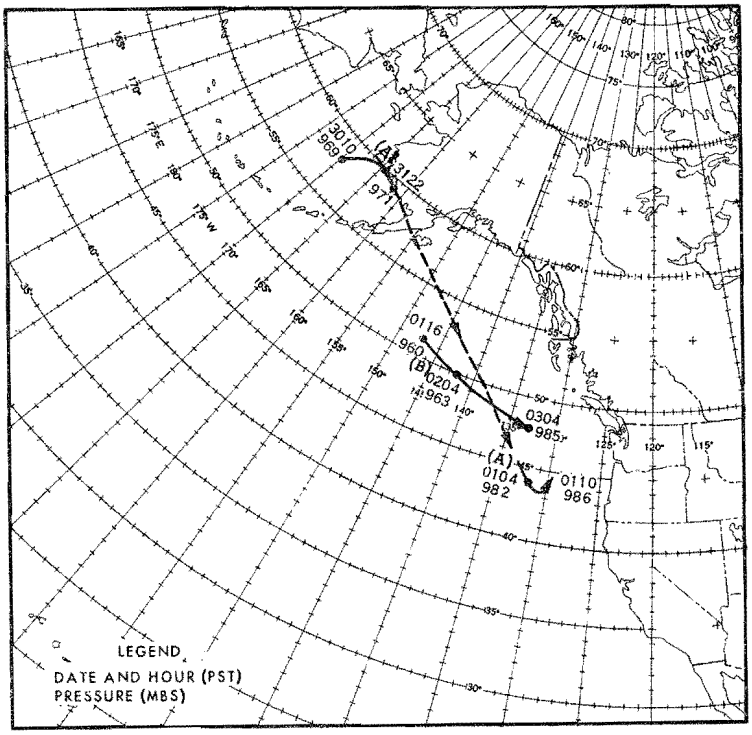

Fig. 5-17. TRACKS OF LOWS, MARCH 30-APRIL 3, 1958

5-C-5. Seasonal variation of instability

There is an apparent seasonal variation in storm type occurrence, based on major storms of record, which favors early winter occurrence of storms involving highest moisture (3-B-3) and stability, such as the Low-latitude and Southerly Mid-latitude types. Hence stability is probably somewhat more typical of air reaching the coast in major storms in early winter than in late winter. This is indirectly supported by the climatological occurrence of tornadoes, half of which are reported in March and April; also by 60-year ratio of recorded occurrence of thunderstorms to rainfall amount at San Francisco, which is high in February and April relative to other cool-season months.

Over the land surface of California, the destabilizing effect of surface heating is greatest during the initial and final weeks of the major storm season when the insolational heating during daytime periods of clearing results in greater local cumulus development than in midwinter.

5-D. RELATIVE ROLES OF CONVERGENCE PRECIPITATION MECHANISMS

Comparison of the relative roles of the three convergence precipitation mechanisms in major storms has specific application as well as general interest; for example, rainfall depth-duration-area relations depend on the

relative role of instability. The difficulties involved in comparisons are considerable; high values of different convergence mechanisms could be compared most effectively when they appear alone but they have an affinity for combination.

The bases for the following comparisons are ratios of observed precipitation to water vapor (P/M ratios), for various durations at stations relatively free from orographic effects.

5-D-1. Comparison of convergence mechanisms in storms of high 24-hour precipitation intensity

One approach to a study of the relative role of instability, frontal lifting and ageostrophic convergence is to compare the synoptic sequences involved in large 24-hour precipitation amounts. This is done below at a long-established non-orographic station, Sacramento. In table 5-5 are listed the 8 storms with highest 24-hour amounts at Sacramento since 1900 and one in 1880, along with pertinent data.

Four of the storms (1911, 1916, 1931 and 1945) involved an occluding wave approaching the coast. These are situations in which lengthy ageostrophic convergence and short-period frontal lifting are the more important factors compared to instability, except near the end of the rain sequence. In two of the storms (1955 and 1940) the more important feature in the locally heavy precipitation at Sacramento was stagnation of a front in the vicinity, although it was followed by approach of an offshore wave. San Francisco, in a less favorable position with respect to the front, received half or less the precipitation experienced at Sacramento. Ageostrophic convergence is believed to have contributed much more to 24-hour amounts in these 6 storms than did direct frontal lifting.

The January 1943 storm involved intense deepening of a Low near the coast (chapter 2-B-4). This pattern suggests strong ageostrophic convergence over a large area. Instability near the occlusion was a possible contributor to locally heavy rain. Another local effect may have been retardation of the occlusion by a strong southeast surface flow in the Central Valley to prolong the frontal precipitation at Sacramento.

The 1935 storm involved local instability precipitation in a thunderstorm at the center of a deep Low, resulting in high short-period intensity.

The apparent factors causing extreme vertical motion evident in the P/M ratio of the April 1880 storm can be surmised from the storm history as discussed in chapter 2-D-1, and are reviewed here. First, the approach of an occluded front near the time of highest 3-hour intensity resulted in convergence. Second, irregular movement of a semi-stationary Low centered on the Northern California coast resulted in strong but changing pressure gradient and thus the possibility of strong ageostrophic convergence during much of the 24-hour period. Third, converging low-level wind trajectories in the general vicinity of Sacramento between air entering through the

Table 5-5

TABULATION OF LARGE 24-HOUR RAINFALLS AT SACRAMENTO

Date	24-Hr Amount (In.)	24-Hr P/M Ratio	3/24-Hr Precip. Ratio	Max. 1-Hr S. F. Wind (mph)	Number of Fronts	
4/20-21/80*	7.24	8.6	.39	32	1	Quasi-stationary 1000-mb Low 100 miles NNW
1/13-14/11*	3.15	4.4	.17	29	1	Weak wave moves out of stagnant offshore Low
1/2-3/16*	3.18	4.0	.30	48	2	Wave in deep Low
12/26-27/31*	2.99	4.0	.17	24	3	Occlusion followed by wave
4/7/35*	3.35	3.6	.80	21	1	Thunderstorm in a deep Low
2/26-27/40	3.30	3.2	.24	34	2	Stationary front followed by occluding wave
1/20-21/43	3.52	3.3	.43	35	1	Occlusion in deepening Low
1/31-2/1/45	2.99	2.8	.26	32	3	Two occlusions followed by recently occluding wave
12/18-19/55	3.28	3.6	.25	36	3	Occlusion followed by open wave

*Not part of a major storm.
S. F. - San Francisco.

San Francisco Bay area and that flowing northward parallel to the valley floor, which was 4 to 5°F colder, provided a stationary frontal surface.

5-D-2. Comparison of convergence mechanisms during high 1- and 2-hr precipitation intensity

In table 5-6, high 1- and 2-hour intensities at San Francisco and Sacramento in 5 recent major storms are listed. All but the 1950 storm appear also in table 5-5. In the following paragraphs, the available evidence on the character of the convergence mechanisms in these short-period rainfalls is summarized in the same manner as for the 24-hour amounts in the previous section. "Burst" in the first column of the table refers to an identifiable non-frontal convergence precipitation line or area.

Table 5-6

COMPARISON OF PRECIPITATION INTENSITIES WITH SYNOPTIC PATTERNS IN FIVE MAJOR STORMS

Synoptic Pattern	Approx. Time (PST)		Highest Intensity (Inches) Hourly S.F.	Hourly Sac.	2-Hourly S.F.	2-Hourly Sac.	P/M Ratio 1-Hr	P/M Ratio 2-Hr	Representative Dew Point (°F)
December 18-19, 1955									
	Sac.								
Occlusion*	18	2300	--	.31	--	.59	.32	.61	53
Burst	19	0700	.16	.26	.27	.52			53
Cold Front	19	1300	.19	.24	.27	.43			54
*No front by San Francisco									
December 21-23, 1955									
	S.F.								
Burst (1)	22	0000	.44	.23	.66	.33	.37	.57	57
Burst (2)	22	1900	.39	.38	.68	.58			58
Burst (3)	22	2300	.38	.16	.51	.28			58
Cold Front	23	1100	.14	.30	.19	.49			59
November 18, 1950									
	S.F.								
Warm Front	0300		.34	.29	.49	.48	.26	.37	59
Burst	0900		.22	.11	.37	.17			60
February 1, 1945									
	S.F.								
Burst (1)	0000		.18	.18	.30	.27			52
Occlusion (1)	0500		.25	.26	.41	.39			54
Occlusion (2)	0900		.16	.11	.24	.22			57
Burst (2)	1700		.19	.47	.25	.62			57
Occlusion (3)	1900		.13	.18	.23	.33			57
January 20-22, 1943									
	Sac.								
Warm Front	20	0900	.25	.17	.41	.31			50
Burst	21	0200	.25	.17	.36	.31			55
Occlusion (1)	21	1200	.35	.63	.49	1.09	.56	.96	56
Occlusion (2)	22	1700	.35	.38	.48	.57			54
February 26-28, 1940									
	S.F.								
Prefrontal Burst	27	0100	.18	.25	.34	.53	.30	.47	56
Near Occlusion	27	0600	.22	.35	.24	.55			57
Occlusion	28	0500	.62	.28	.65	.44			56

S.E - San Francisco
Sac. - Sacramento

In the December 1955 storm, the 2-hour intensity of the non-frontal convergence burst near 190700 PST approached that of the occlusion on the 18th. Each of 3 bursts on the 22d was more intense at San Francisco than rainfall with the front at either station. Instability appears in some layers in table 5-4 near time of the latter two bursts of the 22d, as well as that at 190700 PST.

In the November 1950 storm the warm front rain early on the 18th exceeded in intensity any later bursts. At Sacramento, the fact that the large 2-hour amount occurred far in advance of the warm front eliminates the role of frontal lifting (chapter 5-B-1d).

On February 1, 1945 the intensity of burst (2) at Sacramento was influenced by a thunderstorm.

In the January 1943 storm, intensity was greatest near the two occlusions. It is likely that ageostrophic convergence contributed greatly because of the extreme pressure gradient about the deep moving Lows. The 1.09-inch 2-hour amount at Sacramento near the first occlusion, a record November-March value for over 50 years, suggests an instability contribution, although 5- and 10-minute intensities were less than half record values in those months.

In the February 1940 storm, fairly heavy rain occurred at Sacramento both ahead of and near the occlusion on the morning of the 27th. On the morning of the 28th local instability was evident in the higher intensity with passage of the final occlusion as .37 inches fell at San Francisco in a 10-minute period, a 55-year record for February.

Summarizing, highest hourly and 2-hourly amounts occurred with non-frontal bursts in the 1955 and 1945 storms, a warm front in the 1950 storm and with occlusions in the 1943 and 1940 storms. Instability is shown to have been a factor in these high values in the 1945 and 1940 storms and in all bursts in the 1955 storm except that at 220000 PST.

Selected 1- and 2-hour P/M ratios are listed in table 5-6. These are for high-intensity bursts not identified with instability in the preceding paragraph. The January 1943 occlusion, of unknown instability characteristic has highest ratio. But ratios of non-frontal bursts compare favorably with other front-associated ratios. This suggests that sizeable short-period convergence mechanisms occur independently of fronts even with a fairly stable lapse rate. But in making these comparisons it is acknowledged that 6-hourly raob sampling seldom furnishes adequate information to evaluate the role of instability near fronts or other areas of marked convergence; its presence there in some degree is implied by the occurrence of the heavy rain.

5-E. LIMITATIONS ON CONVERGENCE PRECIPITATION

A persisting convergence mechanism usually results in more wide-spread

but less intense rain than a short-period mechanism; conversely, short-period storms of high intensity tend to be small. These relations pose questions as to what limitations on storm area, duration and even moisture content of the air are imposed by intensity of the convergence mechanism. These are practical questions because they affect the extrapolation of the maximum observed values of convergence precipitation to hypothetical values greater than the record. Complete answers are not forthcoming from the extremely limited area in California available for study of convergence precipitation uncontaminated by orographic effects; yet trends are suggested in past storms.

5-E-1. Area limitations on convergence precipitation

Depth-area relations of convergence precipitation in California storms, though complicated by orographic contamination, are known to vary widely in differing situations. Examples are known of extremely heavy short-period instability precipitation bordering in time and/or area the main part of large-area storms. These examples display extreme concentration of intensity in a small area. One is the thunderstorm centered 7 miles north of Redding September 18, 1959, described in chapter 6-A-1, for which 6-hour isohyets are shown in the inset of figure 5-18. In contrast, small areal variation of convergence precipitation appears in some major storms where neither instability nor frontal lifting are an important part of the total in a steady flow of moist air. An example in the November 18, 1950 storm is shown in figure 5-18 by 6-hour rain at non-orographic locations.

These examples suggest what is well-known from depth-area studies for non-orographic areas of the eastern U. S., namely that isohyetal gradients of convergence precipitation are increasingly large as the contribution of instability to the convergence mechanism increases. The relatively minor contribution of instability in most areas during the main part of recent major California storms, especially those noted for high moisture transport, suggests that isohyetal gradients of convergence rain in these storms are much less than values in intense local storms. Therefore, in extrapolating individual station values of convergence rain to the convergence component of a large cool-season storm over an area (a step required, for example, in HMR 36) a relatively gradual decrease of average precipitation intensity with area is warranted. By contrast, extrapolating the largest intense local thunderstorm values in California should be accomplished with a relatively sharp decrease of average intensity with area.

5-E-2. Duration limitations on convergence precipitation

The type of the convergence mechanism and seasonal and geographic factors affect the duration of convergence precipitation. Each is discussed below.

a. Dependency on type of convergence mechanism. Shortest duration is associated with precipitation primarily due to instability, longest with ageostrophic convergence. This is illustrated by comparison of lowest and

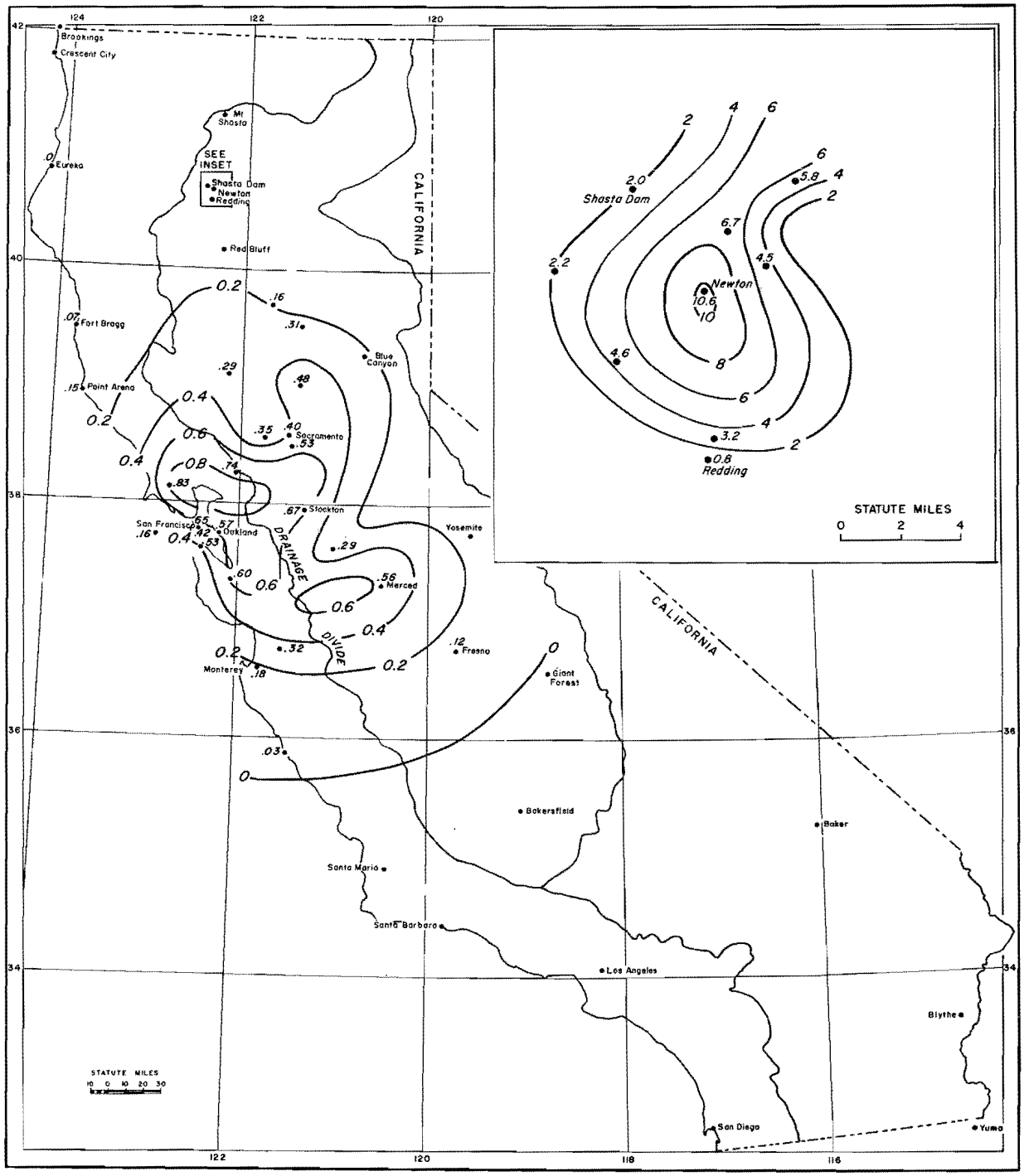

Fig. 5-18. COMPARISON OF ISOHYETS (INCHES) OF 6-HOUR CONVERGENCE RAIN, 0600-1200 PST, NOVEMBER 18, 1950 AND (INSET) ISOHYETS OF 5-HOUR RAIN NORTH OF REDDING, 1700-2200 PST, SEPTEMBER 18, 1959

highest 3/24-hour ratios of large 24-hour storms at Sacramento, listed in table 5-5. The 3/24-hour ratio is the ratio of the highest 3-hour precipitation to the 24-hour total. A low ratio indicates lengthy duration of more or less uninterrupted convergence mechanisms; a high ratio indicates intense convergence for a limited period. The following two large (though not major) storms with extremely low ratios involved persistent horizontal convergence in stable air.

A low ratio of .17 occurred with 3.15 inches in 24 hours January 13-14, 1911. This storm involved a Low which moved southward just off the coast from Washington to near Monterey, then eastward as it filled. A period of several hours of warm front rain was involved, but the more important feature at Sacramento was persistent ageostrophic convergence in connection with the moving Low. Because the track of the Low center was to the west and south of Sacramento, it is thought that fairly stable air was involved there.

On December 26-27, 1931, a storm with ratio .17 occurred with a 3.00-inch 24-hour rainfall at Sacramento. This storm was similar to the southerly Mid-latitude type major storm of December 1937 (ratio .21). A well occluded front extending out of a deep offshore Low moved north-northeastward to the west of Sacramento. It was followed quickly by a deepening wave on the trailing front along the same track, its Low center moving north-northeastward, also to the west of Sacramento. No fronts passed Sacramento until the cold front passage just prior to the end of the storm. Ageostrophic convergence associated with the deepening wave was the main mechanism accounting for the persistent rain.

The intense short-period instability storm of April 7, 1935 is in contrast to the above examples. The 3/24-hour ratio was .80 with a 24-hour amount of 3.35 inches. A wave deepened to 990 mbs as it moved east-southeastward into Nevada, the center passing slightly to the north of Sacramento. A severe thunderstorm occurred at Sacramento near the sharp cold front separating a southwest tropical flow from cold polar air from the northwest.

b. Season and geography. Trends toward longer duration of convergence precipitation in midwinter are suggested by lower precipitation ratios for various time ratios. One study of 6/24-hour convergence precipitation ratios is based on data from 21 Central California stations relatively free from orographic effects, mostly with short hourly records. Ratios for the storms containing the highest 6-hourly and highest 24-hourly amounts of record from each station were averaged in monthly groups. These values, plotted in figure 5-19, show a seasonal variation in mean ratio from .54 in midwinter to .70 in spring and fall.

A similar seasonal trend is indicated in table 5-7 which lists mean 3/24-hour precipitation ratios in storms ranking high in 24-hour amount at each of several stations with lengthy hourly precipitation records. (Some of these stations are subject to an orographic effect at times. Lower limit of 24-hour amount depends on season and station.) Average coastal winter ratios are lower than spring-fall ratios.

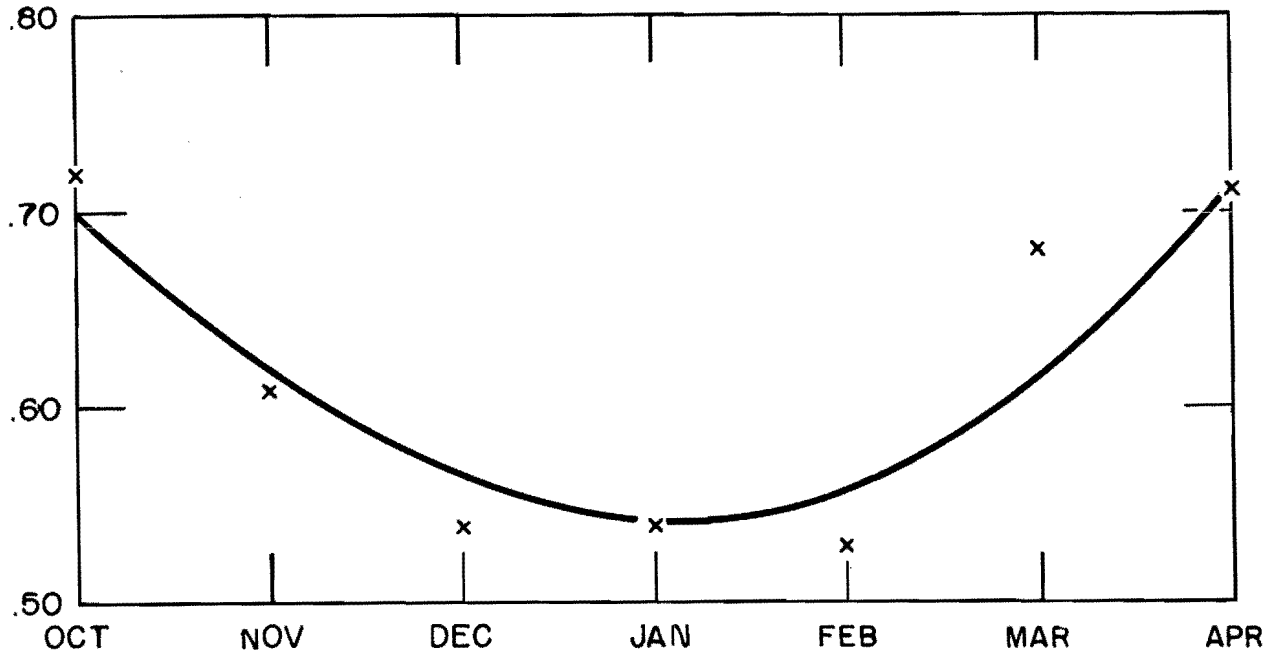

Fig. 5-19. SEASONAL VARIATION OF 6/24-HOUR RAINFALL RATIO. AVERAGE OF 21 CENTRAL VALLEY STATIONS

A geographical variation is also noted in table 5-7. Increase in ratios with lower latitude along the California coast from Eureka to San Diego suggests a decrease in duration of convergence mechanisms. In the Central Valley the lower ratios at Sacramento suggest that it is affected by a coastal stabilizing influence while Fresno and Red Bluff ratios are more representative of an inland location.

5-E-3. Highest moisture not combined with most intense convergence mechanism

Study of large 24-hour precipitation amounts at California stations relatively free of orographic effects indicates that the highest point-rainfall amounts do not depend primarily on unusually high moisture, but on the inherent convergence mechanisms that produce vertical motion, particularly instability. This is evident by the scatter of data in the plot of 24-hour rainfall against moisture during cool-season months in figure 5-20a. These data involve highest known 24-hour convergence rainfall, including such storms as the April 1880 storm at Sacramento (but not the convective storms peculiar to the Northern Sacramento Valley foothills). The convergence mechanisms in some of these storms (as measured by precipitation/moisture ratio) are large compared to those in the storms of table 3-3, p. 83 which contain high moisture. This is explained by the good correlation in winter-season storms between instability (as evidenced by thunderstorms and extreme local precipitation) and a recent offshore air trajectory from a higher latitude. Moisture content of this air is low compared to highest observed values in air reaching the coast from a low latitude.

Table 5-7

MEAN 3/24-HOUR RAINFALL RATIOS FOR LARGEST 24-HR STORMS

	Coast				
	Eureka	San Francisco	San Luis Obispo	Los Angeles	San Diego
Winter (Nov-Mar.)	.30 (32)*	.34 (30)	.35 (31)	.38 (30)	.40 (19)
Spring-Fall (Sept., Oct., Apr., May)	.40 (14)	.41 (9)	.48 (11)	.43 (7)	.50 (7)

	Central Valley		
	Red Bluff	Sacramento	Fresno
Winter (Nov.-Mar.)	.41 (16)	.26 (21)	.34 (7)
Spring-Fall (Sept., Oct., Apr., May)	.54 (11)	.50 (8)	.67 (6)

*Number of storms in parenthesis.

The conclusion from this rainfall-moisture comparison is that the rainy-season California storm with highest orographic precipitation potential has a limited convergence precipitation potential because of the restriction on instability; conversely, the storm with highest convergence precipitation potential has restricted moisture.

The contrast between the above California relation and that found in larger 24-hour point rainfalls in cool-season (Nov.-Apr.) storms of the eastern United States is seen by noting in figure 5-20b that there, high moisture and great instability (indicated by magnitude of 24-hour rain) are compatible.

5-F. COMPARISON OF CONVERGENCE AND OROGRAPHIC PRECIPITATION IN RECENT MAJOR STORMS

The native vegetation, the type of agriculture, and mean annual isohyets make the topographic control of precipitation so obvious in California that there is sometimes a tendency to regard all precipitation on windward slopes as essentially orographic in cause. Actually the normal storm processes, - the "convergence precipitation" of this chapter - make a contribution here as elsewhere. Though no absolute dichotomy exists, a survey of causes of storms would be incomplete without some assessment of the relative roles of convergence and orographic precipitation in different storms, similar to the comparison of the various convergence mechanisms in the preceding section.

Compared to orographic precipitation, convergence precipitation tends to be smaller in areal extent and subject to much wider fluctuations in intensity. Its relative contribution to totals varies considerably with major storms. There is a tendency for high values of convergence to be in the band of high moisture transport. These points are discussed below.

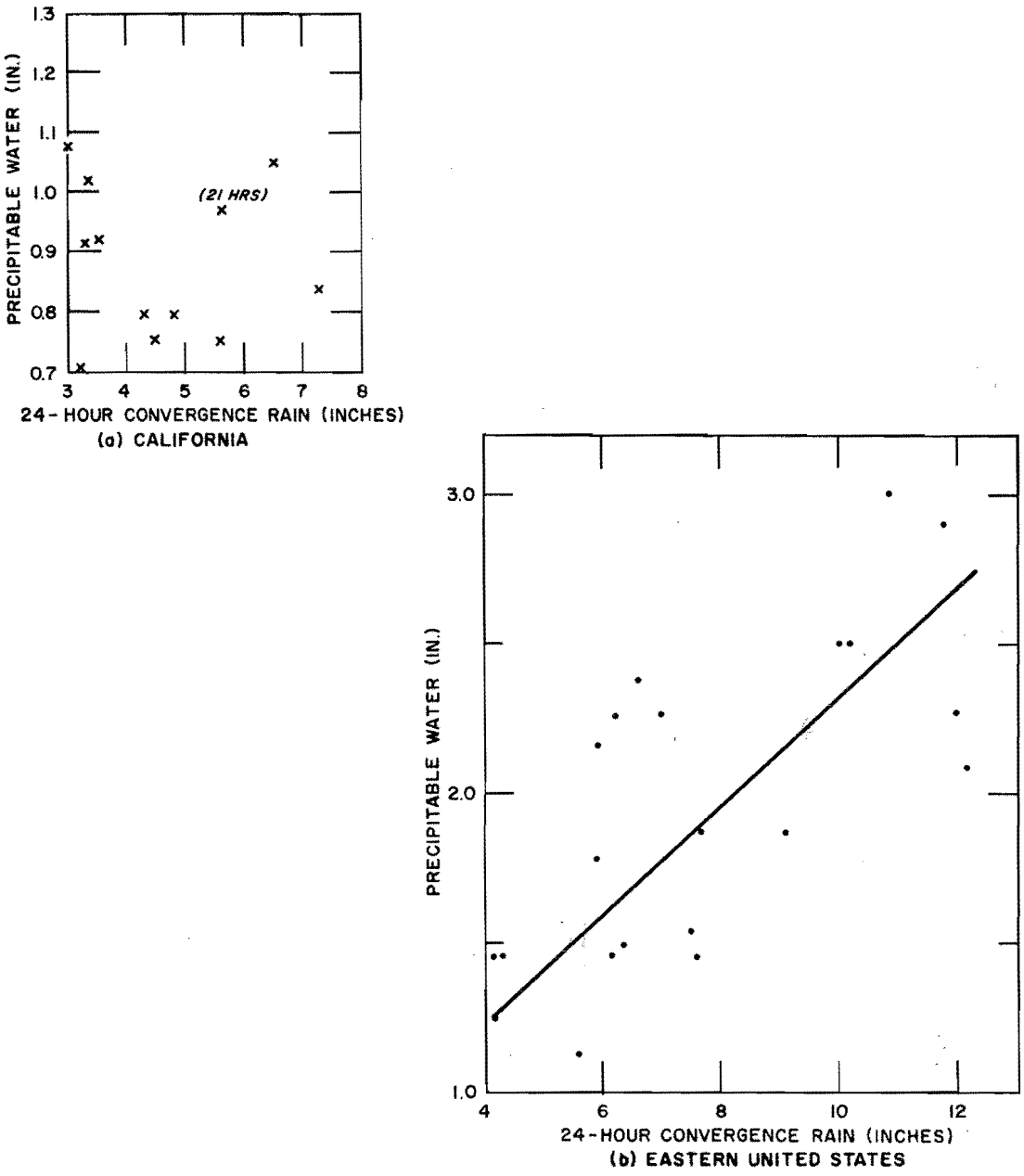

Fig. 5-20a and b. VARIATION OF LARGE 24-HOUR NOVEMBER-APRIL POINT RAINFALL VALUES WITH MOISTURE (PRECIPITABLE WATER) (a) IN CALIFORNIA AND (b) IN THE EASTERN U. S.

5-F-1. Areal limitations on convergence precipitation compared to orographic

In some major storms the band of strong winds subject to orographic lifting and well-laden with moisture covered over half of the orographic area of California during much of the storm. An example is the January 1943 storm. In contrast, the area in this moist flow subject at any given time to substantial additional vertical motion due to horizontal convergence mechanisms was of smaller size. This is evident in most major storms by the shortness of the period of significant convergence precipitation at a point resulting from a well-defined moving burst pattern in saturated air, and the limited number of such patterns effective in the storm area at a given time. Instability release not only contributes to convergence precipitation but also tends to localize it, especially in orographic areas.

The contrast in areal extent of the simultaneous convergence and orographic precipitation is less marked in the case of approach parallel to the coast of a strong occluded front. In a few major storms (as in December 1937) convergence precipitation fell at a modest rate almost continuously over a large area as a result of a cyclonic circulation of slowly fluctuating strength and position.

5-F-2. Comparison of orographic and convergence precipitation time-intensity graphs in recent storms

High values of wind and moisture, parameters of orographic precipitation, tend to occur in that part of a storm when the various other factors in the storm itself which cause convergence precipitation are most pronounced. This relation is seen in figure 3-2, p. 76 with respect to actual windspeeds and periods of convergence precipitation at Oakland in the December 1955 storm. Highest windspeeds occurred during the heavy rain periods on the nights of the 18th, 21st and 22d. It is seen with respect to geostrophic winds and moisture for recent major storms in figures 3-3a to 3-3e, pp. 77 to 79. Comparison of times of high windspeed and high moisture with convergence rain indicates general agreement.

Intensity of convergence precipitation usually has greater fluctuation over short periods of time than does orographic precipitation. Whereas moisture transport and orographic precipitation over an area increase and recede gradually over a period of several hours, convergence precipitation bursts of large enough areal extent to be subject to synoptic analysis tend to have a somewhat shorter effect at a particular location. This conclusion is drawn from the following comparison in selected storms of a time-intensity graph at an essentially non-orographic station with a similar graph from a nearby mountain station whose precipitation is predominantly orographic.

a. November 1950 storm. An example of a particularly simple orographic precipitation time-intensity variation is found in the main part of the November 1950 storm in the south-central Sierras, as illustrated in figure

5-21 by the graph for Wawona (elevation 3960 feet), where rainfall was primarily orographic. There was a rather broad peak in intensity on the afternoon of the 18th following a gradual rise, then a more abrupt fall during the night. The individual burst patterns of convergence rain are numbered above the Wawona graph and the graph of Merced, upwind of Wawona in the Central Valley. (These numbers identify precipitation lines traced across a broad area of the storm.) Figure 5-21 illustrates the relative time scale involved in variation in the two types of precipitation. It indicates the relative unimportance in this storm of the convergence precipitation at higher elevations compared to orographic precipitation at those elevations and to the convergence precipitation at upwind Valley stations. Pertinent to this relation was the lack of instability in this storm.

b. December 1955 storm. Time-intensity graphs over Central California December 21-23, 1955 were complicated by greater fluctuation in both orographic and convergence precipitation intensity than in the 1950 storm. The main convergence bursts of the storm occurred in the strong moist flow south of the frontal systems.

The trend toward simultaneous occurrence (allowing for travel time) of peak convergence precipitation at a Valley station and combined convergence precipitation at a downwind mountain station is seen in the time-intensity plots of figure 5-22 for Sacramento and Blue Canyon (elevation 5280 feet). The main peaks in rainfall at Blue Canyon on the nights of the 21st and 22d were related respectively to the two periods of strong moist flow described in chapter 2-B-1. (Burst (2) did not extend as far to the northeast as Blue Canyon; in that area a sharp peak was centered about time of highest moisture transport. The peak near 1200 PST on December 23 preceded passage of the polar front.) This association suggests control of the main broad Blue Canyon precipitation peaks by moisture transport and thus by the orographic precipitation contribution. This leads to the conclusion that the convergence and orographic component peaks were more or less simultaneous.

Whereas the convergence precipitation contribution in the 1950 storm appears to have been depleted with elevation, in the 1955 storm it appears to have been magnified at times by greater release of instability in mountain areas than upwind and perhaps by more direct upslope flow under less stable conditions (chapter 4-B-3). This magnifying effect is suggested in the coastal mountains in figure 5-23 by comparison of intensity at San Francisco and Boulder Creek (elevation 2200 feet 45 miles to the south), particularly with burst (4) near 2000 PST, December 22. It is supported by lightning reports in that area at the time and the convective instability value in the 900 to 700-mb layer shown in the 2000 PST Oakland sounding (table 5-4).

The sharpness of rainfall intensity fluctuation in pronounced bursts, especially those involving instability, appears to be increased by depletion, through divergence, of the orographic component just prior to and/or following the burst. For example, rainfall was negligible at Boulder Creek just prior to and following burst (4). A study of winds and weather maps shows that the fluctuation in lifting of moist air during this sequence was less

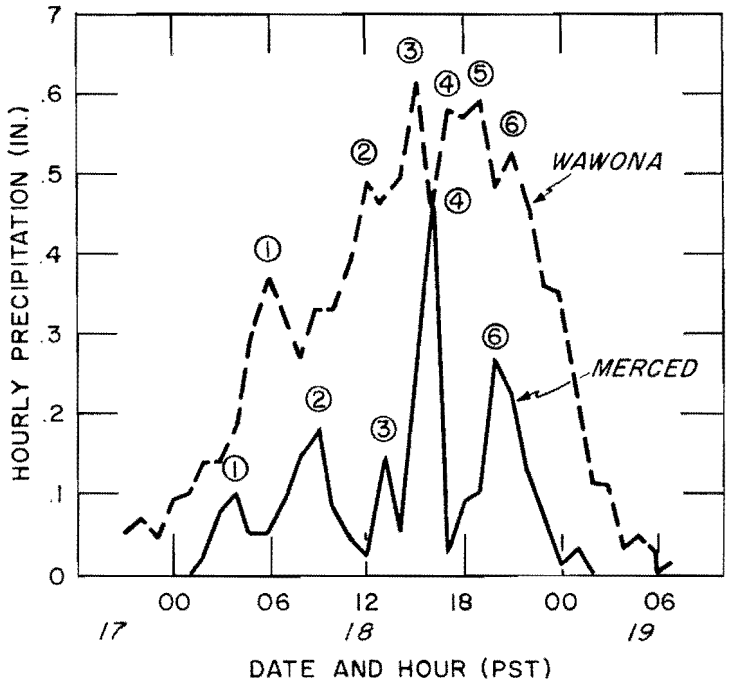

Fig. 5-21. TIME-INTENSITY GRAPHS - NOVEMBER 17-19, 1950. CIRCLED NUMBERS IDENTIFY BURSTS

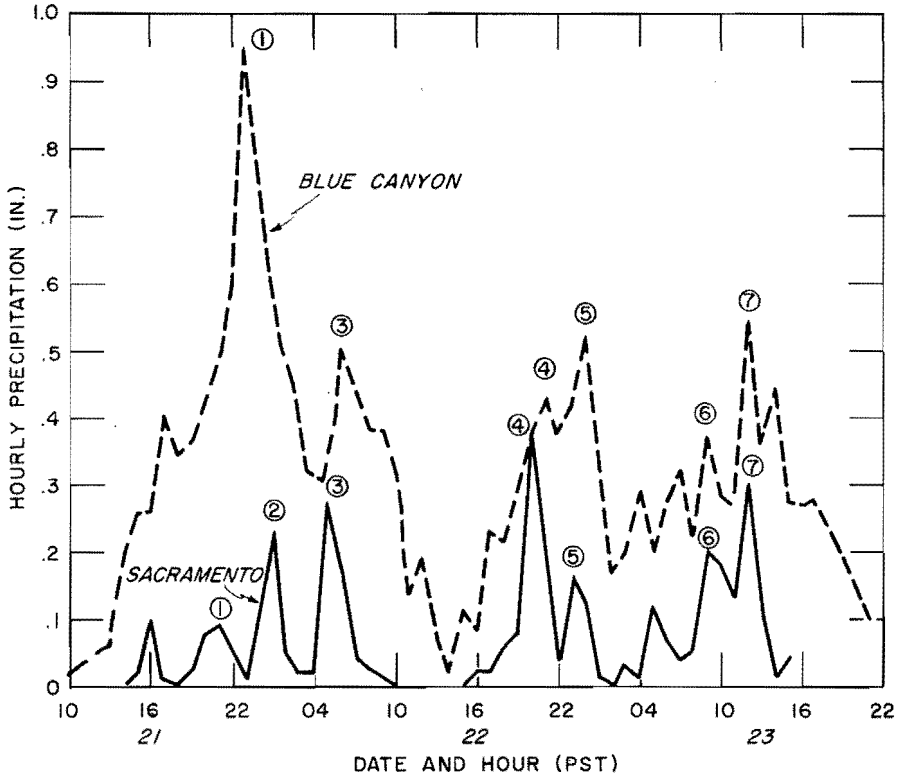

Fig. 5-22. SIERRA TIME-INTENSITY GRAPHS - DECEMBER 1955

than that of rainfall intensity. It appears that divergence resulted in sufficient downward motion to partially offset at times the orographically-induced upslope motion, thus reducing the net precipitation for short periods.

c. January 30-February 2, 1945. The intensity graphs in this storm, illustrated by those from San Francisco (City), Boulder Creek, Merced and Wawona, are shown in figure 5-24. The symbol "F" indicates time of passage of occluded fronts at San Francisco and Merced; passage at the downwind mountain station was slightly later.

The amplitude of intensity fluctuation was less extreme in this storm than in the December 1955 storm. This is attributed partly to a less marked concentration of effects of instability in this storm. The two broad peaks in precipitation in the Wawona graph, centered about the morning and night of February 1, suggest a predominance of orographic precipitation there,

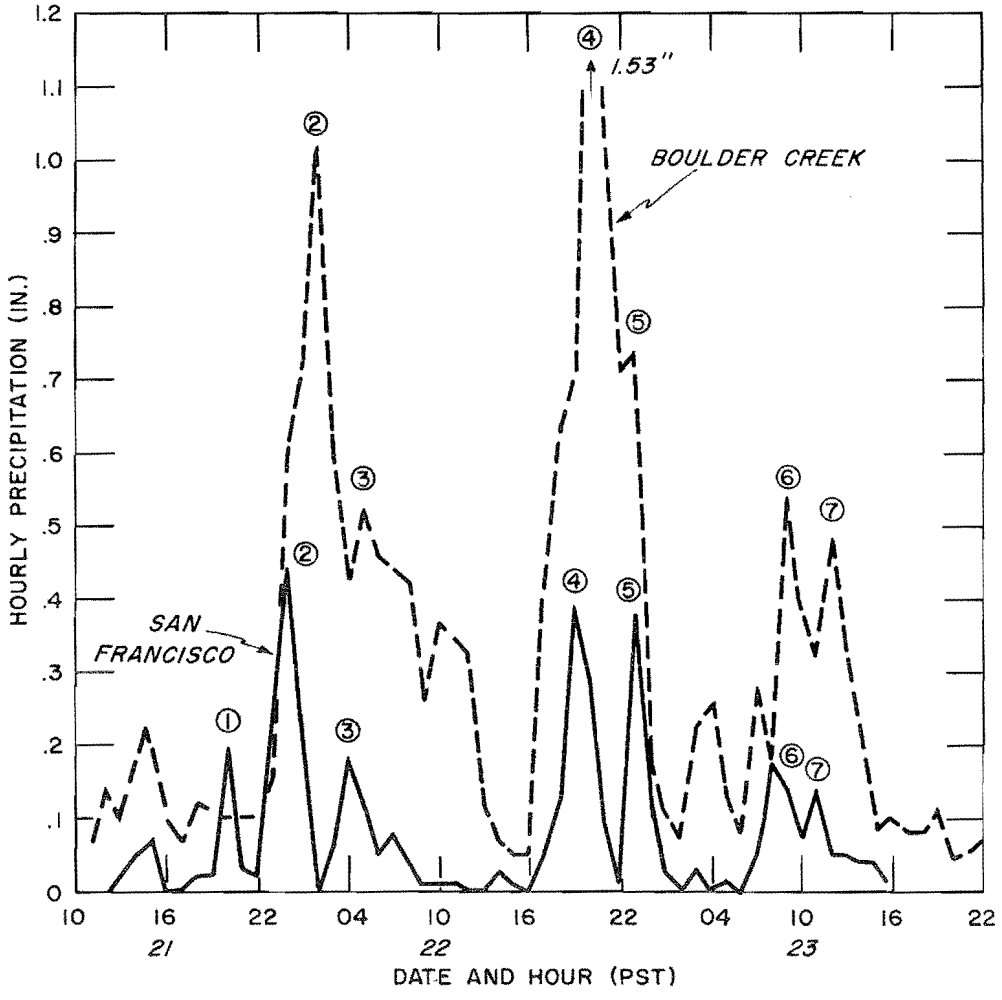

Fig. 5-23. COASTAL TIME-INTENSITY GRAPHS - DECEMBER 1955

with no intense short-period instability contributions. (The latter is suggested also by the Merced curve.) The coastal orographic precipitation less clearly dominates the Boulder Creek graph, centered around the same two peaks; in it there is more evidence of short-period convergence-produced fluctuations in intensity, including those associated with occluded fronts, fluctuations apparent also in the San Francisco graph.

The above comparison of the nature of the precipitation components in the Wawona and Boulder Creek graphs is intended to show that depletion of frontal-associated convergence rain by the effect of the coastal mountains limits in the maximum storm the convergence precipitation potential of foothill windward Sierra slopes not accessible to direct low-level flow from the coast, as compared to the potential at the same elevation on coastal windward slopes. This applies to most of the San Joaquin foothills and to a lesser extent in the Northern Sacramento Valley.

5-F-3. Comparison of orographic with convergence precipitation contribution to storm totals in recent storms

The importance of convergence precipitation relative to orographic precipitation in a major storm may be estimated in a general way by comparing the storm totals at Central Valley stations with those at downwind Sierra stations, and coastal with downwind (or nearby) coastal mountain stations. (The main source of error in such a comparison is the unknown convergence component at the mountain station. In coastal comparisons there is also the likelihood of some orographic component in the coastal station precipitation. Because of the smaller elevation difference and less definite topographic variations, the coastal comparisons are in general less reliable than inland comparisons as an index to convergence/orographic precipitation.)

Table 5-8 presents storm precipitation ratios of coastal to nearby mountain stations and of Central Valley to downwind Sierra stations in recent storms. Also shown is the elevation difference between stations in each pair. Station locations are shown in figure 5-25.

Sierra ratios averaged a little higher in the 1955 and 1945 storms than in the 1950 and 1943 storms, possibly because of weakness of the 1950 storm convergence mechanisms in a pressure field devoid of large pressure gradient fluctuations, and the enhancement of the 1943 storm orographic precipitation by strong and persistent gradients.

The ratios for the 1945 storm averaged less on the coast and no more inland than in the 1955 storm, despite the much greater frequency of frontal passages in the 1945 storm. Such a comparison points up the fact that the number of fronts involved in a major storm is not a reliable indication of the convergence precipitation potential in the storm. This is particularly true of storms similar to the 1945 storm in which most of the occlusions have little temperature contrast or wind shift across them as they move out of the main offshore trough. The above statement is especially applicable to areas reached by these fronts only after suffering the modifying effects of an upwind barrier.

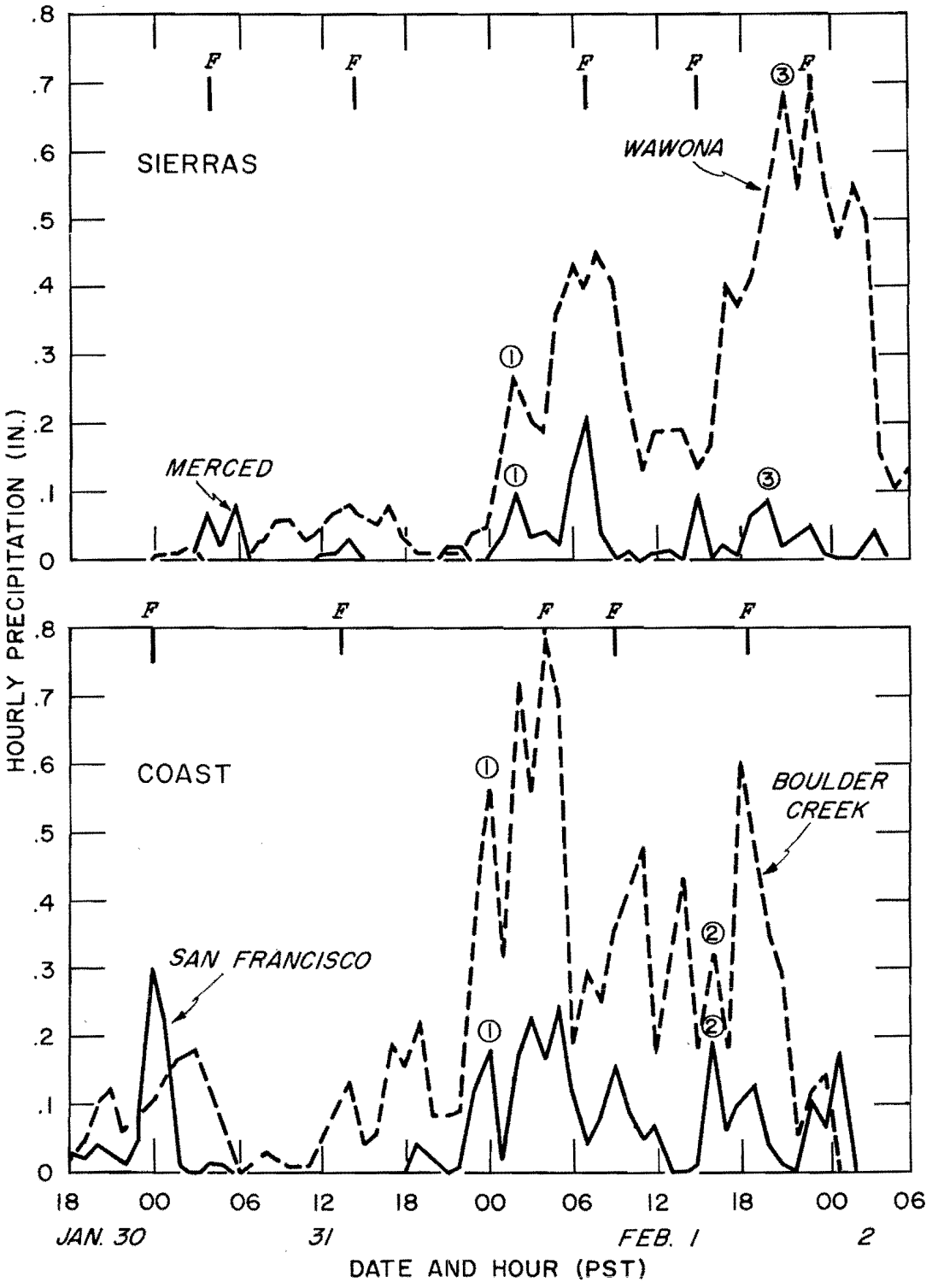

Fig. 5-24. TIME-INTENSITY GRAPHS JANUARY - FEBRUARY 1945

Table 5-8

RATIO OF STORM TOTAL PRECIPITATION AT LOW ELEVATION STATION TO THAT AT NEARBY OR DOWNWIND MOUNTAIN STATION

Sierra	Dec. 1955	Nov. 1950	Jan.-Feb. 1945	Jan. 1943	Feb. 1940	Elevation Difference (ft)
Oroville/Brush Cr.	.34	.25	.33	.30	--	3260
Sacramento/Grizzly Flat	.31	.28	.53	.39	--	3900
Stockton/Calaveras R. S.	.28	.23	.32	--	--	3400
Merced/Wawona-Yosemite	.30	.27	.18	.11	.23	3800
Fresno/Giant Forest	--	.08	.14	.06	.21	6250
Average	.31	.26	.30	.22	--	
Coastal						
San Francisco/Mt. Tamalpais	.57	.42	.44	.39	--	900
Morgan Hill (SCS)/Highland	.54	.24	--	--	--	1150
Hollister/Stayton Mine	.65	.28	.57	.57	--	2750
Average	.59	.31	.50	.53	--	

5-F-4. Comparison of areal location of highest convergence and orographic precipitation in recent storms

The data in table 5-8 for inland stations shows for each storm rather consistent values between stations, with a few exceptions. This consistency implies that the areas of convergence precipitation were generally rather well centered with respect to the areas of downwind orographic precipitation.

A radical fluctuation from one pair of stations to the next, not apparent in other storms, implies an areal displacement, north or south, of one component relative to the other (assuming that the station data are representative of an area). An example of a northward displacement of the area of highest convergence rain in the Central Valley with respect to the area of highest orographic precipitation downwind is seen in the much higher ratio in table 5-8 in the 1945 storm for Sacramento/Grizzly Flat (.53) than for Merced/Wawona-Yosemite (.18). The Merced/Sacramento ratio was only .44 compared to the normal seasonal precipitation ratio of .64 while the downwind mountain ratio Wawona-Yosemite/Grizzly Flat was 1.36 compared to the normal seasonal ratio of .88. This comparison to normal seasonal precipitation values, borne out by data from other stations, illustrates in this storm a relative northward placement of convergence rain in the Valley in comparison to the orographic precipitation downwind. Table 5-8 suggests a similar but less marked displacement in the 1943 storm. In the 1945 storm the heavier rainfall to the north in the Central Valley reflects at Merced dampening of the effect of several frontal trough passages by coastal

mountains upwind, and at Sacramento development of a surface Low to the northwest on the afternoon of February 1. In the Sierras the greater storm totals to the south reflect the longer duration and higher intensity there with the final deepening wave of the storm, as shown in the Wawona plot of figure 5-24.

There is basis in chapter III for the conclusion that in the optimum storm the band of high moisture transport has a degree of both persistence and stability of position which concentrates storm orographic precipitation totals. To this is added the conclusion that convergence precipitation characteristic of this storm may be centered within this band and that the most intense convergence precipitation may occur simultaneously with that of orographic precipitation.

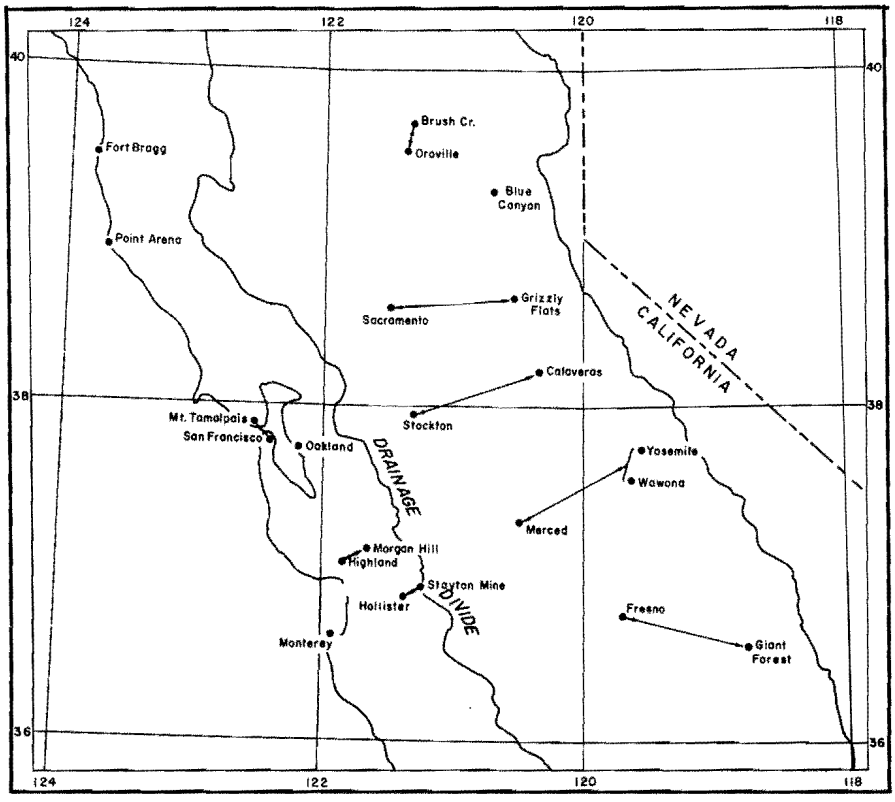

Fig. 5-25. LOCATION OF STATION PAIRS IN TABLE 5-8

Chapter VI

CONVECTIVE AND TROPICAL STORMS

This chapter describes and gives examples of three types of hydrologically critical storms that do not fall into the cool-season, large-area classification of chapter II. Extreme local intensity is the significant characteristic of the first two types, and sometimes also characterizes the third type, tropical storms.

6-A. NORTHERN SACRAMENTO VALLEY FOOTHILL STORMS

Topographic factors appear to be especially favorable to occurrence of intense local storms, sometimes as part of general storms, in the foothills at the head of the Sacramento Valley. The fact that those described here occurred in the months of May and September suggests seasonal controls which favored months bordering the cool season both when vigorous Pacific storms are possible and when inland warm-season modifying factors are prevalent. But the topographic controls seem to be paramount. For there is evidence that unusual local intensification of precipitation occurs in this area also in the winter. An example is the report of heavy local convergence precipitation in the Shasta Lake region on December 20, 1955 during the lull between the two main storm periods.

6-A-1. The Newton storm of September 1959

This storm is of particular interest, both because of the record local short-period intensity for Northern California centered at Newton north of Redding, and because of record or near-record rainfall for September in most areas of Northern and Central California.

The general storm. This was a cool-season storm, early for the season, of 1 to 2 day's duration. The main storm sequence can be visualized from figure 6-1. A Low deepened as it moved east-southeastward across the Southern Gulf of Alaska, stagnating off the Washington coast on the 18th. The strong occluded front continued inland passing through Northern California during the morning. By late afternoon it extended southwestward from Idaho across Central California, as shown. Except for the locally intense center near Newton, most of the storm rainfall in Northern California had fallen by then, having been centered ahead of time of frontal passage.

Storm isohyets are shown in figure 6-2. An orographic effect is seen in the rainfall centers in the Northern and Central Sierras and coastal mountains. One is in the coastal mountains north of Monterey Bay; there 13.6 inches in 30 hours at Boulder Creek approaches highest 30-hour intensity in the December 1955 storm when a 20-year record 24-hour amount fell.

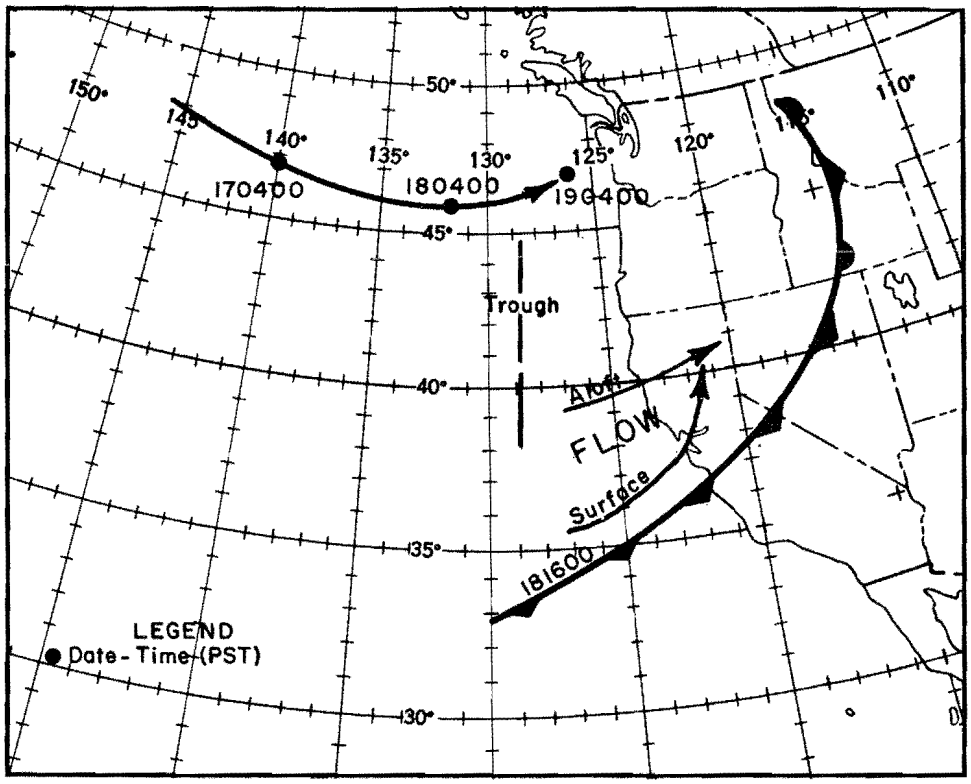

Fig. 6-1. LOW TRACK AND FRONTAL POSITION IN SEPTEMBER 18, 1959 NEWTON STORM

Convergence rainfall in this storm was an unusually important part of the total. Ratio of low-level to downwind Sierra rainfall was twice that of the average of 4 major storms listed in table 5-8. The rainfall center north of Monterey Bay is believed to include considerable convergence rain, judging from the large amounts at nearby low-level locations.

The local storm. The deep offshore trough behind the front remained stationary into the 19th, with unstable polar air entering the coast from this trough. This post-frontal flow was strong southerly in the lower layers through the Sacramento Valley from the San Francisco Bay region but was southwesterly at upper levels. It was in this flow that the local storm center north of Redding occurred during the evening of the 18th. This isohyetal center is reproduced on an enlarged scale in figure 5-18 for the more intense period of rainfall only, 1700-2200 PST. For this 5-hour period, a 10-inch center is shown near Newton. (Newton is at an elevation of 700 feet. Since the Newton gage was not a recorder, the 10.6-inch value for the 5-hour period was obtained by subtraction from the storm total the amounts indicated there on isohyetal maps for contiguous periods. The isohyetal patterns were simple on these maps, permitting good approximations for the 5-hour period.)

The magnitude of the convergence mechanism at Newton for this 5-hour period, in terms of P/M ratio, far exceeds that for a comparable time period

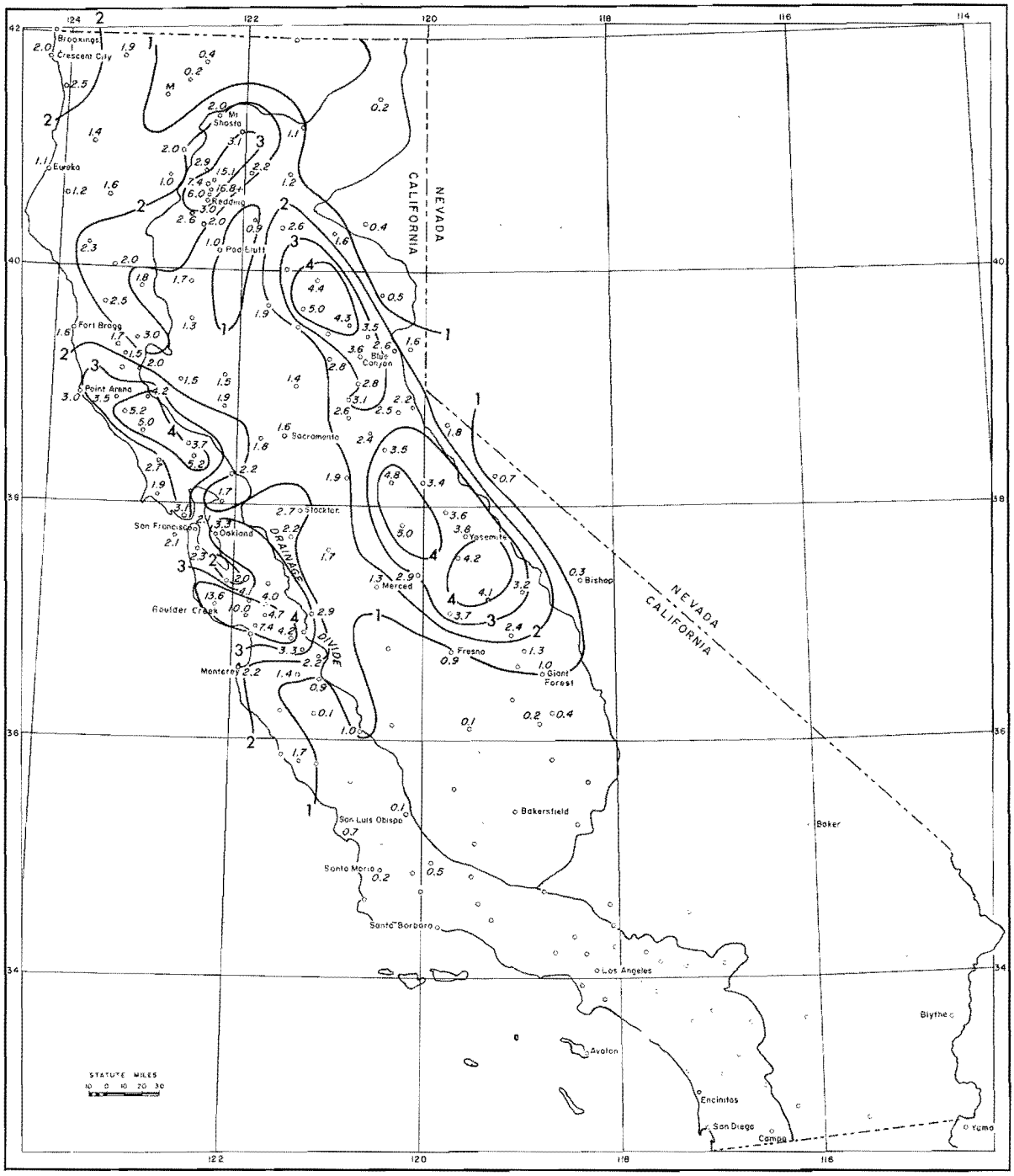

Fig. 6-2. STORM ISOHYETS (INCHES) - SEPTEMBER 17-19, 1959

in any cool-season storm shown in figure 4-8 of HMR 36. The relative importance of factors involved in such a tremendous convective development is obscure. Conditional instability values, as defined in chapter V, were close to zero on the 1600 PST soundings at Oakland and Merced, Calif. and Medford, Ore. Scanty rainfall at stations in the Trinity Mountains to the west during and prior to this period indicates that lifting of the southwest onshore flow was not sufficient for appreciable release of instability there. Probably a necessary additional factor to the observed release over Newton was the superimposing of this upper flow upon a southerly moist flow at the head of the valley in such a manner as to develop instability not shown at the raob stations. The latter flow was potentially warmer because of its source at a lower latitude and because of surface warming in transit northward up the valley during the afternoon. It was lifted both by elevation rise and constriction of valley width.

It is believed that stability of position of the convective area near the center of the valley, contributing to lengthy duration of convective development in one area, was the result of constancy of position of the low-level inflow afforded by the terrain. The center of this downpour seems to have favored the western side of the valley at first and later moved with the upper flow slightly toward east-northeast, since rainfall at Shasta Dam was mostly at the beginning of this period.

6-A-2. The Kennet storm of May 9, 1915

This storm was in most respects typical of a cool-season storm, unusually severe for so late in the season. Rainfall accompanying the two frontal systems shown in figure 6-3 was heavy in Northern California mountain areas. The 4-day totals beginning on the 9th were 5 to 10 inches generally in the Northern Sierras and 12 inches or more on some southward-facing slopes. Sacramento Valley and Northern Coastal amounts were 1 to 3 inches generally with highest amounts to the north. Amounts were more or less evenly divided between the two rain periods which merged in mountain areas.

A fairly strong pressure gradient accompanied the first frontal passage in the Sacramento Valley on the 9th; 1000-mb dew point was 57°F. Rain spread over Northern California and northern Nevada with approach of this front whose position in figure 6-3 is that at the time of the heavy rain at Kennet. (The Kennet site was 11 miles north of Redding at an elevation of 730 feet; it has since been submerged by Shasta Lake.)

The local convective storm at Kennet was an integral part of the general storm of that date. Heavy rain preceding the front began at Kennet about noon, reaching an intensity of 2.20 inches per hour near 6 p.m. with 8.25 inches having fallen in 8 hours to 8 p.m. The localization of intensity in that area is apparent; Kennet had 9 inches in 24 hours compared with 1.3 inches at Redding in the same period. It is verified by reports of extreme damage to railroad right-of-way downstream from Kennet.

Development of the local storm is thought to have been aided by juxtaposition of contrasting airflows even more than in the Newton storm. This would have been brought about by the typical continuance of the low-level southerly flow into the head of the valley after passage of the front aloft had brought potentially cooler air across the Trinity Mountains and over this flow. Lifting of the surface flow by elevation and constriction of valley width, along with lifting of the flow above by the Trinitys, were also probable factors in release of instability.

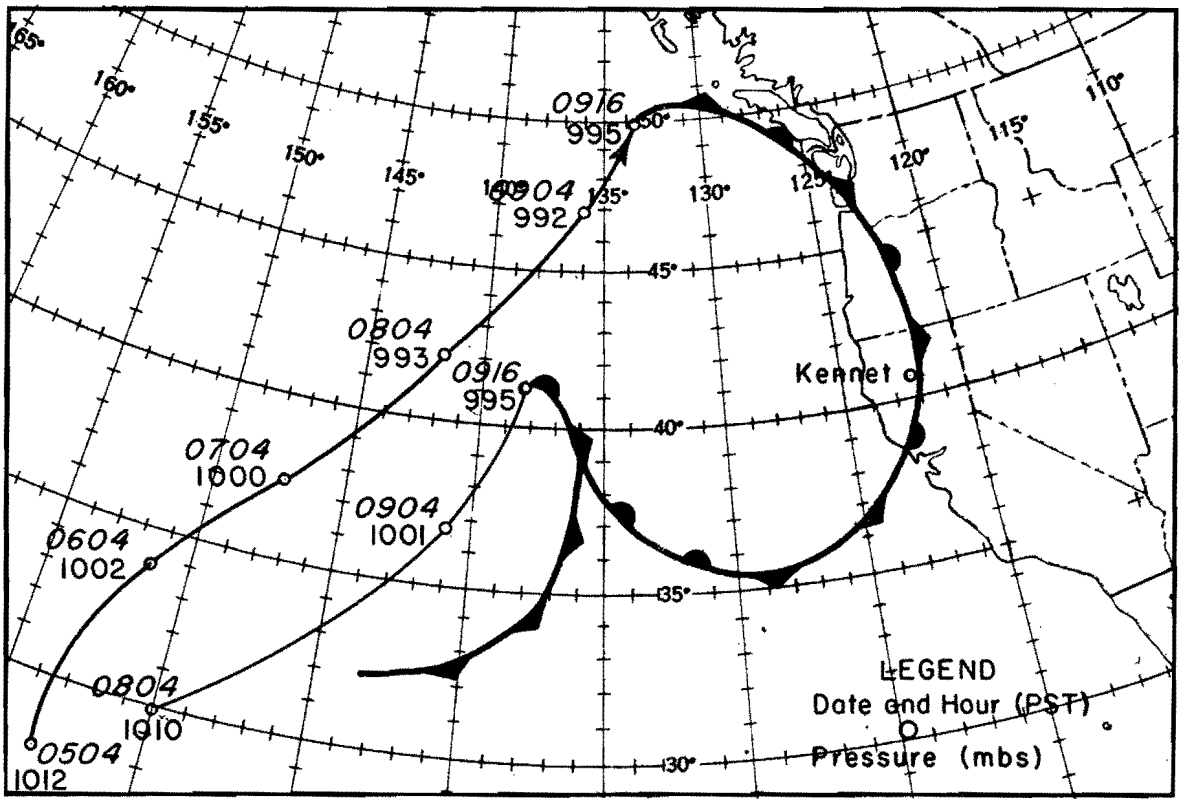

Fig. 6-3. TRACKS OF LOWS PRIOR TO AND FRONTAL POSITIONS AT HEIGHT OF KENNET STORM OF MAY 9, 1915

6-B. STORMS INVOLVING AIR FROM THE GULF OF MEXICO

Intense short-period local convective storms in a flow from the Gulf of Mexico occur in summer or early fall and are more frequent in mountain and desert areas of Southern California than farther north or west. Although the Sierras occasionally experience such storms, particularly on the eastern slopes, records of intense storms are extremely scanty. An unconfirmed report of over 8 inches in a little over 2 hours on July 19, 1955 in a portable

rain gage near the crest of the White Mountains northeast of Bishop is an example of such a storm in the area just east of the Sierras (16).

These storms are of interest primarily for their heavy short-period local rainfall. Their moisture source, similar to that of midwest storms, excludes their use as prototypes of cool-season short-period rainfall potential. Two such storms, described briefly below, are outstanding because of their high intensity.

6-B-1. The Campo storm of August 12, 1891

This storm occurred in the mountains near the Mexican border (see figure 6-2 for location). The reader is referred to a rather complete and graphic description in U. S. Weather Bureau Technical Paper No. 38, page 48 (17). The 11.5 inches reported in 80 minutes is considered valid. No other comparable intensity has been reported in California. The description emphasizes the merging of two intense thunderstorm cells.

6-B-2. The Encinitas storm of October 12, 1889

This storm occurred on the coast 25 miles north of San Diego. Date of occurrence was late for storms of this type. The thermal Low, typical of summer months, was present over southeastern California on the 10th and 11th; it extended northward through the Central Valley and western Oregon on the 12th, as is often the case when Gulf of Mexico air reaches California.

The intense thunderstorm at Encinitas on the evening of the 12th presumably developed as a local cell in the southeasterly flow over the coastal mountains to the east. In 8 hours, 7.58 inches of rain were measured; only .44 inch fell at San Diego and .04 inch at Los Angeles on that date. The effect of the upwind coastal range in development of the cell was probably important; but the direct orographic contribution to rainfall was probably negligible in view of the light pressure gradient and the location of Encinitas at the coast.

6-C. TROPICAL STORMS

With few exceptions, tropical storms approaching middle latitudes from off the Mexican coast turn westward, veer northeastward across northwestern Mexico, or dissipate offshore due to loss of an energy source over a relatively cold ocean surface. Only a very few of these storms enter California. Certain considerations limit the rainfall potential of tropical storms in California relative to tropical storms elsewhere and to some cool-season storms in California, as outlined in paragraph 3.32 of HMR 36. These limitations apply primarily to orographic precipitation as it is related to low-level moisture and wind. California tropical storm history reveals extremely few storms reaching the coast with a strong low-level circulation (and none with extreme winds). One such storm is discussed below. A few have passed

across California as an upper circulation; they are identifiable mainly by their precipitation pattern which, though largely convergent, is centered in mountain areas. Two of these storms are discussed below. The three storm tracks are compared in figure 6-4.

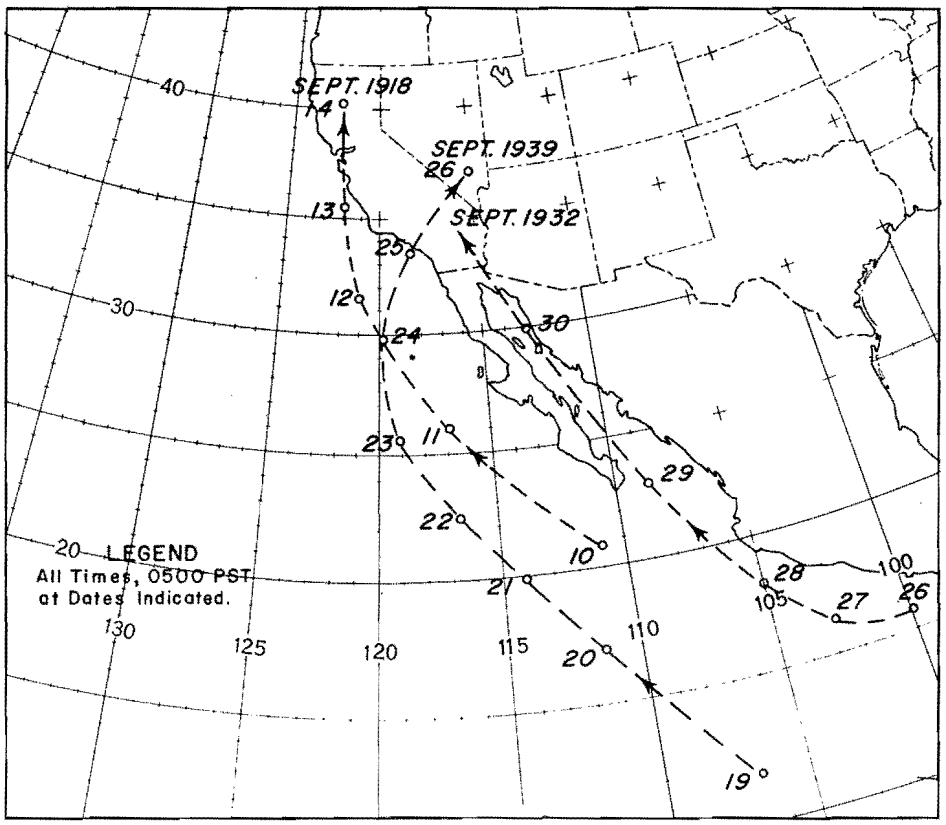

Fig. 6-4. TRACKS OF 3 TROPICAL STORMS

6-C-1. The Southern California tropical storm of September 25, 1939

This was a violent storm in its early offshore history. On the morning of September 22, while west of the southern tip of Baja California, winds of 60 knots and barometer 971 mb were reported near its center. Its offshore track from that point was parallel to the coast (figure 6-4). This track was made possible by a strong ridge over the western United States and another offshore, separated by an elongated inverted trough extending along the coast both at the surface and aloft. This trough persisted from the 19th through the 23d, resulting in extremely high coastal and coastal mountain temperatures in Southern and Central California.

By the 24th, the ridge over the west had weakened, allowing the storm to veer toward NNE and then toward northeast as it approached the Southern California coast. Windspeed at San Pedro reached 37 knots before the 998-mb Low center entered the coast in that vicinity about 0800 PST on the morning

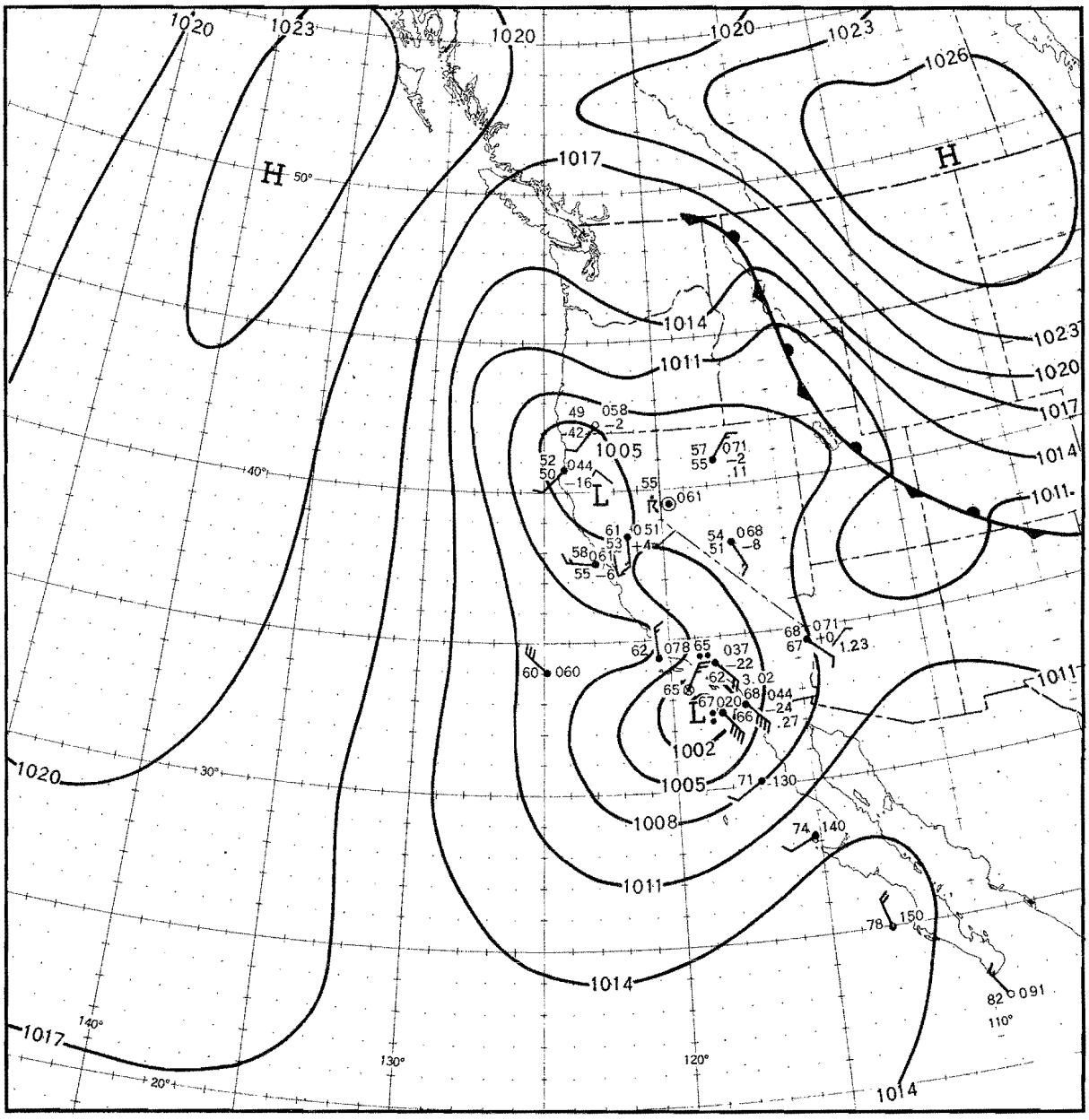

Fig. 6-5. TROPICAL STORM NEAR LOS ANGELES - 0500 PST, SEPTEMBER 25, 1939

of the 25th (figure 6-5). Damage in the area was estimated at $1,500,000, largely from wave action at the coast. But the surface circulation quickly dissipated as the center moved into the rugged mountain terrain to the east-northeast.

The considerable moisture in the storm is indicated by a surface dew point of 66°F at Los Angeles and San Diego, higher than record cool-season dew points.

Storm rainfall is indicated for the significant storm area by the isohyets in figure 6-6. Highest amounts occurred near the crest of mountain ranges in a manner characteristic of a strong orographic influence. Mt. Wilson received over 11 inches. The lee effect in the valley to the northeast of the Santa Ana Mountains and beyond the Coast Range is evident in the much smaller amounts there.

Rain began over most of the area during the afternoon or evening of the 24th, rather far in advance of the tropical Low center. Highest intensity in the Los Angeles area is shown in figure 6-7 as occurring early on the morning of the 25th. Passage of the Low center at the coast was associated with the secondary rainfall peak near 0700 PST.

There is little evidence of locally intense convective development in the area of and during the storm itself. The only thunderstorm reported at this time was at Claremont, in the foothills east of Los Angeles. (Heavy local showers and thunderstorms not included in figure 6-6 occurred over the southeastern interior from 12 to 24 hours prior to the beginning of the storm, presumably in a flow of moisture from the Gulf of Mexico. Indio reported 6.45 inches in 7 hours prior to 1100 PST of the 24th.)

6-C-2. The Northern California storm of September 12-14, 1918

This storm is the only one known to have moved northward offshore as far as Central California before veering inland (figure 6-4). By this time its surface circulation had been dissipated by loss of energy in traversing the cool water offshore. But evidence of strong convergence in the circulation aloft is found in the general 2-day rain over Central and Northern California; evidence of instability is found in reports of locally heavy thunderstorm rainfall.

The features of the general circulation necessary to allow northward movement of a tropical storm into mid-latitudes were present from the 10th. These features were, as in the September 1939 storm, an inverted trough along the coast between north-south ridges centered over the Western States and off the Pacific Coast.

The high moisture content of the tropical air is probably underestimated by the near-record surface dew points of 64-66°F persisting at San Francisco and Sacramento through most of the storm period.

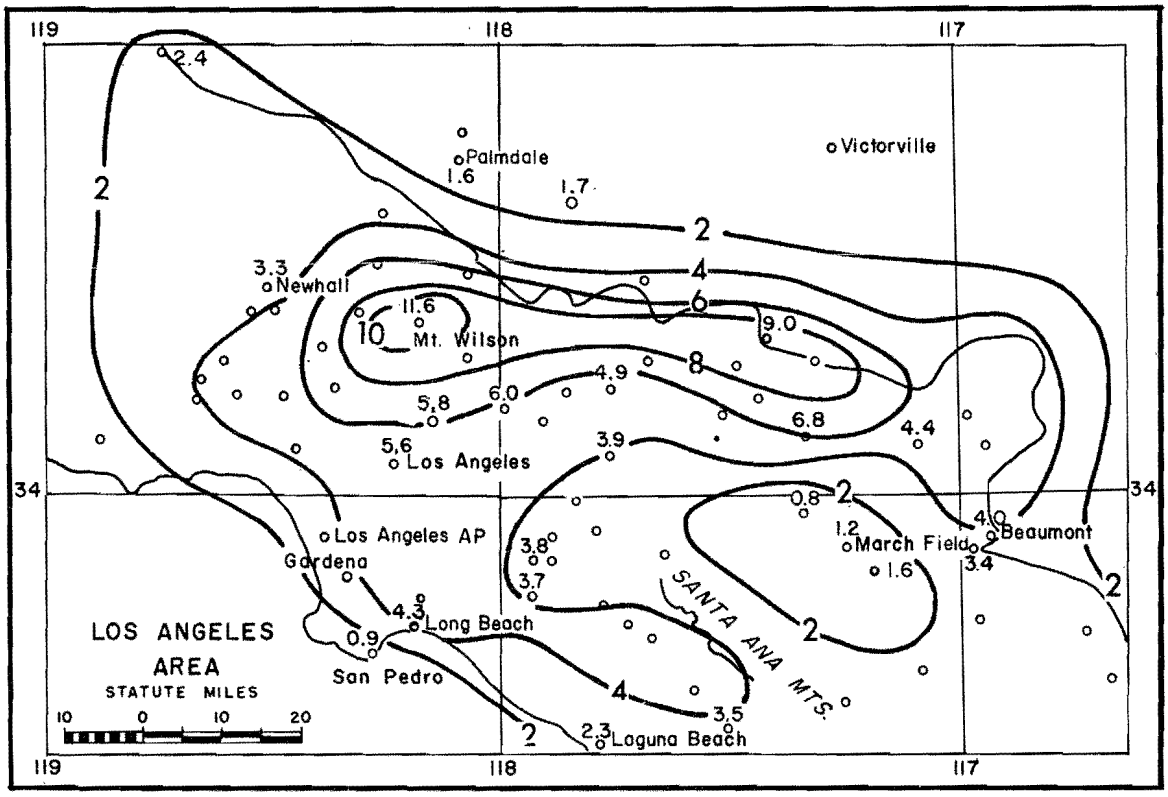

Fig. 6-6. ISOHYETS (INCHES) FOR THE SEPTEMBER 24-25, 1939 TROPICAL STORM

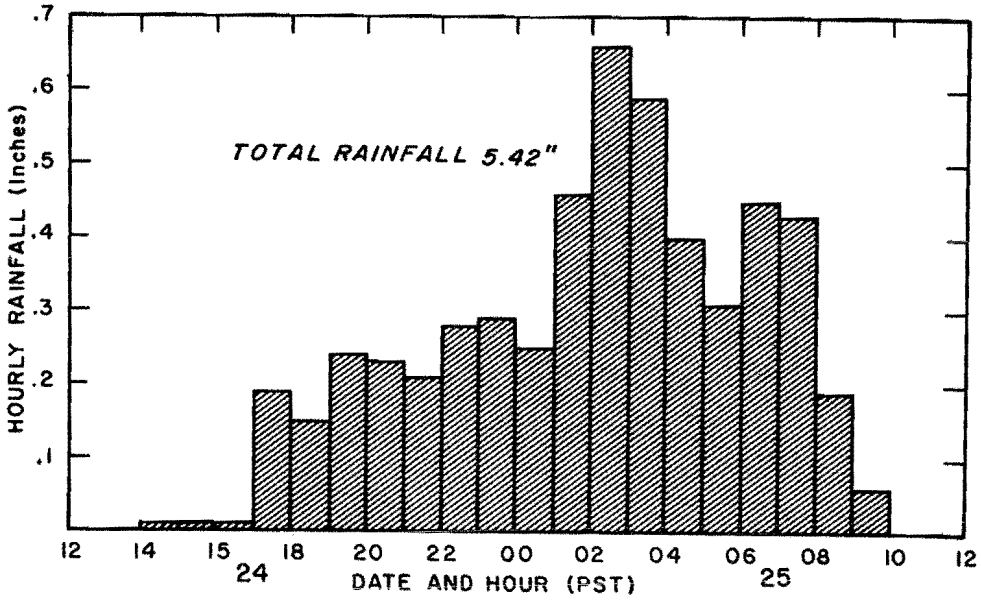

Fig. 6-7. HOURLY RAINFALL AT LOS ANGELES - SEPTEMBER 24-25, 1939

The rainfall sequence indicates that the upper circulation had spread out in the north-south trough. Rain began over Central California on the afternoon of the 11th, far in advance of the weak surface center. It continued through the 12th in a rather narrow north-south band extending into Northern California. By the morning of the 13th the trough had opened to the north as a cold front approached the Washington coast from northwest. The remnant of the surface center moved northward in the trough on the 13th, passing San Luis Obispo early that morning and Sacramento by evening, and continuing northward that night, ending the rain as it passed.

Isohyets of storm rainfall shown in figure 6-8 indicate an elongated north-south center extending along the storm path from Monterey northward along the east side of San Francisco Bay. This axis coincides with the axis of reported thunderstorm activity (not shown). Whereas nearly all of this rainfall was due to convergence or instability release, it is likely that the isohyetal center shown in the mountains northeast of Sacramento was influenced by release of instability due to orographic lifting and to some extent by orographic lifting directly.

The isohyetal center near Red Bluff reflects the extreme release of instability in a thunderstorm early on the morning of the 14th, presumably as the center of the remaining tropical circulation reached that area coincident with approach of cool air from northwest. Its occurrence in the area subject to intense thunderstorms described in chapter 6-A suggests also that terrain influences peculiar to that area were involved. The 3-hour amount at Red Bluff was 4.70 inches and 24-hour amount 6.12 inches, record short-period amounts for that station.

This marked release of instability precipitation at Red Bluff contrasts with the nearly continuous nature of rainfall at stations in the central part of the storm area, including stations reporting thunderstorms nearby. The small 3/24-hour rainfall ratios at stations other than Red Bluff listed in table 6-1 suggest that in areas other than where thunderstorms occurred, instability was a minor factor in rainfall.

Table 6-1

HIGHEST HOURLY RATES AND 3/24-HOUR RATIOS IN THE SEPTEMBER 1918 STORM

Station	Highest Hourly Rate	3/24-Hour Ratio	Thunderstorm
Mt. Tamalpais	.19	.22	No
San Francisco	.20	.31	No
San Jose	.57	.29	Nearby
Sacramento	.38	.31	Nearby
Red Bluff	2.14	.77	Yes

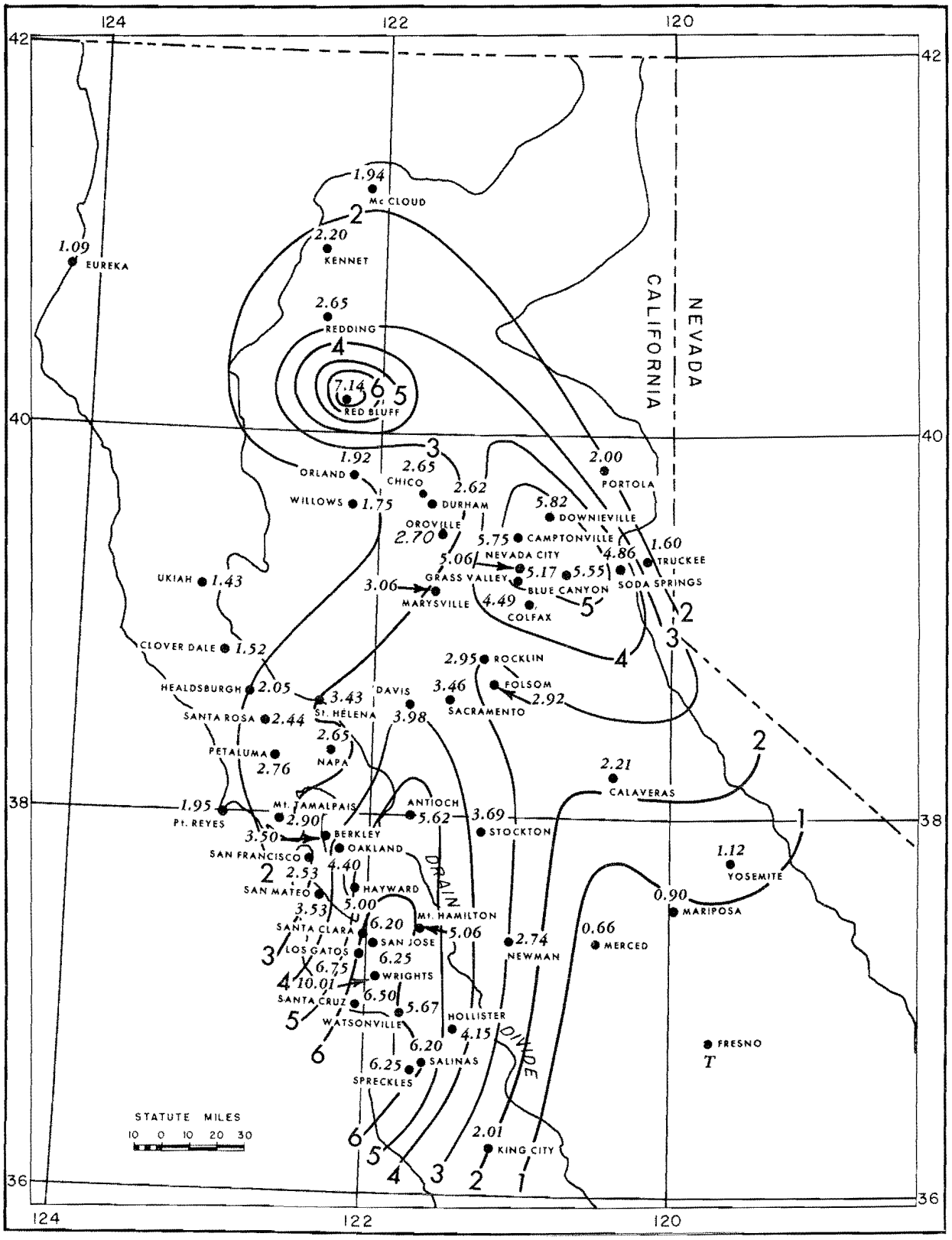

Fig. 6-8. STORM ISOHYETS (INCHES), SEPTEMBER 11-14, 1918

On the 12th a thunderstorm and heavy 24-hour rainfall (8.75 inches) occurred at Wrights, at the crest of the coastal range northeast of Santa Cruz, at an elevation of 1600 feet. Its development at this elevation was not hampered by stability in the ocean-cooled lower layers; it was probably facilitated by some orographic lifting in the weak surface circulation.

6-C-3. The Tehachapi storm of September 30, 1932

On this date 4.38 inches of rain was measured at Tehachapi between 1330 PST and 2000 PST, causing loss of several lives and property damage downstream toward Bakersfield. Description of the flood indicates that the Tehachapi observation did not sample the center of this local cloudburst and that most of the rain fell in a much shorter time interval than stated above. Tehachapi is located in the pass of the Tehachapi Mountains, southeast of Bakersfield.

Figure 6-4 indicates movement of the tropical storm center northward through the Gulf of California. Its surface Low lost its identity after moving on land during the morning. Rainfall from the upper circulation, mostly less than 1/2 inch, was general over Southern California and the southern San Joaquin Valley with lighter amounts near the coast.

Development of the local convective cell was favored by both time of day and terrain as a moist southeasterly flow reached this location after having been lifted to the crest of the Tehachapis. Precipitation was most intense on the lee side of the range toward Bakersfield, since flooding was mainly on Agua Caliente and Tehachapi Creeks draining northwestward.

The behavior of the storm was not unlike that of the 1939 tropical storm in respect to a prior southeasterly flow from the Gulf of Mexico. Such a flow caused scattered showers east of the Sierra crest on the 3 preceding days. It may have contributed to the moisture in the Tehachapi area on this date.

ACKNOWLEDGMENTS

This report was prepared under the supervision initially of Dr. Charles S. Gilman and later of his successor as Chief of the Hydrometeorological Section, Mr. Vance A. Myers. Credit is due Mr. George A. Lott and Mr. Myers for chapter IV. Acknowledgment is due Mr. Leon Hunsaker, Pacific Gas and Electric Co. Meteorologist, for searching much of the data in the December 1884 storm study. Thanks are due Mr. Sydney Molansky for editing figures and coordination of publication.

REFERENCES

1. U. S. Weather Bureau, "Interim Report - Probable Maximum Precipitation in California", Hydrometeorological Report No. 36, Washington, 1961.

2. U. S. Weather Bureau, "Maximum Possible Precipitation, Sacramento River Basin", Hydrometeorological Report No. 3, Washington, 1943.

3. U. S. Weather Bureau, "Revised Report on Maximum Possible Precipitation, Los Angeles Area, California", Hydrometeorological Report No. 21B, Washington, 1945.

4. U. S. Weather Bureau, "Rainfall Frequency Atlas of the U. S. for Durations from 30 Minutes to 24 Hours and Return Periods from 1 to 100 Years", Weather Bureau Technical Paper No. 40, Washington, 1961.

5. Robinson, M., "Sea-Temperatures in the North Pacific Area 20°-40°N, 125°-155°W.", Scripps Inst. of Oceanography, 1951.

6. Robinson, M., "Sea Temperatures in the Gulf of Alaska and in the Northeast Pacific Ocean, 1941-52", Bulletin of Oceanography, Vol. 7, No. 1, 1957.

7. Myers, Vance A., "Airflow on the Windward Side of a Large Ridge", Journal of Geophysical Research, Vol. 67, 1962.

8. Myers, Vance A., and George A. Lott, "Three-Dimensional Windflow and Resulting Precipitation in a Northern California Storm", U. S. Weather Bureau, Washington, 1962 (Unpublished.)

9. Elliott, Robert D., and Russell W. Shaffer, "The Development of Quantitative Relationships between Orographic Precipitation and Air-Mass Parameters for Use in Forecasting and Cloud Seeding Evaluation", Journal of Applied Meteorology, Vol. 1, No. 2, June 1962, pp. 218-228.

10. Goodyear, Hugo V., "A Graphical Method for Computing Horizontal Trajectories in the Atmosphere", Monthly Weather Review, Vol. 87, No. 5, 1959, pp. 188-195.

11. Bergeron, Tor, "Preliminary Results of 'Project Pluvius'," Publication No. 53 of the I.A.S.H., Committee on Precipitation, Gentbrugge, 1960.

12. U. S. Weather Bureau, "Rainfall and Floods of April, May, and June 1957 in the South-Central States", Weather Bureau Technical Paper No. 33, Washington, 1958, p. 14.

13. Haltiner, George J. and Frank L. Martin, "Dynamical and Physical Meteorology," McGraw-Hill Book Co., Inc., New York, 1957, p. 191.

REFERENCES (Cont'd.)

14. U. S. Weather Bureau, "On Quantitative Precipitation Forecasting," National Hurricane Research Project Report No. 38, Washington, 1960. Part 1.

15. Elliot, Robert D., "California Storm Characteristics and Weather Modification", Journal of Meteorology, Vol. 15, No. 6, 1958, pp. 486-493.

16. Kesseli, J. E., and C. B. Beatty, "Desert Flood Conditions in the White Mountains of California and Nevada", Technical Report EP-108, Headquarters, Quartermaster Research & Engineering Command, U. S. Army, Natick, Mass., April 1959, p. 23.

17. U. S. Weather Bureau, "Generalized Estimates of Probable Maximum Precipitation for the United States West of the 105th Meridian", Weather Bureau Technical Paper No. 38, Washington, 1960.

APPENDIX

Included in this appendix are isohyetal maps of the heaviest 24-hour precipitation (to the nearest six hours) in five major winter storms of the last twenty-five years.

The precipitation amounts are derived mostly from the tabulations of storm precipitation by the Corps of Engineers known as "Storm Studies, Part II." In these studies 6-hour amounts are listed for all stations in study area. The subdivision of less frequent readings is estimated from a comparison with adjacent recorder stations and from meteorological factors.

The isohyets, where the observations themselves are inadequate in detail, are patterned after the mean annual precipitation charts of the Corps of Engineers.

The isohyets for each storm are shown only over the portion of the state of heaviest precipitation, and for which the 6-hour amounts were readily available.

☆ U.S. GOVERNMENT PRINTING OFFICE: 1963 O—669657

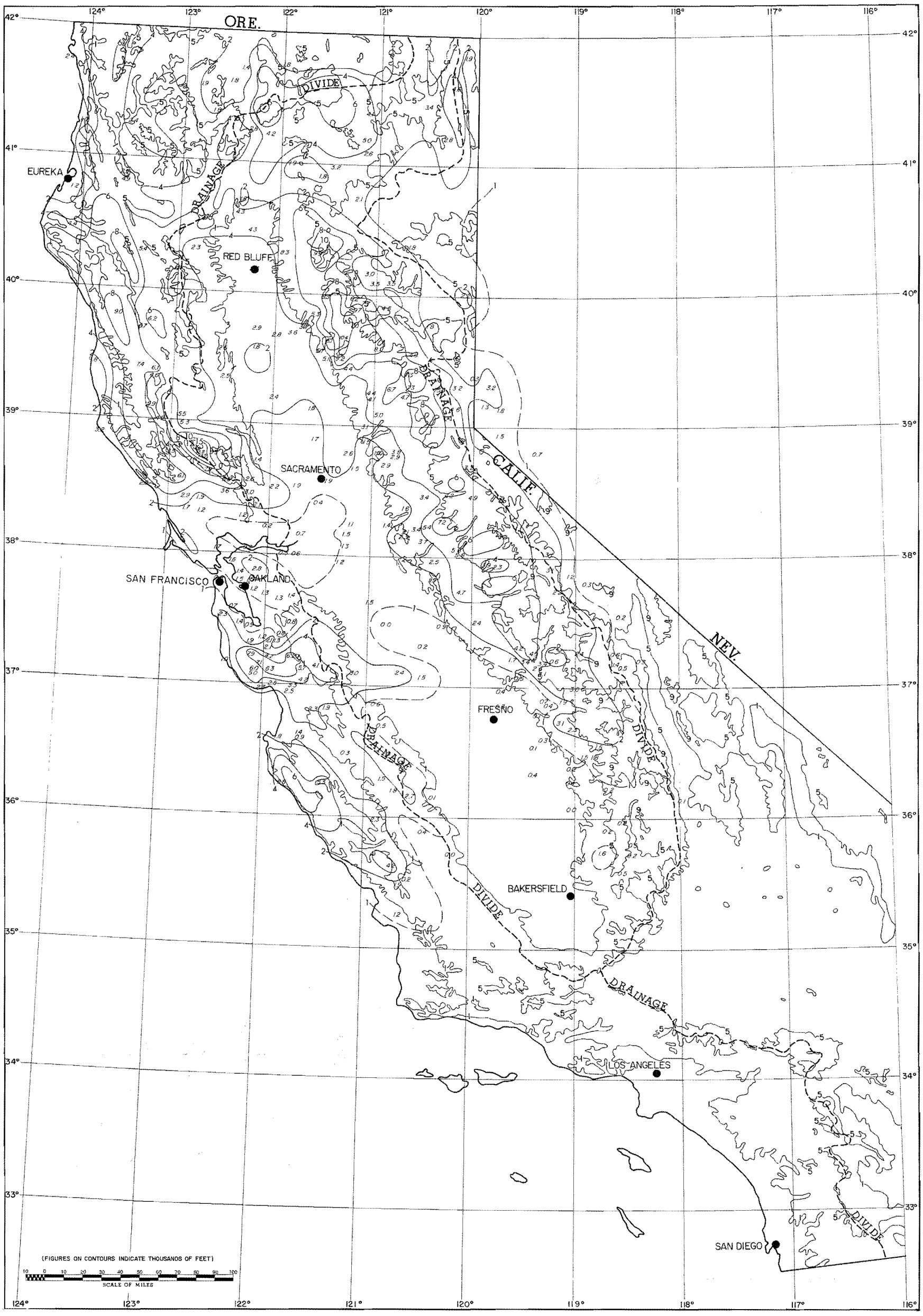

FIG. A-1. 24-HOUR ISOHYETAL CHART (INCHES) ENDING 0600 PST, DEC. 11, 1937

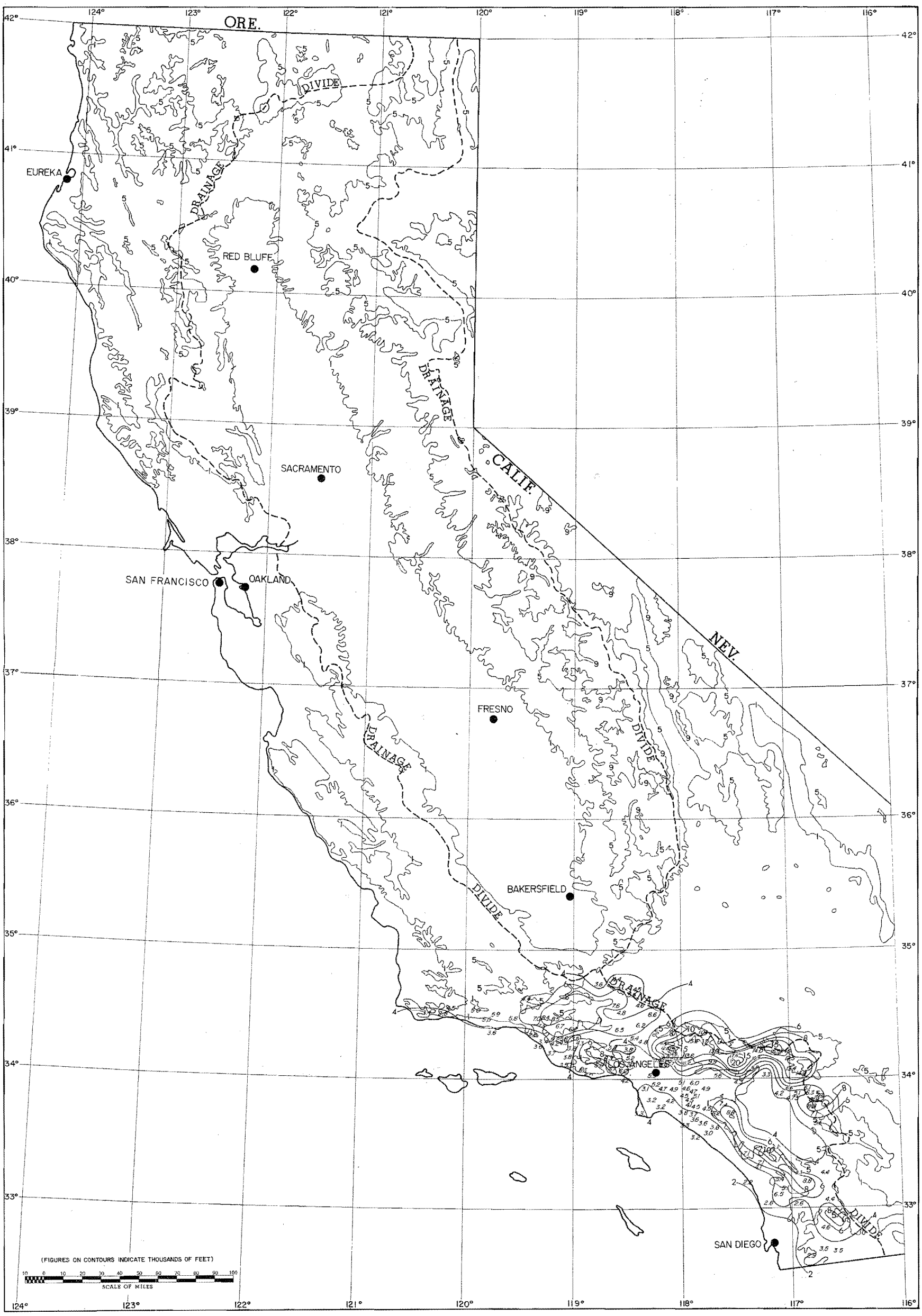

FIG. A-2. 24-HOUR ISOHYETAL CHART (INCHES) ENDING 2400 PST, MAR. 2, 1938

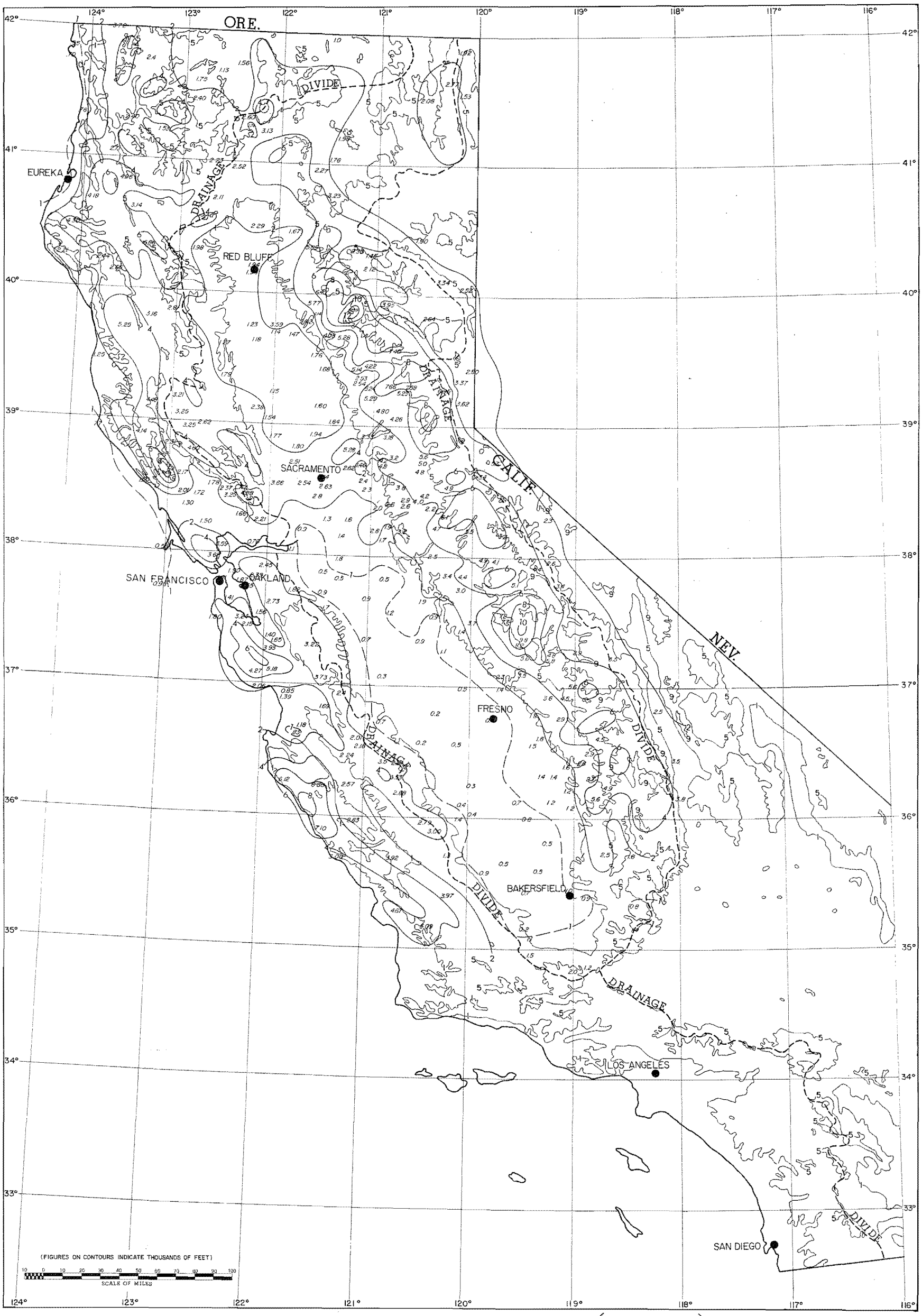

FIG. A–3. 24-HOUR ISOHYETAL CHART (INCHES) ENDING 2400 PST, JAN. 21, 1943

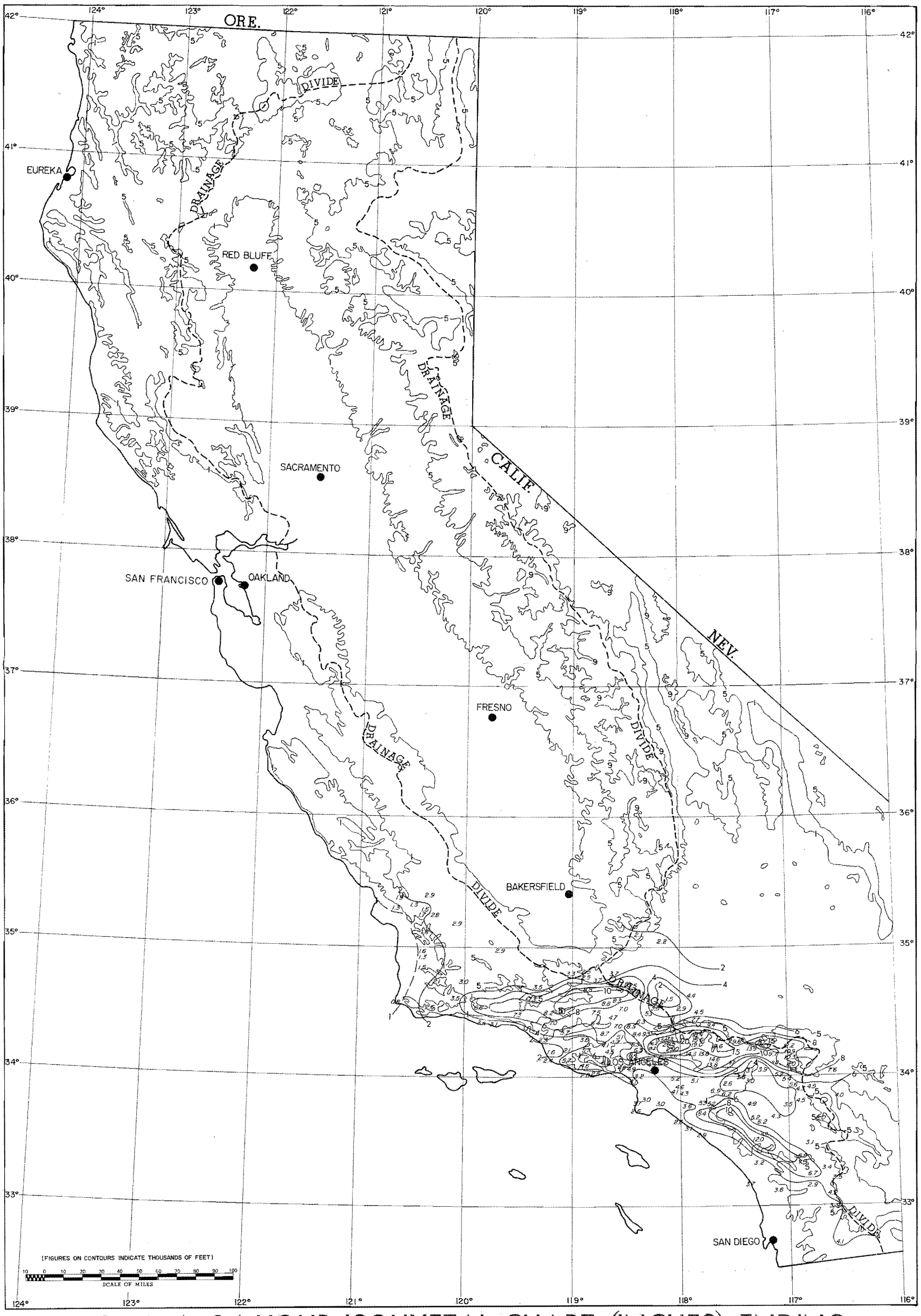

FIG. A–4. 24-HOUR ISOHYETAL CHART (INCHES) ENDING 0600 PST, JAN. 23, 1943

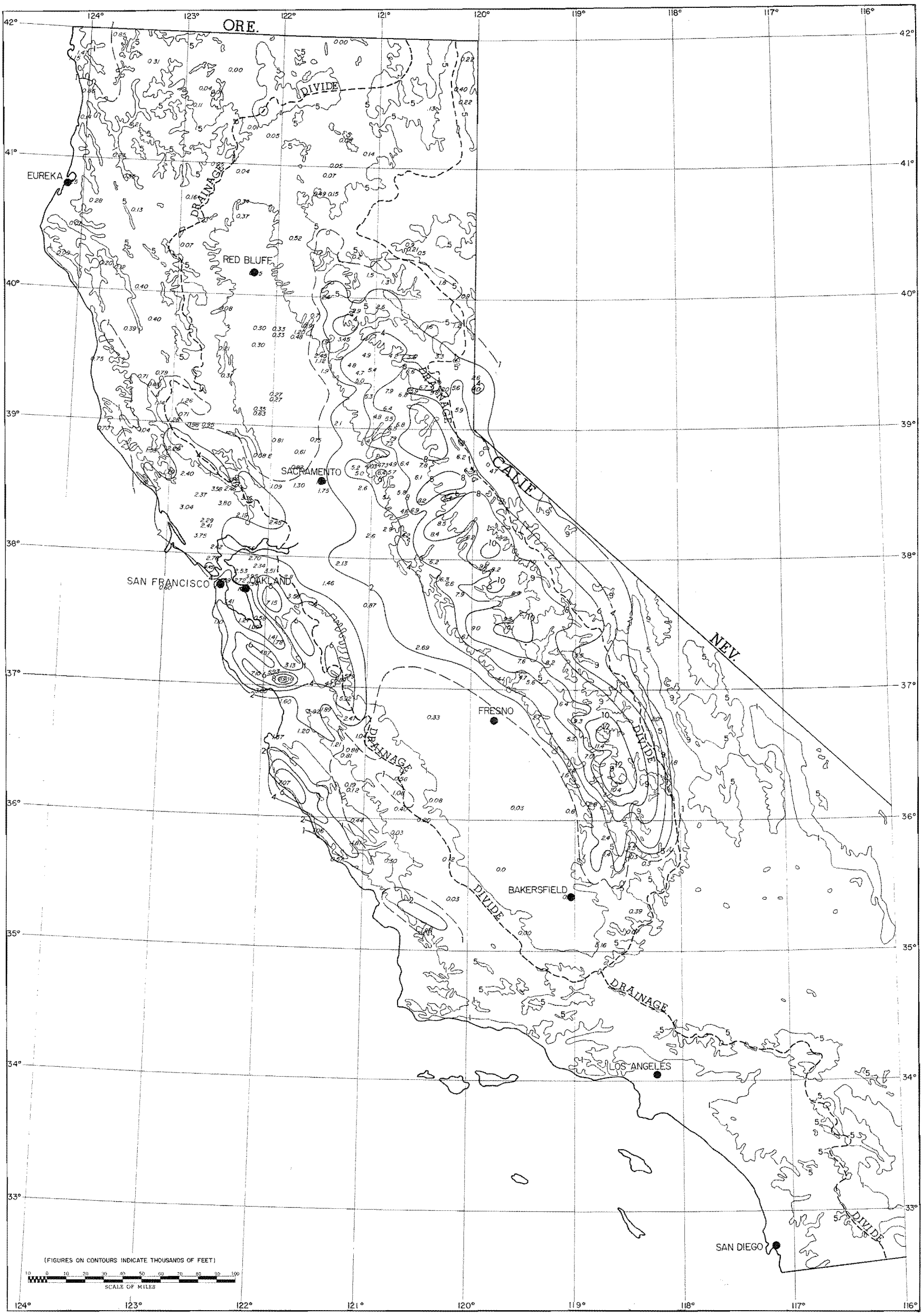

FIG. A-5. 24-HOUR ISOHYETAL CHART (INCHES) ENDING 2400 PST, NOV. 18, 1950

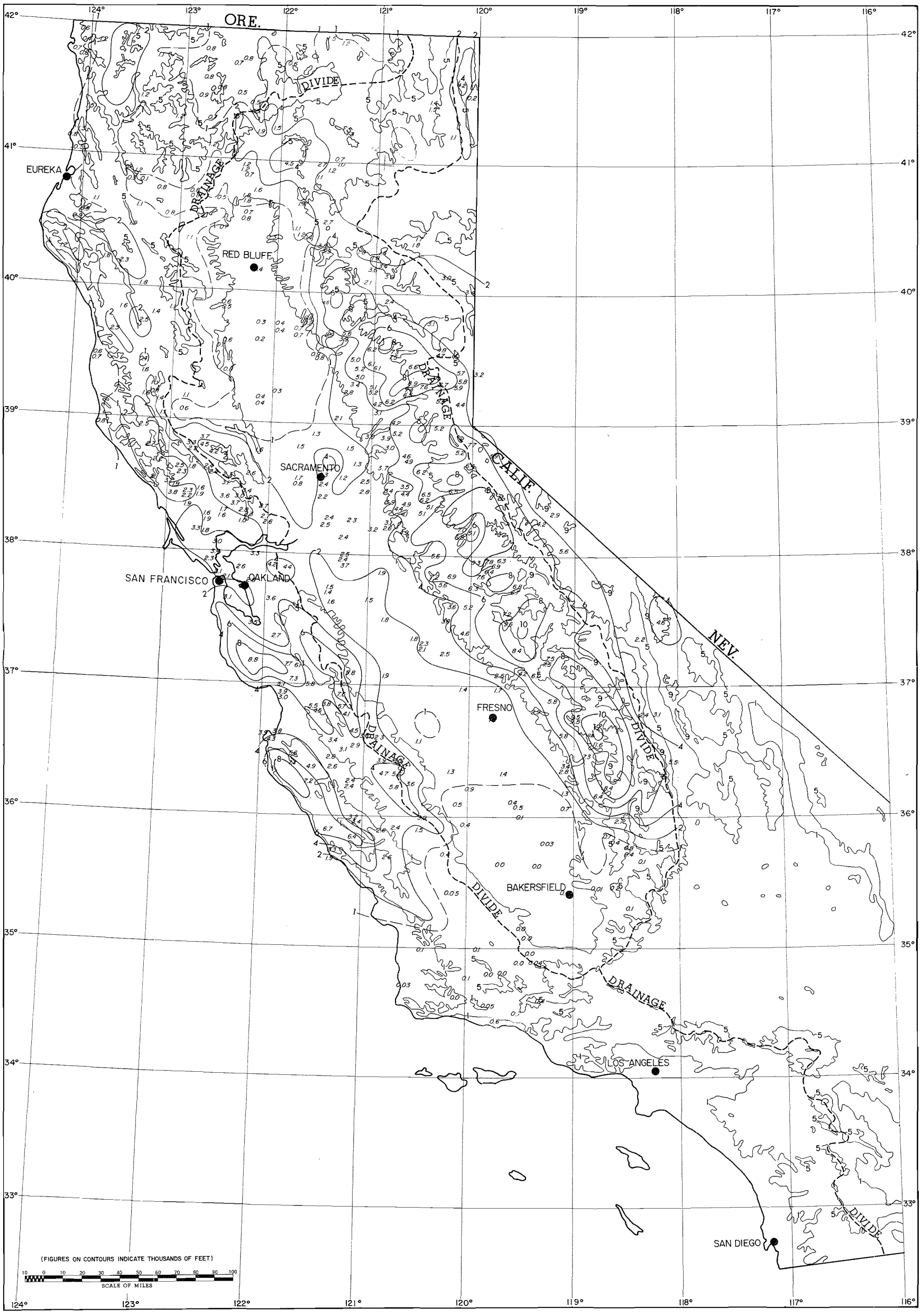

FIG. A-6. 24-HOUR ISOHYETAL CHART (INCHES) ENDING 1800 PST, DEC. 23, 1955